DEVELOPMENT OF SOME MAGNETIC GREEN ADSORBENTS FOR THE REMOVAL OF POLLUTANTS FROM AQUEOUS SOLUTIONS

Thesis Submitted for the Award of the Degree of

DOCTOR OF PHILOSOPHY (Ph.D.)

in

Chemistry

By

Dimple Sharma

Registration Number: 41700144

Supervised By

Dr. Harminder Singh (11839)

School of Chemical Engineering and

Physical Sciences (Professor)

Lovely Professional University,

Phagwara, Punjab

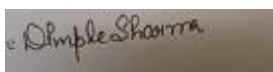

LOVELY PROFESSIONAL UNIVERSITY, PUNJAB

2024

Dedicated

To

My Beloving Daughters

Srishti

&

Aradhana

DECLARATION

I declare that thesis entitled "DEVELOPMENT OF SOME MAGNETIC GREEN ADSORBENTS FOR THE REMOVAL OF POLLUTANTS FROM AQUEOUS SOLUTIONS." has been prepared by me under the guidance of Dr. Harminder Singh, Professor, School of Chemical Engineering and Physical Sciences, Lovely Professional University, Phagwara. No part of this thesis has formed the basis for the award of any degree or fellowship previously.

Dimple Sharma

(Reg. no. 41700144)

School of Chemical Engineering and Physical Sciences

Lovely Professional University

Phagwara, Punjab, India

Date: 1 0 . 0 9 . 2 4

CERTIFICATE

This is to certify that the work reported in the Ph.D. thesis entitled **"DEVELOPMENT OF SOME MAGNETIC GREEN ADSORBENTS FOR THE REMOVAL OF POLLUTANTS FROM AQUEOUS SOLUTIONS"** submitted in fulfillment of the requirement for the award of degree of **Doctor of Philosophy (Ph.D.)** CHEMISTRY in the School of Chemical Engineering and Physical Sciences, is a research work carried out by Dimple Sharma, Registration No. 41700144, is bonafide record of her original work carried out under my supervision and that no part of thesis has been submitted for any other degree, diploma or equivalent course.

(Signature of Supervisor)

Dr. Harminder Singh

Professor in Chemistry

School of Chemical Engineering and Physical Sciences

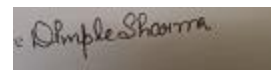Lovely Professional university, Phagwara, Punjab-144001

Acknowledgment

Date: 10.09.24   Dimple Sharma

<u>ABSTRACT</u>

Water is necessary for survival of life on this planet. The drinking water resources are decreasing due to human activities in name of industrialization and urbanization. The challenge before the researchers is to resolve the problem of waste water. The main pollutants of water include- dyes, heavy metals, and ionic impurities along with numerous other organic and inorganic pollutants. These may be very toxic for human beings as well as for aquatic biota. Various physical and chemical techniques have been developed till date to remove dyes and ionic pollutants from water. From all available methods, the one with cost effectiveness, eco-friendly nature, less time consuming and reusability is preferred. Adsorption, therefore is suitable technique because it possesses all such properties. Adsorption is widely used in treatment of waste water. Natural adsorbents are not very costly and are available in large amounts. These show less potential for removing pollutants from water. So, need of synthetic adsorbents arises. Synthetic adsorbents are prepared from agricultural or industrial wastes. They show remarkable performance in eliminating pollutants from water as compared to traditional adsorbents. Nano materials can also be utilised for removal of pollutants from waste water in the form of mesoporous compounds, metal oxides or Nano ferrites. Nano ferrites give good results in removing contaminants from water but these are not very stable in solution. So, need of their modification arises. Different surfactants, polymers or bio-polymers, doping agents etc. are used for the modification of spinel ferrites. Biopolymers modified spinel ferrites are gaining interest of researchers in waste water treatment these days. This is due to the reason that such materials like chitosan, alginate, silica, starch etc. are available in abundant quantities, as these are obtained from agricultural wastes, fruit peels, plant residues (dried leaves, seeds, kernels etc.), etc. When these materials are combined with spinel ferrites, these are termed as magnetic green adsorbents or magnetic green composites.

Therefore, in the present study some selected materials like, rice husk silica, mango starch and carboxy methyl mango starch were utilized for the modification of spinel metal ferrites of zinc, nickel and copper and used as magnetic green adsorbents to remove dyes, heavy metal and fluoride ions from water.

For studying the adsorption behavior of magnetic green composites, preliminary studies were done with various dyes and metal ions. Magnetic green composites Viz. ZFN-RHS, ZFN-MS and ZFN-CMS were selected for further studies as these exhibited good adsorption potential in preliminary studies. The synthesized magnetic green composites were characterized using

Fourier Transform Infrared Spectroscopy (FTIR); X-ray Diffraction (XRD); Fe-Scanning Electron Microscope (FESEM); Energy Dispersive Spectra (EDS); Brunauer-Emmett-Teller (BET) analysis; Thermo Gravimetric Analysis (TGA) and pH point zero charge (pH$_{pzc}$). Adsorption behavior of ZFN-RHS, ZFN-MS and ZFN-CMS magnetic green composites were studied with some selected dyes- Methylene Blue (MB), Crystal Violet (CV), Brilliant Green (BG) and Malachite Green (MG), in single, binary and ternary dye systems; Ni (II) ions and fluoride ions in single ion system using batch adsorption method. Various kinetic models and adsorption isotherms were utilised to study different adsorption parameters, which revealed that synthesized magnetic green composites were suitable to remove various pollutants like dyes, heavy metal and fluoride ions. Kinetic studies using ZFN-RHS, ZFN-MSand ZFN-CMS magnetic green composites, revealed that pseudo second order model fitted best. This indicated that adsorption of dyes in single and multiple dye system; Ni (II) ion and fluoride ion in single ion system, using magnetic green composites was chemical in nature. Similarly, the optimum pH value for removing dyes and fluoride ions was 5 for ZFN-RHS whereas it was 8 for ZFN-MS and ZFN-CMS. The adsorption behavior of selected cationic dyes, Ni (II) ions and fluoride ions, was studied at varying concentration (50-250 mg/L for a single and 20- 100 mg/L for binary and ternary dye systems) by using magnetic green composites. Results revealed that removal efficiency of cationic dyes/Ni (II) ions/fluoride ions, declined by increasing concentration of dyes in single and multiple system. On the other hand, adsorption capacity (Q$_e$) of cationic dyes/Ni (II) ions/fluoride ions, was increased by increasing concentration. But with increase in temperature both percentage removal and Q$_e$, increased. Because of large size of pores of magnetic green composites at high temperature, the surface area accessible for the adsorption of dyes/Ni (II) ions/fluoride ions increased thereby percentage removal increased. By increase in temperature, the stronger electrostatic interactions between adsorbate and adsorbent molecules lead to increase in adsorption capacity. Different adsorption isotherm models viz. Langmuir, Freundlich, Temkin, and Dubinin-Radushkevich (D-R) were utilized for studying adsorption behavior of ZFN-RHS, ZFN-MS and ZFN-CMS magnetic green composites in single and multiple systems. It was noted that using ZFN-CMS, Langmuir and Temkin isotherms fitted best. Using ZFN-RHS and ZFN-MS magnetic green composites, Freundlich isotherm gave best results for removing pollutants (dyes, metal ion and fluoride ions). Regeneration of magnetic green composites after adsorption is important parameter to check their cost-effectiveness. Regeneration of magnetic green composites used in this study was done by using different desorbing agents up to 5 cycles. It was found that ZFN-RHS, ZFN-MS and ZFN-CMS retained regeneration efficiencies of 93%, 80% and 90%, respectively

for dyes in single system. Regeneration efficiency of ZFN-MS and ZFN-CMS for removing Ni (II) ions were 72% and 79%, respectively. In the removal of fluoride ions using ZFN- RHS, ZFN-MS and ZFN-CMS, regeneration efficiencies were 74%, 85% and 84%, respectively. These results conclude that magnetic green composites synthesized in present study are nature friendly, selective and cost effective, hence are suitable adsorbents for removing cationic dyes/metal ions and fluoride ions from water.

Table of Content

CHAPTER 4: RESULTS AND DISCUSSION

Part-1

4.0 Characterization of magnetic green composites (ZFN-RHS, ZFN-MS and ZFN-CMS)

Part II

4.2 Batch adsorption studies with dyes

CHAPTER 5: SUMMARY AND CONCLUSIONS

LIST OF TABLES

LIST OF FIGURES

List of Abbreviations

Abbreviation	Meaning
BG	Brilliant green
CMS	Carboxy methyl starch
CNTs	Carbon Nano tubes
CR	Congo red
CuFN	Copper ferrite
CV	Crystal violet
DW	Distilled water
MB	Methylene blue
MG	Malachite green
MS	Mango starch
MWCNTs	Multi walled carbon Nano tubes
NiFN	Nickel ferrite
ODH	Oxalyl dihydrazide
RHA	Rice husk ash
RHS	Rice husk silica
SiO_2	Silica
ZFN	Zinc ferrite
ZFN-RHS	Zinc ferrite- rice husk silica
ZFN-MS	Zinc ferrite- mango starch
ZFN-CMS	Zinc ferrite- carboxy methyl starch

Symbols Used

Parameter	Symbol	Unit
Percentage	%	NA
Temperature	T	^{o}C
Initial Concentration	C_o	mg/L
Concentration at time t	C_t	mg/L
Adsorption Capacity at equillibrium	Q_e	mg/g
Adsorption Capacity at time t	Q_t	mg/g
Gibbs free energy change	ΔG^o	kJ/mol
Enthalpy change	ΔH^o	kJ/mol
Entropy change	ΔS^o	J/mol/K
Lagergren pseudo first order rate constant	k_1	g/mg/min
Pseudo second order rate constant	k_2	g/mg/min
Chemisorption rate constant	α	mg/min
Chemisorption activation energy	β	g/mg
Absolute temperature	T	K
Maximum binding energy	A	L/g
Temkin constant	b_T	J/mg
Langmuir adsorption capacity	Q	mg/g
D-R adsorption capacity	Q_m	mg/g
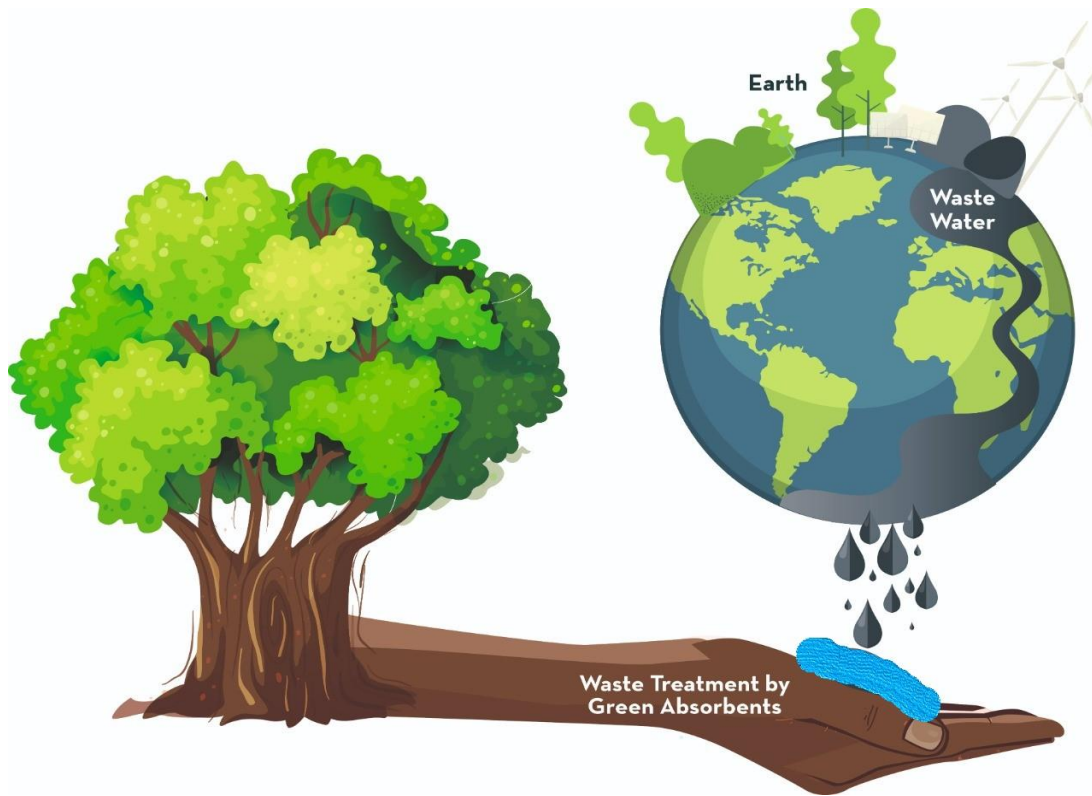
CHAPTER 1

INTRODUCTION

1.0 General Introduction

Out of 70% water present on the surface of earth only 3% is available as fresh water for human and other living beings. Glaciers contribute to 2/3rd of fresh water. Due to increase in the population, the demands of using fresh water supplies in the industries and other activities is increasingday by day. Water contamination is a significant environmental challenge. This can be attributedto domestic wastes, industrial wastes or agricultural wastes which are disposed of into water bodies without any prior treatment. Thus, the future challenge before the world is to face watercrisis because the quantity and quality of water is declining rapidly[1]. The various contaminants responsible for waste water are heavy metals, colored dyes, pesticides, inorganic chemicals and antibiotics etc. These may cause serious health problems in human beings as well as to the aquatic biota. The various diseases caused by these pollutants include infection of lungs, kidney failure, cardiac attacks, failure of nervous system etc.[2,3]. So, treatment of waste water is a challenging issue before the researchers. Various strategies had been adopted till date to treat contamination of waste water which include flocculation, coagulation, membrane filtration, photochemical degradation, adsorption etc.[4]. In the following sections some common waste water treatment methods are discussed.

1.1 Different methods for treatment of waste water

Some common methods for the treatment of waste water include-

1.2 Physical methods

Physical methods utilised in the removal of dyes and heavy metals from waste water include:

a) Adsorption
b) Ion exchange
c) Irradiation
d) Membrane filtration
e) Electro kinetic coagulation
f) Aerobic and anaerobic degradation

1.2.1 Adsorption

Adsorption is commonly employed process for the treatment of waste water due to its cost-effective, eco-friendly nature and ease of operation. Various adsorbents are used for waste

water treatment with high removal capacity. The process of adsorption involves the adhesion of adsorbate onto the surface of adsorbent[5]. The advantage of this method is its high efficiency and simplicity. However, activated carbon conveniently used in the process of adsorption is very expensive.

1.2.2 Ion exchange

Ion exchange is highly efficient technique and it has wide applications in the field of waste water treatment. Natural zeolites and synthetic resins are used in the process of ion exchange.The advantage of this method includes high percentage removal of pollutant and its selectivity. Butit is very expensive so it cannot be used on large scale[6].

1.2.3 Irradiation

Irradiation is one of the most advanced technology for the degradation of pollutants from waste water. In this method gamma rays along with oxidants like oxygen, hydrogen peroxide, sodium hypochlorite, etc. are used for the degradation of dyes. This method has advantages like it does not require any chemical additives. It involves the breakdown and oxidation of pollutants for which large amount of oxygen is required. Mostly the sewage treatment is done using irradiation method[7].

1.2.4 Membrane filtration

Membrane filtration is indeed a versatile method for the removal of both organic and inorganic pollutants from waste water. Commonly used membrane filtration methods are- microfiltration, ultrafiltration, Nano filtration and reverse osmosis. The main advantage of using this method is less amount of chemicals and less production of sludge. But it requires high maintenance and operational cost[8].

1.2.5 Electro kinetic coagulation

Electro kinetic coagulation is indeed an emerging technology utilised for removing in situ pollutants from industrial sludge. For this purpose an electric field is required. This method is suitable for large scale waste water treatment. But this is very expensive method and has disposal problems[9].

1.2.6 Aerobic and anaerobic degradation

In aerobic degradation there is involvement of oxygen for the degradation of organic matter by micro-organisms whereas in anaerobic degradation no oxygen is required[10]. Aerobic Degradation process is fast as compared to anaerobic degradation. But large waste is generated in aerobic process which created disposal problems whereas in anaerobic process less waste is generated.

1.3 Chemical methods

The various chemical methods utilised for removing dyes and heavy metals from waste water include:

(a) Fenton method
(b) Chemical precipitation
(c) Coagulation

1.3.1 Fenton method

Fenton method is advanced oxidation. In this process, hydrogen peroxide and a source of Fe^{2+}ions are used and hydroxyl radicals produced decompose the organic impurities present in water[11]. This method is inexpensive. Disadvantage of this method is that it is based on pH. Because above pH 3 radicals are not stable.

1.3.2 Chemical precipitation

Chemical precipitation is mostly utilised for removing heavy metals from waste water. It is used for removing ionic impurities from water by adding their counter ions which results into decrease of solubility[12]. This method is effective for the removal of various contaminants, including heavy metals, phosphates, making it versatile in waste water treatment. But this method is very expensive.

1.3.3 Coagulation

This method is used for the removal of organic and inorganic impurities from waste water. Some common coagulants used in this method includes aluminium sulphate, ferric sulphate, ferric chloride, etc. In this method after treatment with chemicals small particles aggregate to form large particles. Thereafter, filtration is done. Selection of proper coagulant is the main drawback of this methodand also this method is based upon temperature[13].

1.4 Biological methods

In biological treatment of waste water, the pollutants are degraded with the help of microbes/plants instead of harmful chemicals. By using biological methods, the adverse effects caused by accumulation of chemicals in water bodies can be prevented. It involves aerobic and anaerobic treatment of organic or inorganic effluents present in waste water. In aerobic treatment process, biological sludge is produced. On the other hand, in anaerobic treatment, sludge produced is very less and it has low operating cost. The various biological methods employed for removing dyes and heavy metal ions from waste water are- biological degradation of pollutants by bacteria, fungi, enzymes, plant species, etc.[14-18].

These methods have their own merits and demerits. From all available methods for waste water treatment, adsorption is found to be most reliable because of its eco-friendly nature, cost-effectiveness, low energy requirement and simplicity[19]. In adsorption, dissolved solute particles (adsorbate) are attached on a solid surface (adsorbent) by intermolecular forces of attraction between liquid and solid surface.

1.5 Different types of adsorbents for removal of pollutants from water

The various types of adsorbents utilised for removing dyes and heavy metal ions from waste water have been categorized into two types-

 A) Natural
 B) Synthetic

1.5.1 Natural

Adsorbents such as clay, charcoal, glass, wool, sand, zeolites etc. which are obtained from nature and utilised as such for the removal of pollutants from waste water are classified as natural adsorbents. These are very easily available and are cheap. Their efficiency for the removal of pollutants can be enhanced by modification. The modification can be physical, chemical or biological in nature[20].

1.5.2 Synthetic

The efficiency of removal of pollutants by natural adsorbents were low so the need of synthetic or manmade adsorbents arise. These synthetic adsorbents can be prepared from various industrial or agricultural waste materials. The agricultural waste materials like coconut shells, peels of fruits like orange, banana, walnut shells, baggasse wastes, rice husk, wheat husk, silica, pine cone, saw dust, tea waste, fly ash, etc. can be used to synthesize synthetic adsorbents[21].

Nano materials can be used as adsorbents due to their high adsorption capacity. In the last two decades, wastewater treatment process started utilizing nanomaterials and their composites[22]. These materials have a strong ability to adsorb contaminants from water, both inorganic and organic. These materials have a number of special qualities, including a large surface area, a reactive surface, reusability and cost effectiveness. Nano materials include mesoporous compounds, non-metal oxides, and nano ferrites. Nano ferrites stand out among other nanomaterials because of their additional magnetic properties, which facilitates their separation after processing.

Recently, biopolymers combined with magnetic spinel ferrites have been reported as efficient adsorbents for removing pollutants like dyes and heavy metals from waste water. In the present work magnetic green adsorbents have been synthesized by combining spinel metal ferrites with silica extracted from rice husk, mango starch extracted from mango seed kernel and carboxy methyl starch prepared from mango starch.

References

(1)   Damkjaer, S.; Taylor, R. The Measurement of Water Scarcity: Defining a Meaningful Indicator. *Ambio* **2017**, *46* (5), 513–531. https://doi.org/10.1007/s13280-017-0912-z.

(2)   Mehra, S.; Singh, M.; Chadha, P. Adverse Impact of Textile Dyes on the Aquatic Environment as Well as on Human Beings. *Toxicol. Int.* **2021**, *28* (2), 165–176. https://doi.org/10.18311/ti/2021/v28i2/26798.

(3)   Kahlon, S. K.; Sharma, G.; Julka, J. M.; Kumar, A.; Sharma, S.; Stadler, F. J. Impact of Heavy Metals and Nanoparticles on Aquatic Biota. *Environ. Chem. Lett.* **2018**, *16* (3), 919–946. https://doi.org/10.1007/s10311-018-0737-4.

(4)   Crini, G.; Lichtfouse, E. Advantages and Disadvantages of Techniques Used for Wastewater Treatment. *Environ. Chem. Lett.* **2019**, *17* (1), 145–155. https://doi.org/10.1007/s10311-018-0785-9.

(5)   Alaqarbeh, M. Adsorption Phenomena: Definition, Mechanisms, and Adsorption Types: Short Review. *RHAZES Green Appl. Chem.* **2021**, *13*, 43–51.

(6)   Ma, A.; Abushaikha, A.; Allen, S. J.; McKay, G. Ion Exchange Homogeneous Surface Diffusion Modelling by Binary Site Resin for the Removal of Nickel Ions from Wastewater in Fixed Beds. *Chem. Eng. J.* **2019**, *358*, 1–10. https://doi.org/10.1016/j.cej.2018.09.135.

(7)   Rani, U. A.; Ng, L. Y.; Ng, C. Y.; Mahmoudi, E. A Review of Carbon Quantum Dots and Their Applications in Wastewater Treatment. *Adv. Colloid Interface Sci.* **2020**, *278*, 102124. https://doi.org/10.1016/j.cis.2020.102124.

(8)   Hube, S.; Eskafi, M.; Hrafnkelsdóttir, K. F.; Bjarnadóttir, B.; Bjarnadóttir, M. Á.; Axelsdóttir, S.; Wu, B. Direct Membrane Filtration for Wastewater Treatment and Resource Recovery: A Review. *Sci. Total Environ.* **2020**, *710*. https://doi.org/10.1016/j.scitotenv.2019.136375.

(9)   Jorfi, S.; Pourfadakari, S.; Ahmadi, M. Electrokinetic Treatment of High Saline Petrochemical Wastewater: Evaluation and Scale-Up. *J. Environ. Manage.* **2017**, *204*, 221–229. https://doi.org/10.1016/j.jenvman.2017.08.058.

(10)   Patil, B. S.; Agnes Anto, C.; Singh, D. N. Simulation of Municipal Solid Waste Degradation in Aerobic and Anaerobic Bioreactor Landfills. *Waste Manag. Res.* **2017**, *35* (3), 301–312. https://doi.org/10.1177/0734242X16679258.

(11)   Zhang, M. hui; Dong, H.; Zhao, L.; Wang, D. xi; Meng, D. A Review on Fenton Process for Organic Wastewater Treatment Based on Optimization Perspective. *Sci.*

Total Environ. **2019**, *670*, 110–121. https://doi.org/10.1016/j.scitotenv.2019.03.180.

(12)   Zhang, Y.; Duan, X. Chemical Precipitation of Heavy Metals from Wastewater by Using the Synthetical Magnesium Hydroxy Carbonate. *Water Sci. Technol.* **2020**, *81* (6), 1130–1136. https://doi.org/10.2166/wst.2020.208.

(13)   Cui, H.; Huang, X.; Yu, Z.; Chen, P.; Cao, X. Application Progress of Enhanced Coagulation in Water Treatment. *RSC Adv.* **2020**, *10* (34), 20231–20244. https://doi.org/10.1039/d0ra02979c.

(14)   Ahmed, S.; Aktar, S.; Zaman, S.; Jahan, R. A.; Bari, M. L. Use of Natural Bio-Sorbent in Removing Dye, Heavy Metal and Antibiotic-Resistant Bacteria from Industrial Wastewater. *Appl. Water Sci.* **2020**, *10* (5), 1–10. https://doi.org/10.1007/s13201-020-01200-8.

(15)   Younas, F.; Mustafa, A.; Farooqi, Z. U. R.; Wang, X.; Younas, S.; Mohy-Ud-din, W.; Hameed, M. A.; Abrar, M. M.; Maitlo, A. A.; Noreen, S.; Hussain, M. M. Current and Emerging Adsorbent Technologies for Wastewater Treatment: Trends, Limitations, and Environmental Implications. *Water (Switzerland)* **2021**, *13* (2), 1–25. https://doi.org/10.3390/w13020215.

(16)   Arris, S.; Bencheikh, L. M.; Miniai, H. A. Preparation and Characterisation of an Natural Adsorbent Used for Elimination of Pollutants in Wastewater. *Energy Procedia* **2012**, *18*, 1145–1151. https://doi.org/10.1016/j.egypro.2012.05.129.

(17)   Madiraju, S. V. H.; Hung, Y. T.; Paul, H. H. C. Synthetic Wastewater Treatment Using Agro-Based Adsorbents. *Walailak J. Sci. Technol.* **2021**, *18* (11). https://doi.org/10.48048/WJST.2021.10337.

(18)   Kumar, M.; Singh Dosanjh, H.; Sonika; Singh, J.; Monir, K.; Singh, H. Review on Magnetic Nanoferrites and Their Composites as Alternatives in Waste Water Treatment: Synthesis, Modifications and Applications. *Environ. Sci. Water Res. Technol.* **2020**, *6* (3), 491–514. https://doi.org/10.1039/c9ew00858f.

(19)   Achour, Y.; Bahsis, L.; Ablouh, E. H.; Yazid, H.; Laamari, M. R.; Haddad, M. El. Insight into Adsorption Mechanism of Congo Red Dye onto Bombax Buonopozense Bark Activated-Carbon Using Central Composite Design and DFT Studies. *Surfaces and Interfaces* **2021**, *23* (January), 100977. https://doi.org/10.1016/j.surfin.2021.100977.

(20)   El-Azazy, M.; El-Shafie, A. S.; Issa, A. A.; Al-Sulaiti, M.; Al-Yafie, J.; Shomar, B.; Al-Saad, K. Potato Peels as an Adsorbent for Heavy Metals from Aqueous Solutions: Eco-Structuring of a Green Adsorbent Operating Plackett-Burman Design. *J. Chem.*

2019, *2019* (Ii). https://doi.org/10.1155/2019/4926240.

(21)   Mondal, N. K. Natural Banana (Musa Acuminate) Peel: An Unconventional Adsorbent for Removal of Fluoride from Aqueous Solution through Batch Study. *Water Conserv. Sci. Eng.* **2017**, *1* (4), 223–232. https://doi.org/10.1007/s41101-016-0015-x.

(22)   El-Azazy, M.; Kalla, R. N.; Issa, A. A.; Al-Sulaiti, M.; El-Shafie, A. S.; Shomar, B.; Al-Saad, K. Pomegranate Peels as Versatile Adsorbents for Water Purification: Application of Box–Behnken Design as a Methodological Optimization Approach. *Environ. Prog. Sustain. Energy* **2019**, *38* (6), 1–12. https://doi.org/10.1002/ep.13223.

CHAPTER 2

Literature review

In this study synthesis of magnetic metal ferrites composite with green material for removing dyes, heavy metal ion and fluoride ion from aqueous solution is involved. Therefore, it is quite important to understand the current scenario of work done in this regard already and reported elsewhere. Therefore, in this chapter, detailed literature review related to various adsorbents in general and nano ferrites and their composites in particular are discussed. Apart from the adsorption capabilities, regeneration aspect of these materials has also been discussed as it is quite significant from economic as well as environmental point of view.

2.0 Natural materials as adsorbents (Green adsorbents)

Natural adsorbents are those which are made from natural materials such as plant biomass, agricultural and industrial wastes, natural fibres, animal shells, etc. These are utilised in their raw form as natural adsorbents. Till date many natural materials have been utilised for removing various pollutants from waste water. Some examples of natural adsorbents utilised for removing dyes and heavy metals from water are discussed in this section. In a study conducted for the removal of methylene green 5 (MG5) using orange peel, maximum adsorption capacity for MG5 was found to be 92 mg/g[1].

Potato peel was used to remove Cd^{2+} ions from waste water following lagergren pseudo first order kinetics and Temkin model. Maximum adsorption capacity was found to be 239.64 mg/g[2].

Potential of banana peels was checked for the removal of fluoride ions from waste water at pH 4.0, following pseudo second order kinetics and Bahangam adsorption isotherm. Maximum adsorption capacity for removing fluoride ion using natural banana peel was 1.212 mg/g[3].

Table 2.1 enlists potential of different natural adsorbents for removing dyes and heavy metal ions from waste water.

Table 2.1- Adsorption behavior of natural adsorbents

Sr. no.	Adsorbent	Adsorbate	Max. adsorption capacity(mg/g)/ % removal efficiency	Optimu pH	Optimum temp.(°C)	Best fit isotherm model	Best fit kinetic model	Ref.
1.	Pomegranate peel	Ni^{2+}	99.99%	----	----	----	Pseudo second order	[4]
2.	Rice husk	Methylene blue	24.48	----	----	Langmuir	Pseudo second order	[5]
		Crystal violet	25.46				Pseudo first order	
3.	Green horse chest nut shell	Cu^{2+}	95-97%	5.0	---	---	Pseudo second order	[6]

Sr. no.	Adsorbent	Adsorbate	Max. adsorption capacity(mg/g)/ % removal efficiency	Optimu pH	Optimum temp.(°C)	Best fit isotherm model	Best fit kinetic model	Ref.
4.	Chitosan	Malachite green (MG)	166	-----	----	-----	Pseudo second order	7
		Reactive red (RR)	1250					
		Direct yellow(DY)	250					
5.	Almond gum	Malachite green (MG)	196.07	----	35	Langmuir and Freundlich	Pseudo second order	8

2.1 Use of Nano materials as adsorbents

Nano materials as adsorbents have gained importance in waste water remediation field from last two decades. Nano materials include carbon based nano materials, metal oxide nano particles, nano ferrites etc. They possess unique properties like high adsorption capacity and large surface area. These unique properties of nano materialsmake them suitable for removing pollutants from waste water[9]. Nano materials have applications in various fields like space science, environmental science, bioengineering andmedical science[10]. Wadhawan et.al.[11] focussed on the utilisation of nano materials inremoval of heavy metal ions from waste water. Cai et. al.[12] reviewed nano materials utilised for removing organic dyes from water. Among all nano materials, nano ferrites are important in removal of contaminants from waste water[13].

2.1.1 Carbon based Nano materials and their modified forms in removal of pollutants from waste water

Carbon based nano materials have great attraction of researchers for waste water treatment. Physiochemical properties of nano materials are responsible for removing various pollutants from water[14]. They possess unique properties like capability for the removal of pollutants i.e. dyes and heavy metals from water at low concentration, small size and high surface area. Their adsorption capacities can be enhanced by modification with polymers. Their regeneration and reusability makes them suitable for the removal of pollutants.

Carbon based nano materials include: carbon nano tubes (CNTs), multi-walled carbon nano tubes (MWCNTs), Graphene, Graphene oxide and their modified forms. They possess properties like large surface area, nano size, different functionalities and are recyclable. Carbon Nano tubes have cylindrical shape and are used in air and water filters,electronics, semiconductors, field emission, energy storage, and in biomedical applications.In addition, carbon nano tubes can be functionalized with organic molecules to enhance their adsorption capacities and make them specific in nature. CNTs were synthesized frompetrochemical waste oil and utilised in the systematic removal of both cationic and anionicdyes from waste water. Maximum adsorption capacities for removing Methylene blue (MB) and Methyl orange (MO) using CNT were 84.44 and 85.04 mg/g, respectively. The dyes uptake by CNT followed Langmuir adsorption isotherm model and Pseudo second order kinetics[15].

Carbon nano tubes which have multiple rolled layers of graphene are named as multi-walled carbon nano tubes (MWCNTs). These possess properties like large surface area, high electrical and thermal conductivity. For the removal of Methylene blue (MB) multi walled carbon nanotubes were used and maximum adsorption capacity for MB was found to be 440 mg/g[16].

Graphene based nano adsorbents and their composites are excellent adsorbents for sequestration of organic and inorganic impurities from water. They have size in nano scale dimensions, possess large surface area and are capable of making hydrogen bonds.

In a study conducted on tourmaline/graphene oxide composite used for removing methylene blue dye and Hg (II) ions from water, the maximum adsorption capacities were found to be 454 and 294 mg/g, respectively. The adsorption followed Langmuir isotherm model, pseudo second order kinetics and gave good reusability in removing methylene blue dye and Hg (II) ion for 6 cycles[17].

Table 2.2 depicts carbon based nano materials and their modified forms in removal of pollutants from water.

2.1.2 Metal oxide Nano materials and their composites for the removal of pollutants from waste water

Numerous studies have been conducted by researchers to demonstrate the role of metal oxide nano particles as adsorbents in removing pollutants from waste water. Because of low solubility, mechanical structure and thermal stability, metal oxides are excellent adsorbents for removing dyes and heavy metals from waste water. The limitation in the use of metal oxides in waste water treatment was their tendency to aggregate. So, modification is needed to control dispersion and aggregation of these Nano particles. The modified metal oxide Nano particles have less surface energy and are thermodynamically stable[18].Table 2.3 depicts the adsorption capacities, pH, temperature, applicable kinetic model and adsorption isotherm of metal oxide and their composites for removal of dyes, heavy metals and fluoride ions from waste water.

Table 2.2- Carbon nano tubes (CNTs) and their modified forms for the removal of pollutants from water

Sr. no.	Adsorbate	Adsorbent	Percentage (%) removal/ adsorption capacity (in mg/g)	pH	Best fit adsorption isotherm	Best fit Kinetic model	Ref.
			Carbon nano tubes				
1.	Reactive yellow15 Reactive yellow 42	CNT	36.04 48.1	3	Langmuir and Freundlich	Pseudo second order	[19]
2.	Pb^{2+}	CNT	17.44	7.0	Freundlich	------	[20]
			Modified carbon nano materials				
3.	Ni^{2+}	MWCNT functionalized by DES	115.8	7.2	-----	Pseudo second order	[21]
4.	Cu^{2+}	Chitosan/Poly(vinyl) alcohol modified amino fuctionalised MWCNT	11.1	---	Freundlich	-------	[22]

Sr. no.	Adsorbate	Adsorbent	Percentage (%) removal/ adsorption capacity (in mg/g)	pH	Best fit adsorption isotherm	Best fit Kinetic model	Ref.
5.	Cd^{2+}	Humic acid modified MWCNTs	18.4	----	Langmuir	-------	[23]
6.	Cu^{2+}	CNTs/Calcium alginate Composites	339	2.1	Langmuir	Pseudo second order	[24]
7.	Pb^{2+}	Oxidised MWCNTs	17	7.0	Freundlich	Pseudo second order	[25]
8.	Acid blue 45 Acid black 1	CNT-NH_2	714 666	---	Langmuir	Pseudo second order	[26]
9.	Rhodamine B	Grapheme oxide-CNT	41.5	---	Langmuir	Pseudo second order	[27]
10.	Fluoride ion	Hydroxyapatite- MWCNT	97.15%	---	Langmuir and Freundlich	Pseudo second order	[28]

2.1.3 Role of magnetic nano ferrites for removal of pollutants from waste water

The following properties of nano ferrites are responsible for their excellent performance in waste water treatment [13]:

1. Nano ferrites have size in the range 1-100 nm. Thus, they provide large surface areafor the adsorption of pollutants from waste water.
2. Nano ferrites have tendency to change the oxidation states of hazardous pollutants from higher to lower.
3. The nano ferrites can be easily separated from solution after their use.
4. The surface of nano ferrites is highly reactive and can be easily modified according to the requirement of adsorbent.
5. Nano ferrites are cost effective in nature and they can be regenerated.

The aforementioned properties of nano ferrites make them superior over other commercial adsorbents. Spinel nano ferrites have been widely utilised for the removal of pollutants i.e. dyes, heavymetals and fluoride ions from waste water, due to their high efficiency. Researchers haveemployed magnetic nano ferrites for the removal of pollutants from waste water[29]. Nanoferrites and their composites, among other nanomaterials, are currently receiving a lot of attention in wastewater treatment. Among these spinel ferrites are most popular choice.Spinel ferrites have general formula MFe_2O_4 where M depicts metal ion which might be Mn, Co, Ni or Zn.

$ZnFe_2O_4$ nanospheres were utilised in removing Congo red dye at 25°C and at optimum pH 6, the maximum adsorption capacity was found to be 16.5mg/g[30].

2.1.4 Need for the modification of magnetic spinel ferrites

Spinel nano ferrites have a high surface-to-volume ratio but upon exposing the pure metal particles like iron, cobalt and nickel, their stability becomes an important aspect. So, modification is required to increase their stability. Coating of magnetic spinel ferrites is one of the option. This may include surfactant or polymer coating, doping with various metals and their oxides to increase the stability of magnetic spinel ferrites. Coating/doping protects the core shell and also adds functional groups for specific removal of pollutant in wastewater treatment. Thus, there is need of modification of magnetic spinel ferrites[31].

Table 2.3 –Adsorption behavior of metal oxide nano particles in removal of pollutants from waste water

Sr.No.	Adsorbent	Adsorbate	Adsorption capacity (in mg/g)	Optimum pH	Temp. (in°C)	Best Fit Kinetic model	Best Fit Isotherm	Ref.
Metal oxide Nano particles in removal of pollutants from water								
1. [32]	α-Fe$_2$O$_3$	Methyl orange	0.72	7	-----	Pseudo second order	Langmuir	[32]
2. [33]	Fe$_2$O$_3$	Acridine orange	59	4	----	Pseudo second order	Freundlich	[33]
Composites of metal oxide nano particles in removal of pollutants from water								
3.	ACSO/Fe$_3$O$_4$	Methylene blue	60.60	7	---	Pseudo second order	Freundlich	[34]
		Methyl violet	59.88					
4.	Rice bran/SnO$_2$/ Fe$_3$O$_4$	Reactive blue 4	218.82	2.9	333	Pseudo second order	Langmuir	[35]
		Crystal violet	159.24					

Sr.No.	Adsorbent	Adsorbate	Adsorption capacity (in mg/g)	Optimum pH	Temp. (in °C)	Best Fit Kinetic model	Best Fit Isotherm	Ref.
5.	$Fe_3O_4@SiO_2/P(AM\text{-}AMPS)$	Crystal violet	2106.37	----	298.15	Pseudo second order	Langmuir	[36]
		Methylene blue	1462.34					
6.	$Hap/Fe_3O_4/PDA$	Ni^{2+}	48.09	6	----	Weber Morris intaparticle diffusion model	Langmuir and Freundlich	[37]
7.	$\beta CD@Fe_3O_4/MWCNT$	Ni^{2+}	103	---	----	Pseudo second order	Langmuir	[38]
8.	$Fe_3O_4/Al(OH)_3$	Fluoride ion	6.67	---	----	Pseudo second order	Freundlich	[39]
9.	$Fe_3O_4@LDH/poly$	Fluoride ion	167.62	---	----	Pseudo second order	Freundlich	[40]
10.	PPy/Fe_3O_4	Fluoride ion	78.2%	6	---	Pseudo second order	Freundlich and Temkin	[41]

2.1.5 Doping with metals and their oxides

Doping is a technique which incorporates substitutional ions into the crystalline structure of materials to generate exciting properties. With the increase in concentration of doping agent, structure and size of magnetic spinel ferrites is affected. This can be explained with ion exchange mechanism. The active sites of spinel ferrites increases because there is a difference in the atomic size of doping agents and parent metal ions. The oxidation state of pollutants is reduced from high to low due to the free electrons present on the crystal lattice surface. This helps in easy adsorption of pollutants on the surface of magnetic spinel ferrites[42].

Aluminium doped nano manganese copper ferrite was used as an adsorbent for the removal of arsenic from aqueous solution. The maximum adsorption capacity of arsenic was found to be 0.053 mg/g[43].

2.1.6 Surfactant coating

In surfactant coating single or multiple long chain layers of compounds is formed onto the surface of magnetic spinel nano ferrites. As a result, the sites on the surface of spinel ferrites becomes active for adsorption of pollutants like dyes and heavy metals. Some examples of the surfactants used are sodium dodecyl sulphate (SDS), cetyltrimethylammonium bromide (CTAB) etc.[44].

Nickel ferrite nanoparticles modified with sodium dodecyl sulphate were utilised in removing Basic blue 41, Basic green 4, and Basic red 18 from waste water and maximum adsorption capacities were found to be 0.50 mg/g, 0.41 mg/g and 0.25 mg/g respectively using pure nickel ferrite and 111 mg/g, 17 mg/g and 44 mg/g respectively using nickel ferrite- SDS composite[45].

2.1.7 Polymer Coating

Various polymers like polyvinyl alcohol (PVA), poly aniline (PANI), chitosan and alginate have been used for the modification of surface of magnetic spinel ferrites[22]. Coating increases the stability of spinel nano ferrites and prevent their oxidation and degradation[46]. Additionally it also provide certain functional groups on the surface of the adsorbent which impart specificity towards particular type of pollutant. Magnetic Zinc ferrite-alginic composite was synthesised and used to remove Congo red (CR), Crystal violet (CV) and Brilliant green (BG) dyes with adsorption capacities of 103.2, 123.5 and 99.9 mg/g

respectively[47]. Table 2.4 depicts some examples of magnetic Nano ferrites and their composites in removing various pollutants from waste water.

2.2 Regeneration of adsorbents

Regeneration of adsorbents is an important aspect to study. Advantages of regeneration are as follows-

(i)   Regeneration reduces the need of new adsorbent.

(ii)   The problem of disposal of used adsorbent is solved by regeneration.

(iii)   Economical benefits.

In regeneration process, various desorbing agents are used to regenerate the adsorbent used after saturation. This regenerated adsorbent is again utilised to check the efficiency of adsorbent for various cycles. The desorbing agents renew the active sites of the saturated adsorbents.

For the regeneration of $CoFe_2O_4$ reported in the adsorption of Titan yellow dye, 0.1 M NaCl:acetone (2:1) was utilised as desorbing agent and regeneration efficiency of $CoFe_2O_4$ was found to be 90% after three regeneration cycles[48].

In another report, $ZnFe_2O_4$/alginic was utilised for the removal of Congo red (CR), Crystal violet (CV) and Brilliant green (BG) dyes from water. 0.1 M HCl was utilised as desorbing agent and after seven cycles regeneration efficiencies for Congo red (CR), Crystal violet (CV)and Brilliant green (BG) dyes was found to be 91.8, 92.3 and 90.3 respectively[47].

Table 2.5 depicts information about the regeneration capacity of various adsorbents.

Table 2.4- Adsorption behavior of different magnetic nano ferrites and their composites for the removal of dyes and heavy metal ions from waste water

Sr. No	Adsorbent	Adsorbate	Adsorption Capacity (in mg/g)/ % removal	pH	Temp. (in ºC)	BestFit Kinetic Model	Best fit Adsorption isotherm	Ref.
			Pure ferrites in removal of pollutants from water					
1.	$CuFe_2O_4$	Cd(II)	13.9	6	---	Pseudo second order	Langmuir	[49]
2.	$BiFeO_3$	RhodamineB	64.2	---	---	Pseudo first order	Langmuir	[50]
3.	$CoFe_2O_4$	Titan yellow Congo red	212.8 200.0	3	---	Pseudo second order	Langmuir	[48]
			Metal oxide doped spinel ferrites in removal of pollutants from water					
4.	$Mn_xCu_{1-x}Fe_2O_4$	As(III)	25.5	---	----	Pseudo second order	Freundlich	[43]

Sr. No	Adsorbent	Adsorbate	Adsorption Capacity (in mg/g)/ % removal	pH	Temp. (in °C)	BestFit Kinetic Model	Best fit Adsorption isotherm	Ref.
5.	NiFe$_2$O$_4$-graphene oxide	Pb(II)	121.9	---	----	-----	Langmuir	[51]
		Cr(III)	126.5					
6.	MnFe$_2$O$_4$-graphene oxide	Ni^{2+}	152.67	---	----	Pseudo second order	Langmuir	[52]
		Methylene blue	89.29					
7.	Ni$_x$Zn$_{1-x}$Fe$_2$O$_4$	Cr(VI)	48.5	---	-----	Pseudo second order	Langmuir	[53]
		Mo(VI)	38.8					
		V(V)	28.0					
8.	CuFe$_2$O$_4$-CeO$_2$	Pb(II)	972.4	---	----	Pseudo second order	Langmuir	[54]
		Ni(II)	686.1					
		V(V)	798.6					
Surfactant coated spinel ferrites in removal of pollutants from water								
9.	ZnFe$_2$O$_4$/SDS	Basic Blue41	42.0	---	----	Pseudo second order	Langmuir	[55]
		Basic Red18	61.0					

Sr. No	Adsorbent	Adsorbate	Adsorption Capacity (in mg/g)/ % removal	pH	Temp. (in^{o}C)	BestFit Kinetic Model	Best fit Adsorption isotherm	Ref.
10.	Fe$_3$O$_4$/CTAB	Nyloset yellow	136.0	---	----	----	Langmuir	[56]
11.	CoFe$_2$O$_4$/SDS	Crystal violet	105.0	---	----	Pseudo second order	Elovich	[57]
12.	NiFe$_2$O$_4$/PANI	Malachite green	4.09	7	----	Pseudo second order	Langmuir	[58]
13.	ZnFe$_2$O$_4$/CTAB	Direct red23 Direct red31	26.1 55.6	---	----	Pseudo second order	Langmuir	[59]
14.	NiFe$_2$O$_4$/CTAB	Brilliant green	250	6	----	Pseudo second order	Langmuir	[44]

Polymer coated spinel ferrites in removal of pollutants from water

Sr. No	Adsorbent	Adsorbate	Adsorption Capacity (in mg/g)/ % removal	pH	Temp. (in ^{o}C)	BestFit Kinetic Model	Best fit Adsorption isotherm	Ref.
15.	$ZnFe_2O_4$/ alginic	Congo red Crystalviolet	103.2 123.5	----	----	Pseudo second order	Langmuir	46
16.	$ZnFe_2O_4$ /chitosan NiFe$_2$O$_4$/ chitosan CoFe$_2$O$_4$/ chitosan	Fluoride ion	6.9 8.3 6.7	----	----	Pseudo second order	Freundlich	60

Table 2.5-Regeneration of various adsorbents

Sr. no.	Adsorbents	Target pollutant(s)	1st cycle efficiency	Maximum cycle and efficiency	Medium of regeneration	Ref.
1.	$SiO_2@Fe_2O_3$	Ni^{2+}	94-95%	6 cycles, 25%	0.1M HCl	[61]
2.	$ZnFe_2O_4$-Alginic	Pb^{2+}	100%	5 cycles, 95.5%	0.1N HCl	[62]
		Cu^{2+}	99.2%	5 cycles, 92%		
3.	Poly(1-vinyl-imidazole)/Fe_3O_4 /SiO_2	Hg^{2+}	>96%	5 cycles, >94%	0.5M HCl	[63]
4.	Poly(acrylamide)/ Bentonite	Methylene blue, Crystal violet	99%	4 cycles, 90%	0.1M HNO_3	[64]
5.	$ZnFe_2O_4$/chitosan	Crystal violet	98.5	5 cycles, 89.5%	0.1N HCl	[65]
		Brilliant green	99.0	5 cycles, 91.7%		
6.	Poly(ethyleneoxide)/Poly(L-lactide)/oleic acid-coated Fe_3O_4	Malachite green	40%	3 cycles, 40%	Ethanol	[66]

Sr. no.	Adsorbents	Target pollutant(s)	1st cycle efficiency	Maximum cycle and efficiency	Medium of regeneration	Ref.
7.	MOF-801 (Zirconium-metal organic framework)	Fluoride ion	91.81	4 cycles, 78.90	0.1M NaOH	[67]
8.	$MnFe_2O_4$/graphene	Pb(II)	100.0	3 cycles, 98.0	0.1M HCl	[68]
9.	β-CD@Fe_2O_3/MWCNT	Ni (II)	100.0	5 cycles, 85	Na_2EDTA	[38]
10.	Rice bran/SnO_2/Fe_3O_4	CV	100.0	5 cycles, 90	0.1M NaOH	[35]
11.	CTAB-$NiFe_2O_4$ (cetyl tri methyl ammoniumbromide-nickel ferrite)	Brilliant green	100.0	5 cycles, 91.4	0.1N HCl	[44]
12.	NiFCMC	Ni (II)	100.0	6 cycles, 81.3	0.1N HCl	[69]
13.	NiFCMC-Alg	Ni (II)	100.0	6 cycles, 77.2	0.1 N HCl	[69]

2.3 Research gap:

A. From the review of the literature, it has been observed that little work has been reported onmagnetic spinel ferrite-carboxy methyl starch (CMS) composite for removal of dyes andheavy metals from water.

B. Also, it has been observed that negligible work has been done on magnetic spinel ferrite-starch composite for removing pollutants from water in which starch used has been extracted from mango seeds.

C. From the literature study, it has also been found that negligible work has been reportedon spinel ferrite-rice husk silica (RHS) composite for the removal of dyes and heavy metal ions from water.

Therefore, there is scope of development of magnetic green adsorbents by combining green materials (like rice husk silica, carboxy methyl starch and mango starch) with magnetic spinel ferrite nanoparticles. Magnetic spinel ferrites and their composites have greatadvantages in removing pollutants like dyes and heavy metals from waste water. The advantage of making these adsorbents owes to their removal from water, after adsorption, by using magnets.

2.4 RESEARCH OBJECTIVES

1. To extract starch from mango seed and silica from rice husk (RHS) and synthesis of carboxymethylstarch (CMS) from starch obtained from mango seed.

2. To develop bio-waste (Starch, RHS, CMS) based magnetic ferrite composites and their characterization.

3. To analyse the potential of synthesized adsorbents in removal of pollutants (dyes, heavy metal ions and fluoride ions) on parameters viz. contact time, pH, temperature, initial concentration and adsorbent dose.

4. To analyse adsorption behavior of dyes in single and multiple system and for heavy metal,fluoride ions in single system.

5. To regenerate above adsorbents and to reuse the adsorbents.

References

(1)   Tran, H. N.; You, S. J.; Nguyen, T. V.; Chao, H. P. Insight into the Adsorption Mechanism of Cationic Dye onto Biosorbents Derived from Agricultural Wastes. *Chem. Eng. Commun.* **2017**, *204* (9), 1020–1036. https://doi.org/10.1080/00986445.2017.1336090.

(2)   El-Azazy, M.; El-Shafie, A. S.; Issa, A. A.; Al-Sulaiti, M.; Al-Yafie, J.; Shomar, B.; Al-Saad, K. Potato Peels as an Adsorbent for Heavy Metals from Aqueous Solutions: Eco-Structuring of a Green Adsorbent Operating Plackett-Burman Design. *J. Chem.* **2019**, *2019* (Ii). https://doi.org/10.1155/2019/4926240.

(3)   Mondal, N. K. Natural Banana (Musa Acuminate) Peel: An Unconventional Adsorbent for Removal of Fluoride from Aqueous Solution through Batch Study. *Water Conserv. Sci. Eng.* **2017**, *1* (4), 223–232. https://doi.org/10.1007/s41101-016-0015-x.

(4)   El-Azazy, M.; Kalla, R. N.; Issa, A. A.; Al-Sulaiti, M.; El-Shafie, A. S.; Shomar, B.; Al-Saad, K. Pomegranate Peels as Versatile Adsorbents for Water Purification: Application of Box–Behnken Design as a Methodological Optimization Approach. *Environ. Prog. Sustain. Energy* **2019**, *38* (6), 1–12. https://doi.org/10.1002/ep.13223.

(5)   Quansah, J. O.; Hlaing, T.; Lyonga, F. N.; Kyi, P. P.; Hong, S. H.; Lee, C. G.; Park, S. J. Nascent Rice Husk as an Adsorbent for Removing Cationic Dyes from Textile Wastewater. *Appl. Sci.* **2020**, *10* (10). https://doi.org/10.3390/app10103437.

(6)   Parus, A. Copper(II) Ions' Removal from Aqueous Solution Using Green Horse-Chestnut Shell as a Low-Cost Adsorbent. *Chem. Ecol.* **2018**, *34* (1), 56–69. https://doi.org/10.1080/02757540.2017.1396452.

(7)   S.E., S.; Thinakaran, N. Isotherm, Kinetic and Thermodynamic Studies on the Adsorption Behaviour of Textile Dyes onto Chitosan. *Process Saf. Environ. Prot.* **2017**, *106*, 1–10. https://doi.org/10.1016/j.psep.2016.11.024.

(8)   Bouaziz, F.; Koubaa, M.; Kallel, F.; Ghorbel, R. E.; Chaabouni, S. E. Adsorptive Removal of Malachite Green from Aqueous Solutions by Almond Gum: Kinetic Study and Equilibrium Isotherms. *Int. J. Biol. Macromol.* **2017**, *105*, 56–65.

https://doi.org/10.1016/j.ijbiomac.2017.06.106.

(9)   Kumari, P.; Alam, M.; Siddiqi, W. A. Usage of Nanoparticles as Adsorbents for Waste Water Treatment: An Emerging Trend. *Sustain. Mater. Technol.* **2019**, *22*, e00128. https://doi.org/10.1016/j.susmat.2019.e00128.

(10)   Gautam, P. K.; Singh, A.; Misra, K.; Sahoo, A. K.; Samanta, S. K. Synthesis and Applications of Biogenic Nanomaterials in Drinking and Wastewater Treatment. *J. Environ. Manage.* **2019**, *231* (June 2018), 734–748. https://doi.org/10.1016/j.jenvman.2018.10.104.

(11)   Wadhawan, S.; Jain, A.; Nayyar, J.; Mehta, S. K. Role of Nanomaterials as Adsorbents in Heavy Metal Ion Removal from Waste Water: A Review. *J. Water Process Eng.* **2020**, *33* (October 2019), 101038. https://doi.org/10.1016/j.jwpe.2019.101038.

(12)   Cai, Z.; Sun, Y.; Liu, W.; Pan, F.; Sun, P.; Fu, J. An Overview of Nanomaterials Applied for Removing Dyes from Wastewater. *Environ. Sci. Pollut. Res.* **2017**, *24* (19), 15882–15904. https://doi.org/10.1007/s11356-017-9003-8.

(13)   Asha, A. B.; Narain, R. *Nanomaterials Properties*; Elsevier Inc., 2020. https://doi.org/10.1016/B978-0-12-816806-6.00015-7.

(14)   Lu, H.; Wang, J.; Stoller, M.; Wang, T.; Bao, Y.; Hao, H. An Overview of Nanomaterials for Water and Wastewater Treatment. *Adv. Mater. Sci. Eng.* **2016**, *2016*, 4964828. https://doi.org/10.1155/2016/4964828.

(15)   Amon, R. E. C.; Lawagon, C. P. Efficient Removal of Cationic and Anionic Dyes from Wastewater Using Carbon Nanotubes from Petrochemical Waste Oil. *Chem. Eng. Trans.* **2021**, *86*, 349–354. https://doi.org/10.3303/CET2186059.

(16)   Saxena, M.; Sharma, N.; Saxena, R. Highly Efficient and Rapid Removal of a Toxic Dye: Adsorption Kinetics, Isotherm, and Mechanism Studies on Functionalized Multiwalled Carbon Nanotubes. *Surfaces and Interfaces* **2020**, *21* (June), 100639. https://doi.org/10.1016/j.surfin.2020.100639.

(17)   Xue, G.; Luo, X.; Srinivasakannan, C.; Zheng, L.; Miao, Y.; Duan, X. Effective

Removal of Organic Dye and Heavy Metal from Wastewater by Tourmaline/Graphene Oxide Composite Nano Material. *Mater. Res. Express* **2019**, *6* (11), 115618. https://doi.org/10.1088/2053-1591/ab4d22.

(18)   Ahangaran, F.; Navarchian, A. H. Recent Advances in Chemical Surface Modification of Metal Oxide Nanoparticles with Silane Coupling Agents: A Review. *Adv. Colloid Interface Sci.* **2020**, *286*, 102298. https://doi.org/10.1016/j.cis.2020.102298.

(19)   Naghizadeh, A.; Karimi, A.; Derakhshani, E.; Esform, A. Single-Walled Carbon Nanotubes (SWCNTs) as an Efficient Adsorbent for Removal of Reactive Dyes from Water Solution: Equilibrium, Kinetic, and Thermodynamic. *Environ. Qual. Manag.* **2022**, *31* (4), 133–140. https://doi.org/10.1002/tqem.21753.

(20)   Burakov, A. E.; Galunin, E. V.; Burakova, I. V.; Kucherova, A. E.; Agarwal, S.; Tkachev, A. G.; Gupta, V. K. Adsorption of Heavy Metals on Conventional and Nanostructured Materials for Wastewater Treatment Purposes: A Review. *Ecotoxicol. Environ. Saf.* **2018**, *148* (August 2017), 702–712. https://doi.org/10.1016/j.ecoenv.2017.11.034.

(21)   Rahmati, N.; Rahimnejad, M.; Pourali, M.; Muallah, S. K. Effective Removal of Nickel Ions from Aqueous Solution Using Multi-Wall Carbon Nanotube Functionalized by Glycerol-Based Deep Eutectic Solvent. *Colloids Interface Sci. Commun.* **2021**, *40* (December 2020), 100347. https://doi.org/10.1016/j.colcom.2020.100347.

(22)   Mahmoodi, N. M.; Mokhtari-Shourijeh, Z. Preparation of PVA-Chitosan Blend Nanofiber and Its Dye Removal Ability from Colored Wastewater. *Fibers Polym.* **2015**, *16* (9), 1861–1869. https://doi.org/10.1007/s12221-015-5371-1.

(23)   Tian, X.; Yang, K.; Xu, Y.; Lu, H.; Lin, D. Effect of Humic Acids on the Physicochemical Property and Cd(II) Sorption of Multiwalled Carbon Nanotubes. *Funct. Nat. Org. Matter Chang. Environ.* **2013**, *9789400756* (11), 751–755. https://doi.org/10.1007/978-94-007-5634-2_136.

(24)   Lagoa, R.; Rodrigues, J. R. Evaluation of Dry Protonated Calcium Alginate Beads for

Biosorption Applications and Studies of Lead Uptake. *Appl. Biochem. Biotechnol.* **2007**, *143* (2), 115–128. https://doi.org/10.1007/s12010-007-0041-4.

(25)   Xu, D.; Tan, X.; Chen, C.; Wang, X. Removal of Pb(II) from Aqueous Solution by Oxidized Multiwalled Carbon Nanotubes. *J. Hazard. Mater.* **2008**, *154* (1–3), 407–416. https://doi.org/10.1016/j.jhazmat.2007.10.059.

(26)   Maleki, A.; Hamesadeghi, U.; Daraei, H.; Hayati, B.; Najafi, F.; McKay, G.; Rezaee, R. Amine Functionalized Multi-Walled Carbon Nanotubes: Single and Binary Systems for High Capacity Dye Removal. *Chem. Eng. J.* **2017**, *313*, 826–835. https://doi.org/10.1016/j.cej.2016.10.058.

(27)   Hu, C.; Le, A. T.; Pung, S. Y.; Stevens, L.; Neate, N.; Hou, X.; Grant, D.; Xu, F. Efficient Dye-Removal via Ni-Decorated Graphene Oxide-Carbon Nanotube Nanocomposites. *Mater. Chem. Phys.* **2021**, *260* (December 2020), 124117. https://doi.org/10.1016/j.matchemphys.2020.124117.

(28)   Ruan, Z.; Tian, Y.; Ruan, J.; Cui, G.; Iqbal, K.; Iqbal, A.; Ye, H.; Yang, Z.; Yan, S. Synthesis of Hydroxyapatite/Multi-Walled Carbon Nanotubes for the Removal of Fluoride Ions from Solution. *Appl. Surf. Sci.* **2017**, *412*, 578–590. https://doi.org/10.1016/j.apsusc.2017.03.215.

(29)   Kharissova, O. V.; Dias, H. V. R.; Kharisov, B. I. Magnetic Adsorbents Based on Micro- and Nano-Structured Materials. *RSC Adv.* **2015**, *5* (9), 6695–6719. https://doi.org/10.1039/c4ra11423j.

(30)   Etemadinia, T.; Barikbin, B.; Allahresani, A. Removal of Congo Red Dye from Aqueous Solutions Using Znfe2o4/Sio2/Tragacanth Gum Magnetic Nanocomposite as a Novel Adsorbent. *Surfaces and Interfaces* **2019**, *14*, 117–126. https://doi.org/10.1016/j.surfin.2018.10.010.

(31)   Singh, S.; Singhal, S. Transition Metal Doped Cobalt Ferrite Nanoparticles: Efficient Photocatalyst for Photodegradation of Textile Dye. *Mater. Today Proc.* **2019**, *14*, 453–460. https://doi.org/10.1016/j.matpr.2019.04.168.

(32)   Dehno Khalaji, A.; Machek, P.; Jarosova, M. α-Fe2O3 Nanoparticles: Synthesis,

Characterization, Magnetic Properties and Photocatalytic Degradation of Methyl Orange. *Adv. J. Chem. A* **2021**, *4* (4), 317–326. https://doi.org/10.22034/AJCA.2021.292396.1268.

(33) Qadri, S.; Ganoe, A.; Haik, Y. Removal and Recovery of Acridine Orange from Solutions by Use of Magnetic Nanoparticles. *J. Hazard. Mater.* **2009**, *169*, 318–323. https://doi.org/10.1016/j.jhazmat.2009.03.103.

(34) Foroutan, R.; Mohammadi, R.; Razeghi, J.; Ramavandi, B. Performance of Algal Activated Carbon/Fe 3 O 4 Magnetic Composite for Cationic Dyes Removal from Aqueous Solutions. *Algal Res.* **2019**, *40* (January), 101509. https://doi.org/10.1016/j.algal.2019.101509.

(35) Ma, C. M.; Hong, G. B.; Wang, Y. K. Performance Evaluation and Optimization of Dyes Removal Using Rice Bran-Based Magnetic Composite Adsorbent. *Materials (Basel).* **2020**, *13* (12), 1–18. https://doi.org/10.3390/ma13122764.

(36) Zheng, X.; Zheng, H.; Zhao, R.; Xiong, Z.; Wang, Y.; Sun, Y.; Ding, W. Sulfonic Acid-Modified Polyacrylamide Magnetic Composite with Wide PH Applicability for Efficient Removal of Cationic Dyes. *J. Mol. Liq.* **2020**, *319*, 114161. https://doi.org/10.1016/j.molliq.2020.114161.

(37) Foroutan, R.; Peighambardoust, S. J.; Ahmadi, A.; Akbari, A.; Farjadfard, S.; Ramavandi, B. Adsorption Mercury, Cobalt, and Nickel with a Reclaimable and Magnetic Composite of Hydroxyapatite/Fe3O4/Polydopamine. *J. Environ. Chem. Eng.* **2021**, *9* (4), 105709. https://doi.org/10.1016/j.jece.2021.105709.

(38) Lin, S.; Zou, C.; Liang, H.; Peng, H.; Liao, Y. The Effective Removal of Nickel Ions from Aqueous Solution onto Magnetic Multi-Walled Carbon Nanotubes Modified by β-Cyclodextrin. *Colloids Surfaces A Physicochem. Eng. Asp.* **2021**, *619* (8), 126544. https://doi.org/10.1016/j.colsurfa.2021.126544.

(39) Girma, M.; Zewge, F.; Chandravanshi, B. S. Fluoride Removal from Water Using Magnetic Iron Oxide / Aluminium Hydroxide Composite. *SINET Ethiop. J. Sci.* **2020**, *43* (1), 32–45.

(40)   Ammavasi, N.; Mariappan, R. Enhanced Removal of Hazardous Fluoride from Drinking Water by Using a Smart Material: Magnetic Iron Oxide Fabricated Layered Double Hydroxide/Cellulose Composite. *J. Environ. Chem. Eng.* **2018**, *6* (4), 5645–5654. https://doi.org/10.1016/j.jece.2018.08.071.

(41)   Aigbe, U. O.; Onyancha, R. B.; Ukhurebor, K. E.; Obodo, K. O. Removal of Fluoride Ions Using a Polypyrrole Magnetic Nanocomposite Influenced by a Rotating Magnetic Field. *RSC Adv.* **2019**, *10* (1), 595–609. https://doi.org/10.1039/c9ra07379e.

(42)   Abbas, N.; Rubab, N.; Sadiq, N.; Manzoor, S.; Khan, M. I.; Garcia, J. F.; Aragao, I. B.; Tariq, M.; Akhtar, Z.; Yasmin, G. Aluminum-Doped Cobalt Ferrite as an Efficient Photocatalyst for the Abatement of Methylene Blue. *Water (Switzerland)* **2020**, *12* (8). https://doi.org/10.3390/w12082285.

(43)   Malana, M. A.; Qureshi, R. B.; Ashiq, M. N. Adsorption Studies of Arsenic on Nano Aluminium Doped Manganese Copper Ferrite Polymer (MA, VA, AA) Composite: Kinetics and Mechanism. *Chem. Eng. J.* **2011**, *172* (2–3), 721–727. https://doi.org/10.1016/j.cej.2011.06.041.

(44)   Jasrotia, R.; Singh, J.; Mittal, S.; Singh, H. Synthesis of CTAB Modified Ferrite Composite for the Efficient Removal of Brilliant Green Dye. *Int. J. Environ. Anal. Chem.* **2022**, *0* (0), 1–17. https://doi.org/10.1080/03067319.2022.2098485.

(45)   Mahmoodi, N. M. Nickel Ferrite Nanoparticle: Synthesis, Modification by Surfactant and Dye Removal Ability. *Water. Air. Soil Pollut.* **2013**, *224* (2). https://doi.org/10.1007/s11270-012-1419-7.

(46)   Kumar, M.; Dosanjh, H. S.; Singh, H. Magnetic Zinc Ferrite–Alginic Biopolymer Composite: As an Alternative Adsorbent for the Removal of Dyes in Single and Ternary Dye System. *J. Inorg. Organomet. Polym. Mater.* **2018**, *0* (0), 1–18. https://doi.org/10.1007/s10904-018-0839-2.

(47)   Kumar, M.; Dosanjh, H. S.; Singh, H. Magnetic Zinc Ferrite–Alginic Biopolymer Composite: As an Alternative Adsorbent for the Removal of Dyes in Single and Ternary Dye System. *J. Inorg. Organomet. Polym. Mater.* **2018**, *28* (5), 1688–1705.

https://doi.org/10.1007/s10904-018-0839-2.

(48) Ghaemi, M.; Absalan, G.; Sheikhian, L. Adsorption Characteristics of Titan Yellow and Congo Red on CoFe2O4 Magnetic Nanoparticles. *J. Iran. Chem. Soc.* **2014**, *11* (6), 1759–1766. https://doi.org/10.1007/s13738-014-0448-0.

(49) Tu, Y. J.; You, C. F.; Chang, C. K. Kinetics and Thermodynamics of Adsorption for Cd on Green Manufactured Nano-Particles. *J. Hazard. Mater.* **2012**, *235–236*, 116–122. https://doi.org/10.1016/j.jhazmat.2012.07.030.

(50) Soltani, T.; Entezari, M. H. Sono-Synthesis of Bismuth Ferrite Nanoparticles with High Photocatalytic Activity in Degradation of Rhodamine B under Solar Light Irradiation. *Chem. Eng. J.* **2013**, *223*, 145–154. https://doi.org/10.1016/j.cej.2013.02.124.

(51) Lingamdinne, L. P.; Kim, I. S.; Ha, J. H.; Chang, Y. Y.; Koduru, J. R.; Yang, J. K. Enhanced Adsorption Removal of Pb(II) and Cr(III) by Using Nickel Ferrite-Reduced Graphene Oxide Nanocomposite. *Metals (Basel).* **2017**, *7* (6). https://doi.org/10.3390/met7060225.

(52) Thi Mong Thy, L.; Hoan Kiem, N.; Hoang Tu, T.; Minh Phu, L.; Thi Yen Oanh, D.; Minh Nam, H.; Thanh Phong, M.; Hieu, N. H. Fabrication of Manganese Ferrite/Graphene Oxide Nanocomposites for Removal of Nickel Ions, Methylene Blue from Water. *Chem. Phys.* **2020**, *533* (October 2019), 110700. https://doi.org/10.1016/j.chemphys.2020.110700.

(53) Afkhami, A.; Aghajani, S.; Mohseni, M.; Madrakian, T. Effectiveness of Ni0.5Zn0.5Fe2O4 for the Removal and Preconcentration of Cr(VI), Mo(VI), V(V) and W(VI) Oxyanions from Water and Wastewater Samples. *J. Iran. Chem. Soc.* **2015**, *12* (11), 2007–2013. https://doi.org/10.1007/s13738-015-0675-z.

(54) Talebzadeh, F.; Zandipak, R.; Sobhanardakani, S. CeO2 Nanoparticles Supported on CuFe2O4 Nanofibers as Novel Adsorbent for Removal of Pb(II), Ni(II), and V(V) Ions from Petrochemical Wastewater. *Desalin. Water Treat.* **2016**, *57* (58), 28363–28377. https://doi.org/10.1080/19443994.2016.1188733.

(55) Mahmoodi, N. M. Surface Modification of Magnetic Nanoparticle and Dye Removal from Ternary Systems. *J. Ind. Eng. Chem.* **2015**, *27*, 251–259. https://doi.org/10.1016/j.jiec.2014.12.042.

(56) Dalali, N.; Khoramnezhad, M.; Habibizadeh, M.; Faraji, M. Magnetic Removal of Acidic Dyes from Waste Waters Using Surfactant- Coated Magnetite Nanoparticles : Optimization of Process by Taguchi Method. **2011**, *15* (July 2015), 89–93.

(57) Singh, M.; Dosanjh, H. S.; Singh, H. Surface Modified Spinel Cobalt Ferrite Nanoparticles for Cationic Dye Removal: Kinetics and Thermodynamics Studies. *J. Water Process Eng.* **2016**, *11*, 152–161. https://doi.org/10.1016/j.jwpe.2016.05.006.

(58) Patil, M. R.; Shrivastava, V. S. Adsorption of Malachite Green by Polyaniline–Nickel Ferrite Magnetic Nanocomposite: An Isotherm and Kinetic Study. *Appl. Nanosci.* **2015**, *5* (7), 809–816. https://doi.org/10.1007/s13204-014-0383-5.

(59) Mahmoodi, N. M.; Abdi, J.; Bastani, D. Direct Dyes Removal Using Modified Magnetic Ferrite Nanoparticle. *J. Environ. Heal. Sci. Eng.* **2014**, *12* (1), 1–10. https://doi.org/10.1186/2052-336X-12-96.

(60) Kumar, M.; Dosanjh, H. S.; Singh, H. Biopolymer Modified Transition Metal Spinel Ferrites for Removal of Fluoride Ions from Water. *Environ. Nanotechnology, Monit. Manag.* **2019**, *12* (May 2018), 100237. https://doi.org/10.1016/j.enmm.2019.100237.

(61) Ahmad, I.; Siddiqui, W. A.; Ahmad, T.; Siddiqui, V. U. Synthesis and Characterization of Molecularly Imprinted Ferrite (SiO 2 @Fe 2 O 3) Nanomaterials for the Removal of Nickel (Ni 2+ Ions) from Aqueous Solution. *J. Mater. Res. Technol.* **2019**, *8* (1), 1400–1411. https://doi.org/10.1016/j.jmrt.2018.09.011.

(62) Kumar, M.; Dosanjh, H. S.; Singh, H. Removal of Lead and Copper Metal Ions in Single and Binary Systems Using Biopolymer Modified Spinel Ferrite. *J. Environ. Chem. Eng.* **2018**, *6* (5), 6194–6206. https://doi.org/10.1016/j.jece.2018.09.054.

(63) Shan, C.; Ma, Z.; Tong, M.; Ni, J. Removal of Hg(II) by Poly(1-Vinylimidazole)-Grafted Fe3O4 at SiO2 Magnetic Nanoparticles. *Water Res.* **2015**, *69* (Ii), 252–260. https://doi.org/10.1016/j.watres.2014.11.030.

(64)   Jana, S.; Ray, J.; Mondal, B.; Tripathy, T. Efficient and Selective Removal of Cationic Organic Dyes from Their Aqueous Solutions by a Nanocomposite Hydrogel, Katira Gum-Cl-Poly(Acrylic Acid-Co-N, N-Dimethylacrylamide)@bentonite. *Appl. Clay Sci.* **2019**, *173* (October 2018), 46–64. https://doi.org/10.1016/j.clay.2019.03.009.

(65)   Kumar, M.; Dosanjh, H. S.; Singh, H. Magnetic Zinc Ferrite–Chitosan Bio-Composite: Synthesis, Characterization and Adsorption Behavior Studies for Cationic Dyes in Single and Binary Systems. *J. Inorg. Organomet. Polym. Mater.* **2018**, *28* (3), 880–898. https://doi.org/10.1007/s10904-017-0752-0.

(66)   Savva, I.; Odysseos, A.; Evaggelou, L.; Marinica, O.; Vasile, E.; Vekas, L.; Sarigiannis, Y.; Krasia-Christoforou, T. Fabrication, Characterization, and Evaluation in Drug Release Properties of Magnetoactive Poly(Ethylene Oxide)-Poly(L-Lactide) Electrospun Membranes. *Biomacromolecules* **2013**, *14*. https://doi.org/10.1021/bm401363v.

(67)   Tan, T. L.; Krusnamurthy, P. A.; Nakajima, H.; Rashid, S. A. Adsorptive, Kinetics and Regeneration Studies of Fluoride Removal from Water Using Zirconium-Based Metal Organic Frameworks. *RSC Adv.* **2020**, *10* (32), 18740–18752. https://doi.org/10.1039/d0ra01268h.

(68)   Chella, S.; Kollu, P.; Komarala, E. V. P. R.; Doshi, S.; Saranya, M.; Felix, S.; Ramachandran, R.; Saravanan, P.; Koneru, V. L.; Venugopal, V.; Jeong, S. K.; Grace, A. N. Solvothermal Synthesis of MnFe 2 O 4 -Graphene Composite-Investigation of Its Adsorption and Antimicrobial Properties. *Appl. Surf. Sci.* **2015**, *327*, 27–36. https://doi.org/10.1016/j.apsusc.2014.11.096.

(69)   Singh, R. Recyclable Magnetic Nickel Ferrite-Carboxymethyl Cellulose-Sodium Alginate Bio-Composite for Efficient Removal of Nickel Ion from Water. **2023**, 1–33.

CHAPTER 3

MATERIALS AND METHODS

3.0 Materials used

The chemicals used in the present study were all purchased from LOBA CHEMICAL Co. Ltd. All reagents purchased were of analytical grade. The chemicals utilised in present study were-Zinc nitrate, copper sulphate, cobalt nitrate, hydrazine hydride, diethyloxalate, hydrochloric acid, mono chloro acetic acid, sodium fluoride, dyes- crystal violet, congo red, methylene blue, malachite green, brilliant green, glutaraldehyde as binding agent, sodium hydroxide pellets, methyl alcohol, sodium meta bisulphite, ferric nitrate, isopropanol, SPADNS reagent, Zirconyl chloride octahydrate, dimethyl glyoxime, nickel sulphate, tri sodium citrate, conc. Ammonia, potassium iodide and iodine.

3.1 Methodology used

The general methodology used in the present work involved following steps:-

- Step 1- Extraction of starch from mango seeds (MS) and silica form rice husk (RHS).

- Step 2- Preparation of magnetic spinel ferrites of Zn, Ni, Cu and synthesis of carboxy methyl starch (CMS) and development of bio-waste(Mango starch (MS), Rice husk silica (RHS), Carboxy methyl starch (CMS)) based magnetic ferrite composites (Magnetic green composites).

- Step 3- Characterization of prepared magnetic green adsorbents.

- Step 4- Analysis of adsorption potential of synthesized magnetic green adsorbents in the removal of pollutants like dyes (in single and multiple system), heavy metal ions and fluoride ions (in single system).

- Step 5- Regeneration and reuse of adsorbents.

3.1.1 Synthesis of spinel ferrites:-

For the synthesis of various spinel transition metal ferrites, low temperature combustion approach was used[1]. Following are some of the benefits of low temperature combustion method over other traditional methods:

1. Synthesis is achieved at lower temperature.
2. The equipment used is not very expensive.
3. Single phase and stoichiometrically pure ferrites are produced.

4. Ferrites with a small size and large surface area are produced.

By using low combustion method, Zinc ferrite (ZFN), Nickel ferrite (NiFN) and Copper ferrite (CuFN) were synthesized. The procedure used was as follows:

1 mole of diethyl oxalate and 2 moles of hydrazine hydrate were thoroughly mixed to prepare Oxalyl dihydrazide (ODH). Metal salt and iron salt were mixed separately into 1:2 ratio in distilled water and mixed thoroughly. Oxalyl dihydrazide (ODH) solution was gradually added to this while being constantly stirred into the solution of metal salt and iron salt. This mixture was concentrated over a hot water bath for one hour. This mixture was annealed for three hours at 600°C in a muffle furnace, then cooled and grounded.

3.1.2 Synthesis of carboxymethylstarch (CMS)

A) Extraction of starch from mango seed kernel (MS)

The leftover mango seeds are thrown away as garbage. Mango seeds are significant source of starch with high yield[2]. The mango seeds were collected from fruit market in Jalandhar, rinsed with water and cleaned to remove any leftover pulp, dried, and grounded into fine powder. To prevent oxidation, the powder (25 g) was dissolved in 10% sodium metabisulphitesolution and homogenised using a blender at 25°C. The ground slurry was screened with muslin cloth and was continuously washed with distilled water until it turned into a clear solution. After this, when the mixture settled, then the supernatant was discarded. After drying, the extract was kept at roomtemperature[3]. This product was labelled as mango seed kernel starch (MS).

B) Synthesis of carboxy methyl starch (CMS)

Mango seed kernel starch (MS) was used to synthesize carboxy methyl starch (CMS). The mixture of 50 mL of isopropanol/H_2O (3:1), 1 g of starch and 1.2 g of NaOH was heated at 60 °C. Monochloroacetic acid (1.5 g) was gradually added to this solution, and the mixture was constantly agitated for two hours at the same temperature. At a temperature between 45 and 50 °C, the solvent was extracted using rotatory evaporator, and was neutralised using acetic acid. A pH metre was used to verify this. Then, 50 mL of methanol was put into the solution, and the resulting mixture was stored at 4 °C for 12 hours. The washing with methanol was done for three times and the precipitates were dried in vacuum. Thus, carboxy methyl starch (CMS) was synthesized[4].

3.1.3 Extraction of silica from rice husk using Taguchi approach

Rice husk (RH) was grounded and then washed with distilled water while being mechanically stirred for an hour. Then, it was leached in 1M HCl for two hours at 90 °C. After that, distilled water was repeatedly used to neutralise the acid leached rice husk solution. The leached rice husk was put into a muffle furnace for two hours operating at 700 °C. The product obtained was rice huskash that was white in color.

After that, the rice husk ash (RHA) was used as a raw material to develop high surface area silica. In a beaker with 9 mL of 1.5 M sodium hydroxide (NaOH), 300 mg of RHA was added and heated at 90°C for 1 h. During the boiling process, RHA's silica was transformed into sodium silicate solution. To make the concentration of sodium silicate to 1M (monitored with the help of a pH meter), distilled water was added. By gradually adding 1.0 M HCl, the sodium silicate solution was titrated up to pH 7. The mixture was placed in a beaker, wrapped on top, and placed in oven at 70°C for seven days. The product was then washed by using distilled water and centrifuged at 3000 rpm for five minutes. The resulting rice husk silica (RHS) obtained was ground to a fine powder[5].

3.1.4 Synthesis of magnetic green adsorbents

Preparation of magnetic green adsorbents viz. spinel ferrite-carboxy methyl starch (CMS), spinel ferrite-mango starch (MS) and spinel ferrite-rice husk silica (RHS), was done in the following manner:

Homogenous solutions of 2% CMS, MS and RHS were prepared by mixing these in 5% acetic acid solution separately and were mixed continuously for 1 h at 200 rpm. 2 g of selected spinel ferrite in distilled water (10 mL) was put into 2% solutions of CMS, MS, and RHS prepared above and stirred continuously for 30 minutes. The solution obtained was added to mixture of 0.5 M NaOH solution and 10% glutaraldehyde (linking agent) with continuous stirring for 1 h to form magnetic green adsorbents[6]. The prepared magnetic green adsorbents were kept overnight.

- Spinel ferrite –carboxy methyl starch (CMS) and spinel ferrite – mango starch (MS) were dried under vaccum
- Spinel ferrite –rice husk silica (RHS) was dried at 50°C.
- By using this method, Zinc ferrite-rice husk silica (ZFN-RHS), Zinc ferrite-mango starch (ZFN-MS), Zinc ferrite-carboxy methyl starch (ZFN-CMS), Nickel ferrite-rice husk silica (NiFN-RHS), Nickel ferrite-mango starch (NiFN-MS), Nickel ferrite-carboxy methyl starch (NiFN-CMS), Copper ferrite-rice husk silica (CuFN-RHS),

Copper ferrite- mango starch (CuFN), Copper ferrite- carboxy methyl starch (CuFN-CMS), magnetic green composites were synthesized.

3.2 Preliminary adsorption studies of different magnetic green adsorbents with dyes

The selective nature of different magnetic green composites were determined by conducting preliminary studies. Therefore, various cationic and anionic dyes were utilised for studying adsorption behavior.

3.2.1 Preliminary adsorption studies with different dyes:

The adsorption behavior of metal ferrite –RHS, metal ferrite-MS and metal ferrite –CMS composites (magnetic green adsorbents) were studied with various cationic and anionic dyes. Dyes like Congo red (CR), Brilliant green (BG), Methylene blue (MB), Malachite green (MG) and Crystal violet (CV) were utilised to study the adsorption behavior of above mentioned magnetic green adsorbents. In preliminary adsorption, a fixed amount of metal ferrite composite was added in a fixed concentration (50mg/L) of dye solution, in a conical flask, and kept at 200 rpm for fixed interval of time. The reduced concentration of dyes was calculated by noting absorbance with the help of a UV- spectrophotometer (Shimadzu, 1800 scanning Double beam UV-VIS spectrophotometer). The wavelength (λ_{max}) at which the absorption was recorded for CR, BG, MB, CV and MG used were 498nm, 624nm, 664nm, 592nm and 614nm respectively. The results of preliminary studies with metal ferrites and their composites are represented in Table 3.1:

Table 3.1- Percentage removal of different dyes in preliminary studies

Sr. No.	Adsorbent	% removal of BG	% removal of MB	% removal of MG	% removal of CV	% removal of CR
ZFN and their composites						
1	ZFN	30.02	17.02	18.8	32.6	81.84
2	ZFN-RHS	63.35	43.05	45.8	49.4	58.21
3	ZFN-MS	49.51	41.32	41.3	52.1	32.83
4	ZFN-CMS	52.75	48.49	39.7	43.6	13.41
NiFN and their composites						

5	NiFN	23.78	18.23	25.3	15.8	31.76
6	NiFN-RHS	32.98	23.97	28.7	19.9	27.67
7	NiFN-MS	36.58	31.18	26.1	23.4	23.22
8	NiFN-CMS	19.88	39.20	29.6	18.1	29.62
CuFN and their composites						
9	CuFN	0.77	5.93	3.43	11.4	18.28
10	CuFN-RHS	12.16	16.35	5.28	18.6	16.95
11	CuFN-MS	10.08	11.85	8.99	15.3	11.61
12	CuFN-CMS	2.92	18.80	6.54	12.2	6.39

It was observed that ZFN-RHS, ZFN-MS and ZFN-CMS composites showed high percentage removal for cationic dyes BG, MG, CV and MB as compared to ZFN. For anionic CR, percentage removal decreased with ZFN-RHS, ZFN-MS and ZFN-CMS composite as compared to ZFN. It may be due to the fact that upon surface modification, the surface of magnetic green composites became negatively charged due to the presence of certain functional groups present in RHS, MS and CMS. Therefore, negatively charged surface easily attracted cationic dyes toward itself and the percentage removal was increased. However, in case of anionic CR dye, decrease in percentage removal was observed due to similar charges present on the surface of the adsorbent as well as anionic dye molecules. This observation indicated that magnetic green adsorbents synthesized in this study had increased selectivity towards cationic dyes. Based on these studies ZFN-RHS, ZFN-MS and ZFN-CMS composite were selected forfurther adsorption studies of cationic dyes.

3.2.2 Preliminary adsorption studies with fluoride ions

The preliminary studies were conducted by adding 0.1 g of metal ferrite and their composites in 50 mL of fixed concentration (5 mg/L) of fluoride ions solution, and kept at 200 rpm for fixed time interval. The reduced concentration of fluoride ions was calculated by SPADNS method using UV-VIS spectrophotometer (by noting absorbance)[7]. Percentage removal of non-metal fluoride ions with different adsorbents is presented in table 3.2.

Table 3.2- Percentage removal of fluoride ions using different magnetic green composites

Sr. no.	Adsorbent used	% removal of Fluoride ion
1	ZFN	48.10
2	ZFN-RHS	72.20
3	ZFN-MS	73.24
4	ZFN-CMS	67.70
5	NiFN	42.56
6	NiFN-RHS	52.36
7	NiFN-MS	52.13
8	NiFN-CMS	37.60
9	CuFN	43.67
10	CuFN-RHS	47.70
11	CuFN-MS	47.13
12	CuFN-CMS	45.63

From the above data table it is clear that zinc ferrite and its composites gave better results therefore ZFN composites were selected for fluoride ions removal for detailed adsorption study.

3.2.3 Preliminary adsorption studies with Ni (II) ions using different magnetic green composites

Adsorption behavior of nickel (II) ions was analysed using batch adsorption method with all the adsorbents synthesized. To a known concentration of nickel ion solution, 0.1 g of the

adsorbent (magnetic green composites) was added in 50 mL solution taken in a 250 mL conical flask and placed at 200 rpm for fixed interval of time. DMG method was used for the estimation of nickel ions in solution[8].

Percentage removal of nickel ions using synthesized magnetic green composites is mentioned in table 3.3.

Table 3.3- Percentage removal of nickel ions using different magnetic green composites

Sr. no.	Adsorbent used	% removal of Ni(II) ion
1	ZFN	38.20
2	ZFN-RHS	45.67
3	ZFN-MS	63.24
4	ZFN-CMS	57.70
5	NiFN	32.46
6	NiFN-RHS	33.36
7	NiFN-MS	32.93
8	NiFN-CMS	34.60
9	CuFN	33.55
10	CuFN-RHS	37.64
11	CuFN-MS	37.63
12	CuFN-CMS	35.28

From the above table it is clear that zinc ferrite and its composites performed better than other composites and therefore composites of Zinc ferrite were selected for detailed study of nickel ions removal.

3.3 Characterization of magnetic green adsorbents

The characterization of pure ferrites and their composites was made utilising FTIR spectrophotometer (Shimadzu-8400 S); Scanning Electron Microscope with Energy Dispersive spectra (Fe-SEM:JEOL EDS: OXFORD EDS LN 2 free, Au coater: JEOL Smart coater) ; X-Ray diffraction (XRD, Shimadzu Maxima_ XRD-7000 X-Ray Diffractometer); Brunauer-Emmett-Teller (BET, Quanta Chrome Nova-1000 Version 3.70), pH of point zero charge (pH$_{PZC}$) and thermo gravimetric analysis (Perkin Elmer TGA 4000). Fourier transform infrared spectroscopy revealed about the functional groups present in magnetic green adsorbents. XRD revealed the crystalline or amorphous nature of the adsorbents. FESEM gave information regarding the surface morphology of the synthesized adsorbents. BET analysis provided useful information like for surface area, pore volume etc. of the magnetic green adsorbents. pH$_{PZC}$ depicted pH at which total surface charge density on the adsorbent's surface is zero. TGA analysis measured thermal stability of the adsorbent over time as the temperature changes.

3.4 Batch adsorption studies

Batch adsorption process was followed for remediation of water containing pollutants like dyes, heavy metals and/or fluoride ions. The magnetic green adsorbents (ZFN-RHS, ZFN-MS and ZFN-CMS) were used for selective removal of dyes such as Brilliant green, Crystal violet, Methylene blue, Malachite green etc., heavy metals like Ni (II) ions and for removing fluoride ions from water. Extensive studies were performed on different experimental parameters, viz. adsorbent dosage, initial concentration, temperature, pH, time etc.

3.4.1 Effect of contact time

There exists a dynamic equilibrium between the amount of adsorbate adsorbed to and desorbed from surface of adsorbent. The time taken to reach the equilibrium stage is known asequilibrium time. The amount of adsorbate adsorbed on surface of adsorbent is referred to as maximum adsorption capacity (Q$_e$) (at equilibrium time). 50mL of dye solution with dye concentration 50 mg/L (in single dye system) and 20mg/L (in binary and ternary dye system) wasprepared. 0.1g

of adsorbent was added to it (0.1g/50mL) and placed in a thermostatic shaker. The absorbance of solution was noted after certain intervals of time till equilibrium was reached. The adsorption capacity Q_e (in mg/g) and % removal of dyes/metal ions/fluoride ions was calculated by using following equations[9]:

$$Q_e = \frac{C_o - C_t}{m} \times V \tag{1}$$

$$\% \text{ Removal} = \frac{C_o - C_t}{C_o} \times 100 \tag{2}$$

where C_o, C_t and C_e represents initial concentration, concentration at time 't' and equilibrium concentration of adsorbate (in mg/L), 'V' stands for volume of the solution (in L) and 'm' depicts mass of adsorbent used (in g).

3.4.2 Effect of concentration and temperature

To study the effect of concentration on the adsorption process, various concentrations of dyes and metal ion/fluoride ion solution were taken. Took 50 mL of 50-250 mg/L dyes (in single dye system) and 20-100 mg/L of dyes (in binary and ternary system), 5-25 mg/L of fluoride ions and 100-500 mg/L of Ni (II) ions (in single ion system) and adsorbent dose (0.1g/50mL) and was placed in a thermostatic shaker maintained at 25°C at 200rpm. The final dye concentration readings were taken at fixed time interval. The same steps were repeated at 30°C and35°C to see the effect of temperature[10].

3.4.3 Effect of adsorbent Dose

The adsorbent dose plays a crucial role in adsorption. Different amounts of adsorbent ranging from 0.1g to 0.5g were taken and all other parameters were kept constant. A fixed volume of dye (50 mL) of known concentration of dyes i.e.50 mg/L (in single dye system) and 20 mg/L (in binary and ternary dye system) was taken and varied amounts of adsorbent (0.1 to 0.5g) was added. The final dye concentration was noted at fixed interval of time[11].

3.4.4 Effect of pH

The pH of solution is significant in water purification processes. pH governs the surface charge on the surface of the adsorbent[12]. To a fixed volume of dye (50 mL) of known concentration (50 mg/L in single dye system and 20mg/L in binary and ternary dye system) added a fixed

amount of adsorbent (0.1g).The pH of the dye solutions was adjusted from 3 to 11 with dilute HCl or NaOH solution. The absorbance of dyes were measured after separation from adsorbent using a UV spectrophotometer after fixed interval of time.

3.5 Kinetic studies

Kinetic studies were used to identify equilibrium time for the maximum removal of the pollutants (dyes, heavy metals and fluoride ions) from water. Three kinetic models viz. Lagergren pseudo first order, Pseudo second order and Elovich models, were employed for studying kinetic behavior of ZFN-RHS, ZFN-MS and ZFN-CMS for the removal of pollutants (dyes, heavy metals, fluoride ions) from water[13].

3.5.1 Lagergren pseudo first order

Lagergren pseudo first order assumes that rate of adsorption depends on the diffusion of adsorbate on the surface of adsorbent[12].

Linear Lagergren pseudo first order equation is -

$$\text{Log} \ (Q_e - Q_t) = \log Q_{e1} - \frac{k_1}{2.303} * t \qquad (3)$$

3.5.2 Pseudo second order

Pseudo second order kinetics assumes that rate of adsorption is influenced by interactions between adsorbent and adsorption sites throughout the adsorption process[12].

Linear pseudo second order equation is –

$$\frac{t}{Q_t} = \frac{1}{h} + \frac{t}{Q_{e2}} \qquad (4)$$

3.5.3 Elovich equation

It describes a diffusion step controlling the adsorption process. The equation is valid for heterogeneous adsorbing surfaces[12].

The Elovich model equation is represented as-

$$Q_t = \frac{1}{\beta \ln \alpha \beta} + \frac{1}{\beta \ln t} \qquad\qquad (5)$$

Where, Q_{e1} describes Lagergren pseudo 1st order

constant Q_{e2} describes pseudo 2nd order constant

Q_t represents adsorbate adsorbed (in mg/g) on adsorbent at time 't' (min.)

k_1 stands for Lagergren pseudo first order rate constant (g/mg/min)

$$h = \frac{1}{k_2 Q_{2e2}}$$

k_2 stands for rate constant for pseudo second order

(g/mg/min) α is chemisorption rate (mg/min.)

β is chemisorption activation energy (g/mg).

Above equations were plotted for the data collected from single, binary and ternary dye systems, for Ni (II) and fluoride ions. These plots were used to calculate various kinetic constants.

3.5.4 Weber Morris intra particle diffusion model

Weber Morris intra particle diffusion model was applied to study the intra particle diffusion behavior of magnetic green adsorbents (ZFN-RHS, ZFN-MS and ZFN-CMS) and was applied to the kinetic data. The Weber Morris intra-particle diffusion model is expressed as[14]:

$$Q_t = K_{int} t^{0.5} \qquad\qquad (6)$$

where K_{int} describes intra-particle diffusion rate constant.

The graph between Q_t and $t^{0.5}$ indicate the diffusion behavior of ZFN-RHS, ZFN-MS and ZFN-CMS and is considered as a rate limiting step if straight line passes through the origin.

3.6 Adsorption isotherms study

To analyse the adsorption behavior of an adsorbent, various adsorption isotherms are employed. The four most prevalent adsorption isotherms were used in this study namely, the Temkin, Dubinin-Radushkevich (DR), Langmuir and Freundlich isotherms[15]. The adsorption

behavior of magnetic green adsorbents at equilibrium, for single and multiple (binary and ternary) dye systems; Ni (II) ions and for fluoride ions, at three different temperatures were studied using these isotherm models.

3.6.1 Langmuir isotherm

According to Langmuir model, adsorption is homogeneous in nature[16]. It has following assumptions:

    I.   The adsorption sites are uniformly distributed over the surface of the adsorbent.

   II.   Adsorbed molecules do not interact with each other.

  III.   A monolayer is formed at the surface.

Linear form of Langmuir isotherm model equation is:

$$\frac{1}{Q_e} = \frac{1}{Q} + \frac{1}{bQC_e} \tag{7}$$

where Langmuir adsorption capacity is represented by Q (mg/g).

Adsorption energy is represented by b

The important characteristics of Langmuir isotherm is separation factor R_L which is a dimensionless constant and is calculated by using following equation[17]:

$$R_L = \frac{1}{1+bC_o} \tag{8}$$

C_o represents highest initial concentration of adsorbate.

If value of separation factor is in the range 0-1, then the adsorption is favourable in nature. If its value is more than 1, then adsorption will be unfavourable, if its value is 1, adsorption will be linear and if it is 0, then adsorption process will be irreversible in nature[18].

3.6.2 Freundlich isotherm

The Freundlich isotherm model describes adsorption on a heterogeneous surface[11]. Linear form of Freundlich model equation is:

$$\log Q_e = \log K_f + \frac{1}{n \log C_e} \tag{9}$$

Freundlich constant is represented by K_f

'n' represents adsorption intensity

The Freundlich isotherm constants $1/n$ and K_f can be calculated from the slope and intercept of the graph between $\log Q_e$ and $\log C_e$.

3.6.3 Temkin isotherm

The Temkin isotherm is based on the assumption that the heat of adsorption decreases linearly with coverage due to interactions between adsorbate molecules on the surface[19]. It describes non-uniform distribution of heat of adsorption.

Linear form of Temkin model equation is:

$$Q_e = B \ln A + B \ln C_e \tag{10}$$

where RT/b_T parameter is represented by B

Maximum binding energy is represented by A (L/g)

Absolute temperature is represented by T (K)

Temkin constant is represented by b_T (J/mg)

3.6.4 D-R isotherm

According to D-R isotherm porosity occurs homogeneously on surface of adsorbent[20]. Linear form of Dubinin-Raduskevich (D-R) model equation is:

$$\ln Q_e = \ln Q_m - K_{DR} \in^2 \tag{11}$$

$$\text{Where } \in = RT \ln (1 + \frac{1}{C_e}) \tag{12}$$

D-R adsorption capacity is represented by Q_m (mg/g)

D-R isotherm constant is represented by K_{DR}

Polanyi potential is represented by $\in$

Adsorption energy (E), which describes adsorption as physical or chemical, is one of the parameter calculated in the D-R isotherm model to identify the type of adsorption. This calculation is performed using following equation[13]:

$$E = \frac{1}{\sqrt{2K_{DR}}} \qquad (13)$$

Where, K_{DR} is D-R isotherm constant.

'E' value indicates whether the adsorption is chemical or physical. If calculated adsorption energy is less than 40 kJ/mol, adsorption is termed as physisorption, otherwise as chemisorption[9].

3.7. Thermodynamic studies

Using thermodynamic equations, various adsorption thermodynamic parameters- free energy change ($\Delta G°$), entropy change ($\Delta S°$) and enthalpy change ($\Delta H°$) were calculated.

Van't Hoff equation to calculate $\Delta G°$ which is as under[21]:

$$\Delta G° = -RT \ln K_d \qquad (14)$$

Gibb's Helmholtz equation is given as,

$$\Delta G° = \Delta H° - T\Delta S° \qquad (15)$$

From equation (14) and (15), we get

$$\ln K_d = \frac{\Delta S°}{R} - \frac{\Delta H°}{RT} \qquad (16)$$

$$K_d = \frac{C_o - C_e}{C_e} \qquad (17)$$

Where, 'K_d' represents adsorption affinity,

'T' is temperature in Kelvin.

The intercept and slope of the linear plots of $\ln K_d$ vs $1/T$ were used to compute $\Delta S°$ and $\Delta H°$.

References

(1)   Kumar, M.; Dosanjh, H. S.; Singh, H. Synthesis of Spinel ZnFe2O4 Modified with
        SDS via Low Temperature Combustion Method and Adsorption Behaviour of Crystal
        Violet Dye. *Asian J. Chem.* **2017**, *29* (9), 2057–2064.
        https://doi.org/10.14233/ajchem.2017.20827.

(2)   Ramli, R. N.; Lee, C. K.; Kassim, M. A. Extraction and Characterization of Starch
        From Mango Seeds. **2018**. https://doi.org/10.1088/1742-6596/1082/1/012019.

(3)   Tesfaye, T.; Johakimu, J. K.; Chavan, R. B.; Sithole, B.; Ramjugernath, D.
        Valorisation of Mango Seed via Extraction of Starch: Preliminary Techno-Economic
        Analysis. *Clean Technol. Environ. Policy* **2018**, *20* (1), 81–94.
        https://doi.org/10.1007/s10098-017-1457-3.

(4)   Bachra, Y.; Grouli, A.; Damiri, F.; Talbi, M.; Berrada, M. A Novel Superabsorbent
        Polymer from Crosslinked Carboxymethyl Tragacanth Gum with Glutaraldehyde:
        Synthesis, Characterization, and Swelling Properties. *Int. J. Biomater.* **2021**, *2021*.
        https://doi.org/10.1155/2021/5008833.

(5)   Song, S.; Cho, H. B.; Kim, H. T. Surfactant-Free Synthesis of High Surface Area Silica
        Nanoparticles Derived from Rice Husks by Employing the Taguchi Approach. *J. Ind.
        Eng. Chem.* **2018**, *61*, 281–287. https://doi.org/10.1016/j.jiec.2017.12.025.

(6)   Kumar, M.; Dosanjh, H. S.; Singh, H. Magnetic Zinc Ferrite–Chitosan Bio-Composite:
        Synthesis, Characterization and Adsorption Behavior Studies for Cationic Dyes in
        Single and Binary Systems. *J. Inorg. Organomet. Polym. Mater.* **2018**, *28* (3), 880–
        898. https://doi.org/10.1007/s10904-017-0752-0.

(7)   Shanker, A. S.; Srinivasulu, D.; Pindi, P. K. A Study on Bioremediation of Fluoride-
        Contaminated Water via a Novel Bacterium Acinetobacter Sp. (GU566361) Isolated
        from Potable Water. *Results Chem.* **2020**, *2*, 100070.
        https://doi.org/10.1016/J.RECHEM.2020.100070.

(8)   Singh, H.; Rattan, V. K. Adsorption of Nickel from Aqueous Solutions Using Low
        Cost Biowaste Adsorbents. **2011**, 239–249. https://doi.org/10.2166/wqrjc.2011.024.

(9)   de Oliveira, H. A. L.; Campos, A. F. C.; Gomide, G.; Zhang, Y.; Ghoshal, S.
        Elaboration of a Core@shell Bimagnetic Nanoadsorbent (CoFe2O4@γ-Fe2O3) for the
        Removal of As(V) from Water. *Colloids Surfaces A Physicochem. Eng. Asp.* **2020**, *600*
        (May), 125002. https://doi.org/10.1016/j.colsurfa.2020.125002.

(10)   Akharame, M. O.; Fatoki, O. S.; Opeolu, B. O. *Regeneration and Reuse of Polymeric*

Nanocomposites in Wastewater Remediation: The Future of Economic Water Management; Springer Berlin Heidelberg, 2018. https://doi.org/10.1007/s00289-018-2403-1.

(11) Shekhawat, A.; Jugade, R.; Kahu, S.; Saravanan, D.; Deshmukh, S. Mesoporous Cellulose Assemblage Al-Doped Ferrite for Sustainable Defluoridation Process Based on Parameters Optimization through RSM. *Inorg. Chem. Commun.* **2023**, *151*, 110528. https://doi.org/10.1016/J.INOCHE.2023.110528.

(12) Lima, É. C.; Adebayo, M. A.; Machado, F. M. *Kinetic and Equilibrium Models of Adsorption*; 2015; Vol. 0. https://doi.org/10.1007/978-3-319-18875-1_3.

(13) Culita, D. C.; Simonescu, C. M.; Patescu, R. E.; Preda, S.; Stanica, N.; Munteanu, C.; Oprea, O. Polyamine Functionalized Magnetite Nanoparticles as Novel Adsorbents for Cu(II) Removal from Aqueous Solutions. *J. Inorg. Organomet. Polym. Mater.* **2017**, *27* (2), 490–502. https://doi.org/10.1007/s10904-016-0491-7.

(14) Azmi, M. A.; Ismail, N. A. A.; Rizamarhaiza, M.; Hasif, A. A. K. W. M.; Taib, H. Characterisation of Silica Derived from Rice Husk (Muar, Johor, Malaysia) Decomposition at Different Temperatures. *AIP Conf. Proc.* **2016**, *1756*. https://doi.org/10.1063/1.4958748.

(15) Tesfaye Bahir, T.; Eitex, T. T. Valorisation of Mango Fruit By-Products: Physicochemical Characterisation and Future Prospect Crystalline Nanocellulose View Project Valorization of Corncobs View Project Valorisation of Mango Fruit By-Products: Physicochemical Characterisation and Future. **2017**, *50* (Figure 2), 22–34.

(16) Rawat, V.; Rai, P.; Gautam, R. K.; Chattopadhyaya, M. C. Kinetic and Equilibrium Isotherm Studies for the Adsorptive Removal of Brilliant Green Dye from Aqueous Solution by Oplismenus Frumentaceus Husk. *J. Indian Chem. Soc.* **2013**, *90* (5), 577–583. https://doi.org/10.1016/j.jenvman.2006.06.024.

(17) Kumar, M.; Dosanjh, H. S.; Singh, H. Magnetic Zinc Ferrite–Alginic Biopolymer Composite: As an Alternative Adsorbent for the Removal of Dyes in Single and Ternary Dye System. *J. Inorg. Organomet. Polym. Mater.* **2018**, *28* (5), 1688–1705. https://doi.org/10.1007/s10904-018-0839-2.

(18) Hassan Musa, S.; Sagagi, B. S. Extraction and Some Characteristics of Mango Seed Kernel Starch for Industrial Applications. *Sci. Lett.* **2023**, *17* (2), 81–90.

(19) Pathania, D.; Sharma, S.; Singh, P. Removal of Methylene Blue by Adsorption onto Activated Carbon Developed from Ficus Carica Bast. *Arab. J. Chem.* **2017**, *10*, S1445–S1451. https://doi.org/10.1016/J.ARABJC.2013.04.021.

(20)   Mondal, N. K. Natural Banana (Musa Acuminate) Peel: An Unconventional Adsorbent for Removal of Fluoride from Aqueous Solution through Batch Study. *Water Conserv. Sci. Eng.* **2017**, *1* (4), 223–232. https://doi.org/10.1007/s41101-016-0015-x.

(21)   Kumar, M.; Dosanjh, H. S.; Singh, H. Biopolymer Modified Transition Metal Spinel Ferrites for Removal of Fluoride Ions from Water. *Environ. Nanotechnology, Monit. Manag.* **2019**, *12* (May 2018), 100237. https://doi.org/10.1016/j.enmm.2019.100237.

CHAPTER 4

RESULTS AND DISCUSSION

In preliminary studies, it was observed that zinc metal ferrite magnetic green composites viz. Zinc ferrite-rice husk silica, Zinc ferrite-mango starch and Zinc ferrite-carboxy methyl starch (ZFN-RHS, ZFN- MS and ZFN-CMS) performed better therefore these ferrite composites were selected for detailed study to remove various cationic dyes like Brilliant green, Malachite green, Methylene blue and Crystal violet (BG, MG, MB and CV) in single and multiple dye systems; Ni (II) ions and fluoride ions in single ion system. This chapter of thesis is divided in four parts for better representation of results obtained and discussions. First part consists of characterization of magnetic green composites, second part involves removal of dyes using batch adsorption method, third part includes removal of F⁻ ions and fourth part represents removal of Ni (II) ions.

Part I

4.0 Characterization of magnetic green composites (ZFN-RHS, ZFN-MS and ZFN-CMS)

4.1 Different characterization techniques:

The adsorbents must be characterized in order to learn about their structure, morphology, stability, composition, size, and other crucial characteristics for the conformation of desired synthesis and adsorption process. Fourier Transform Infra-red Spectroscopy (FTIR), X-Ray Diffraction (XRD), Fe- Scanning Electron Microscopy (FESEM), Energy Dispersive Spectra (EDS), Brunauer- Emmett-Teller analysis (BET), Thermo Gravimetric Analysis (TGA) and Point Zero Charge pH (pH$_{pzc}$) were utilised to characterize the synthesized adsorbents and have been discussed in the following sections.

4.1.1 Fourier Transform Infra-red Spectroscopy (FTIR)

The FTIR spectra of Zinc metal ferrite (ZFN), Rice husk silica (RHS) and Zinc ferrite-Rice husk silica (ZFN-RHS) magnetic green composites are shown in figure 4.1.1.

FTIR spectra of ZFN- There is a strong peak at 554 cm^{-1} which indicates the metal-oxygen stretching bond at tetrahedral position and second peak at 423 cm^{-1} corresponds to the metal-oxygen stretching bond at octahedral position in FTIR spectra of spinel Zinc ferrite[1]. These two peaks confirmed the formation of spinel zinc ferrite.

FTIR spectra of RHS- FTIR spectra of RHS shows peaks at 1066.7 cm^{-1}, 796.8 cm^{-1} and 458 cm^{-1} which corresponds to siloxane bonds[2].

FTIR spectra of ZFN-RHS- FTIR spectra of Zinc ferrite-Rice husk silica (ZFN-RHS)

magnetic green composite shows peaks at 1064 and 795 cm^{-1} which corresponds to asymmetric stretching and bending respectively[2]. These stretching modes depicts silicon-oxygen-siliconbonds in silica obtained from rice husk. Peaks at 554 cm^{-1} and 423 cm^{-1} are present in FTIR spectra of ZFN-RHS which are similar to ZFN spectra indicating the retention of spinel character. Thus, it is observed that the peaks which were present in pure zinc ferrite spectra and pure rice husk silica spectra were also found in the spectra of zinc ferrite-rice husk silica. All these findings reveal that Zinc ferrite –rice husk silica magnetic green composite was formed successfully.
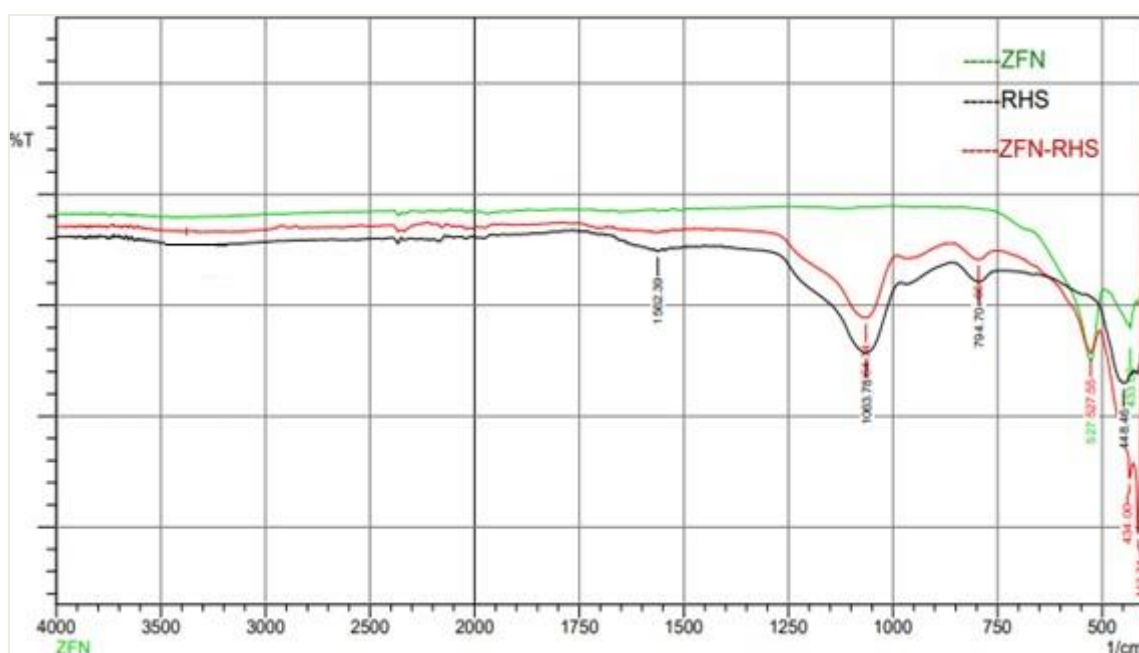
Figure 4.1.1- FTIR spectra of Zinc ferrite (ZFN), Rice husk silica (RHS) and Zinc ferrite-ricehusk silica (ZFN-RHS)

Figure 4.1.2 shows FTIR spectra of Zinc ferrite (ZFN), Mango starch (MS) and Zinc ferrite-mango starch (ZFN-MS) magnetic green composite.

FTIR spectra of MS- Peaks at 3295.49 cm^{-1} and 1649.19 cm^{-1} are visible in FTIR spectra of the MS (Figure 4.1.2), which are associated with stretching and angular deformation of the hydroxyl groups in glucose and residual water, respectively[3]. Another peak at about 2930 cm^{-1} represents C-H stretch in MS. Peaks at around 1160 cm^{-1} are indicative of asymmetric C-O-C stretching associated with glycoside couplings. Peak at 1012 cm^{-1} corresponds to C-O band in starch component [3].

FTIR spectra of ZFN-MS- Peak at 2930 cm^{-1} can be seen in the FTIR spectra of ZFN-MS

which is also present in the spectra of pure mango starch. Similarly, peaks at 554 cm^{-1} and 423 cm^{-1} are observed which corresponds to tetrahedral and octahedral sites present in the spectra of pure zinc ferrite. Peak at 3200 cm^{-1} represents the presence of hydroxyl group in ZFN-MS. Peaks at 1077, 996 and 930 cm^{-1} attributed to C-OH and CH$_2$ deformations. In ZFN-MS spectra, peaks at 1012 cm^{-1} corresponds to C-O band in starch component[4] and 2930 cm^{-1} corresponds to axial deformation of CH$_2$ group[5]. Thus, it can be seen that peaks which were present in the ZFN-MS spectra are similar to the peaks present in the pure zinc ferrite and mango starch spectra. It reveals the successful formation of ZFN-MS.
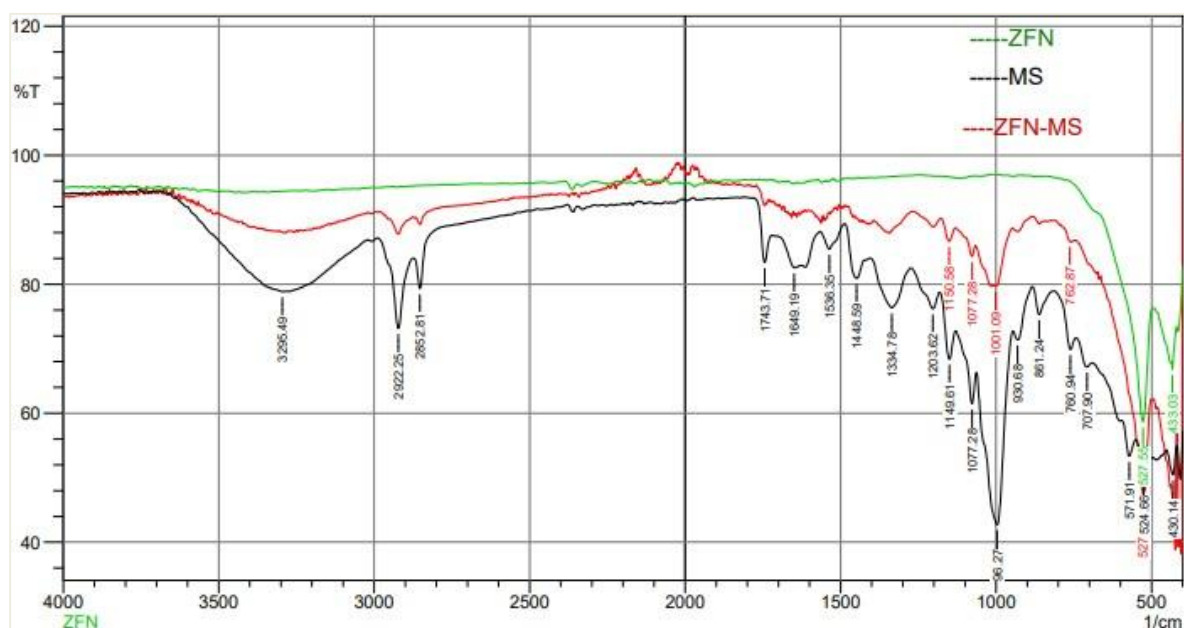
Figure 4.1.2- FTIR spectra of Zinc ferrite (ZFN), mango starch (MS) and Zinc ferrite-mangostarch (ZFN-MS)

Figure 4.1.3 represents FTIR spectra of Zinc ferrite (ZFN), Carboxy methyl starch (CMS) and Zinc ferrite-carboxy methyl starch (ZFN-CMS) magnetic green composite

FTIR spectra of CMS- The bands in the 2000–1500 cm^{-1} range in the CMS spectra (Figure 4.1.3) are caused by C=C and C=O stretching[6]. Peak at 1550 cm^{-1} confirms the presence of COO$^-$ group in carboxy methyl mango starch. The -CH$_2$ group is responsible for the peak at about 1411.94 cm^{-1}. Peaks at 3375 cm^{-1} and 2900 cm^{-1} are associated with stretching vibrations of –OH (hydroxyl) groups and C-H (alkyl) groups, respectively. These peaks provide information about the functional groups present in the carboxy methyl starch[6].

FTIR spectra of ZFN-CMS- A band at 2000–1500 cm^{-1} range similar to that present in the spectra of pure carboxy methyl starch is also present in ZFN-CMS spectra but absent in ZFN

spectra. The ZFN-CMS's FTIR displays an absorption band at around 1557.57 cm^{-1}, confirming the COO$^-$ group's presence. Peaks at 3375 cm^{-1} and 2900 cm^{-1} which were found in spectra of both CMS and ZFN-CMS indicate presence of hydroxyl and alkyl groups in them. The spectra of ZFN do not have these peaks. Peaks at 554 cm^{-1} and 423 cm^{-1} corresponds to tetrahedral and octahedral sites and indicated retention of spinel properties. This demonstrates that CMS and ZFN were successfully attached to form the composite.
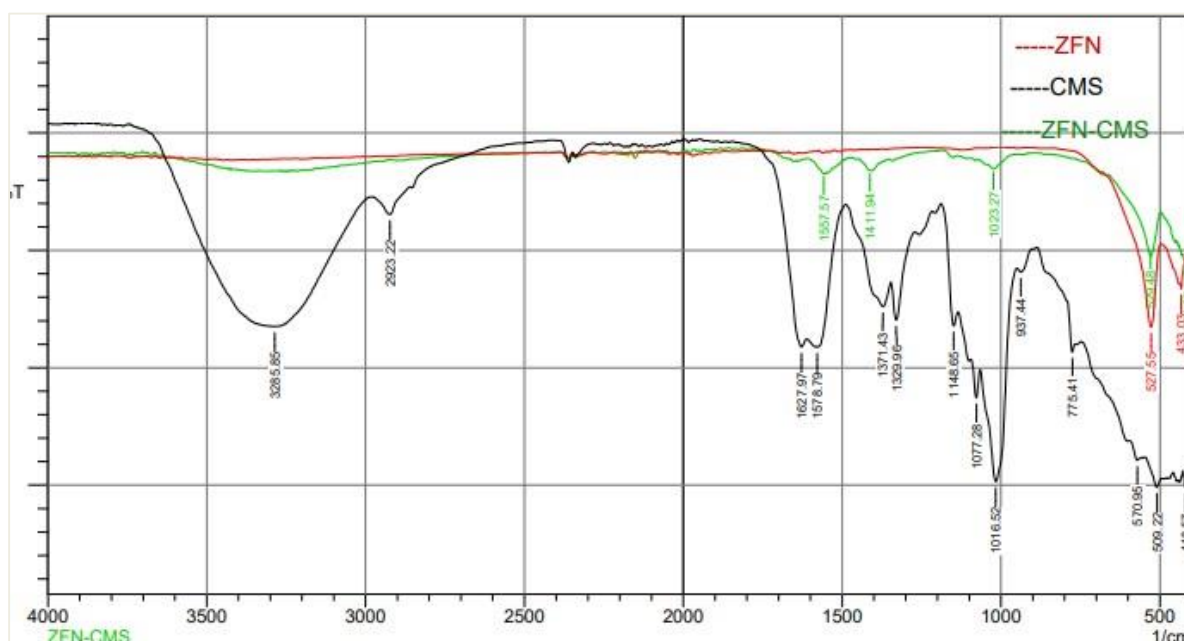
Figure 4.1.3- FTIR spectra of Zinc ferrite (ZFN), Carboxy methyl starch (ZFN-CMS) and Zinc ferrite-Carboxy methyl starch (ZFN-CMS)

4.1.2 X-Ray Diffraction (XRD)

Figure 4.1.4 represents the XRD pattern of Zinc ferrite and its magnetic green composites ZFN-RHS, ZFN-MS and ZFN-CMS. ZFN is showing the diffraction pattern having Miller indices (220), (311), (222), (400), (511), (440) with diffraction angles at 29.8º, 33.2º, 35.2º, 42.7º, 49.5º, 57.5º [7]. These results correspond to the spinel structure of Zinc metal ferrite [8]. On the other hand, XRD diffraction patterns of Zinc ferrite-rice husk silica, Zinc ferrite-mango starch and Zinc ferrite-carboxy methyl starch, magnetic green composites showed same results at slightly different diffraction angles. Diffraction angles of 28º, 31º, 35.5º, 43º, 48º, 58º for ZFN-RHS; 29.7º, 33.4º, 35.6º, 43.1º, 50.2º, 57.8º for ZFN-MS and 27º, 33º, 38º, 42º, 48º, 55º, 57.5º for ZFN-CMS, respectively. These have little differences from 2θ of ZFN.

Thus, the spinel character of ZFN-RHS, ZFN-MS and ZFN-CMS was retained. Average crystallite size ofZinc ferrite and its composites was calculated by Scherrer formula as given below[9]:

$$D = \frac{0.89\lambda}{\beta Cos\theta} \qquad (1)$$

(Where D is crystallite size, λ is X-ray wavelength, β is broadening peak and θ is diffraction angle for maximum peak).

Average crystallite size of ZFN, ZFN-RHS, ZFN-MS and ZFN-CMS magnetic green composites was found to be 28nm, 31nm, 43nm and 38nm, respectively, calculated using Scherrer formula. The size of composites was found to be more than pure ZFN, which indicated the formation of desired composites. The crystallite size indicated that all synthesized material were in nano size range.
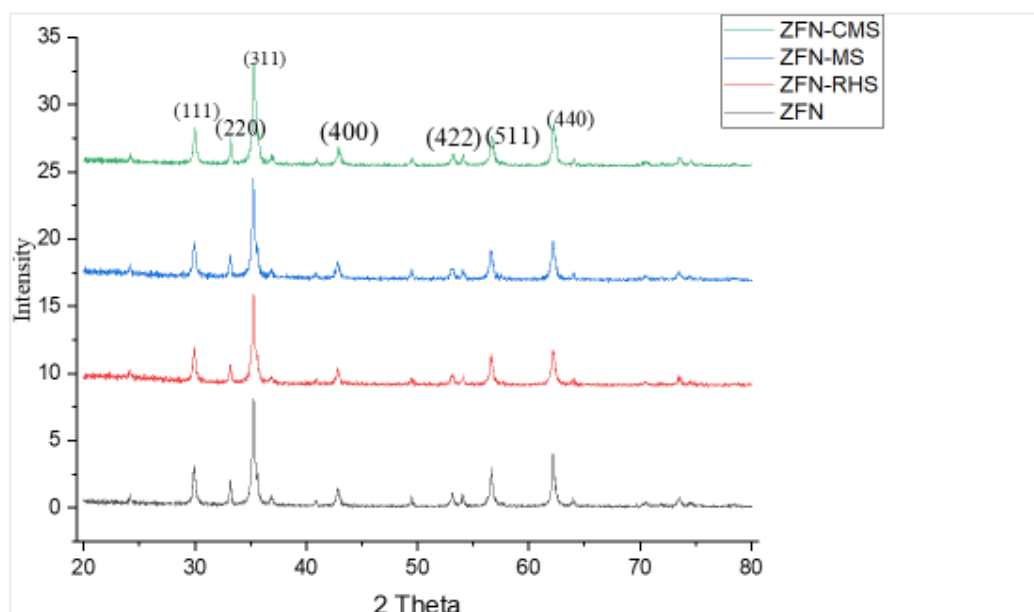
Figure 4.1.4- X-Ray Diffraction pattern of Zinc ferrite and its magnetic green composites viz.Zinc ferrite-rice husk silica, Zinc ferrite-Mango starch and zinc ferrite-carboxy methyl starch

4.1.3 Fe-Scanning Electron Microscopy (FESEM)

FESEM is used to capture the micro structure image of the material. FESEM has brighter electron source which helps to capture the magnified image of the nanomaterials. FESEM images of Zinc ferrite and its magnetic green composites viz. ZFN-RHS, ZFN-MS and ZFN-

CMS have been shown in figures 4.1.5(a-d), respectively. FESEM detects reflected electrons to provide a topographic picture of sample. From these images, the detailed information about the shape and structure of Zinc ferrite and its composites was observed. Zinc ferrite has spinel crystalline structure (fig. 4.1.5 a). When zinc ferrite was modified with rice husk silica small granules appeared on the surface of ZFN- RHS composite (fig. 4.1.5 b). When mango starch is attached with ZFN, the surface of ZFN-MS became flaky (fig. 4.1.5 c). On the other hand, zinc ferrite-carboxymethyl starch (ZFN-CMS) has irregular structure (fig. 4.1.5 d).
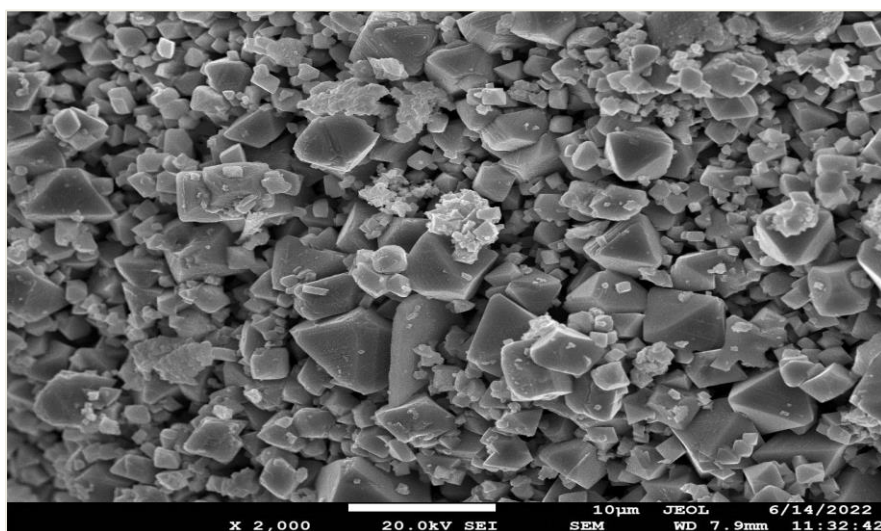
(a)
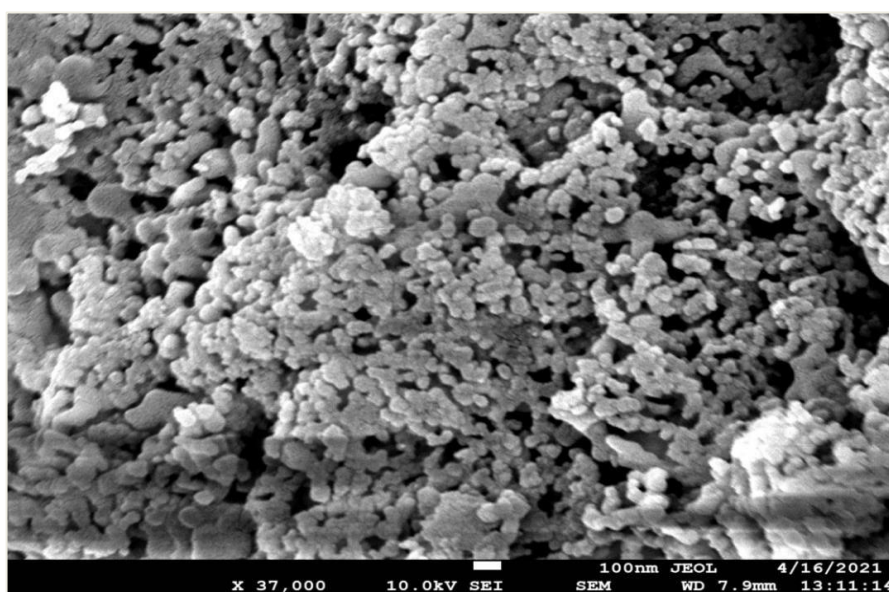
(b)
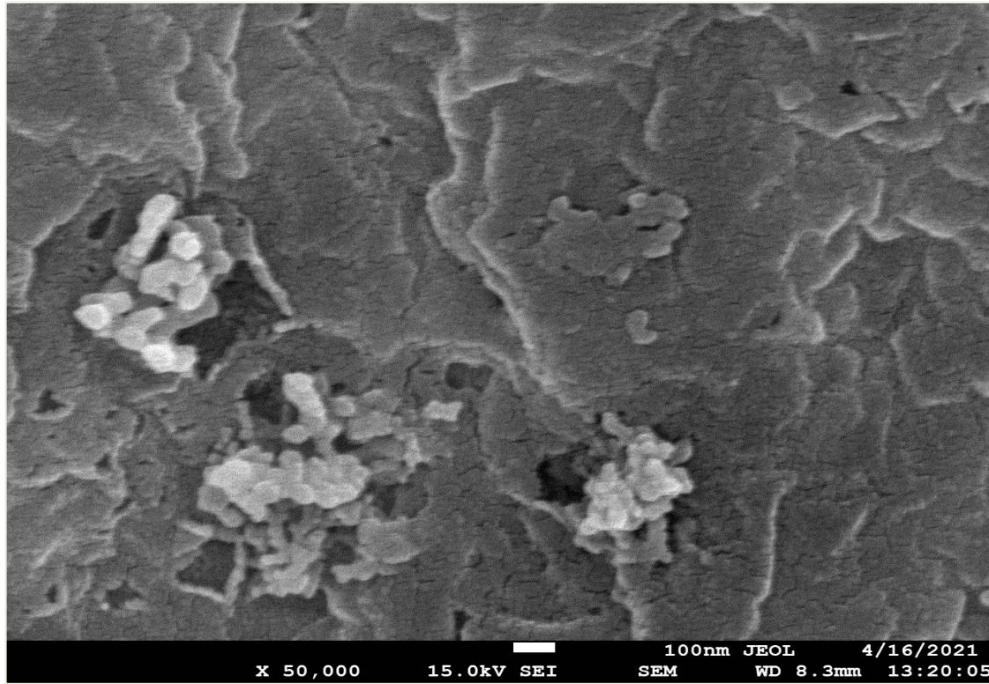
(c)
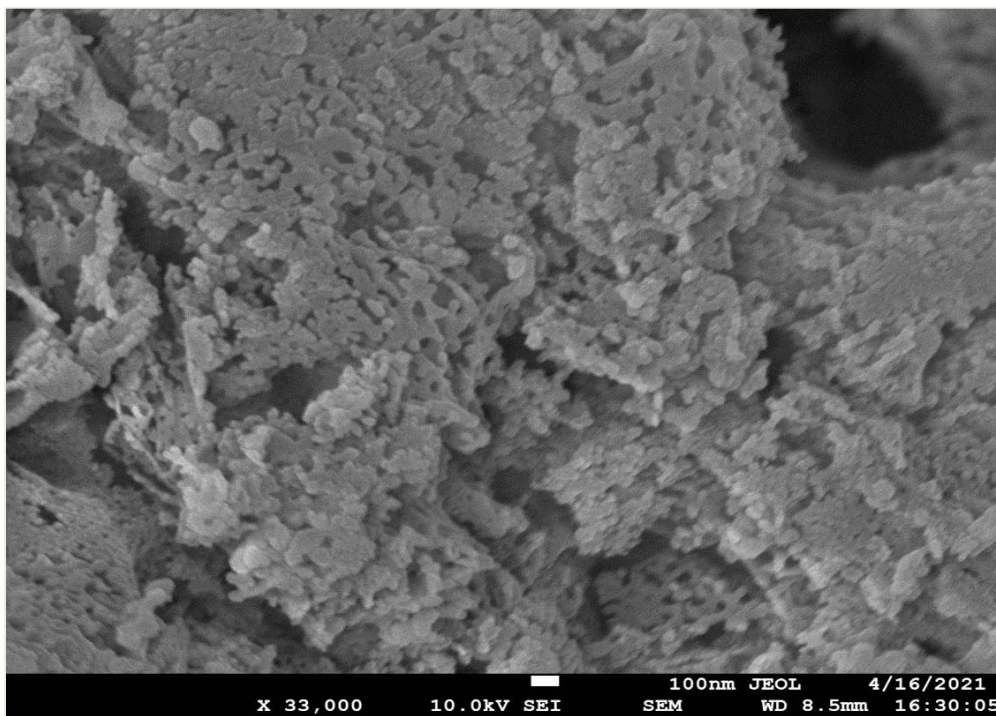
(d)

Figure 4.1.5- FESEM images of (a) Zinc ferrite, (b) Zinc ferrite-rice husk silica (c) Zincferrite-mango starch (d) Zinc ferrite-carboxy methyl starch

4.1.4 Energy Dispersive Spectra (EDS)

Energy dispersive spectra (EDS) is a technique used to analyze the elemental composition of a sample. Energy Dispersive spectra of Zinc metal ferrite and its magnetic green composites viz. ZFN-RHS, ZFN-MS and ZFN-CMS have been shown in figures 4.1.6 (a-d), respectively. The results of EDS are shown in table 4.1.1. Table 4.1.1 revealed that silicon is present in ZFN-RHS, whichis absent in ZFN. This indicated that rice husk silica is successfully attached with zinc ferrite. Carbon as an element was found in significant amount in ZFN-MS and ZFN-CMS compositeswhich was not present in pure ZFN, which confirms the modification of ZFN with mango starch and carboxy methyl mango starch.
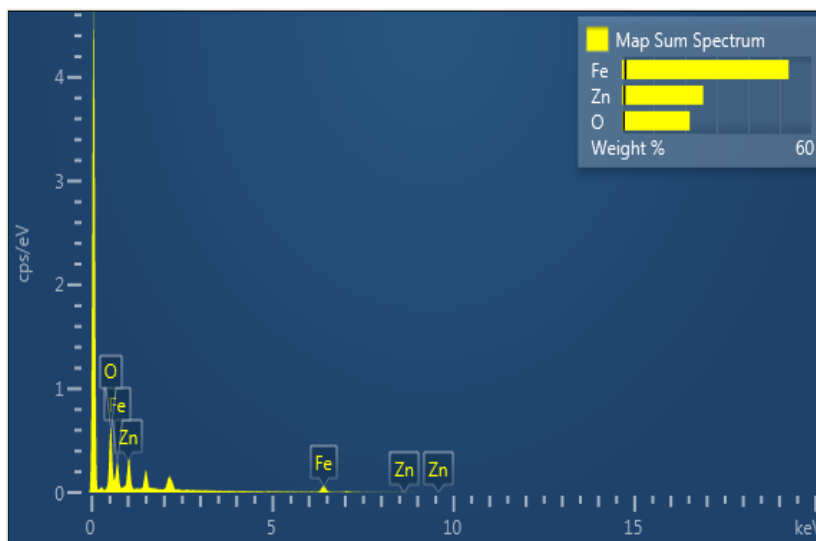
(a)
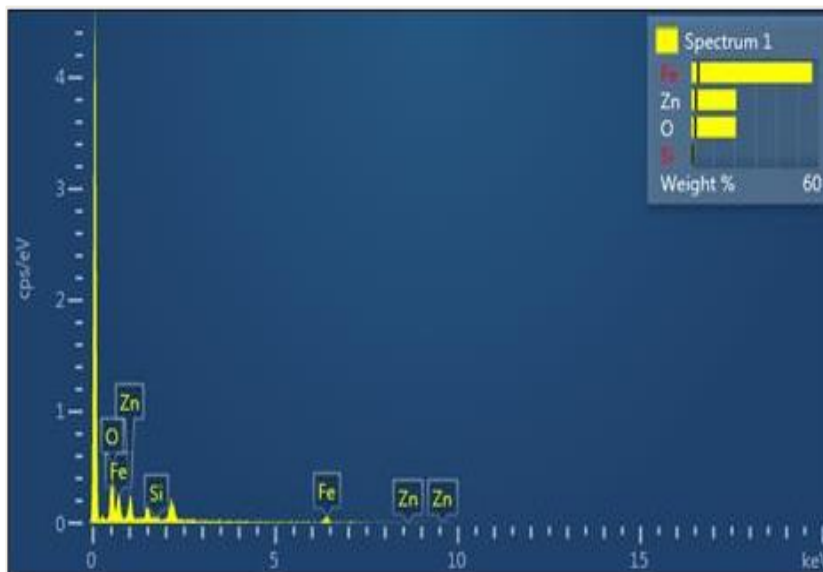
(b)
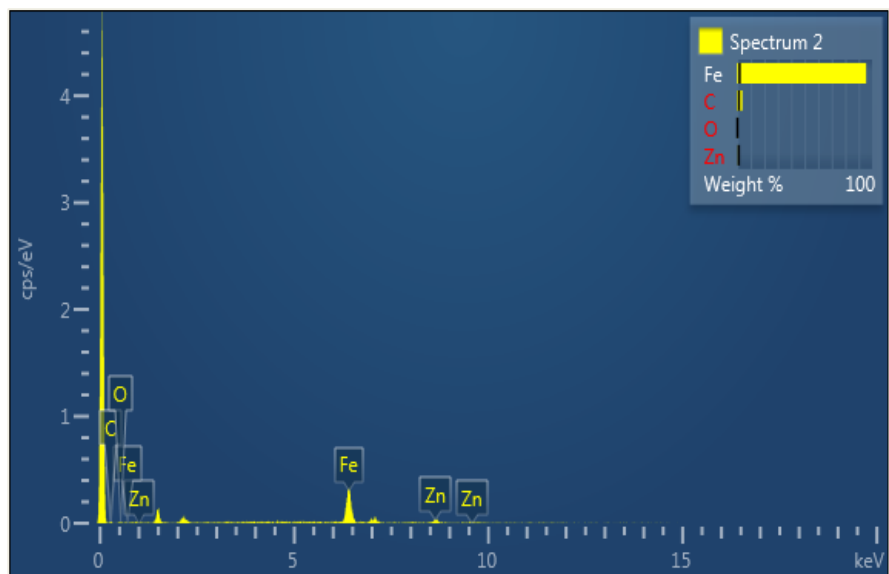
(c)
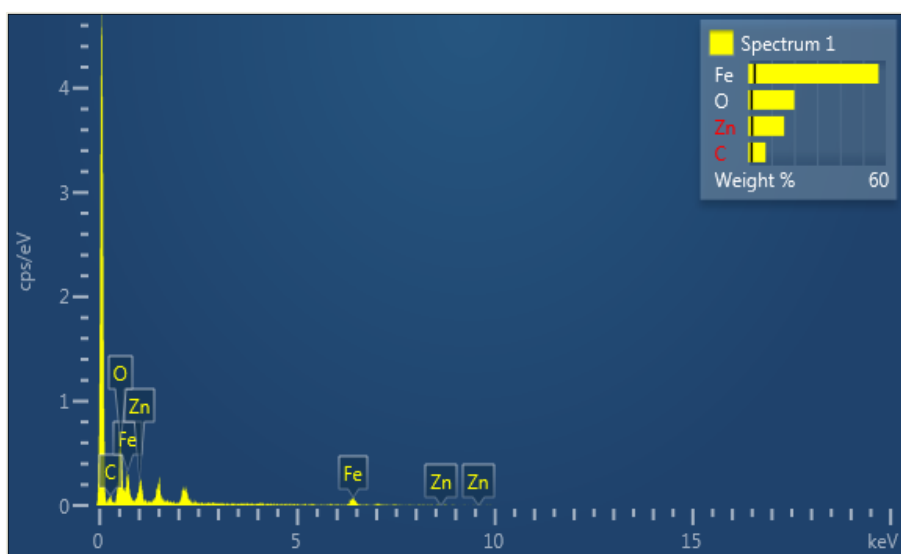
(d)

Figure 4.1.6- Energy Dispersive Spectra of (a) Zinc ferrite, (b) Zinc ferrite-rice husk silica, (c) Zinc ferrite-mango starch, (d) Zinc ferrite-carboxy methyl starch

Table 4.1.1- Composition of elements in Zinc ferrite and its magnetic green composites(ZFN-RHS, ZFN-MS and ZFN-CMS)

Constituent Elements	Zinc-ferrite (ZFN)		Zinc-ferrite-rice husk silica (ZFN-RHS) composite		Zinc-ferrite-mango starch (ZFN-MS) composite		Zinc-ferrite-carboxymethyl starch (ZFN-CMS) composite	
	Weight %	Atomic %	Weight %	Atomic %	Weight %	Atomic %	Weight %	Atomic %
Si	------	------	1.24	1.65	------	-------	------	------
C	------	------	------	------	3.90	15.72	7.51	19.93
O	21.43	50.00	20.84	48.47	20.48	41.44	20.07	40.01
Fe	52.83	35.31	52.48	37.90	56.52	32.77	56.84	32.46
Zn	25.74	14.70	25.44	11.97	19.10	10.07	15.58	7.60
Total	100		100		100		100	

4.1.5 Brunauer-Emmett-Teller analysis (BET)

Brunauer- Emmett- Teller (BET) measures specific surface area (m^2/g) through nitrogen gas adsorption-desorption analysis. In this technique, an inert gas such as nitrogen is flowed over the sample continuously. It is a reliable technique to measure specific surface area, pore size/pore diameter and pore volume of a given solid sample. With the help of Brunauer-Emmett-Teller analysis (BET), specific surface area, volume of pores and diameter of pores of Zinc ferrite and its magnetic green composites viz. Zinc ferrite-rice husk silica, Zinc ferrite-mango starch and Zinc ferrite-carboxy methyl starch was calculated and is represented in table 4.1.2. There is a decrease in the specific surface area of magnetic green composites as compared to pure ZFN's specific surface area (specific surface area of ZFN, ZFN-MS, ZFN-CMS and ZFN-RHS were found to be 3.7020, 3.0233, 2.7790 and 0.4268 m^2/g respectively). There was a decrease of specific surface area because of the attachment of RHS, MS and CMS[10]. There is an increase in the pore volume and pore diameter values (pore volume of ZFN was 0.6519 cm^3/g whereas for ZFN-MS it was found to be 3.6785 cm^3/g, for ZFN-CMS

1.0954 cm^3/g and for ZFN-RHS 1.30201 cm^3/g and the average pore diameterfor ZFN, ZFN-MS, ZFN-CMS and ZFN-RHS were found to be 410.79, 454.25, 416.87 and 423.82 A^o respectively)) as compared to pure ZFN.

Table 4.1.2- BET results of Zinc ferrite and its magnetic green composites viz. ZFN-RHS, ZFN-MS and ZFN-CMS

Parameters	Zinc ferrite (ZFN)	Zinc ferrite-mango starch (ZFN-MS)	Zinc ferrite-carboxy methyl starch (ZFN-CMS)	Zinc ferrite-rice husk silica (ZFN-RHS)
Specific surface area (in m^2/g)	3.7020	3.0233	2.7790	0.4268
Pore vol. of pores (in cm^3/g)	0.6519	3.6785	1.0954	1.30201
Average pore diameter (in A^o)	410.79	454.25	416.87	423.82

4.1.6 Thermo Gravimetric Analysis (TGA)

Thermo Gravimetric Analysis (TGA) shows thermal stability of substance. TGA results for Zinc metal ferrite and its magnetic green composites viz. ZFN-RHS, ZFN-MS and ZFN-CMS have been shown in figure 4.1.7. TGA analysis for ZFN, ZFN-MS, ZFN-CMS and ZFN-RHS magnetic green composites was carried out at temperature ranging from 50 to 600°C at 10°C per minute of heating in air atmosphere.

ZFN- It was observed that around 100°C, there was approximately 11% weight loss in pure ZFN due to the vaporization of trapped moisture in it. Thereafter, no weight loss was observed in the TGA of ZFN indicating its thermal stability at higher temperature.

ZFN-MS-At 120°C, approximately 10% weight loss was observed in ZFN-MS magnetic green composite due to the vaporization of water molecules in the sample. At about 250°C, another 28% loss in weight was observed because functional groups present in ZFN-MS were lost. Another loss of 8% in weight was noted in temperature range 400-450°C, due to complete

degradation of mango starch in ZFN-MS. Based on the data it was found that approximately 0.40g of starch was attached in 1g of ZFN-MS magnetic green composite.

ZFN-CMS-A weight loss of approximately 7% was noted at temperature about 100°C, which might be caused by evaporation of water molecules in ZFN-CMS magnetic green composite. Further, weight loss of 23% was observed between 250-300°C. This was observed due to degradation of carboxyl and other functional groups present in ZFN-CMS. Additional loss in weight about 19% was noted in temperature between 400-450°C, which may be due to complete degradation of carboxyl and other functional groups present in ZFN-CMS. Based on the data it was estimated that approximately 0.45g of carboxy methyl starch was found to be attached with 1g of ZFN-CMS.

ZFN-RHS-At 100°C, approximately 10% weight loss was observed in ZFN-RHS. This was due to the vaporization of the moisture in the magnetic green composite. Then, it followed a sharp weight loss of 33% from 170°C to 350°C. The total weight loss of 52% at 350°C indicated the decomposition of silica and other functional groups present in ZFN-RHS. Further, weight loss of 12% was observed above 350°C. Based on the data it was found that approximately 0.50g of silica was attached with 1g of ZFN-RHS.
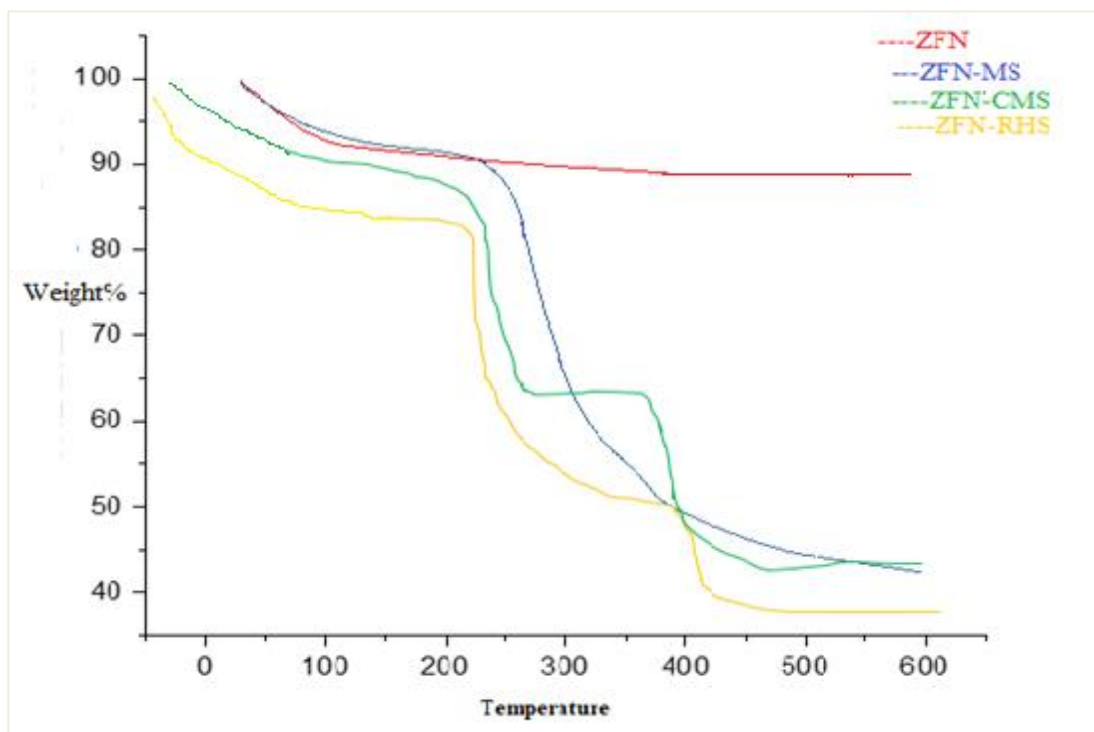
Figure 4.1.7- TGA plots for Zinc ferrite, Zinc ferrite-rice husk silica, Zinc ferrite-mango starch and Zinc ferrite-carboxy methyl starch

### 4.1.7 Point Zero Charge pH (pH$_{pzc}$)

pH$_{pzc}$ depicts the value of hydrogen ion concentration where the electric charge density on the surface of adsorbent comes out to be zero. This was calculated using solid addition method[11]. Figure 4.1.8 shows the graph plotted between difference of initial pH (pH$_i$) and final pH (pH$_f$) v/s pH$_i$. From these plots pH$_{PZC}$ of Zinc ferrite and its magnetic green composites viz. ZFN-RHS, ZFN-MS and ZFN-CMS was noted (where the graph touches pH$_i$ i.e. x-axis depicted the pH$_{PZC}$ value). The pH$_{pzc}$ of ZFN, ZFN-RHS, ZFN-MS and ZFN-CMS magnetic green composites is 8.4, 4.3, 7.4 and 7.2, respectively. The pH$_{pzc}$ of magnetic green composites is less than pH$_{pzc}$ of pure ZFN, which is due to the presence of RHS, MS and CMS.
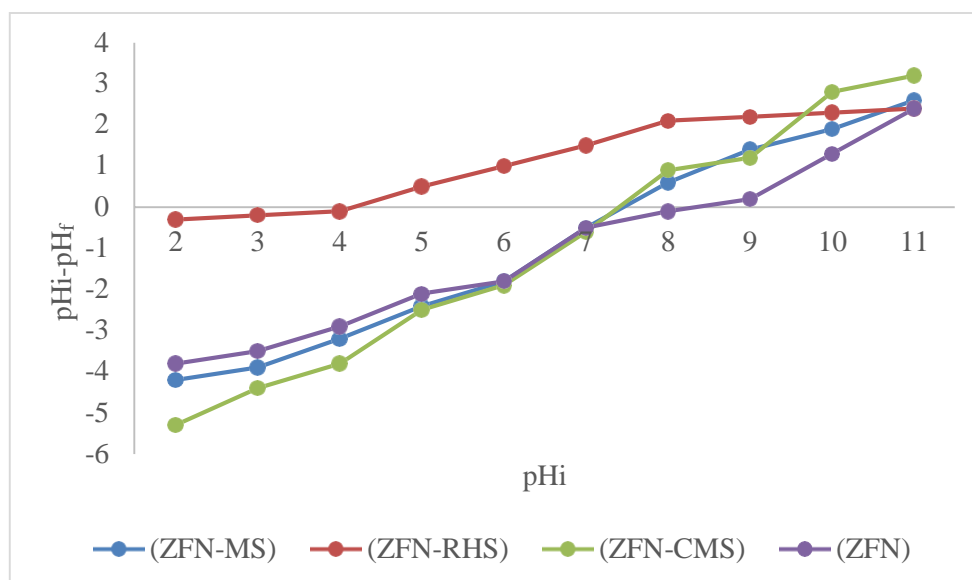
Figure 4.1.8- pH$_{pzc}$ of Zinc ferrite and its magnetic green composites viz. ZFN-RHS, ZFN- MS and ZFN-CMS

Part II

4.2 Batch adsorption studies with dyes

Different dyes selected in preliminary studies (Crystal violet, Brilliant green, Malachite green and Methylene blue) were taken for the adsorption studies with magnetic green composite ZFN-CMS in single dye system.

4.2.1 Adsorption of dyes using ZFN-CMS magnetic green composite

4.2.2 Single dye system

Batch mode of adsorption was preferred for analyzing adsorption potential of ZFN-CMS magnetic green composite for removal of selected dyes-Methylene blue(MB), Brilliant green (BG), Crystal violet (CV) and Malachite green (MG) in single dye system. Various parameters like effect of contact time, dose of composite, concentration of dye solution, varying temperature and pH were taken into consideration in batch mode adsorption studies. Parameter wise effect is described in the following sections.

4.2.3 Effect of contact time

Time is a factor on which adsorption depends greatly. For the study of this parameter concentration of dyes selected was 50 mgL^{-1} for single dye system. 50 mL of solution of dyes was kept in contact with 0.1g of magnetic green composite (at temperature 25°C) in a thermostatic shaker. After every 15 min. the samples were drawn and the absorbance of dyes was recorded using a UV-visible spectrophotometer from which the residual concentration was calculated. It was noted that as time increased, adsorption also increased and reached equilibrium stage at around 180 min. Effect of time on concentration and percentage removal of dyes using ZFN-CMS is shown in figure 4.2.1 for single dye system. It can be observed in the figure that the residual concentration of dyes decreased with time, whereas percentage removal increased with time. At initial stage, removal of dyes was very fast and after some time it achieved equilibrium stage. This was observed because a large number of vacant sites were available on ZFN-CMS magnetic green composite's surface at initial stage and after sometime more competition was observed among dye molecules to occupy vacant sites. When all vacant sites were occupied, equilibrium was assumed to be achieved[12].
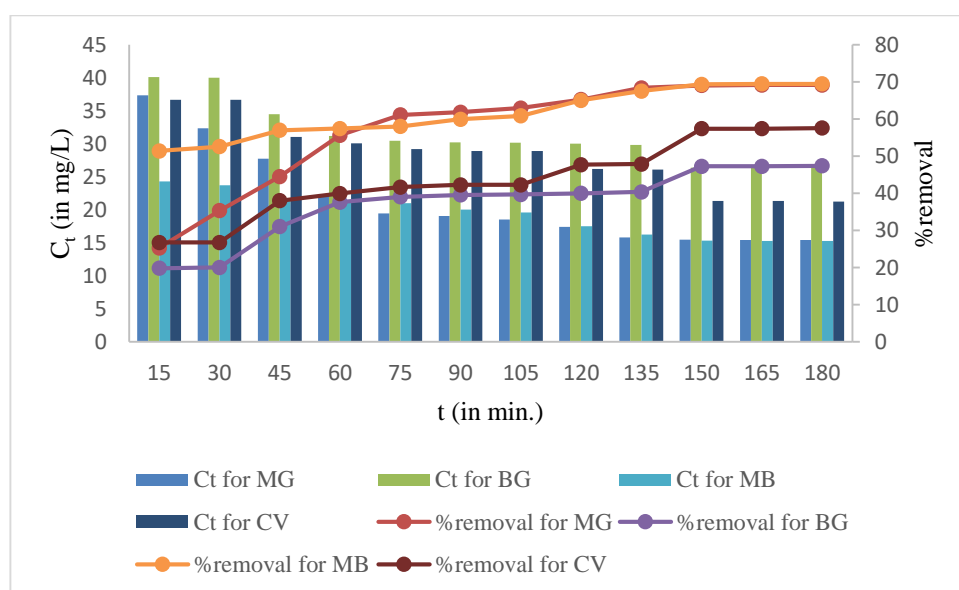
Figure 4.2.1- Effect of contact time in single dye system using ZFN-CMS

4.2.4 Kinetic studies

Adsorption kinetics revealed nature of adsorption of dyes by adsorbent. To describe the adsorption behavior of ZFN-CMS, kinetic models like Lagergren pseudo first order, Pseudo second order, Elovich and Weber Morris intra-particle diffusion models were used. Figures 4.2.2, 4.2.3 and 4.2.4 represent Lagergren pseudo first order, Pseudo second order and Elovich model of kinetics respectively for the removal of cationic dyes used in this study. Table 4.2.1 represents the kinetic constants associated with kinetic models calculated for removing selected dyes by using ZFN-CMS. The correlation coefficient (R^2) value were used to check which model fitted better for removing dyes using ZFN-CMS. More closely a model fits the data, if its R^2 value is near to 1. If the computed R^2 value for Lagergren pseudo-first order model is very near to 1, adsorption has a physisorption character and follows Lagergren pseudo-first order model. The adsorption, however, shows chemisorption characteristics if R^2 value for the pseudo second order model is higher[13]. In this study, the R^2 values were greater for pseudo-second order model, for the removal of dyes CV, BG, MB and MG from aqueous solution using ZFN-CMS according to table 4.2.1. Thus, the sequestration of dyes in single dye system using ZFN-CMS followed pseudo-second order model followed by Elovich and then Lagergren pseudo first order kinetics. As a result, the nature of adsorption of dyes in single system using ZFN-CMS is chemical in nature.
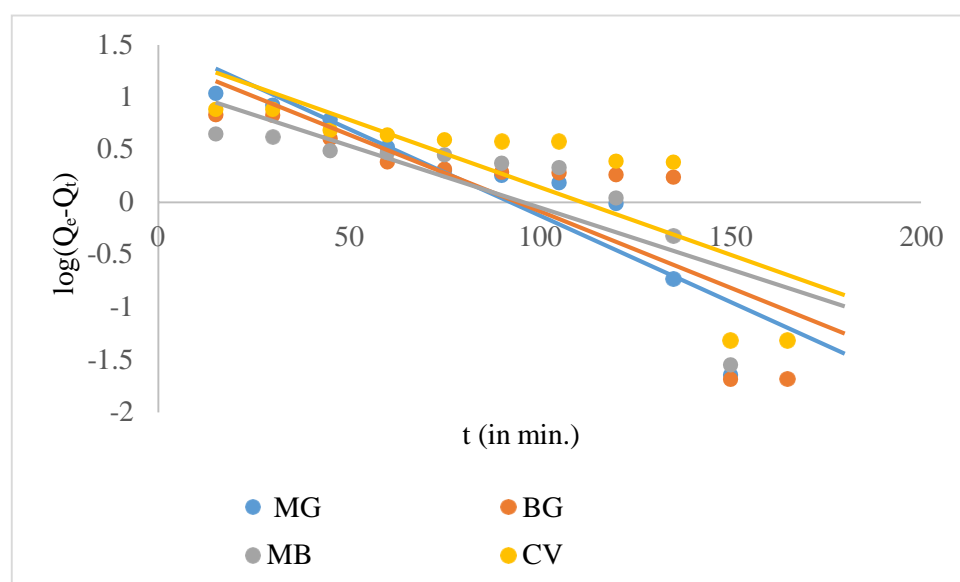
Figure 4.2.2- Lagergren pseudo first order kinetics for single dye system using ZFN-CMS
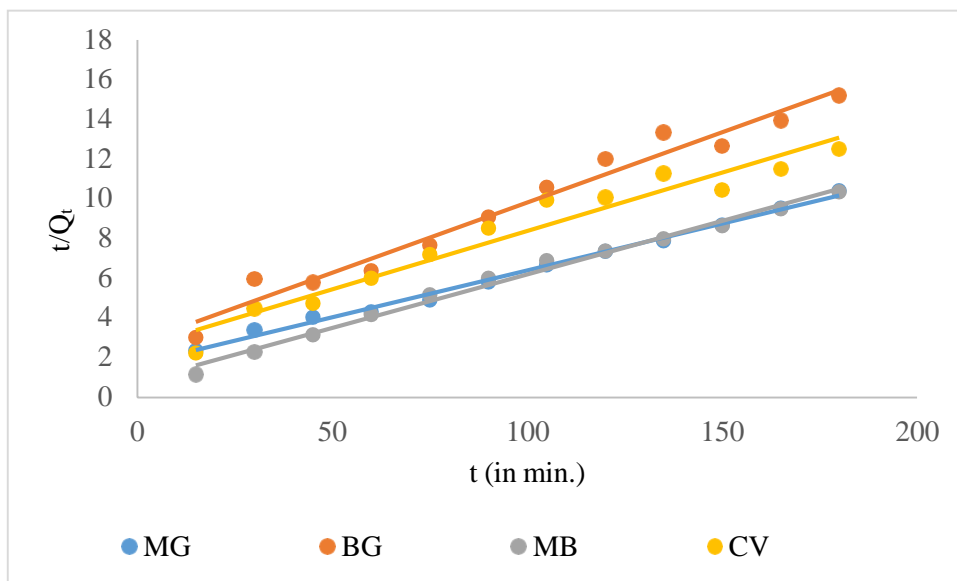
Figure 4.2.3- Pseudo second order kinetics for single dye system using ZFN-CMS
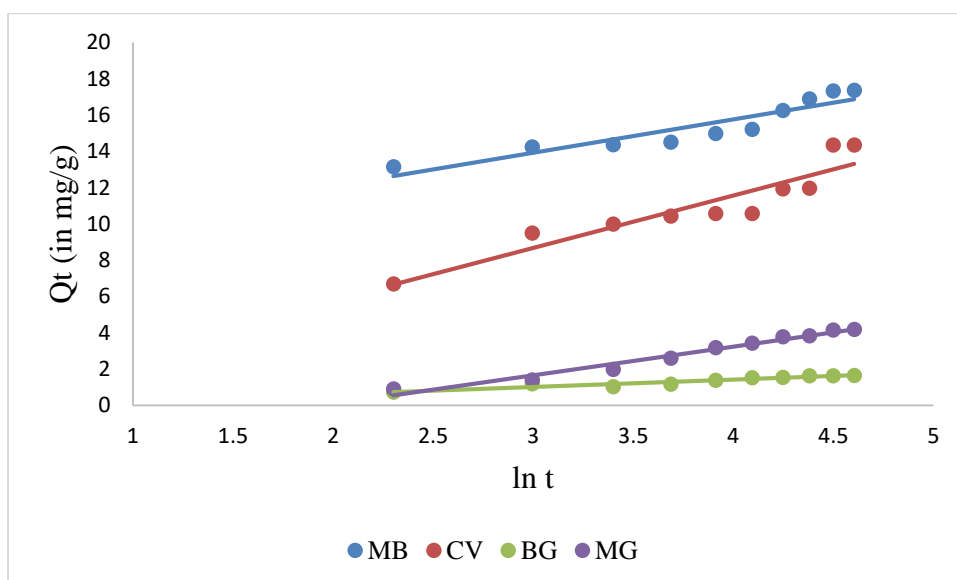
Figure 4.2.4- Elovich model of kinetics for single dye system using ZFN-CMS

Table 4.2.1- Kinetic constants calculated for single dye system using ZFN-CMS

Model of kinetic study	Kinetic constants	Methylene Blue (MB)	Crystal Violet (CV)	Malachite Green (MG)	Brilliant Green (BG)
Lagergren pseudo first order	Q_{e1}	12.851	25.698	29.457	22.825
	K_1	0.023	0.032	0.029	0.033
	R^2	0.753	0.698	0.547	0.737

	SD	0.132	0.059	0.189	0.122
Pseudo second order	Q_{e2}	21.222	17.341	15.889	24.935
	h	1.112	0.405	1.131	0.371
	K_2	0.0030	0.0012	0.0014	0.0012
	R^2	0.9987	0.9799	0.9981	0.9581
	SD	0.142	0.156	0.163	0.176
Elovich model	α	0.812	1.173	1.152	0.823
	β	0.267	0.324	0.425	0.198
	R^2	0.845	0.886	0.864	0.9123
	SD	0.285	0.439	0.348	0.348

The Weber Morris intra-particle diffusion model was utilised for studying intra-particle diffusion behavior of adsorbent. Figure 4.2.5 shows Weber Morris plot for removing the selected cationic dyes (CV, BG, MB and MG) using ZFN-CMS. The intra-particle diffusion rate constant is depicted by K_{int}, and if slope on the graph of Q_t v/s $t^{0.5}$ is a straight line, then it is considered as rate limiting step. The straight line should pass through origin[14], if this is the rate-limiting step. However, in figure 4.2.5, neither the plot is linear nor it is passing through origin. This suggested that there were additional elements other than intra-particle diffusion (electrostatic force of attraction such as electrostatic interaction) that affected adsorption of dyes in single system using ZFN-CMS.
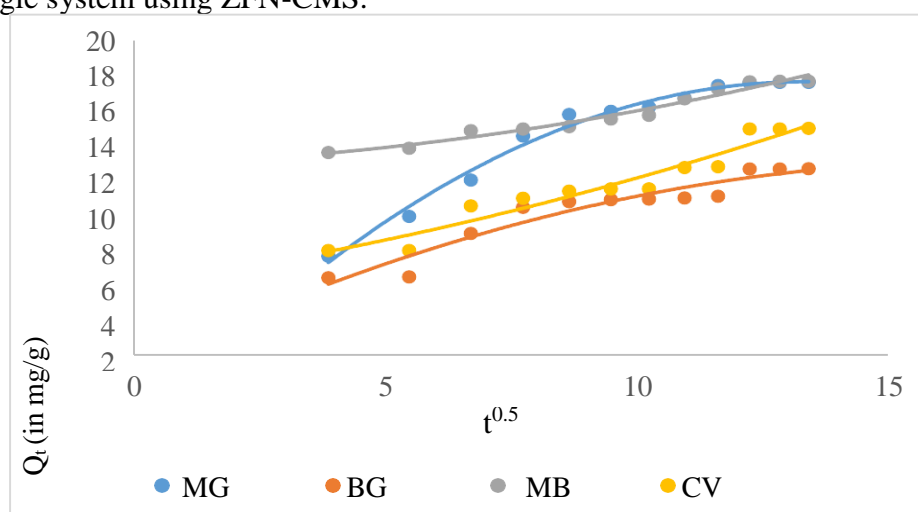
Figure 4.2.5- Weber Morris intra particle diffusion curves for single dyes using ZFN-CMS

4.2.5 Effect of pH

The potential of adsorbent to remove dye is influenced by the pH of aqueous solution as pH of

solution affect the surface charge of adsorbent. It significantly contributes to the adsorption process. At various pH levels, the adsorption of individual dyes viz. MG, CV, BG, and MB with ZFN-CMS magnetic green composite was investigated. With initial dye concentration 50 mg/L and an equilibrium time three hours, initial pH value of solution was changed from 3-11 in order to evaluate the effect of pH (at 25°C and at 200 rpm)[15]. It was noted that the dyes removal percentage grew steadily as the solution's pH rose, reaching a maximum at pH 7-8 (Figure. 4.2.6) before declining at higher pH values. The pH_{pzc} value of the ZFN-CMS composite, which is 7.2, correlates to a maximum pH range of 7-8. It showed that at pH 7-8, the most dye molecules attached to the surface of ZFN-CMS magnetic green composite. As the pH value exceed from pH_{pzc} value, the surface of ZFN-CMS becomes negatively charged and therefore, cationic dye molecules get attached with the surface of adsorbent. The maximum efficiency for removing dyes in single dye system using ZFN-CMS for MG, BG, MB and CV dyes were found to be 74%, 56%, 76% and 62%, respectively.
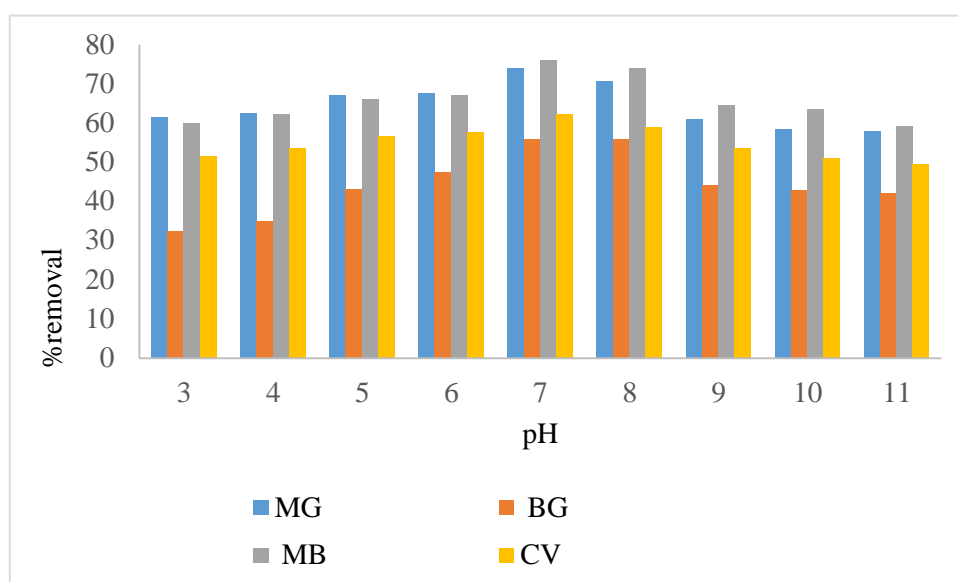
Figure 4.2.6- Effect of pH for single dye system using ZFN-CMS

4.2.6 Effect of adsorbent dose

The amount of ZFN-CMS magnetic green composite was altered from 0.1 to 0.5 g in 50 mL of 50 mg/L dye solution for single dye system for the selected dyes. Figure 4.2.7 shows that an increase in the amount of ZFN-MS magnetic green composite, lead to increase in percentage removal of dyes CV, MB, BG and MB. By increasing adsorbent dose, an increase in number of active sites for adsorption of dyes was achieved, which was the cause

of increasein the percentage removal of various dyes[16]. Using ZFN-CMS, removal efficiency of MG, BG, MB and CV dyes increased from 69.1% to 79.9%, 47.3% to 59.1%, 69.4% to 77.5% and 57.5% to 74.4%, respectively. On the other hand, when the amount of adsorbent increased, the adsorption capacity (Q_e) decreased. This was observed because additional active sites were present onto the surface of adsorbent, which remained empty as adsorbent concentration increased[17].
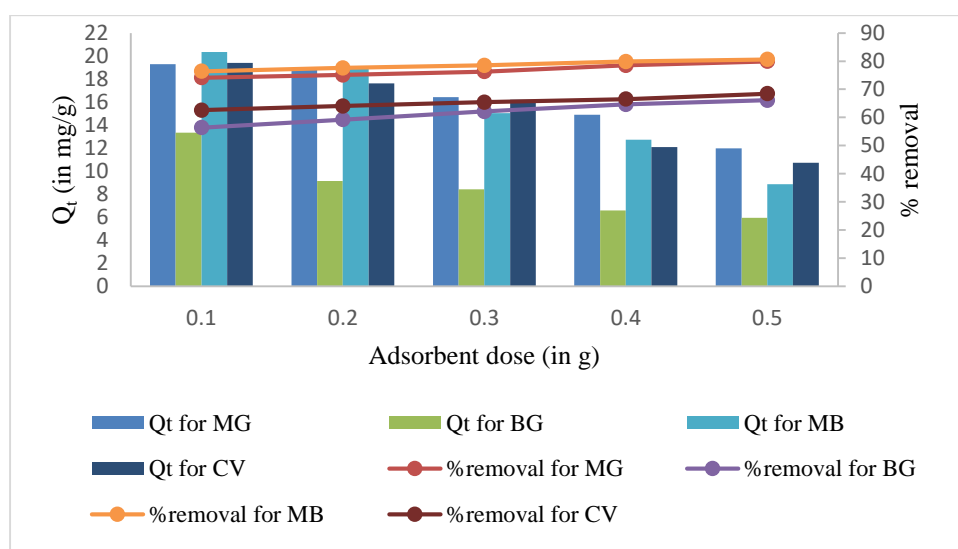
Figure 4.2.7- Effect of adsorbent dose in single dye system using ZFN-CMS

4.2.7 Effect of Concentration and temperature

Effect of change in concentration of dyes MG, CV, BG, and MB was investigated at different temperatures -25°C, 30°C, and 35°C using ZFN-CMS. Initial concentration of dyes were varied from 50-250 mg/L, 0.1g of adsorbent and 50 mL of dye solution was taken. Figure 4.2.8 shows the concentration and temperature effect on removal of selected cationic dyes using ZFN-CMS magnetic green composite. Adsorptioncapacity (Q_e) for various dyes increased as dye concentration was increased. This increase in adsorption capacity may be brought about by stronger interactions between molecules of adsorbate and adsorbent due to increased collision rate. On the other hand, as the concentration of dyes (CV, BG, MB and MG) increased, the percentage removal of various dyes decreased. It might be explained by the fact that as dye concentration rises, fewer active sites become available for adsorption. It is evident from figure 4.2.8 that adsorption of various dyes increased as temperature increased, revealing that adsorption process was endothermic in nature[18]. A stronger electrostatic interaction between molecules of dyes and adsorbent lead to increase in adsorption capacity with temperature[19]. The surface area accessible for the adsorption of various dye molecules increased as a result of increase in the size of adsorbent'spores with the rise in temperature[20].
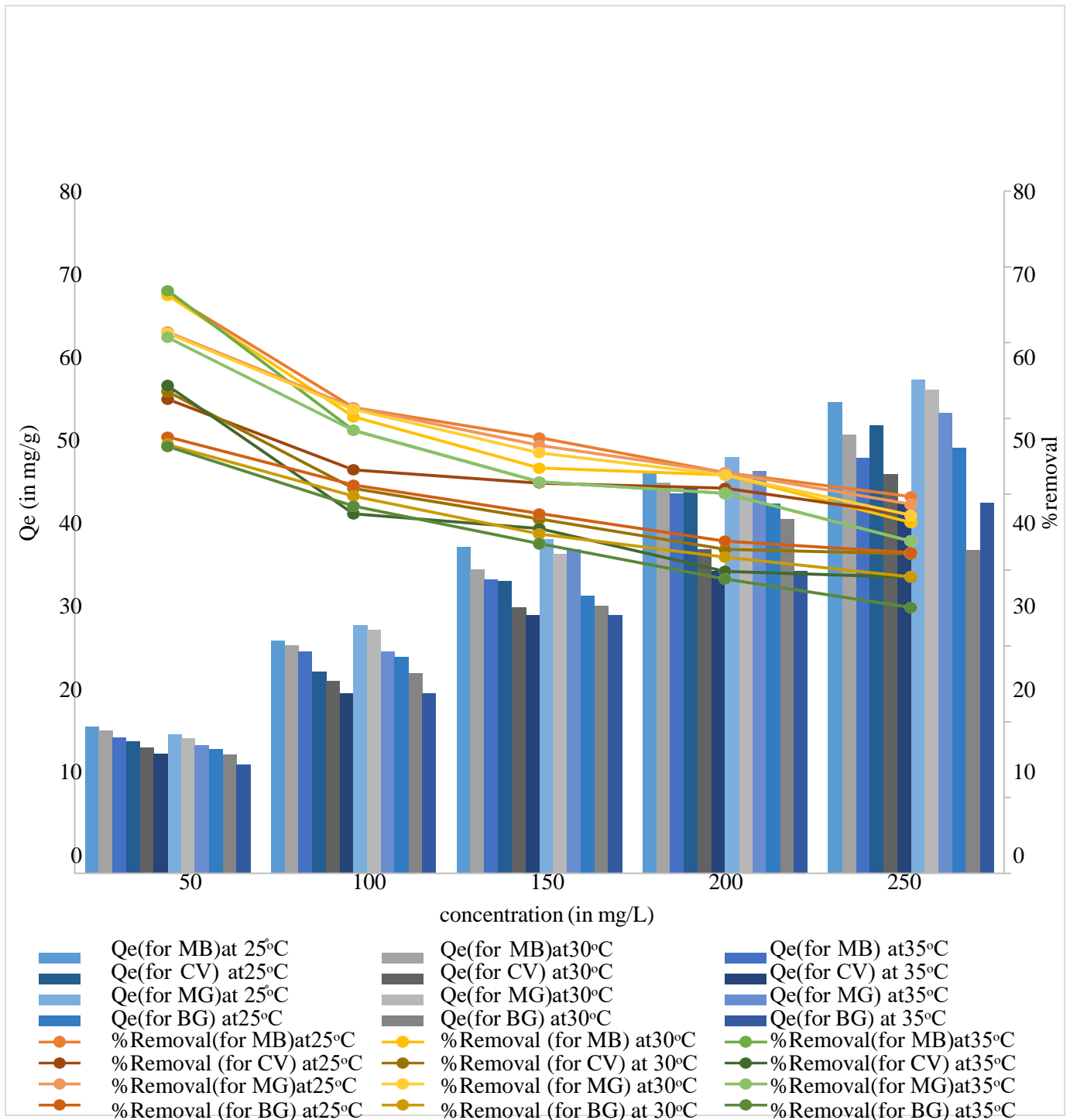
Figure 4.2.8-Effect of concentration and temperature in single dye system using ZFN-CMS

4.2.8 Adsorption isotherms

The adsorption behavior of MG, CV, BG, and MB dyes was described using isotherm models-
Langmuir, Freundlich, Temkin, and Dubinin-Raduskevich (D-R), at three distinct temperatures
-25ºC, 30ºC, and 35ºC. The adsorption isotherm plots are shown in Figures 4.2.9 (a-d).
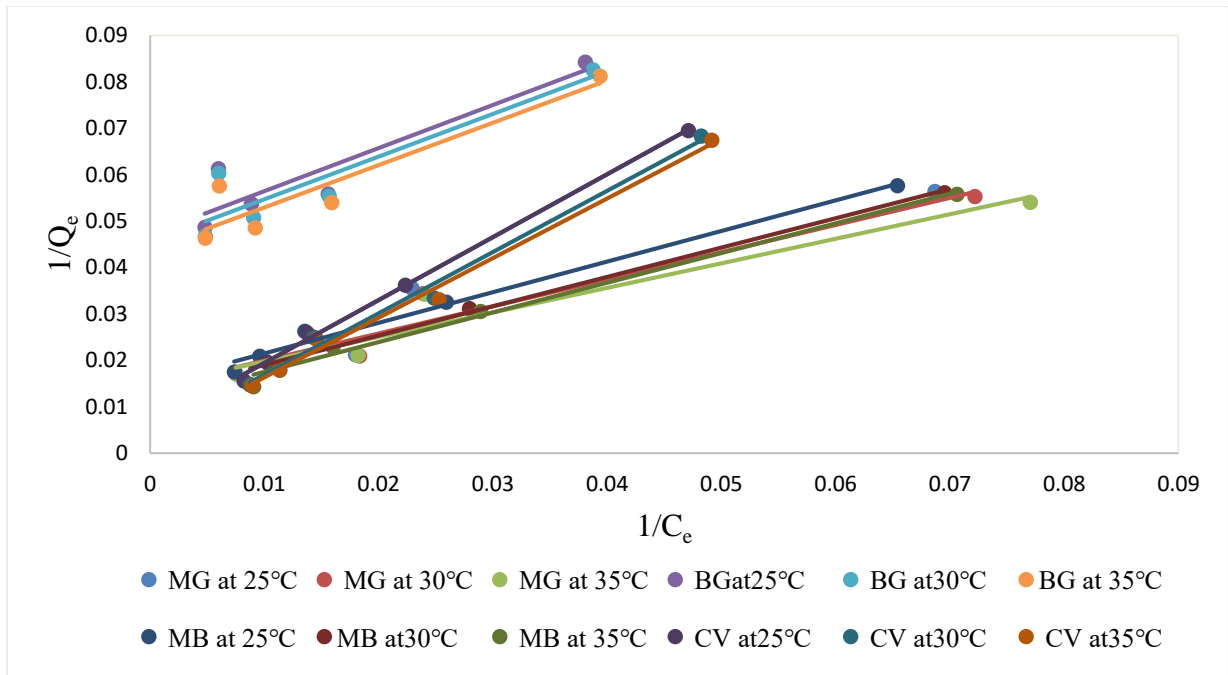
Figure 4.2.9 (a) - Langmuir isotherm for single dye system using ZFN-CMS
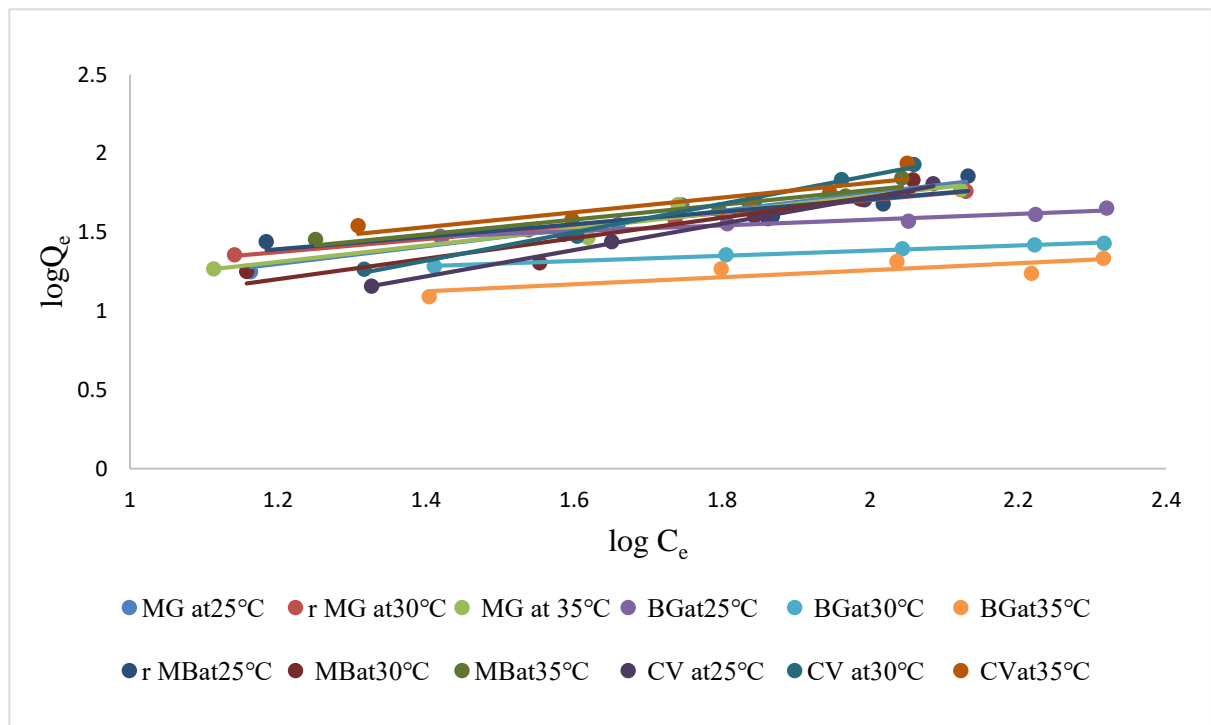
Figure 4.2.9 (b) - Freundlich isotherm for single dye system using ZFN-CMS
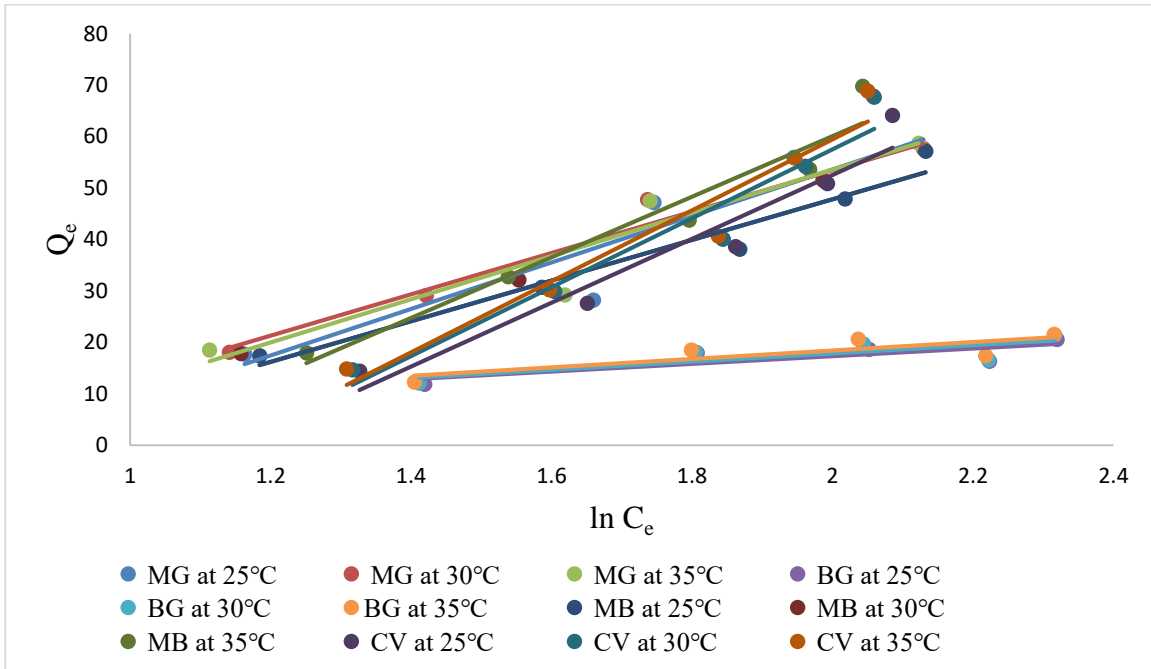
Figure 4.2.9 (c) - Temkin isotherm for single dye system using ZFN-CMS
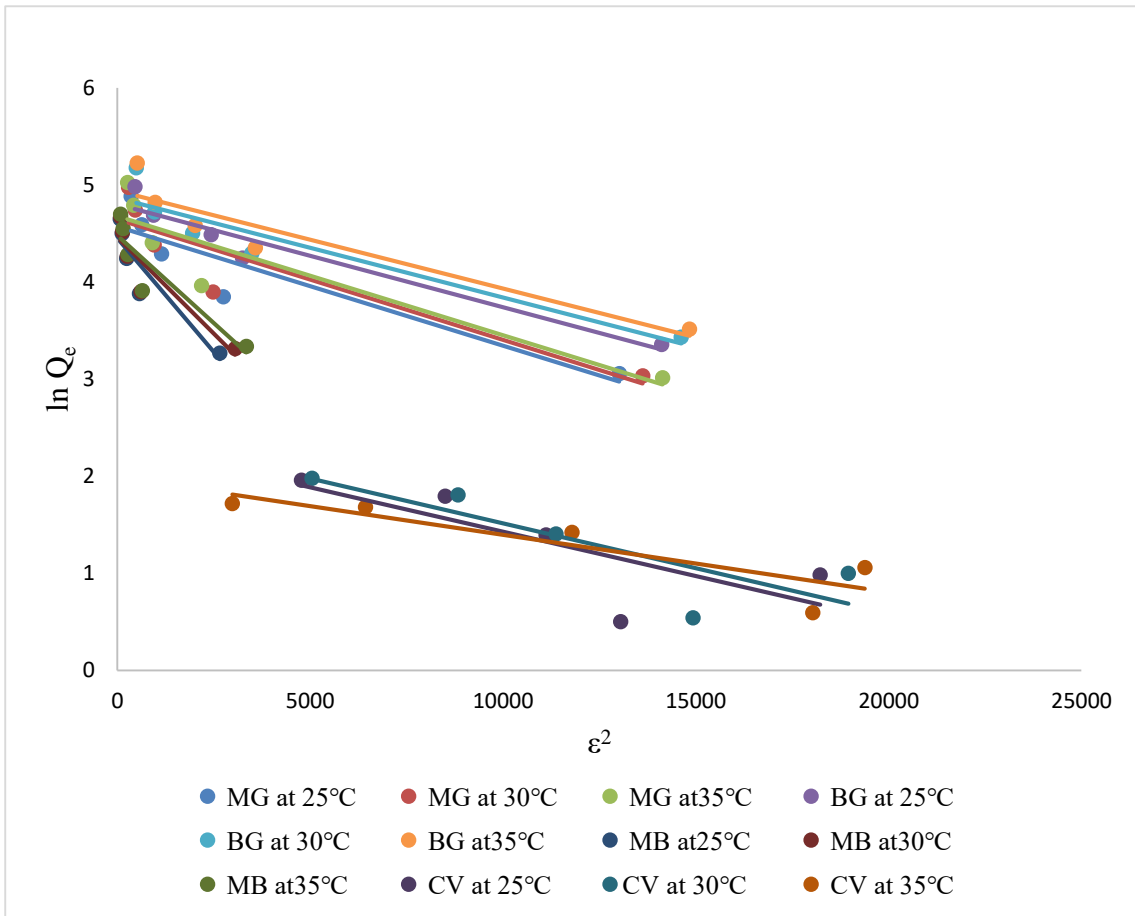
Figure 4.2.9 (d) – D-R isotherm for single dye system using ZFN-CMS

Different adsorption isotherm constants were calculated using adsorption isotherm plots. The derived values of various adsorption isotherm constants for various dyes (CV, BG, MB and

MG) are shown in Table 4.2.2. The calculated R^2 values for Langmuir and Temkin model came out to be the highest among various adsorption isotherm models. As a result, according to the Langmuir adsorption isotherm hypothesis, ZFN-CMS magnetic green composite has active sites which were uniformly distributed on its surface, and adsorption of various dyes (CV, BG,MB and MG) resulted in the formation of a monolayer on the surface. According to Temkin's hypothesis, the heat of adsorption increased linearly, confirming the adsorbent's uniform surface. Additionally, a separation factor (R_L) which is associated with Langmuir isotherm can be calculated to describe the nature of Langmuir isotherm. According to the values of R_L, there are four different types of adsorption taking place: irreversible ($R_L=0$), linear ($R_L =1$), favourable ($0< R_L<1$), and unfavourable ($R_L>1$)[21]. It was found that the predicted values of R_L for various dyes (CV, BG, MB and MG) ranged from 0 to 1. It demonstrated favourable adsorption of selected cationic dyes onto ZFN-CMS magnetic green composite. One of the constants associated with the D-R isotherm model that is useful to ascertain the nature of the adsorption process is adsorption energy (E). Adsorption can be classified as physical if the adsorption energy E is less than 40 kJ/mol[22]. More than 100 kJ/mol of adsorption energy was calculated in the present study, confirming the chemisorption character of the adsorption using ZFN-CMS magnetic green composite (Table 4.2.2). Maximum adsorption capacities using ZFN –CMS magnetic green composite for removal of dyes MG, BG, MB and CV were found to be 101.3, 132.1, 98.3 and 114.9 mg/g, respectively.

.

4.2.9 Thermodynamics of adsorption

Different thermodynamic relationships (Gibbs Helmholtz equation and Van't Hoff equation mentioned in section 3.7) were used to determine various thermodynamic parameters, including enthalpy change, free energy change, and entropy change. The slope and intercept of the graph between lnK_d and 1/T were used to compute the values of enthalpy change and free energy change[23]. Figure 4.2.10 shows the graph between lnK_d and 1/T for the data obtained in removing selected cationic dyes from aqueous solution using ZFN-CMS at various concentrations. Table 4.2.3 shows the thermodynamic constants for removing selected cationic dyes (CV,BG, MB and MG) using ZFN-CMS magnetic green composite at various concentrations.

Table 4.2.2- Adsorption isotherm constants for single dye system using ZFN-CMS

System→ Isotherm Model ↓	Const.	Malachite green			Brilliant green			Methylene blue			Crystal violet		
Temperature →		25ºC	30ºC	35ºC	25ºC	30ºC	35ºC	25ºC	30ºC	35ºC	25ºC	30ºC	35ºC
Langmuir	Q	96.7	97.8	101.3	118.9	127.5	132.1	95.9	97.7	98.3	108.4	112.3	114.9
	b	0.01	0.014	0.103	0.012	0.014	0.015	0.012	0.014	0.012	0.012	0.013	0.013
	R^2	0.993	0.996	0.998	0.997	0.995	0.998	0.996	0.998	0.995	0.997	0.998	0.996
	SD	0.001	0..002	0.002	0.002	0.003	0.002	0.001	0.002	0.003	0.002	0.002	0.003
	R_L	0.212	0.226	0.229	0.244	0.252	0.261	0.321	0.342	0.358	0.257	0.262	0.287
Freundlich	K_f	3.6	4.8	5.2	4.2	4.7	4.8	3.9	4.5	5.3	4.1	4.7	4.9
	1/n	0.589	0.596	0.612	0.678	0.688	0.692	0.612	0.638	0.649	0.678	0.681	0.684
	R^2	0.943	0.957	0.962	0.979	0.981	0.972	0.954	0.966	0.969	0.977	0.980	0.984
	SD	0.055	0.059	0.062	0.055	0.061	0.063	0.049	0.054	0.056	0.041	0.045	0.048
D-R	Q_m	52.9	56.2	57.3	65.2	67.7	69.6	51.8	52.3	54.6	58.7	61.3	62.4
	K_{DR}	4×10^{-5}	3×10^{-5}	3×10^{-5}	3×10^{-5}	2×10^{-5}	4×10^{-5}	3×10^{-5}	4×10^{-5}	5×10^{-5}	4×10^{-5}	5×10^{-5}	5×10^{-5}
	R^2	0.979	0.931	0.933	0.917	0.923	0.919	0.913	0.918	0.929	0.908	0.912	0.923
	SD	0.152	0.173	0.184	0.192	0.189	0.194	0.172	0.176	0.181	0.183	0.185	0.182
	E	99.2	115.8	118.9	121.1	124.5	131.6	99.6	105.4	108.9	114.8	121.6	132.5
Temkin	b_T	142.2	145.2	145.8	112.8	118.9	123.2	132.4	134.6	138.9	99.8	102.6	104.5
	A	0.167	0.171	1.176	0.168	0.172	0.179	0.151	0.157	0.164	0.122	0.134	0.140
	R^2	0.997	0.998	0.997	0.998	0.996	0.999	0.998	0.997	0.998	0.996	0.992	0.999
	SD	0.816	0.762	0.818	1.172	1.103	1.115	0.489	0.513	0.583	0.998	1.013	1.105

The values of enthalpy change came out to be positive which depicted endothermic nature of adsorption by ZFN-CMS and positive values of entropy change revealed more randomness at the interface of ZFN-CMS composite and dyes. The spontaneity of adsorption by ZFN-CMS is depicted by negative values of free energy change. It was observed that free energy change (ΔG^o) values were negative at lower concentration, but at higher concentration it came out to be positive. This indicated that the process was spontaneous at lower concentrations whereas it becomes non-spontaneous at higher concentrations.
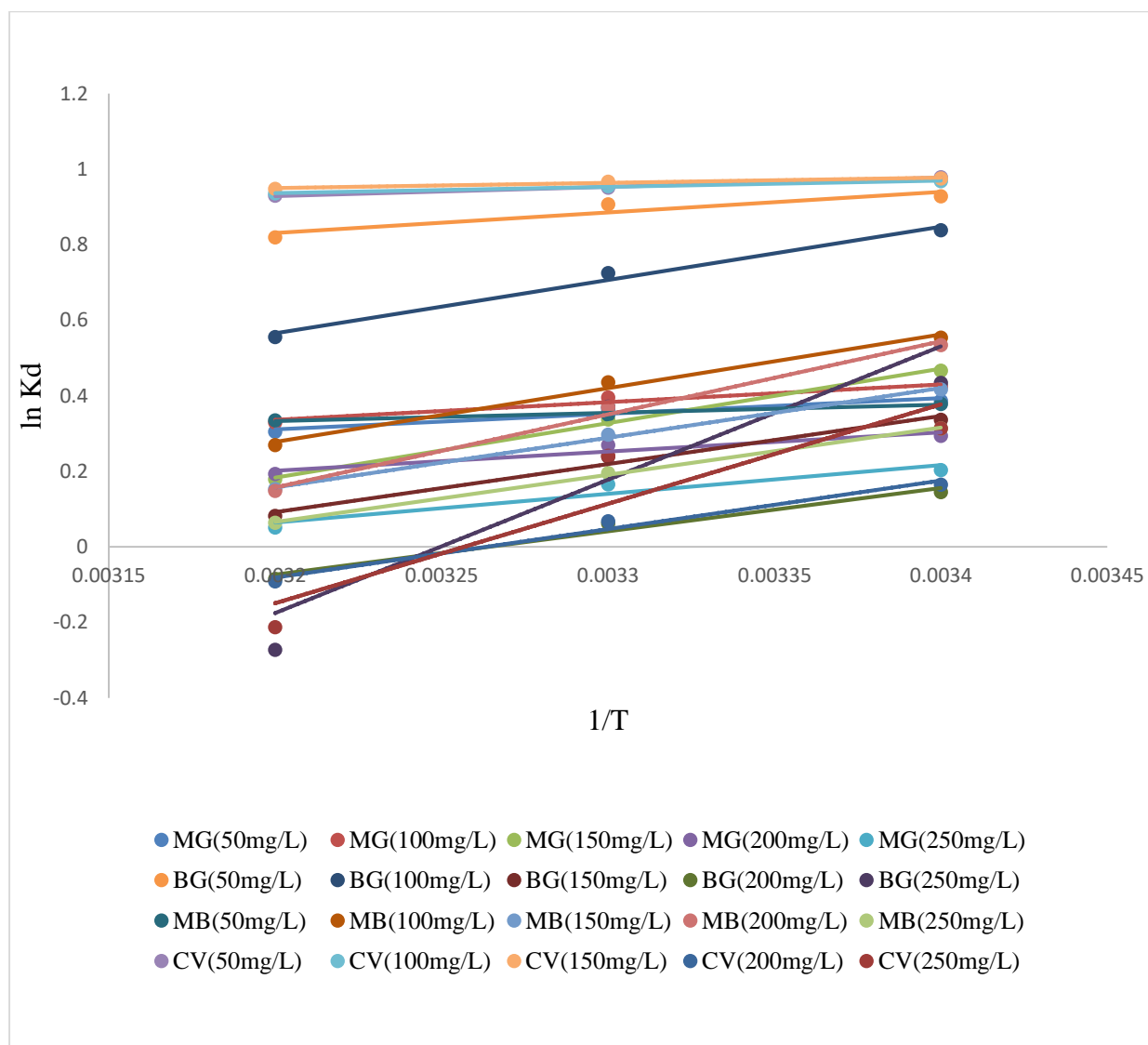
Figure 4.2.10- ln K$_d$ v/s 1/T plot for single dye system using ZFN-CMS

Table 4.2.3- Thermodynamic constants for single dye system using ZFN-CMS

System	Conc. (mg/L)	ΔH^o (kJ/mol)	ΔS^o (J/mol/K)	ΔG^o(25ºC) (kJ/mol)	ΔG^o(30ºC) (kJ/mol)	ΔG^o (35ºC) (kJ/mol)
Malachite green	50	14.9	0.049	-0.292	-0.567	-0.812
	100	14.2	0.048	-0.029	-0.281	-0.538
	150	13.5	0.052	0.698	-0.478	0.285
	200	12.9	0.039	1.112	1.183	0.977
	250	13.3	0.042	1.545	1.656	1.612
Brilliant green	50	12.8	0.044	-0.657	-0.875	-1.112
	100	14.4	0.052	-0.312	0.658	-0.756
	150	15.8	0.056	0.132	-0.143	-0.413
	200	11.3	0.041	0.812	0.612	0.498
	250	12.1	0.039	1.487	1.323	1.213
Methylene blue	50	17.1	0.029	-0.081	-0.353	-0.598
	100	16.8	0.036	0.223	-0.058	-0.364
	150	14.5	0.047	0.934	0.714	0.633
	200	13.7	0.027	1.557	1.432	1.244
	250	12.8	0.028	1.998	1.992	1.714
Crystal violet	50	18.9	0.058	-0.534	-0.867	-1.186
	100	18.3	0.055	-0.029	-0.389	-0.721
	150	16.9	0.046	0.345	0.078	-0.231
	200	15.4	0.039	0.987	0.788	0.602
	250	13.3	0.038	1.487	1.412	1.223

4.2.10 Regeneration of ZFN-CMS

One of the crucial factors to consider when evaluating an adsorbent's performance following an adsorption study is its ability to regenerate and reusage. It determines adsorbent's cost-effectiveness and its performance after recycling. Following the adsorption of various dyes with ZFN-CMS magnetic green composite, regeneration of adsorbent was carried out using 0.1N HCl as desorbing agent[8]. Table 4.2.4 shows the regeneration efficiency up to 5 cycles. ZFN-CMS composite was 82.3%, 73.2%, 74.4% and 73.8% efficient to remove Malachite green (MG), Brilliant green (BG), Methylene blue (MB) and Crystal violet (CV) dyes, respectively in a single dye system. These results indicated that ZFN-CMS magnetic green adsorbent has good re-usability and is a cost-effective adsorbent.

Table 4.2.4- Regeneration efficiency of ZFN-CMS for single dye system

Number of Cycles	Regeneration Efficiency using 0.1 N HCl			
	% MG	% BG	% MB	% CV
1	99.1	99.8	99.4	98.2
2	88.7	88.4	88.2	77.5
3	86.4	75.1	77.5	76.3
4	84.4	74.7	76.1	75.6
5	82.3	73.2	74.4	73.8

4.2.11 Adsorption of dyes using ZFN-RHS magnetic green composite

4.2.12 For single and binary dye systems

Zinc ferrite-rice husk silica magnetic green composite was used for removing Methylene blue and Crystal violet dyes in single and binary system. To examine adsorption behavior of ZFN-RHS with Methylene blue (MB) and Crystal violet (CV) dyes, the batch mode adsorption process was employed. Regeneration and reuse of ZFN-RHS was also tested for up to five cycles to determine whether or not the adsorbent preserved its efficiency. The following details of the various factors, including time, composite dose, solution concentration, temperature, and pH were taken into consideration:

4.2.13 Effect of contact time

0.1g of ZFN-RHS was added to 50 mL of dye solution with known concentrations for single dye system (50 mg/L) and binary dye system (20 mg/L), on a thermostatic shaker set at $25^{\circ}C$ (at 200 rpm). At regular intervals of time, the absorbance of dyes was measured by using Shimadzu-8400S UV-Visible spectrophotometer and from this the residual concentration of dyes was calculated. The effect of time for removing MB and CV dyes in single and binary dye systems is shown in Figure 4.2.11 in terms of percentage dye removal and residual dye concentration at various time intervals (C_t). Initially, the percentage dye removal was rapid, but as time goes on, adsorption approached an equilibrium stage where it became constant. This rapid growth in percentage removal was attributed to the presence of more unoccupied

sites on surface of the adsorbent initially. The vacant sites were available for the occupation of dyes until equilibrium was attained[24]. The equilibrium stage was reached at around 100 min. This was equilibrium time and the concentration at equilibrium time was referred to as C_e i.e. equilibrium concentration. It revealed that the maximum dye adsorption was attained from aqueous solution during this time period.
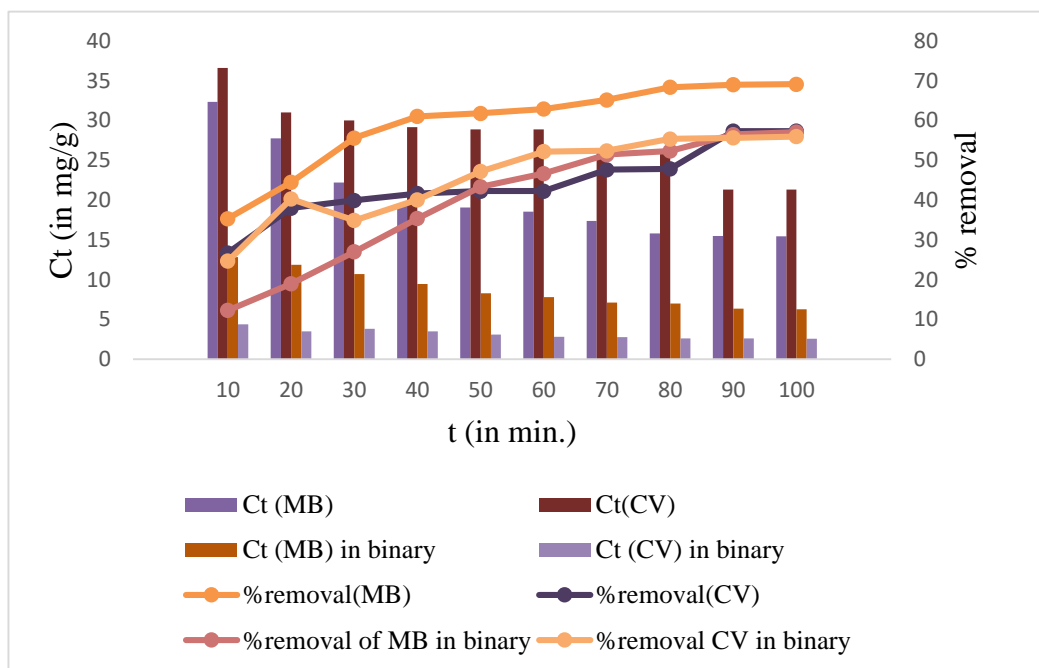
Figure 4.2.11- Effect of time in single and binary dye system using ZFN-RHS

4.2.14 Adsorption kinetics

The physical/chemical nature of dye's adsorption by the adsorbent was revealed by kinetic analysis. To characterize the adsorption behavior of ZFN-RHS for removing MB and CV dyes, different kinetic models viz. Lagergren pseudo first order, Pseudo second order, Elovich model, and Weber Morris intraparticle diffusion models were utilised. Figures 4.2.12, 4.2.13 and 4.2.14 showsLagergren pseudo first order, second order and Elovich models respectively for removing CVand MB dyes, in single and binary dye system by using ZFN-RHS magnetic green composite.The different kinetic constants calculated using scope and intercept of plots of various kinetic models for removing CV and MB dyes using ZFN-RHS magnetic green composite are shown in Table 4.2.5.
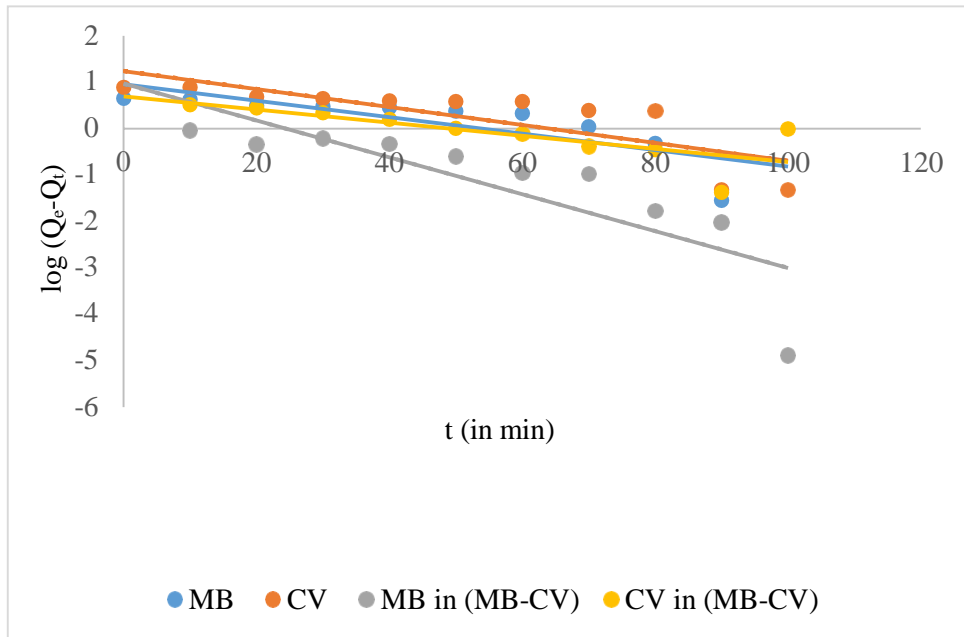
Figure 4.2.12- Lagergren pseudo first order kinetics for single and binary dye systems usingZFN-RHS
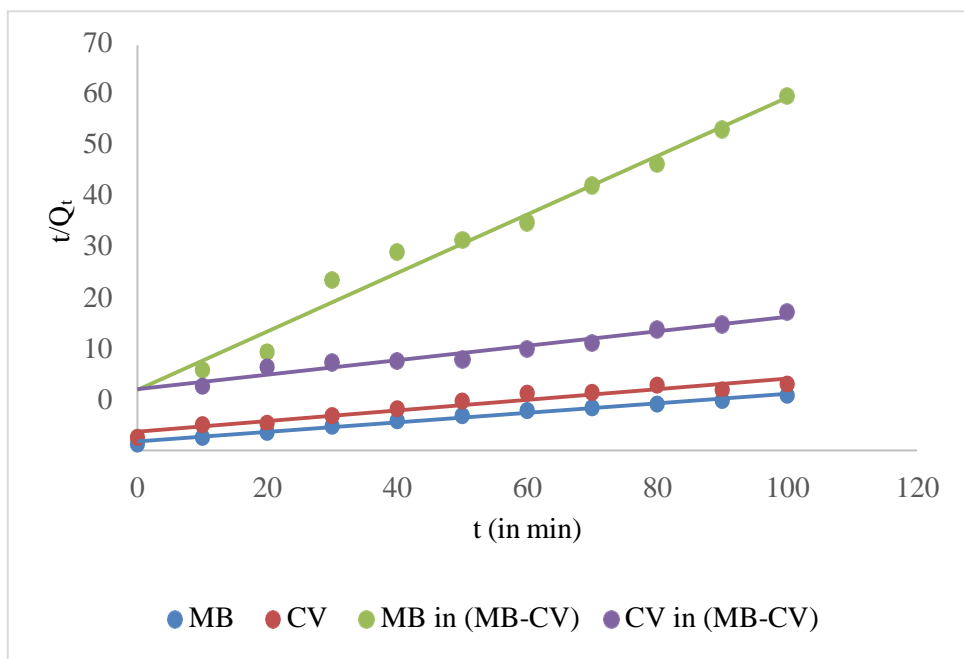
Figure 4.2.13- Pseudo second order kinetics study for single and binary dye systems using ZFN-RHS
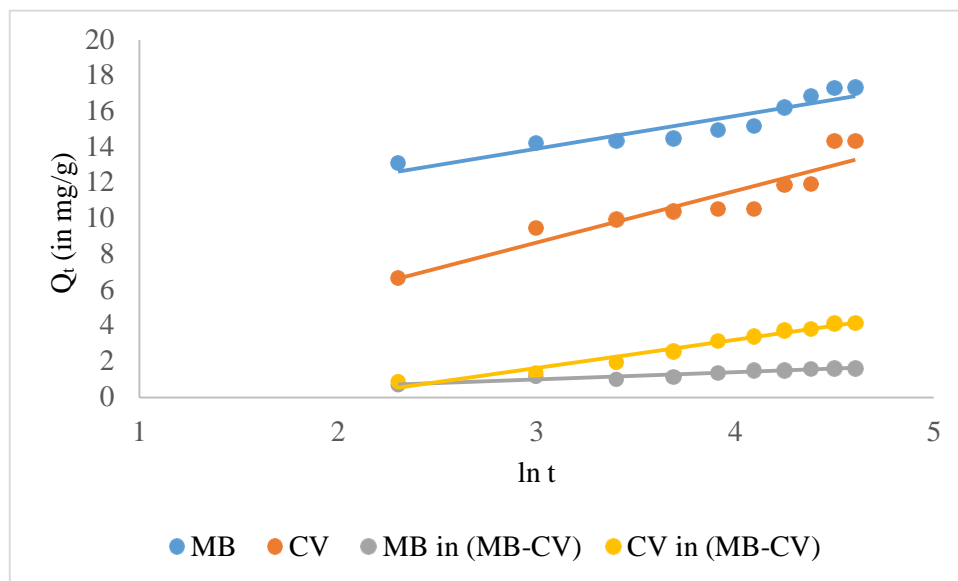
Figure 4.2.14- Elovich kinetic model for single and binary dye systems using ZFN-RHS

The fitness of various kinetic models was evaluated using regression coefficient (R^2). Pseudo-second order plot had highest R^2 values in both single and binary dye systems, according to Table4.2.5. It revealed that the adsorption behavior of Methylene Blue and Crystal Violet dyes in single and binary dye systems, followed pseudo-second order model and that the process was chemisorption in nature.

Table 4.2.5- Kinetic constants for single and binary dye systems using ZFN-RHS

Model of kinetic study	Constants	For Methylene Blue	For Crystal Violet	For Methylene Blue in binary system	For Crystal Violet in binary system
Lagergren Pseudo First order	Q_{e1}	13.551	27.133	8.177	9.315
	K_1	0.027	0.029	0.0462	0.091
	R^2	0.646	0.638	0.8612	0.689
	SD	0.129	0.054	0.168	0.113

Pseudo Second order	Q_{e2}	18.552	16.977	7.993	1.981
	h	1.237	0.398	0.094	0.095
	K_2	0.0035	0.0013	0.0014	0.0243
	R^2	0.9916	0.9668	0.957	0.978
	SD	0.121	0.138	0.585	0.176
Elovich model	α	0.799	1.162	0.224	0.246
	β	0.248	0.304	0.634	2.482
	R^2	0.8795	0.8808	0.913	0.971
	SD	0.278	0.412	0.142	0.204

The Weber Morris intra particle diffusion model for MB and CV dyes in both systems is shown in Figure 4.2.2.5. It suggests that a wide range of factors affect adsorption of dyes in both systems of dyes[14].
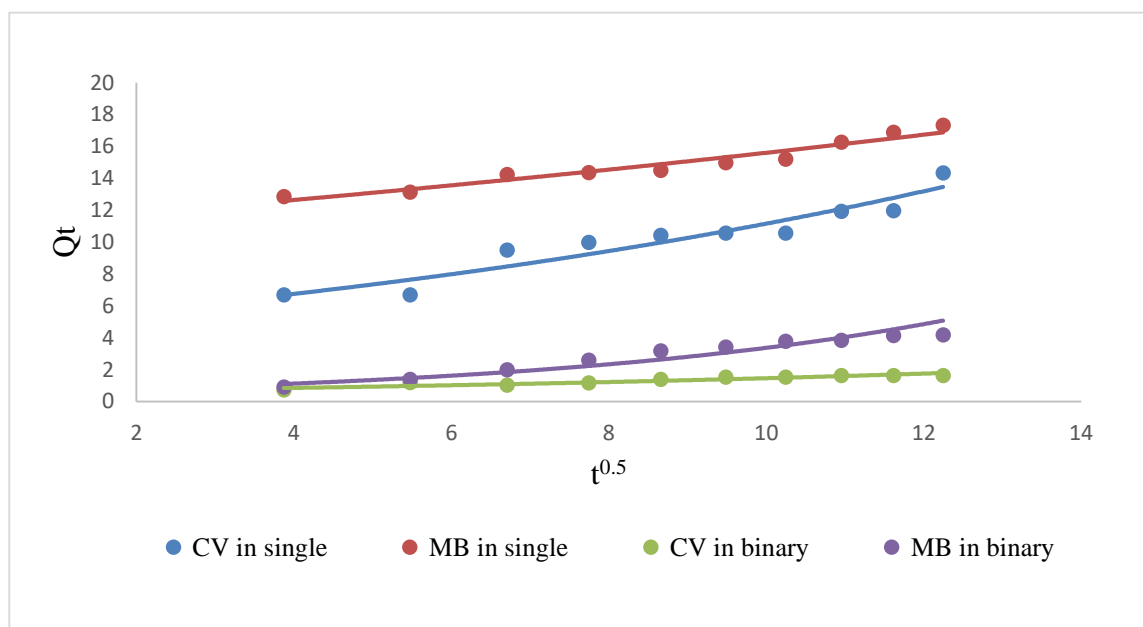
Figure 4.2.15- Weber Morris model for single and binary dye systems using ZFN-RHS

It is evident from figure 4.2.15 that in both single and binary dye system, the straight line does not pass through origin, which indicates that a variety of factors influence adsorption of Crystal Violet and Methylene Blue dyes using ZFN-RHS magnetic green composite. Adsorption slopes were sharp for single dye system which indicated quick adsorption initially and with the passage of time it became flattened indicating slowing down of adsorption process which ultimately lead to equilibrium stage. The slope of the graph in binary dye system is not steep, indicating a decrease in rate of adsorption, due to antagonistic effect of the dyes. The molecules of MB and CV interact electrostatically, resulting in strong bonds between the dye molecules. As a result, rate of adsorption in binary dye systems dropped[8].

4.2.15 Effect of pH

The pH of the solution affects surface charge on surface of adsorbent which result in change of electrostatic and other interactions. The effect of pH was studied with ZFN-RHS in single dye system. To study the effect of pH, initial pH of solution was altered from 3-11 with initial concentration of dye 50mg/L and equilibrium time of two hours. In Figure 4.2.16, the adsorption behavior of Methylene Blue and Crystal Violet dyes utilising ZFN-RHS magnetic green composite at different initial pH values ranging from 3 to 11 is shown.
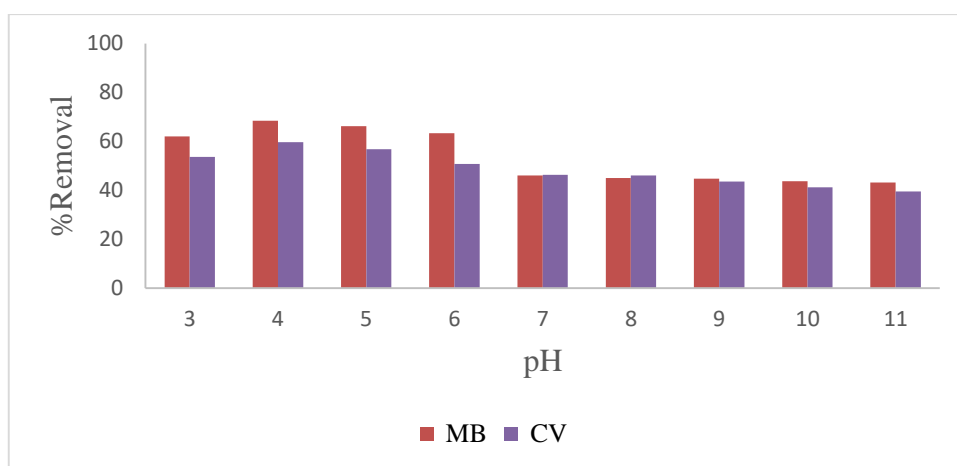
Figure 4.2.16- Effect of pH for removal of CV and MB dyes using ZFN-RHS

At pH 4–5, Methylene Blue and Crystal Violet dyes were removed to the greatest extents 68.4% and 59.7%, respectively. As a result, pH 4–5 was found to be the ideal range for studying adsorption parameters using ZFN-RHS. ZFN-RHS magnetic green composite acquired negative charge above pH of point zero charge ($pH_{PZC} = 4.3$). Therefore, the surface

of adsorbent became suitable to attract cationic species such as MB and CV, which are cationic in nature. Methylene Blue and Crystal Violet dyes were therefore successfully removed from aqueous solution using ZFN-RHS magnetic green composite at pH around 4-5.

4.2.16 Effect of Adsorbent dose

The amount of adsorbent was altered from 0.1-0.5g, to study its effect for removing Methylene blue and Crystal violet dyes in single and binary systems using ZFN-RHS magnetic green composite. Effect of adsorbent dosage in both dye systems is shown in Figure 4.217. Percentage removal for MB dye increased from 69.4% to 77.6% and for CV dye increased from 57.6% to 74.4% in a single system with the addition of more adsorbent. When adsorbent dosage was altered from 0.1 g to 0.5 g in binary system, percentage removal of MB dye increased from 57.1% to 66.0% while for CV dye, it increased from 56.0% to 67.7%. It was observed because with increase in adsorbent dose, number of active sites for adsorption also increased. Additionally, in both systems, dye adsorption capacities (Q_e) decreased as adsorbent dose increased. The unsaturation of adsorption sites caused was responsible for the decrease in Q_e at higher adsorbent dosage[25]. In case of binary dye system the adsorption percentage is less than single system of dyes because of antagonistic effect of dyes[26].
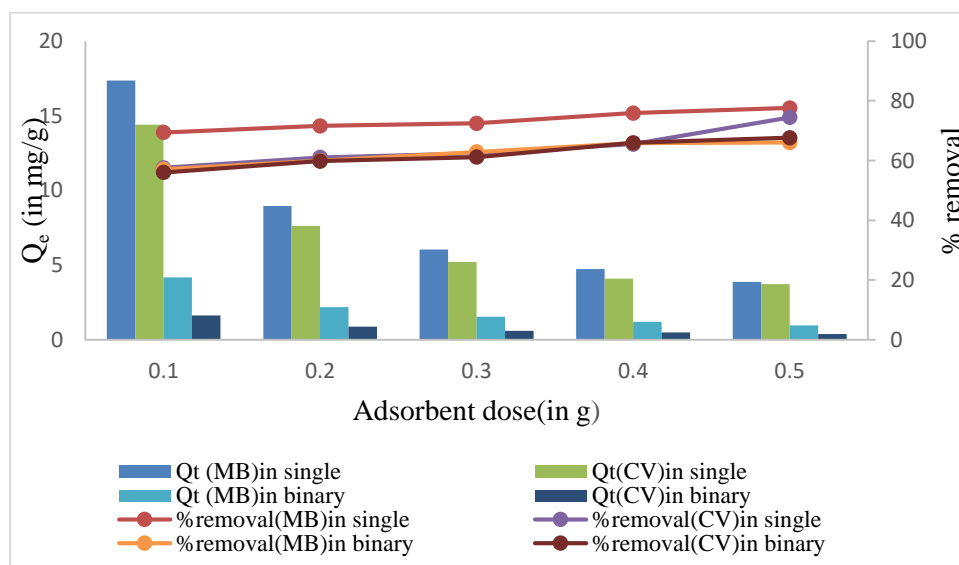
Figure 4.2.17- Effect of adsorbent dose in single and binary dye systems using ZFN-RHS

4.2.17 Effect of concentration and temperature

Concentration of MB and CV dyes was increased from 50-250 mg/L in single dye system and from 20-100 mg/L in binary dye system. The effect of change in concentration for MB and CV dyes using ZFN-RHS magnetic green composite in both system of dyes is shown in Figures 4.2.18 (a) and (b) with respect to Q_e and percentage removal. For both system of dyes, percentage removal declined with increase in concentration of dyes. In single dye system, percentage removal of MB dye decreased from 72% to 44% and for CV dye decreased from 76% to 46% by altering initial concentration of dyes from 50-250 mg/L. In binary dye system, percentage removal of MB dye decreased from63% to 44% and for CV dye decreased from 59% to 39% with the increase in the initial dye concentration. This was observed because of less number of active adsorption sites on ZFN- RHS magnetic green composite's surface with respect to the increased number of dye molecules. In binary dye system, percentage removal of MB and CV was lower as compared to single dyes due to antagonistic effect of dyes (electrostatic and π-π interactions) in multiple dye system[26]. On the other hand, as dye concentration increased, adsorption capacities (Q_e) increased in both systems of dyes. Increase in the value of Q_e was observed due to stronger interactions as a result of more number of collisions between the dye molecules and ZFN-RHS. Furthermore, the effect of concentration was examined at three different temperatures viz. 25°C, 30°C, and 35°C. As temperature increased, percentage removal of dyes also increased. It might be because when the solution's temperature rose, the size of the adsorbent's pores grew larger, increasing the amount of surface area accessible for dye adsorption. It demonstrated the endothermic character of the adsorption process using ZFN-RHS magnetic green composite[27].

4.2.18 Adsorption Isotherms

To understand the nature of adsorption, it is important to study adsorption isotherms. Isotherms are important as these describe the relationship between the adsorbate present in liquid (C_e) and in solid phase (Q_e) at equilibrium time, so they are critical to design adsorption process. Figures 4.2.19 to 4.2.26 represents Langmuir, Freundlich, Temkin and D-R isotherms for removing Crystal Violet and Methylene Blue dyes respectively for in both system of dyes using ZFN-RHS magnetic green composite.
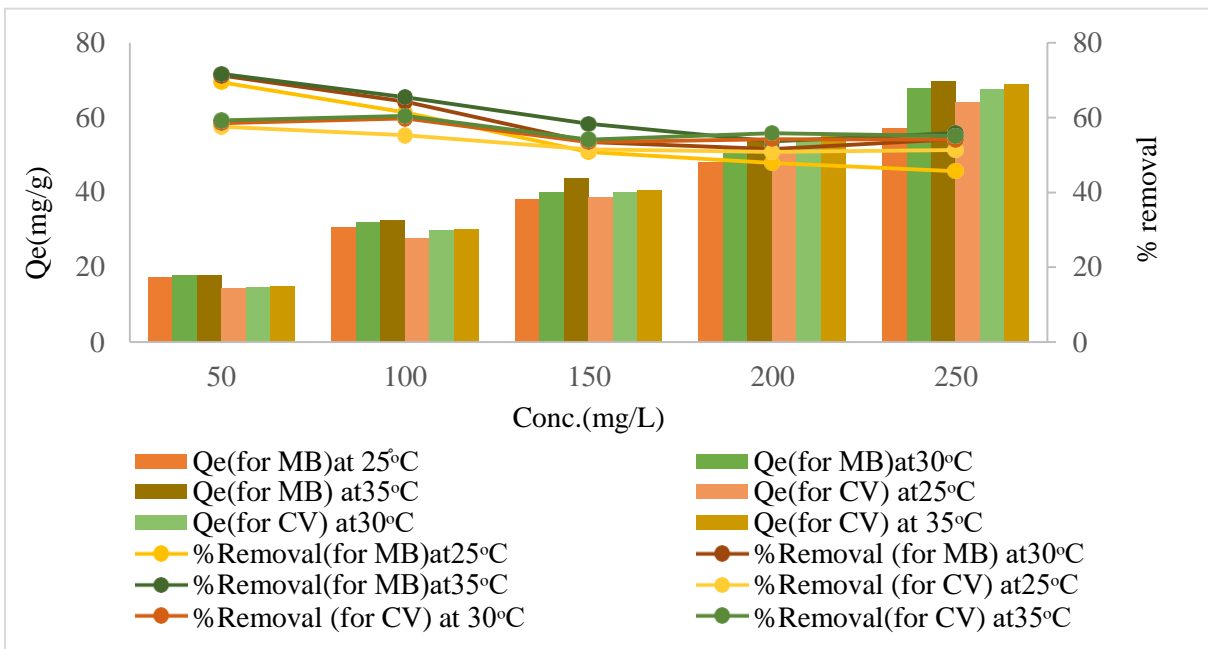
(a) Single dye system
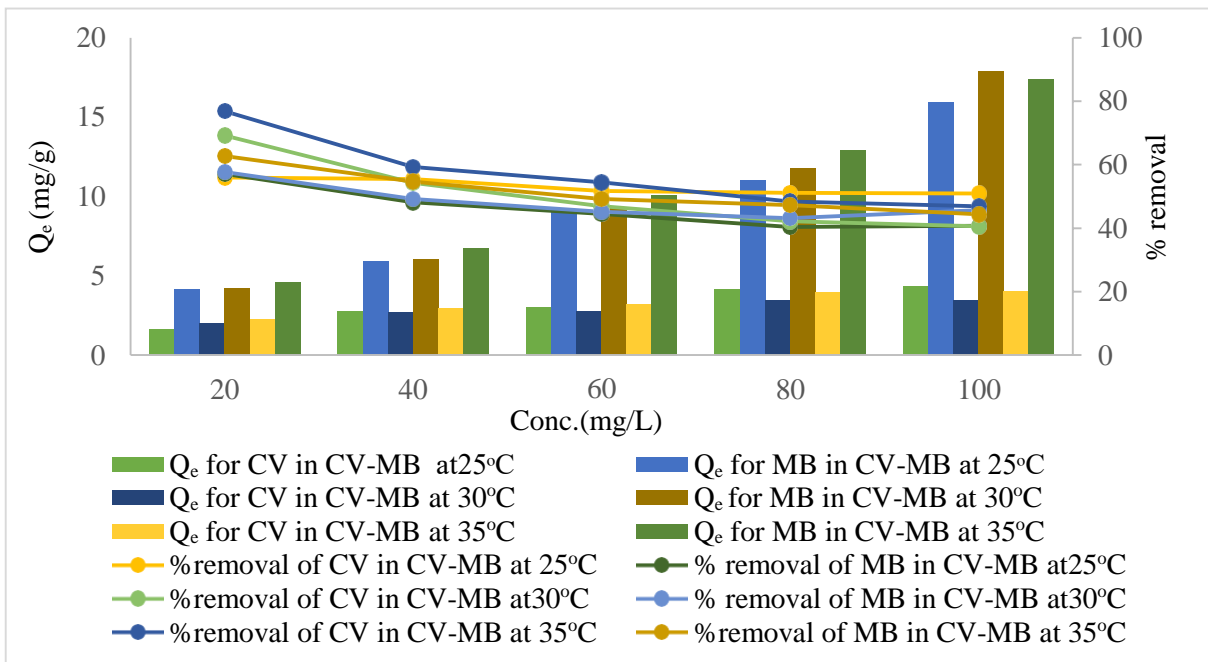
(b) Binary dye system

Figure 4.2.18- Effect of concentration for (a) single and (b) binary dye systems using ZFN-RHS
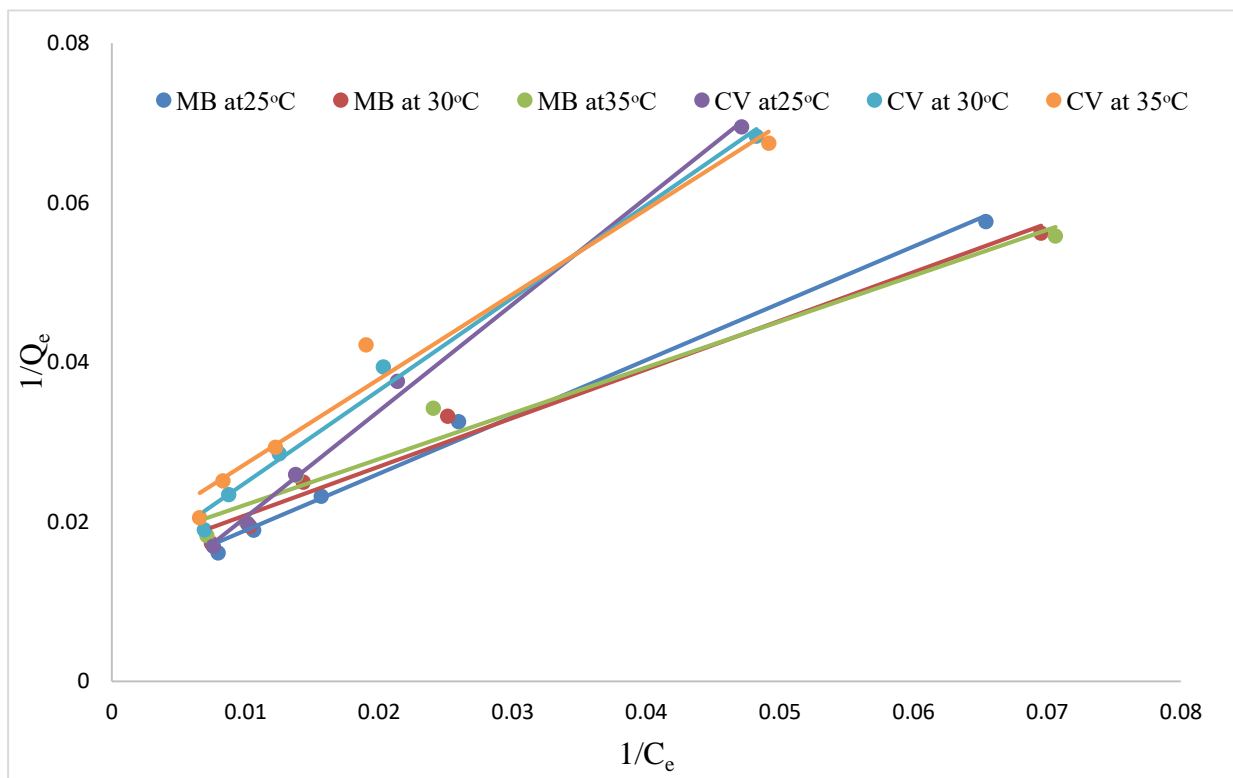
Figure 4.2.19- Langmuir isotherm for single dye system using ZFN-RHS
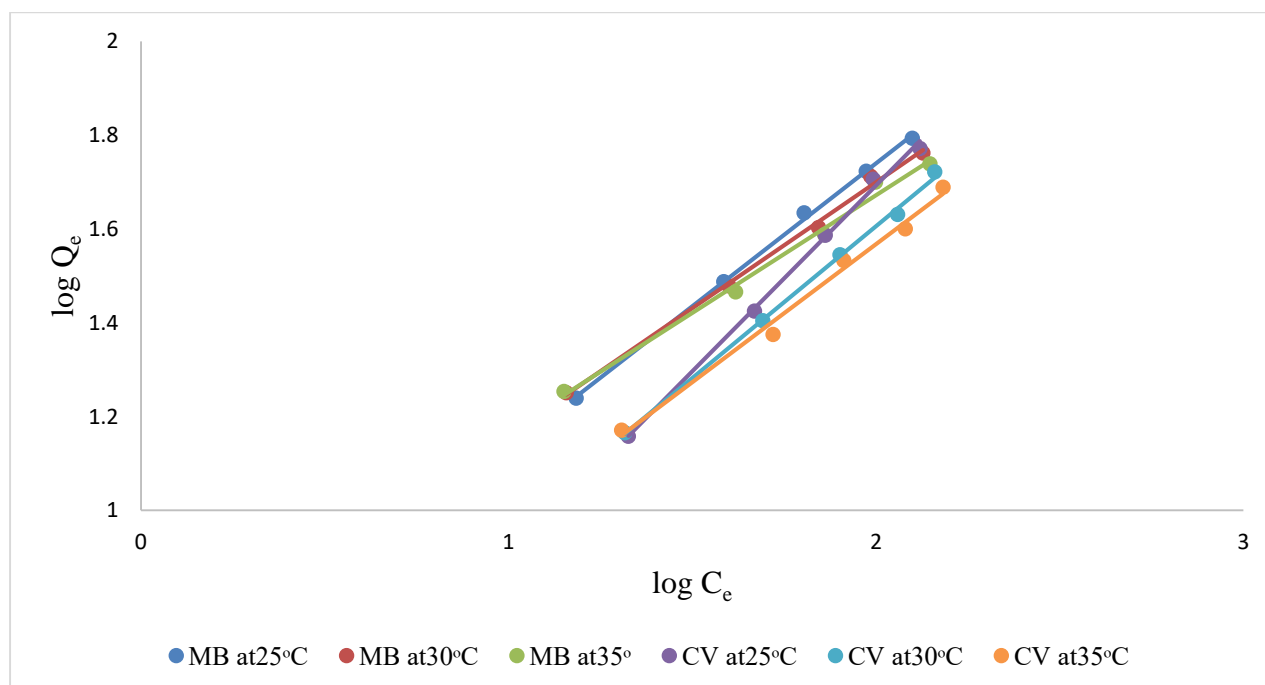
Figure 4.2.20- Freundlich isotherm for single dye system using ZFN-RHS
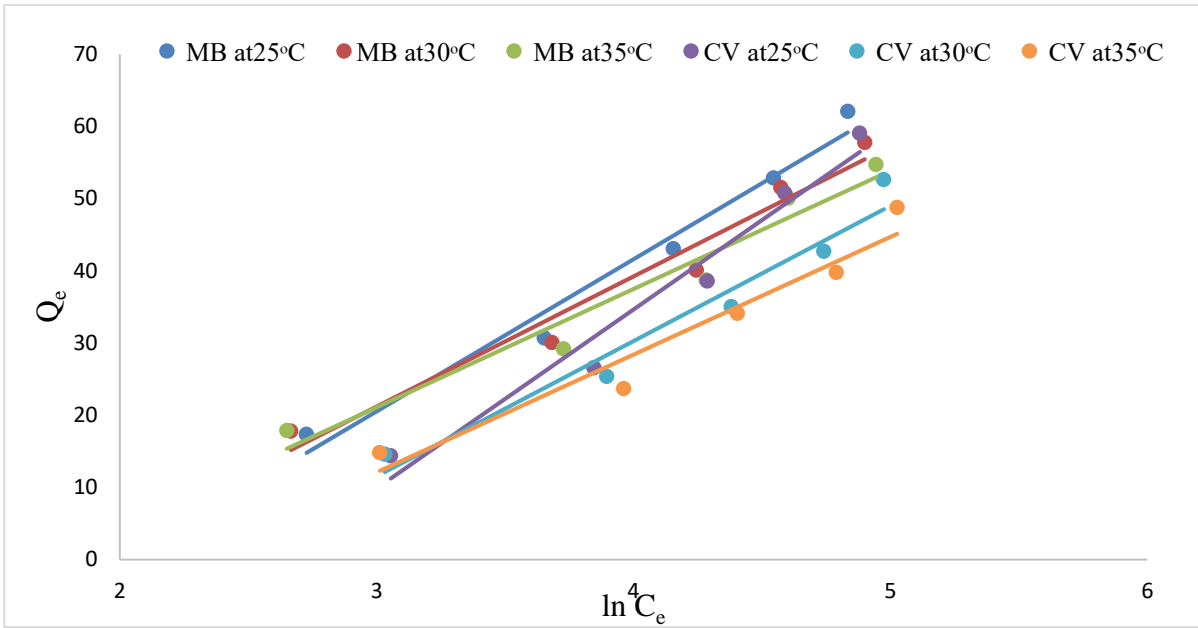
Figure 4.2.21- Temkin isotherm for single dye system using ZFN-RHS
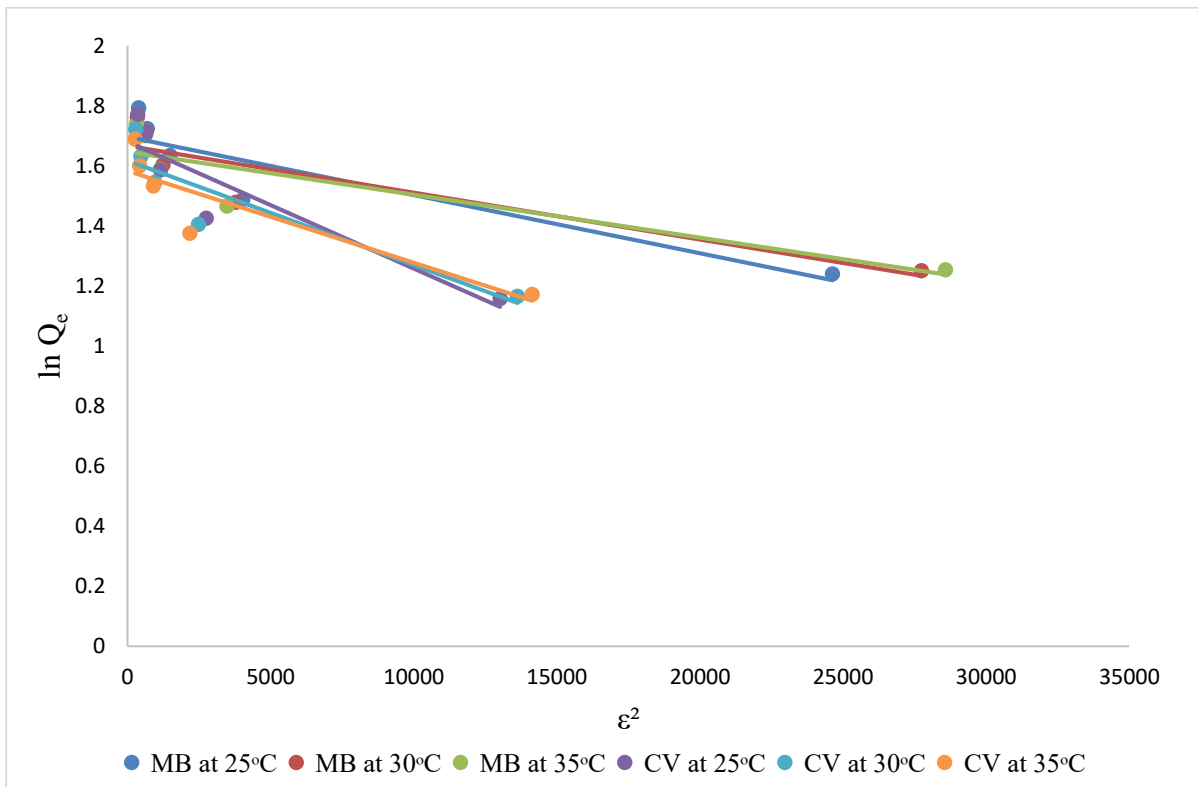
Figure 4.2.22- D-R isotherm for single dye system using ZFN-RHS
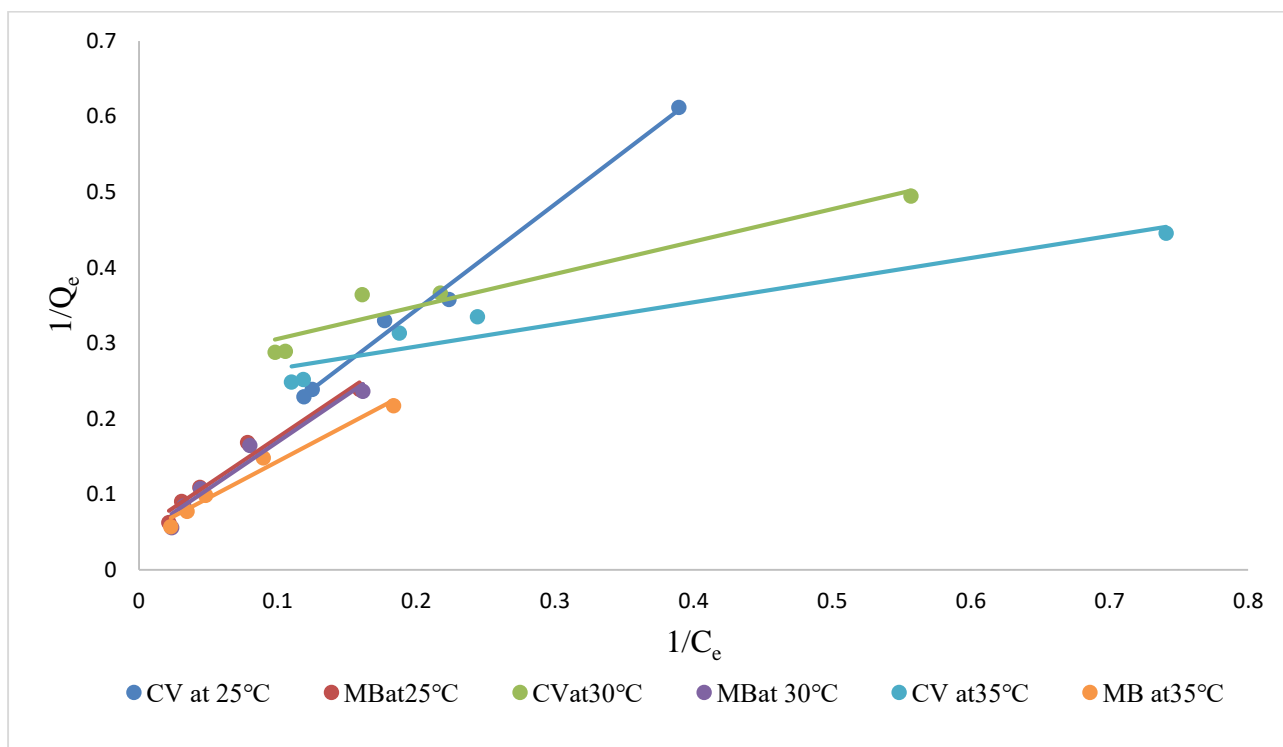
Figure 4.2.23- Langmuir isotherm for binary dye system using ZFN-RHS
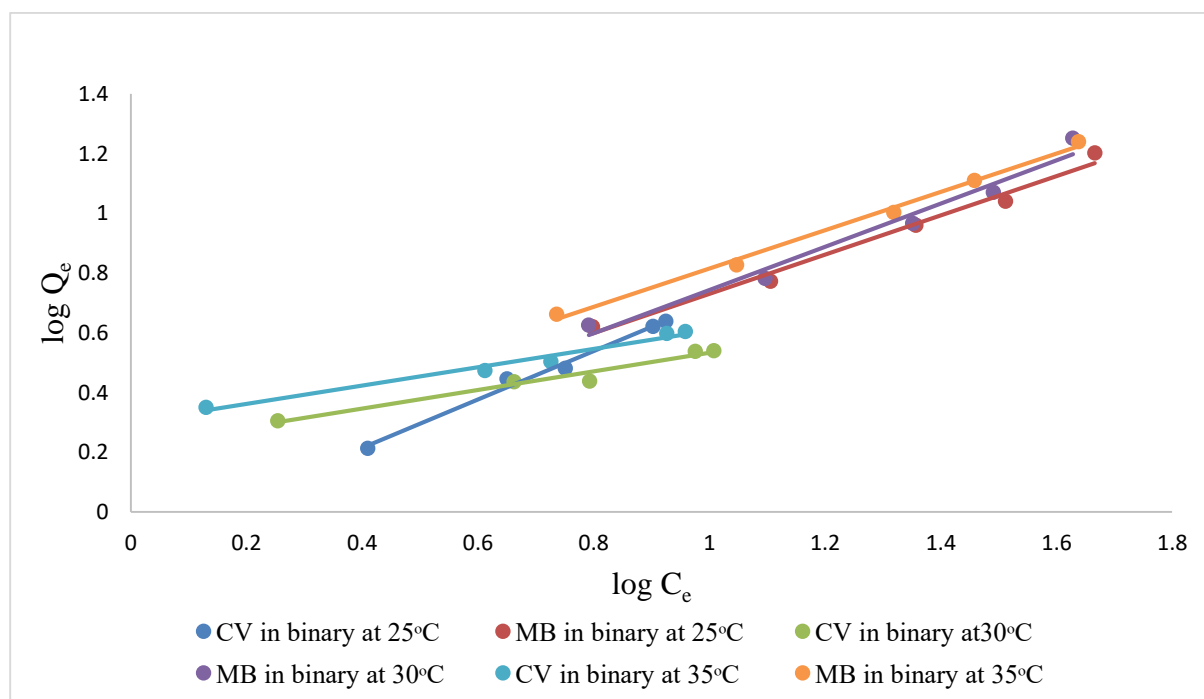
Figure 4.2.24- Freundlich isotherm for binary dye system using ZFN-RHS
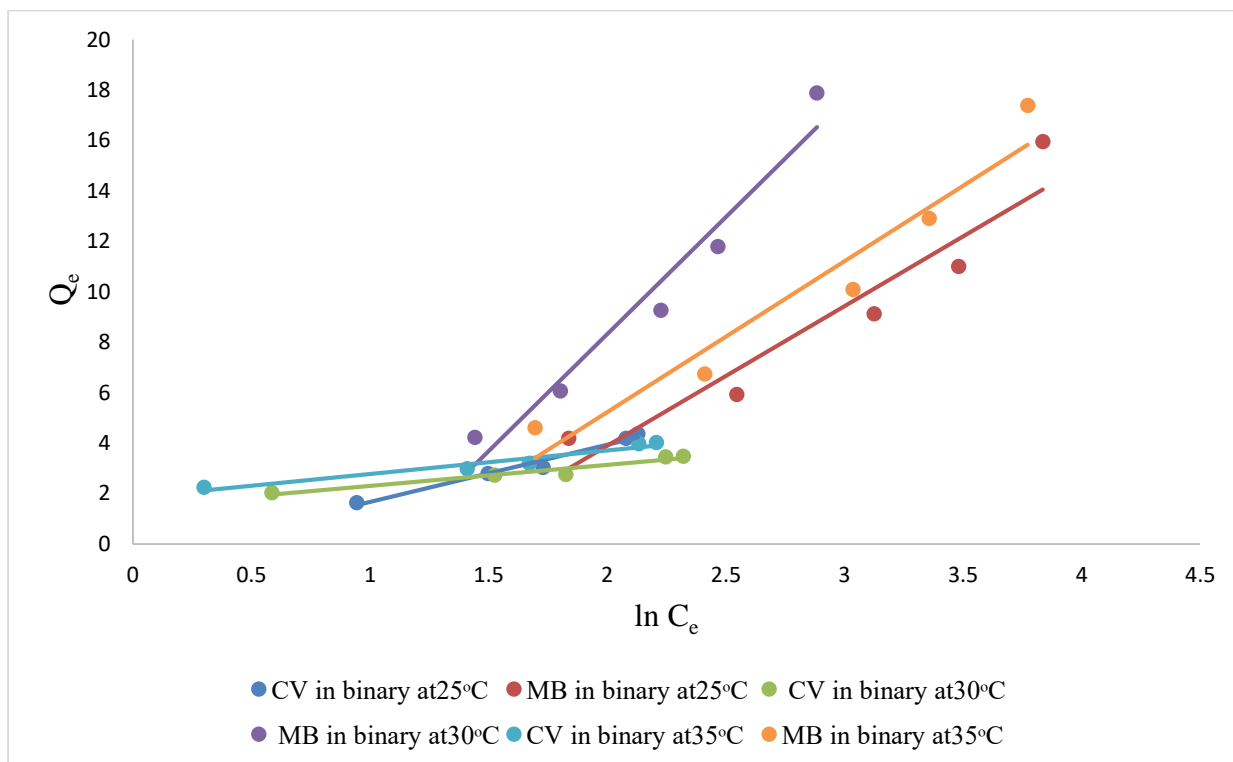
Figure 4.2.25- Temkin isotherm for binary dye system using ZFN-RHS
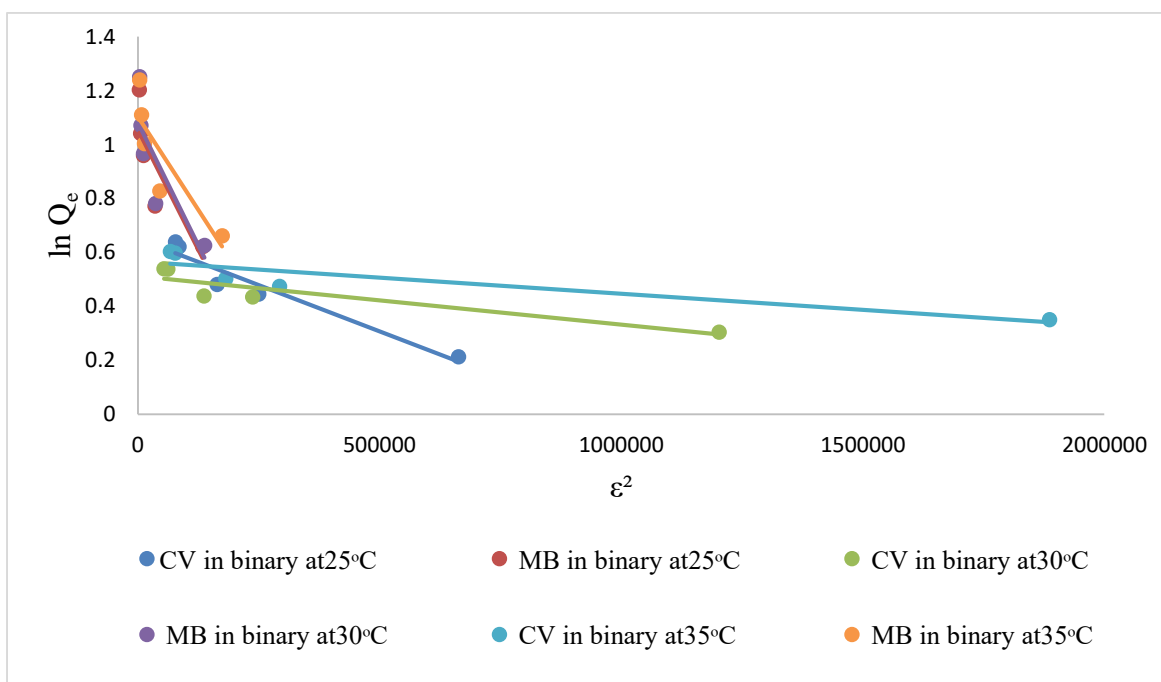
Figure 4.2.26-D-R isotherm for binary dye system using ZFN-RHS

The isotherm constants for single and binary dye systems are shown in Table 4.2.6 based on the slopes and intercepts of graphs of Langmuir, Freundlich, Temkin and D-R isotherms (Figures 4.2.19 to 4.2.26). The fitness of adsorption model was assessed using the regression coefficient (R^2). The Freundlich isotherm model displayed a higher R^2 value for both single and binary dye systems. As a result, it was concluded that Freundlich model best fitted to the obtained experimental data. R^2 values for Langmuir isotherm, however, are comparable, as the table demonstrates. Therefore, utilising ZFN-RHS magnetic green composite, adsorption behavior of CV and MB dyes using ZFN-RHS magnetic green composite was followed in the order Freundlich > Langmuir isotherm. It suggested that adsorption of dyes onto the surface of ZFN-RHS was heterogeneous. Adsorption energy (E) related to D-R isotherm model is helpful in determining the nature of adsorption process. The value of the adsorption energies for Methylene Blue and Crystal Violet dyes in both system of dyes was found to be more than 100 kJ/mol in the current study using ZFN- RHS magnetic green composite. It suggested that adsorption was chemisorption[28]. In this study, the separation factor (R_L) value associated with Langmuir isotherm was found between 0 and 1, indicating that the process of removal of dyes using ZFN-RHS magnetic green composite was favourable in nature. Maximum adsorption capacities for CV and MB dyes were found to be 138.8 and 84.7 mg/g, respectively in single dye system whereas in binary dyes system it was 15.4 and 22.2 mg/g, respectively for CV and MB dyes.

4.2.19 Thermodynamics of adsorption

Thermodynamics of adsorption is very important in the estimation of adsorption mechanism (physisorption or chemisorption). The various thermodynamic parameters like enthalpy change (ΔH^o), Gibbs free energy change (ΔG^o) and entropy change (ΔS^o) give information about the endothermic or exothermic nature of adsorption, spontaneity and nature of the adsorption process. Figures 4.2.27 and 4.2.28 show graphs of ln k_d v/s 1/T for Methylene Blue and Crystal Violet dyes in single and binary system of dyes, respectively. Table 4.2.7 lists several thermodynamic constants for adsorption of Methylene blue and Crystal violet dyes in single and binary dye system utilising ZFN-RHS. In both instances, the ΔH^o and ΔS^o readings were positive, indicating an endothermic reaction with a higher level of unpredictability at adsorbent's surface. It was inferred that adsorption of MB and CV dyes using ZFN-RHS magnetic green composite was spontaneous, based on the negative ΔG^o values[29].

Table 4.2.6- Isotherm constants for single and binary dye systems

SYSTEM		Single CV			Single MB			CV in Binary			MB in Binary		
Isotherm Model	Const.	25ºC	30ºC	35ºC	25ºC	30ºC	35ºC	25ºC	30ºC	35ºC	25ºC	30ºC	35ºC
Langmuir	Q	60.240	75.187	138.88	60.97	68.03	84.75	3.803	4.217	15.408	19.267	21.505	22.271
	b	0.005	0.011	0.015	0.016	0.024	0.028	0.046	0.612	0.810	0.042	0.036	0.047
	R^2	0.997	0.991	0.971	0.993	0.980	0.968	0.992	0.935	0.920	0.962	0.956	0.972
	SD	0.002	0.003	0.021	0.003	0.012	0.020	0.003	0.022	0.024	0.020	0.020	0.020
	R_L	0.800	0.645	0.571	0.555	0.454	0.416	0.303	0.031	0.024	0.322	0.357	0.298
Freundlich	K_f	1.279	2.041	2.454	3.321	4.217	4.653	0.775	1.666	1.994	1.180	1.043	1.490
	1/n	0.792	0.648	0.588	0.609	0.537	0.502	0.811	0.311	0.307	0.658	0.724	0.641
	R^2	0.997	0.998	0.990	0.998	0.996	0.991	0.989	0.968	0.977	0.984	0.971	0.994
	SD	0.002	0.002	0.003	0.002	0.016	0.003	0.038	0.052	0.042	0.034	0.063	0.032
D-R	Q_m	4.870	5.040	5.370	5.189	5.295	5.455	1.669	1.761	1.915	2.866	2.950	3.015
	K_{DR}	5×10^{-4}	0.49×10^{-4}	0.48×10^{-4}	5×10^{-2}	5×10^{-2}	5×10^{-1}	7×10^{-7}	7×10^{-6}	7×10^{-5}	6×10^{-4}	6×10^{-4}	6×10^{-3}
	R^2	0.850	0.831	0.792	0.838	0.809	0.790	0.937	0.826	0.796	0.736	0.712	0.760

	E	111.80	129.10	129.10	158.1	158.11	223.61	845.15	845.15	912.87	353.55	353.55	408.25
	SD	0.103	0.108	0.134	0.106	0.127	0.133	0.025	0.112	0.130	0.159	0.158	0.159
Temkin	br	101.6	134.5	154.5	119.5	139.8	153.7	1109.1	2669.4	3014.0	271.1	421.1	454.9
	A	0.074	0.092	0.104	0.131	0.161	0.180	0.765	5.748	6.999	0.273	0.331	0.872
	R^2	0.963	0.954	0.944	0.975	0.960	0.952	0.976	0.944	0.943	0.903	0.953	0.934
	SD	1.122	1.124	1.130	0.589	0.635	0.834	0.585	1.130	1.118	1.145	0.774	1.192
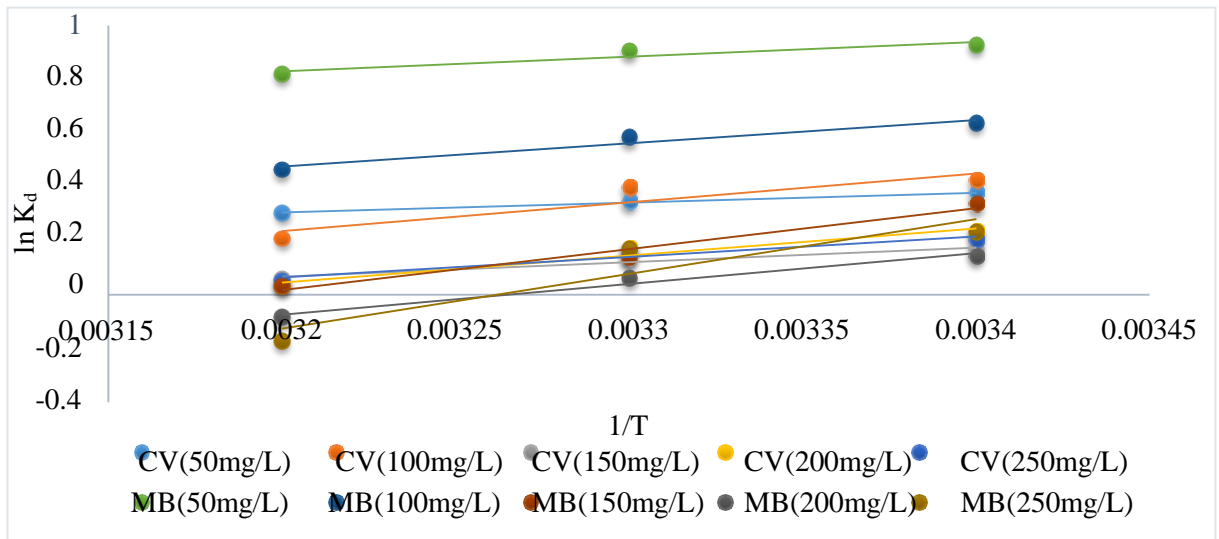
Figure 4.2.27- Graph between ln K$_d$ and 1/T for single dye system using ZFN-RHS
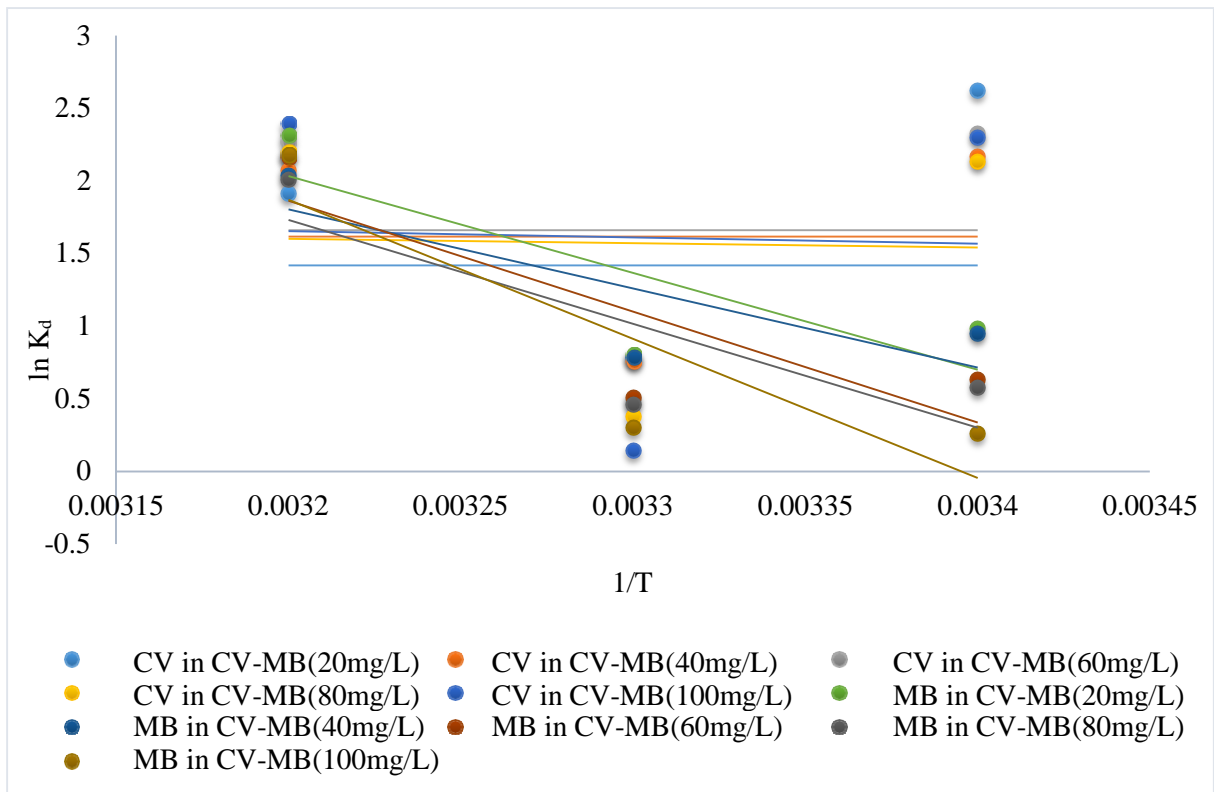
Figure 4.2.28- Graph between ln K$_d$ and 1/T for binary dye system using ZFN-RHS

Table 4.2.7- Thermodynamic parameters for single and binary dye systems using ZFN-RHS

Dyes system	Conc. in mg L^{-1}	ΔS^o in J $mol^{-1}K^{-1}$	ΔH^o in kJ mol^{-1}	ΔG^o at 25°C in kJ mol^{-1}	ΔG^o at 30°C in kJ mol^{-1}	ΔG^o at 35°C in kJ mol^{-1}
Crystal Violet	50	0.007	3.013	-0.755	-0.869	-0.966
	100	0.027	8.907	-0.519	-0.997	-1.085
	150	0.014	4.483	-0.145	-0.346	-0.426
	200	0.026	8.375	-0.081	-0.428	-0.600
	250	0.020	6.314	-0.127	-0.417	-0.521
Methylene Blue	50	0.008	4.523	-2.031	-2.339	-2.378
	100	0.019	7.175	-1.154	-1.608	-1.635
	150	0.040	12.646	-0.079	-0.847	-0.861
	200	0.031	9.532	0.210	-0.364	-0.370
	250	0.055	16.886	0.427	-0.589	-0.599
Crystal Violet in CV-MB binary system	20	0.083	29.553	-4.744	-1.967	-6.724
	40	0.000	4.098	-5.134	-1.912	-5.559
	60	0.005	2.660	-5.613	-1.240	-5.965
	80	0.021	2.486	-5.445	-0.953	-5.474
	100	0.025	3.526	-5.916	-0.367	-5.897
Methylene Blue in CV-MB binary system	20	0.197	55.438	-5.738	-2.021	-2.515
	40	0.160	45.283	-5.056	-1.990	-2.436
	60	0.219	63.494	-5.349	-1.290	-1.617
	80	0.205	59.420	-4.978	-1.159	-1.485
	100	0.270	79.600	-5.392	-0.762	-0.670

4.2.20 Regeneration of ZFN-RHS

Regeneration of adsorbent is important to evaluate its performance. Adsorbent's cost-effectiveness is directly correlated with its recycling potential. The regeneration studies were conducted up to five cycles using 0.1N HCl as desorbing agent. The results of regeneration for CV and MB dyes using ZFN-RHS magnetic green composite in single and binary dye system, are presented in table 4.2.8. In a single system, the regeneration efficiency of CV fell from 97.3 to 79.4%, and for MB, from 98.5% to 80.0%, however in a CV-MB binary dye system, it decreased from 93.7% to 71.0% for CV and from 97.6% to 80.2% for MB. Given that ZFN- RHS maintained its adsorption capacity at significant levels during five regeneration cycles, the current work suggests that it may be a useful as cost-effective adsorbent for removing dyes in single and binary dye system.

Table 4.2.8- Regeneration efficiency of ZFN-RHS magnetic green composite in single and binary dye systems

Regeneration Cycle	Crystal Violet (50 mg/L)	Methylene Blue (50 mg/L)	Crystal Violet in CV-MB binary system (20mg/L)	Methylene Blue in CV-MB binary system (20 mg/L)
1	97.4	98.5	93.7	97.6
2	97.2	96.7	85.4	92.4
3	88.4	94.8	78.8	78.7
4	81.3	90.9	73.7	76.4
5	79.4	80.0	71.0	72.2

4.2.21 Adsorption of dyes using ZFN-MS magnetic green composite

4.2.22 For single and ternary dye system

Magnetic green composite of zinc ferrite and mango starch was used for removal of BG,MB, and CV dyes in single and ternary dye systems. Regeneration and reuse of ZFN-MS was also examined for five cycles, to see if ZFN-MS maintained its effectiveness. The batch mode of adsorption was selected for studying the adsorption behavior of ZFN-MS magnetic green composite for the above mentioned dyes. The following parameters, including contact time, adsorbent dose, concentration, temperature, and pH, was taken into account.

4.2.22 Effect of contact time

To 50 mL of dyes (MB, BG, and CV) of known concentration (for single 50 mg/L and for ternary 20 mg/L), 0.1g of ZFN-MS was added, and the mixture was agitated at 200 rpm at 25ºC. At regular intervals, an aliquot of the dye was taken and residual concentration of dyes were noted with a UV-Visible spectrophotometer. Figures 4.2.29 and 4.2.30 show the effect of time in single and ternary dye systems with respect to concentration and percent removal respectively. The equilibrium stage was reached at around 135 min. This was equilibrium time and concentration at this time was referred to as equilibrium concentration (C_e). Percentage removal of dyes was rapid at first, but over time, it increased to its highest level and achieved equilibrium. Initially, ZFN-MS had a large number of empty sites with to which dye molecules attached rapidly, these sites were decreased with the time which caused decrease in the rate of removal and ultimately achieved equilibrium.
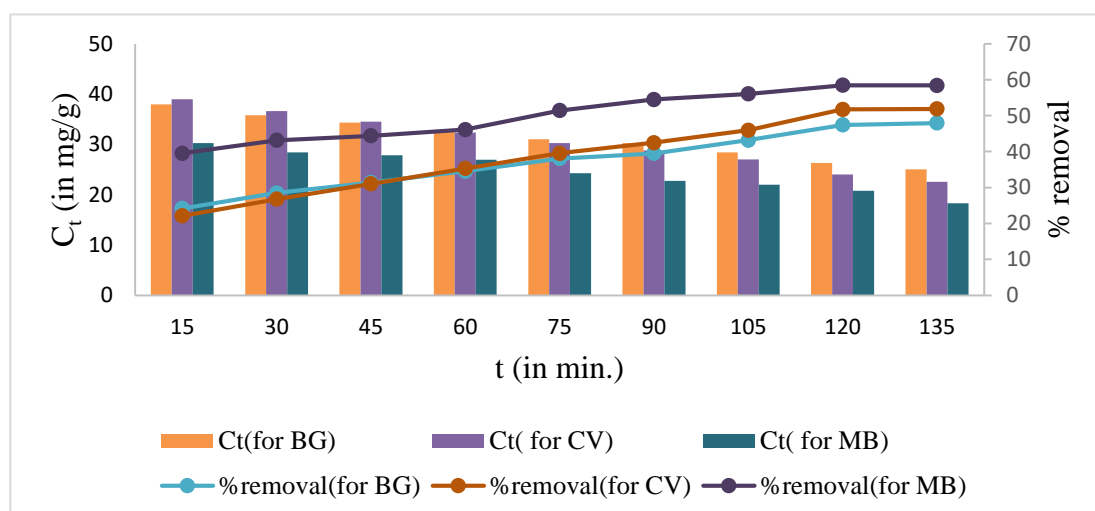
Figure 4.2.29- Effect of time in single dye system using ZFN-MS
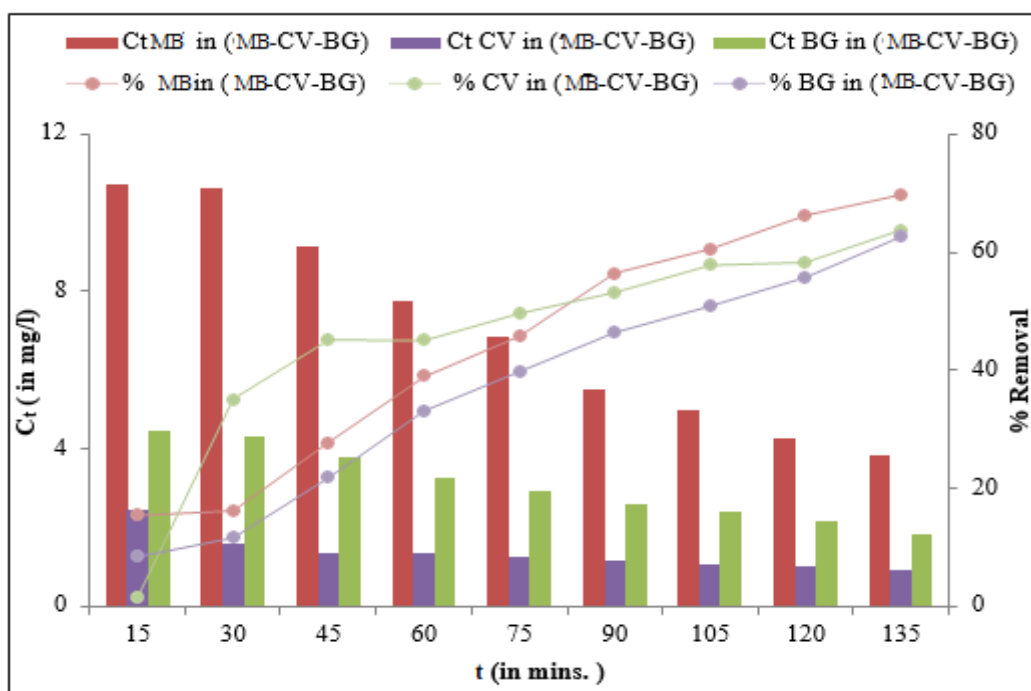
Figure 4.2.30- Effect of time in ternary dye system using ZFN-MS

4.2.24 Kinetic studies

The kinetics of dyes with ZFN-MS magnetic green composite was studied utilising various kinetic models viz. Lagergren Pseudo first order, Pseudo second order, and the Elovich model. Figure 4.2.31 represents Lagergren pseudo first order, figure 4.2.32 represents Pseudo second order and figure 4.2.33 represents Elovich model for the removing CV, BG and MB dyes in single and ternary dye systems by employing ZFN-MS magnetic green composite.

Table 4.2.9 depicts various kinetic constants calculated from the linear equations of kinetic models for removal of CV, MB and BG dyes, using ZFN-MS magnetic green composite in single as well as ternary dye systems. According to the aforementioned table regression coefficient (R^2) for Pseudo second order is highest. In single dye system for CV, MB and BG dyes value of R^2 was found to be 0.992, 0.971 and 0.991 respectively. In ternary dye system using ZFN-MS for the removal of dyes CV, MB and BG, R^2 values were found to be 0.998, 0.997 and 0.998, respectively. Thus, pseudo second order model was most suited for removing CV, BG, and MB dyes using ZFN-MS magnetic green composite in single and ternary system of dyes.
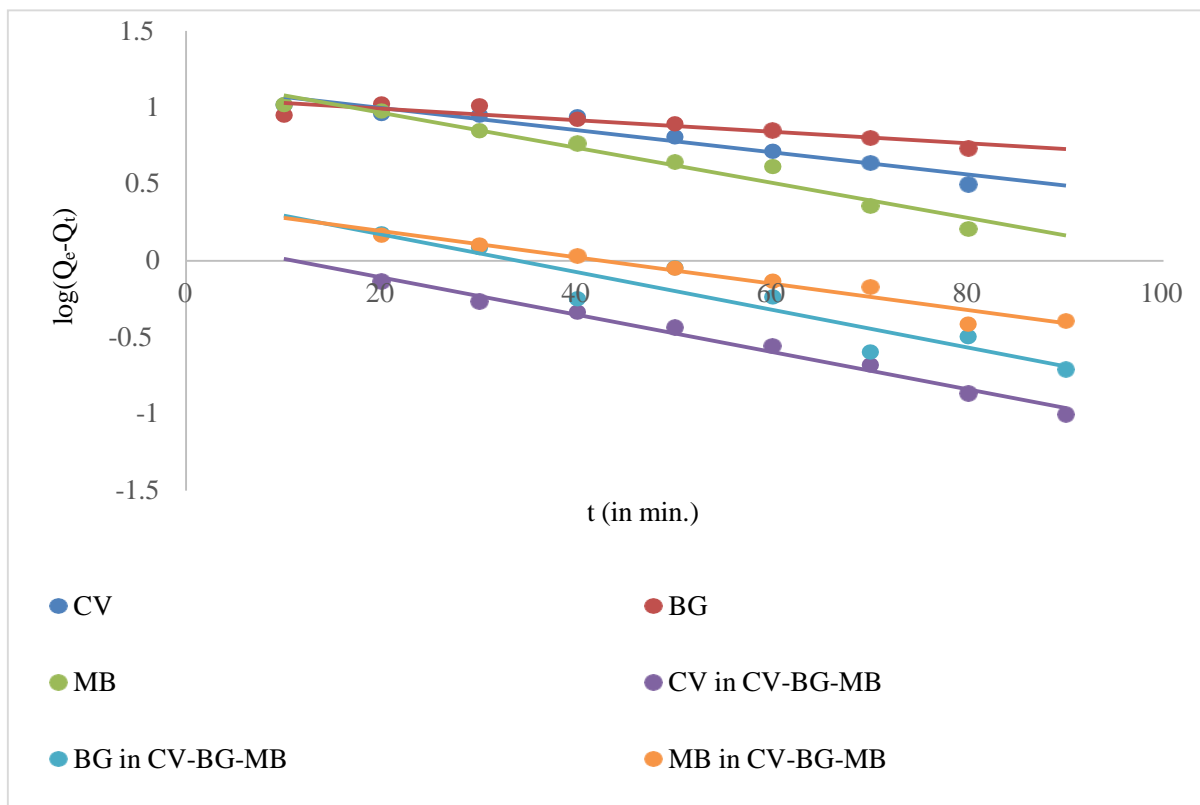
Figure 4.2.31- Lagergren pseudo first order kinetics for single and ternary dye systems using ZFN-MS
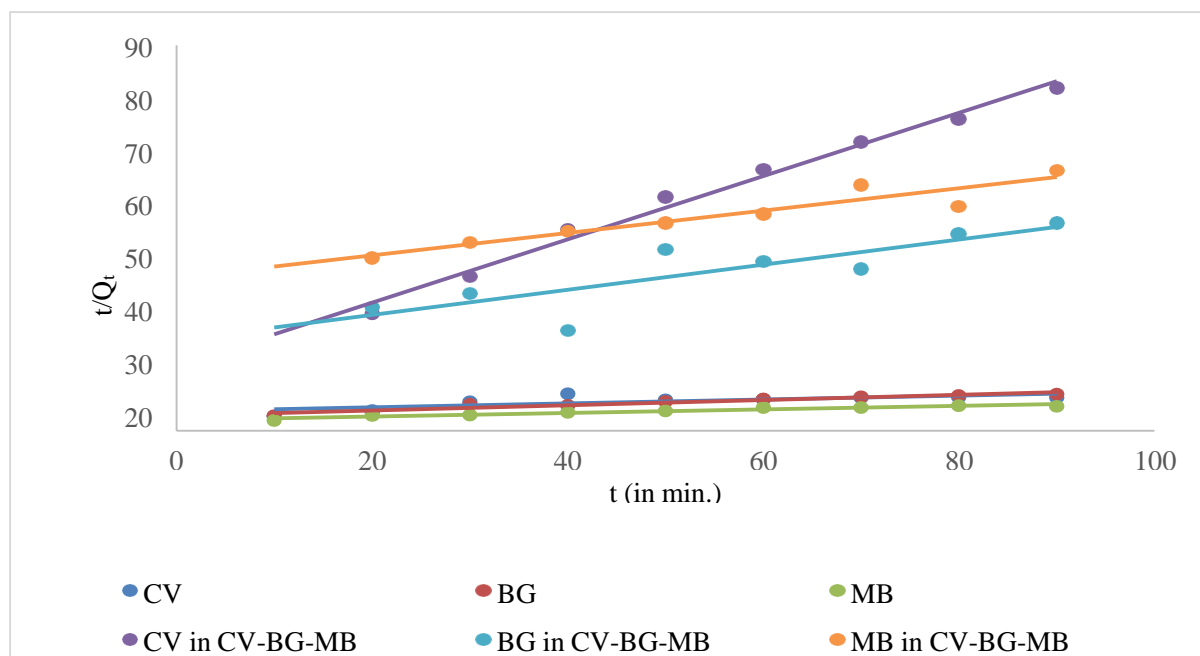
Figure 4.2.32- Pseudo second order kinetics for single and ternary dye systems using ZFN-MS
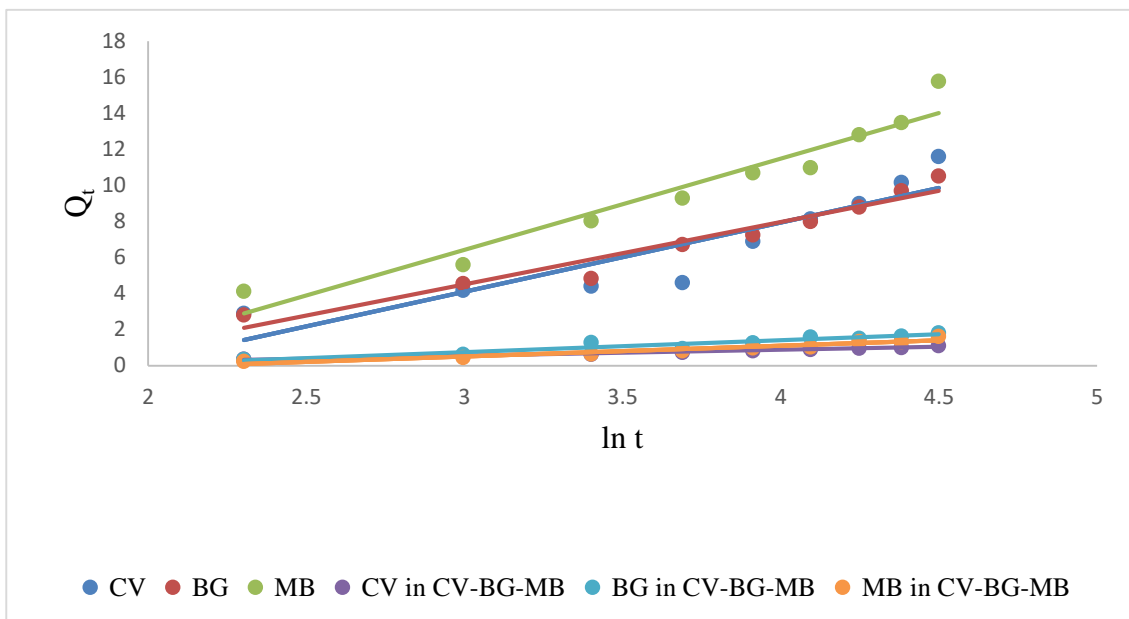
Figure 4.2.33- Elovich model for single and ternary dye systems using ZFN-MS

Table 4.2.9- Kinetic constants for single and ternary dye systems using ZFN-MS

System → Kinetic Model ↓	constants	Single system			Ternary system (CV-BG-MB)		
		Crystal Violet	Methylene Blue	Brilliant Green	CV in (CV-BG-MB)	MB in (CV-BG-MB)	BG in (CV-BG-MB)
Lagergren pseudo first order	Qe_1	2.856	5.786	3.167	0.464	0.375	0.187
	k_1	0.022	0.023	0.034	0.039	0.032	0.049
	R^2	0.659	0.876	0.973	0.887	0.941	0.883
	SD	0.002	0.001	0.002	0.113	0.044	0.091

Pseudo second order	Qe_2	3.857	5.813	5.368	1.763	1.613	1.792
	h	0.179	0.085	0.524	0.413	0.373	1.273
	k_2	0.011	0.004	0.023	0.142	0.162	0.406
	R^2	0.992	0.971	0.991	0.998	0.997	0.998
	SD	0.010	0.012	0.002	0.658	0.623	0.231
Elovich Model	α	0.783	0.163	3.438	1518.3	553.5	890.5
	β	1.351	0.878	1.442	8.764	9.138	19.703
	R^2	0.949	0.975	0.992	0.879	0.952	0.892
	SD	0.058	0.096	0.039	0.066	0.039	0.021
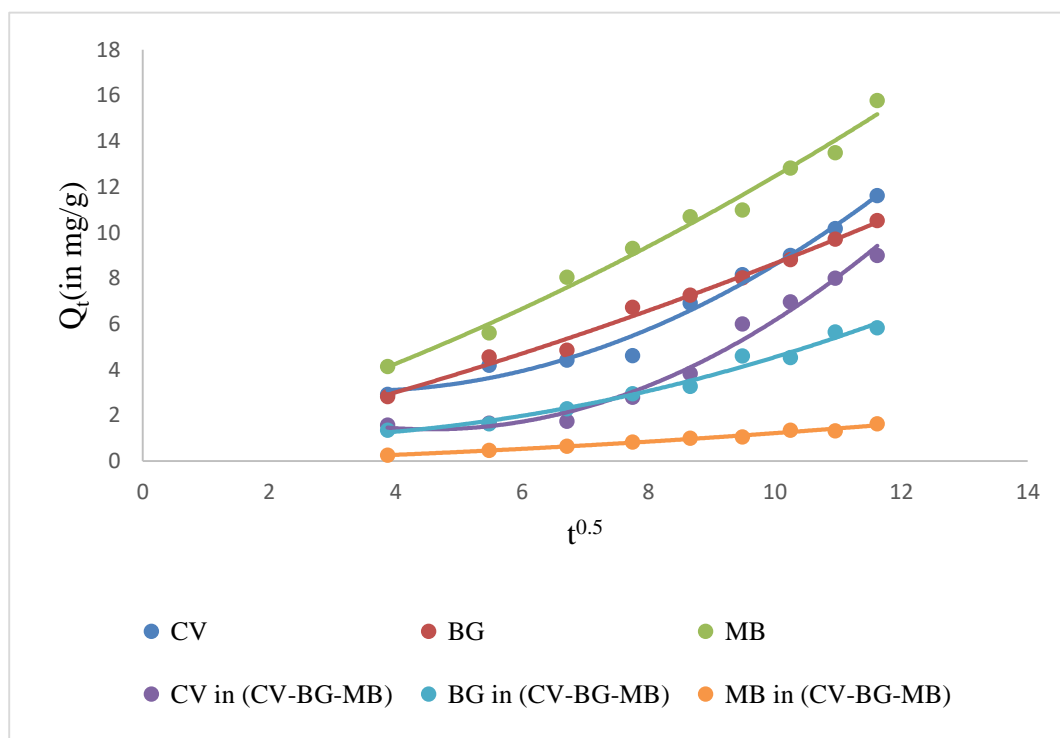
Figure 4.2.34- Weber Morris model for single and ternary dye systems using ZFN-MS

The Weber Morris intra particle diffusion model for the single and ternary dye systems for Methylene Blue, Brilliant Green and Crystal Violet is shown in Figure 4.2.34. The graph clearly shows that straight line does not pass through origin in single and ternary dye systems, which suggested that a number of factors affect adsorption of Crystal Violet, Brilliant Green, and Methylene Blue dyes, using ZFN-MS magnetic green composite and intra particle diffusion is not the sole reason of adsorption. In the ternary system, the slope is not sharp, showing a drop in adsorption rate brought on by the dye's antagonistic interactions. Strong bonds were formed between the molecules of Methylene Blue, Brilliant Green, and Crystal Violet dyes, as a result of electrostatic forces. As a result, rate of adsorption in ternary dye system decreased[30].

4.2.25 Effect of pH

Adsorbent's capacity to remove dyes is strongly affected by the pH of the solution. It affects the adsorbent's adsorption behavior, as the surface charge is controlled by pH of the solution. At various pH levels, ZFN-MS magnetic green composite was utilised for studying the adsorption behavior of CV, BG and MB dyes. For this, 0.1g of ZFN-MS magnetic green composite was added in 50 mg/L of dyes for two hrs at various initial pH levels ranging from 3-11. Effect of pH on percentage removal of ZFN-MS magnetic green composite, to eliminate Crystal violet, Brilliant green, and Methylene blue dyes from aqueous solutions is shown in Figure 4.2.35. The maximum removal was observed around pH~7-8 to remove dyes from solution correlates with the pH_{PZC} of ZFN-MS which was 7.4. When the pH value exceed from pH_{PZC} value, the surface of ZFN-MS became negative and cationic dye molecules get attached with the surface of the adsorbent.
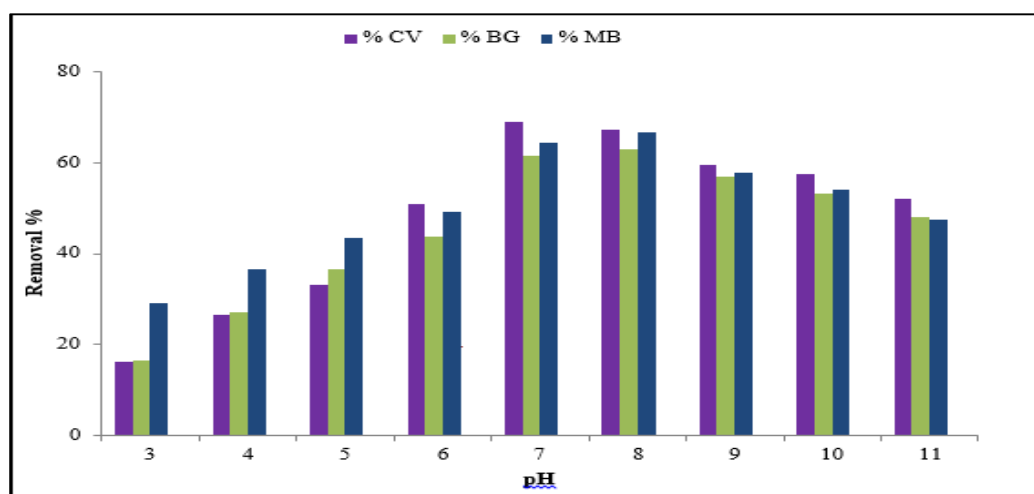
4.2.26 Effect of adsorbent dose

In single system 50mg/L and in ternary system 20 mg/L concentration of dyes were taken and adsorbent dose was changed from 0.1-0.5g in 50 mL of dye solution. Figure 4.2.36 shows the percentage removal ofCrystal Violet, Brilliant Green, and Methylene Blue dyes in single and ternary dye systems, using different doses of ZFN-MS magnetic green composite. It was found that in both systems, as adsorbent dosage increased, percentage removal of dyes also increased. This was noticed because the number of vacant active sites increased as adsorbent dosage increased in single and ternary dye systems[26]. Using ZFN-MS, removal efficiency of MB, CV and BG dyes increased from 69.4% to 77.5%, 59.2% to 79.5% and 53.5% to 75.5%, respectively in single dye system. In ternary dye system, it increased from 52.4% to 75.2%, 55.5% to 74.4% and 53.1% to 72% for MB, CV and BG dyes respectively. Compared to single dyes, percentage removal of dyes in ternary dye system was slightly lower, due to antagonistic effect of dyes due various electrostatic and π-π interactions. In both single and ternary dye systems, adsorption capacity (Q_e) decreased as adsorbent dose increased. The unsaturation of adsorption sites was responsible for the decrease in Q_e at higher adsorbent dose[31].
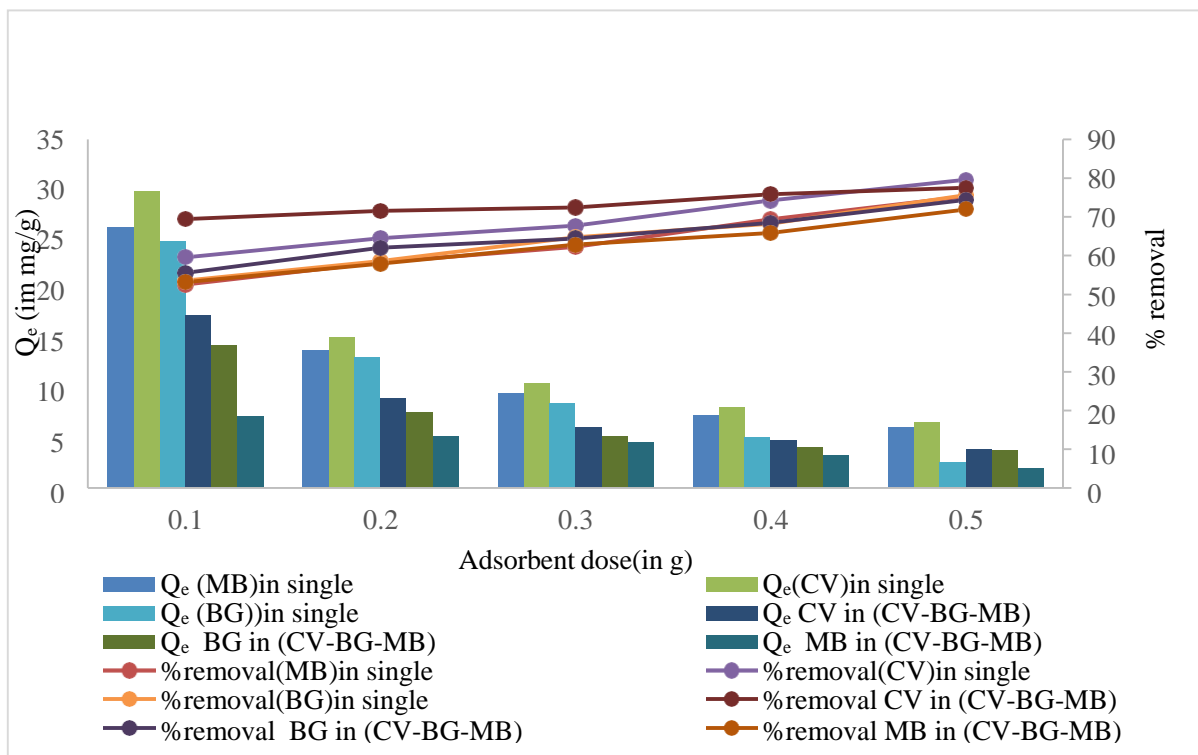
Figure 4.2.36- Effect of adsorbent dose in single and ternary dye systems using ZFN-MS

4.2.27 Effect of concentration and temperature

Effect of concentration on removal of dyes in single and ternary dye systems (50-250 mg/L for single and 20-100 mg/L for ternary dye systems), using ZFN-MS magnetic green composite, is shown in figures 4.2.37 and 4.2.38, respectively. As the initial concentration increased, adsorption capacity (Q_e) also increased. With increase in concentration, more adsorbate and adsorbent molecules came into contact with each other. But percentage removal of dyes decreased by increasing concentration. This was observed because as concentration is increased, less number of active sites were available for adsorption of dyes. As temperature increased, percentage removal of dyes in both systems increased. Because, as temperature was increased, the pore size of adsorbent became large, thus, provided large surface area for adsorption of dyes in single and ternary dye systems[30]. Increase in temperature also increases number of effective collisions due to increase in the kinetic energy of the system. In ternary dye system, percentage removal of dyes was less as compared to single dye system, due to antagonistic effect of dyes (electrostatic and π-π interactions).
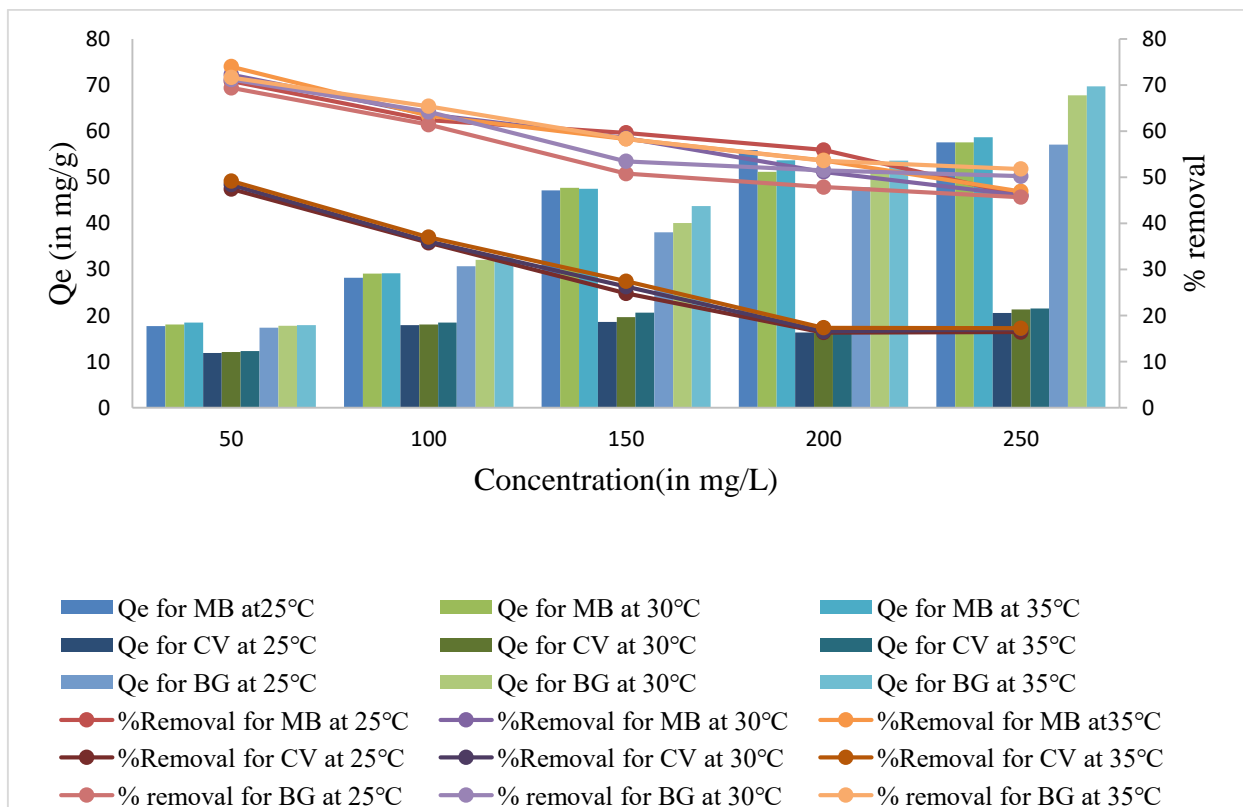
Figure 4.2.37- Effect of concentration in single dye system using ZFN-MS
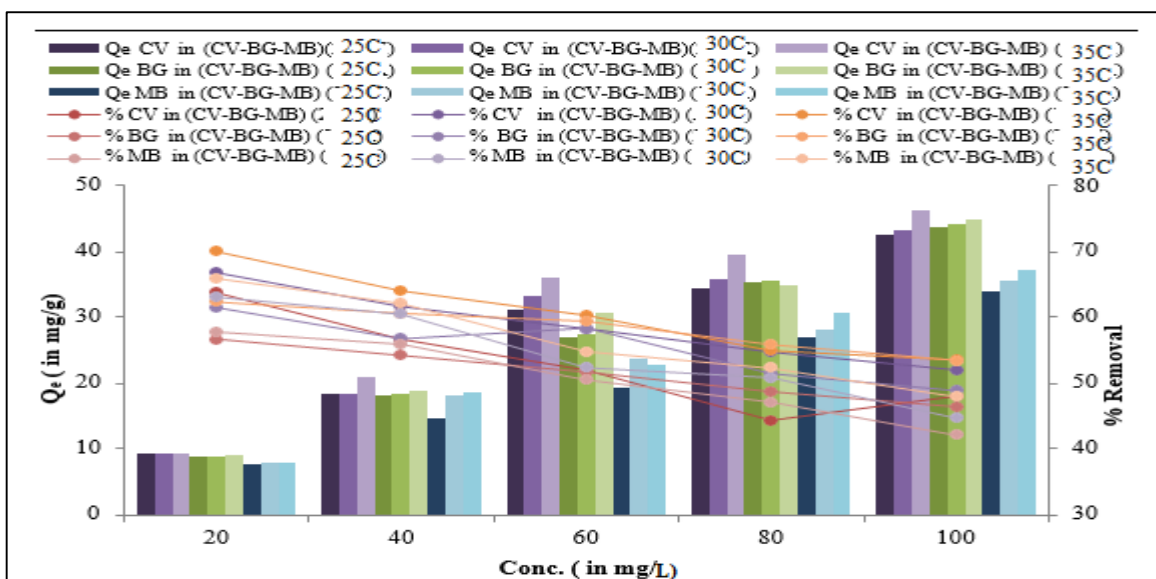
Figure 4.2.38- Effect of concentration in ternary dye system using ZFN-MS

4.2.28 Adsorption isotherms

Several isotherm models have been utilised to describe the equilibrium stage in single and ternary dyes system at three temperatures viz. 25°C, 30°C, 35°C. Figures 4.2.39 to 4.2.46 represent the graphs for different isotherms i.e Langmuir, Freundlich, Temkin and D-R for removing CV, BG and MB dyes in single and ternary dye systems using ZFN-MS magnetic green composite. Different isotherm constants computed from plots of the aforementioned isotherms in both dye systems are depicted in Tables 4.2.10 and 4.2.11. In order to determine which model best described the removal of dyes using ZFN-MS magnetic green composite from aqueous solution, the regression coefficient (R^2) was used. The Freundlich isotherm model displayed a higher R^2 value in both dye systems. Therefore, Freundlich model fitted best while removing dyes from aqueous solution using ZFN-MS magnetic green composite. Separation factor (R_L) which is associated with Langmuir isotherm, had values between between 0 and 1, which demonstrated the favourable nature of adsorption using ZFN-MS[26]. Adsorption energy 'E' indicates whether the process of adsorption of dyes is chemical or physical. The value of E for removal of CV, MB, and BG dyes in both systems is greater than 40 kJ/mol in current study[22]. It suggested that the process of the adsorption of dyes using ZFN-MS was chemical in nature. Maximum adsorption capacities using ZFN-MS for CV, BG and MB dyes were found to be 142.9, 101.2 and 105.8 mg/g, respectively in single dye system whereas in ternary dye system it was found to be 66.8, 53.8 and 54.5 mg/g, respectively for CV, BG and MB dyes.
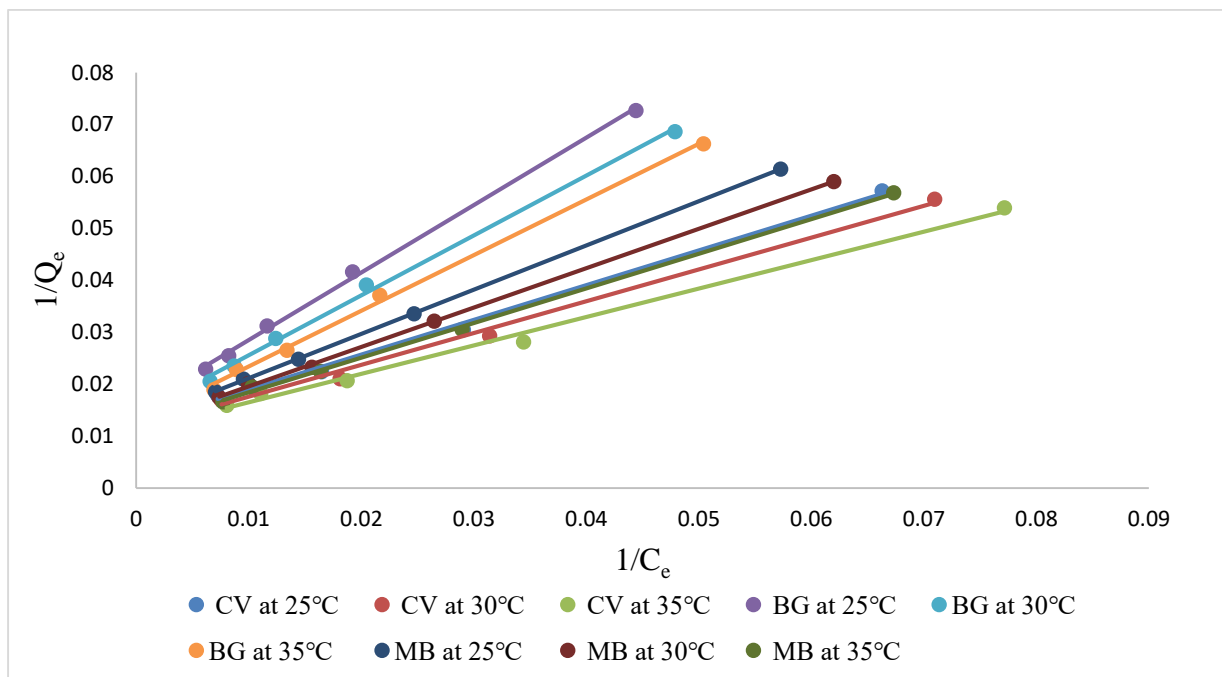
Figure 4.2.39- Langmuir isotherms for single dye system using ZFN-MS
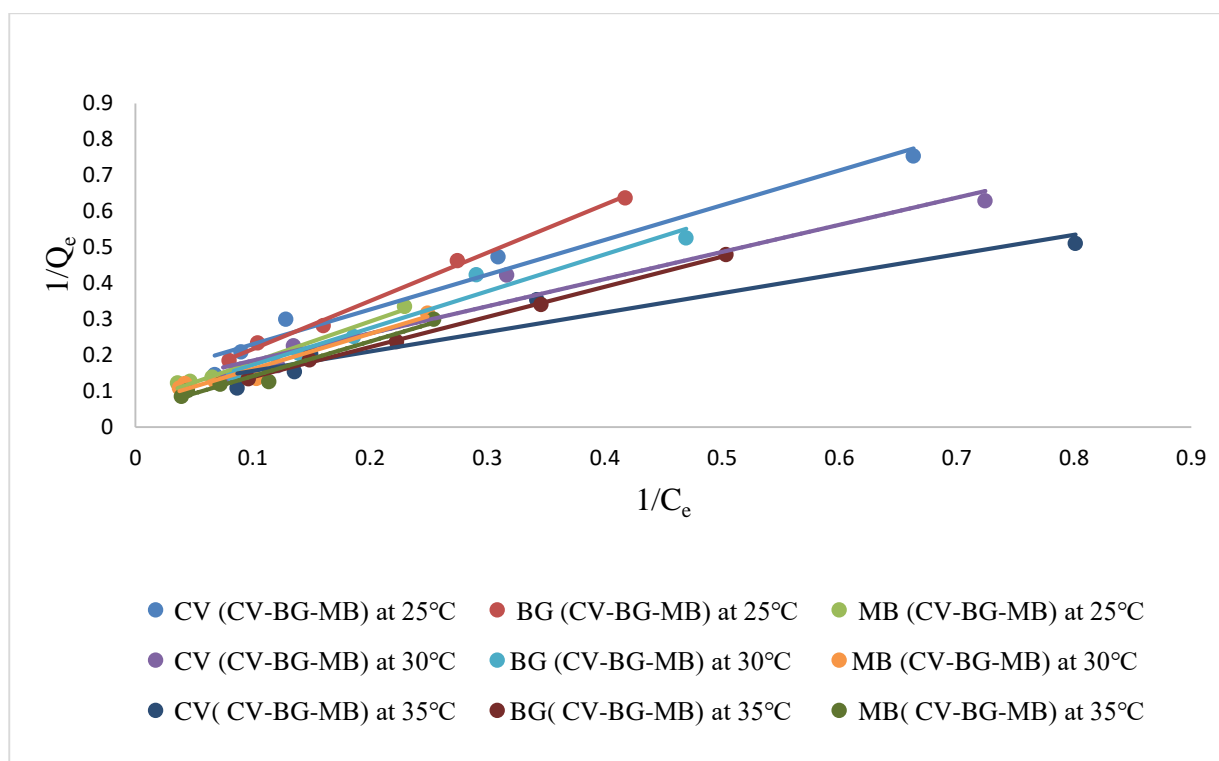
Figure 4.2.40- Langmuir isotherms for ternary dye system using ZFN-MS
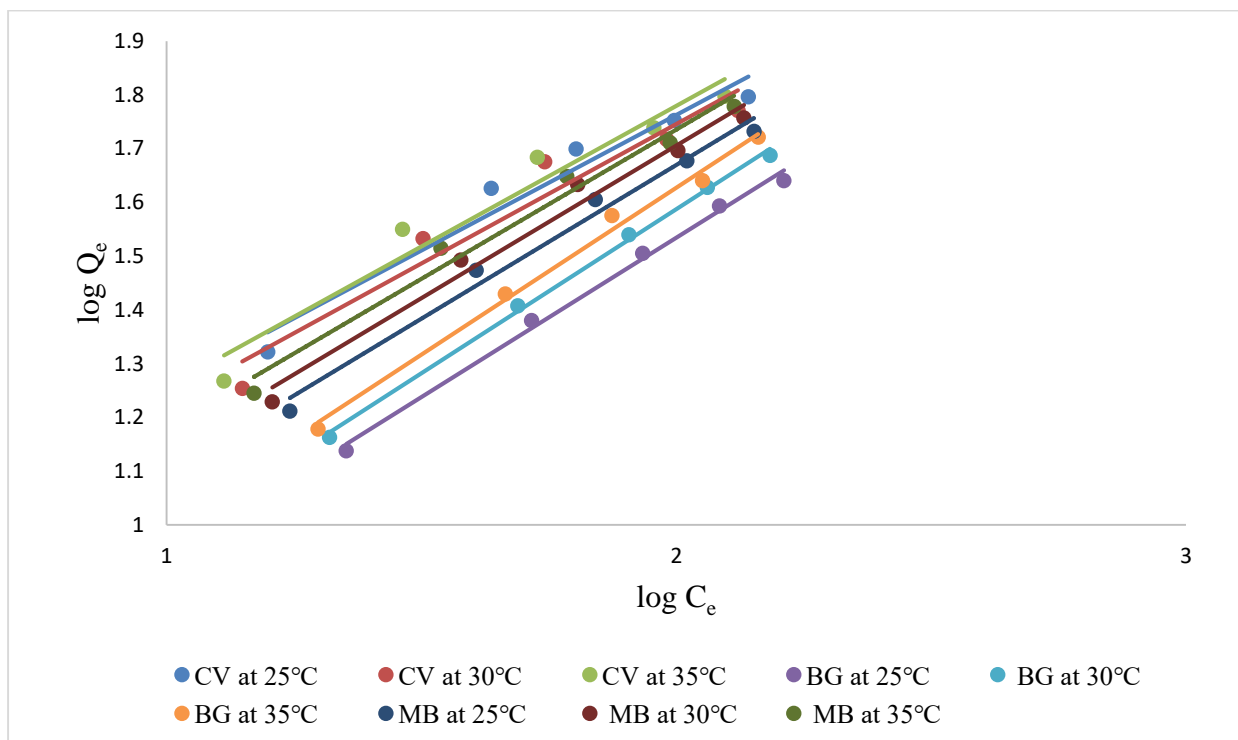
Figure 4.2.41- Freundlich isotherms for single dye system using ZFN-MS
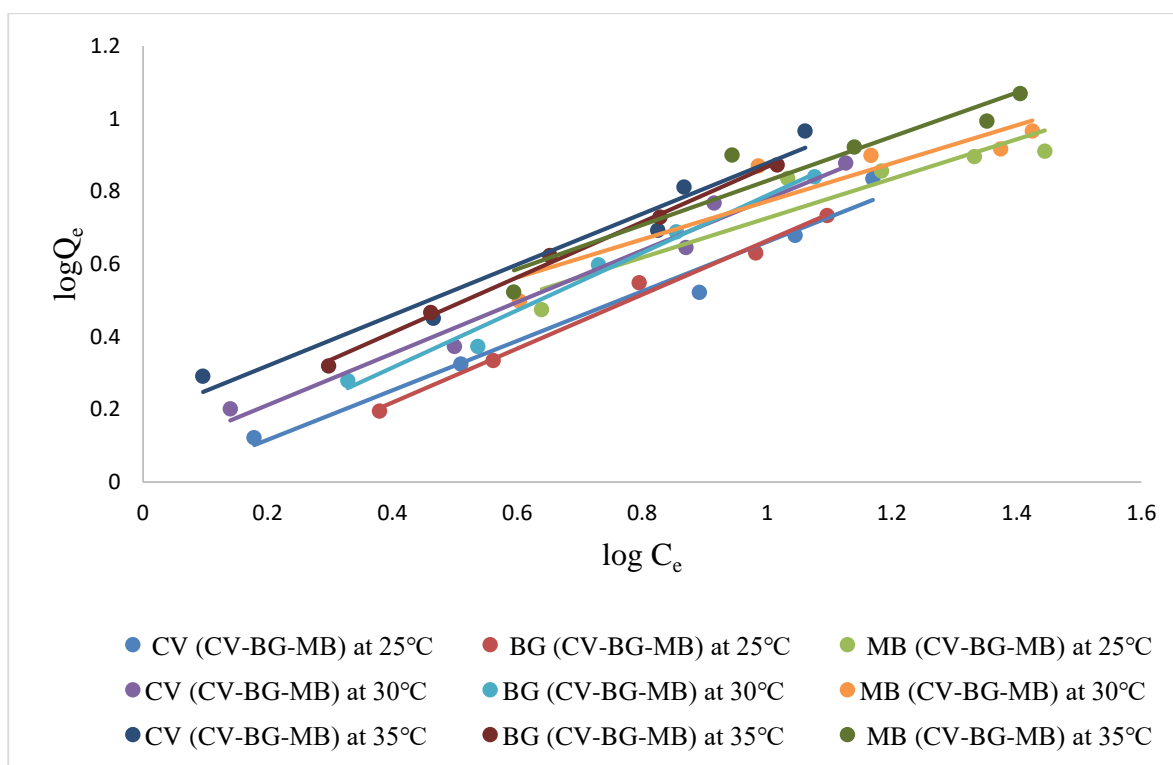
Figure 4.2.42- Freundlich isotherms for ternary dye system using ZFN-MS
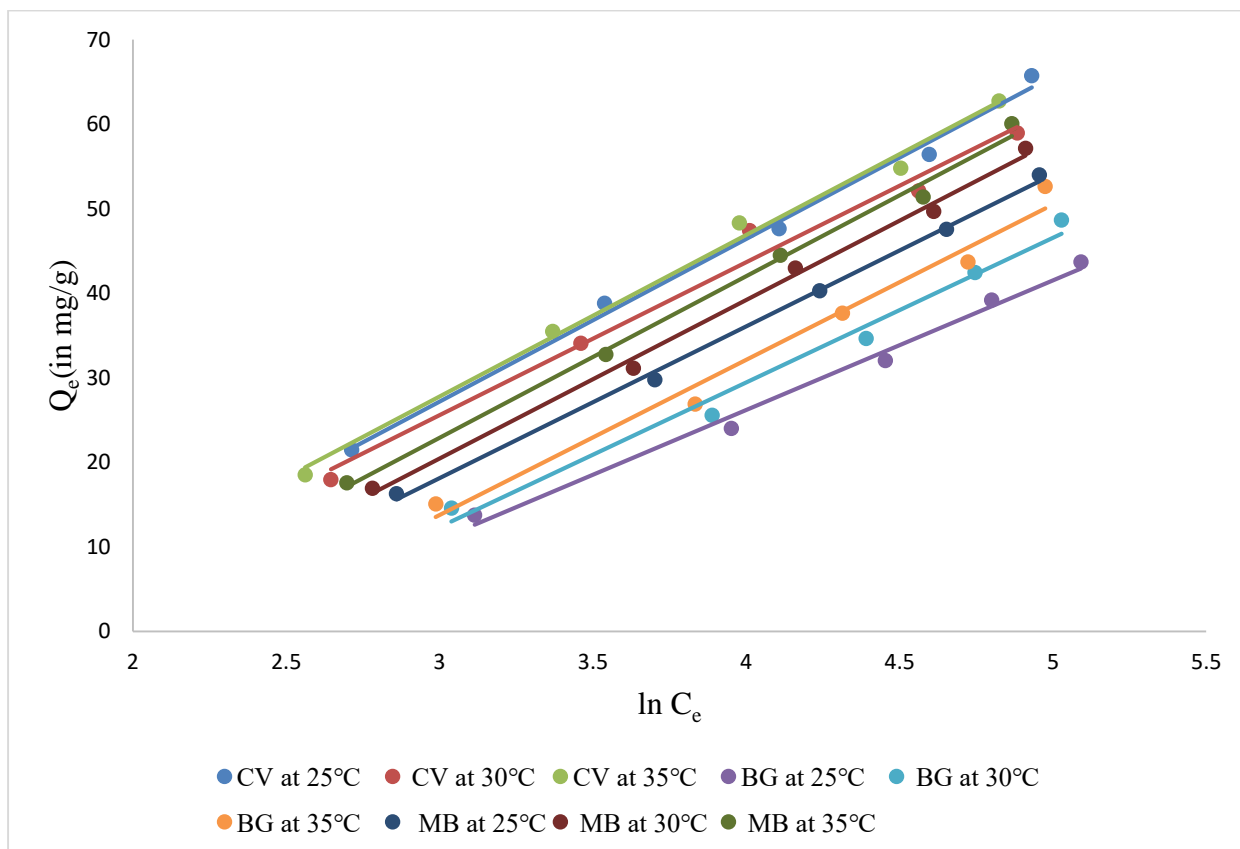
Figure 4.2.43- Temkin isotherms for single dye system using ZFN-MS
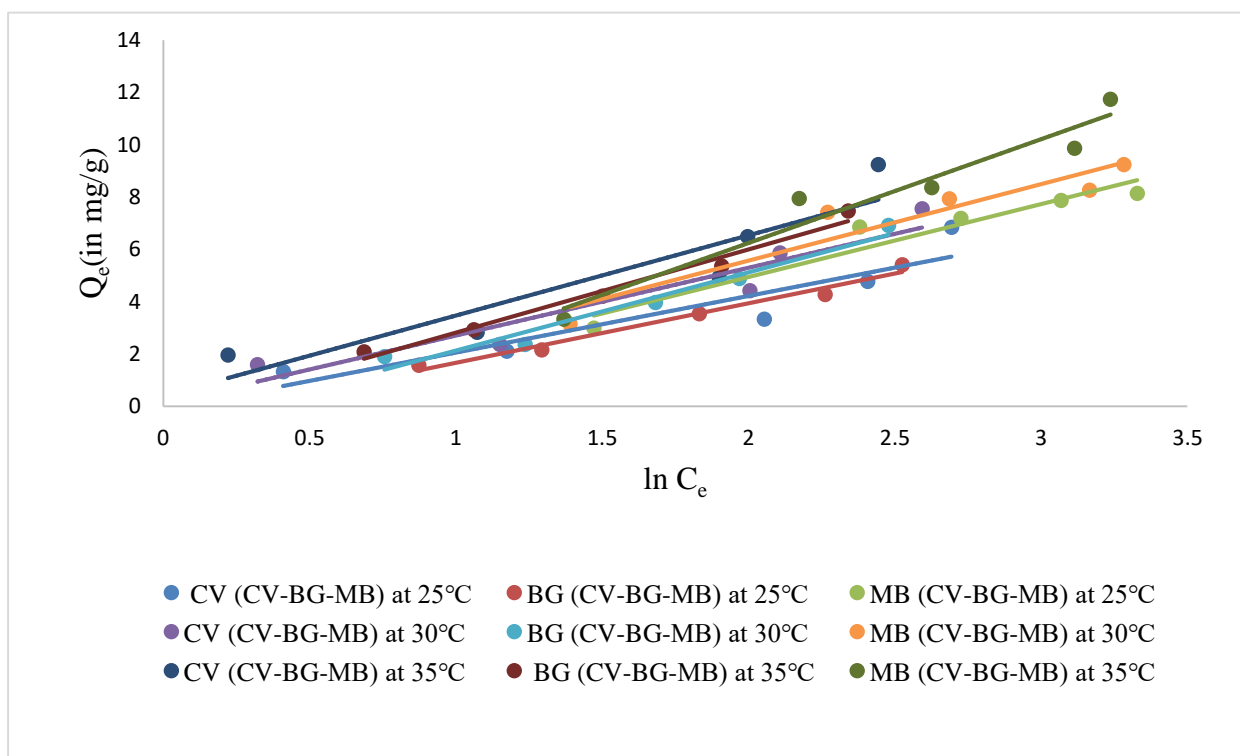
Figure 4.2.44- Temkin isotherms for ternary dye system using ZFN-MS

110
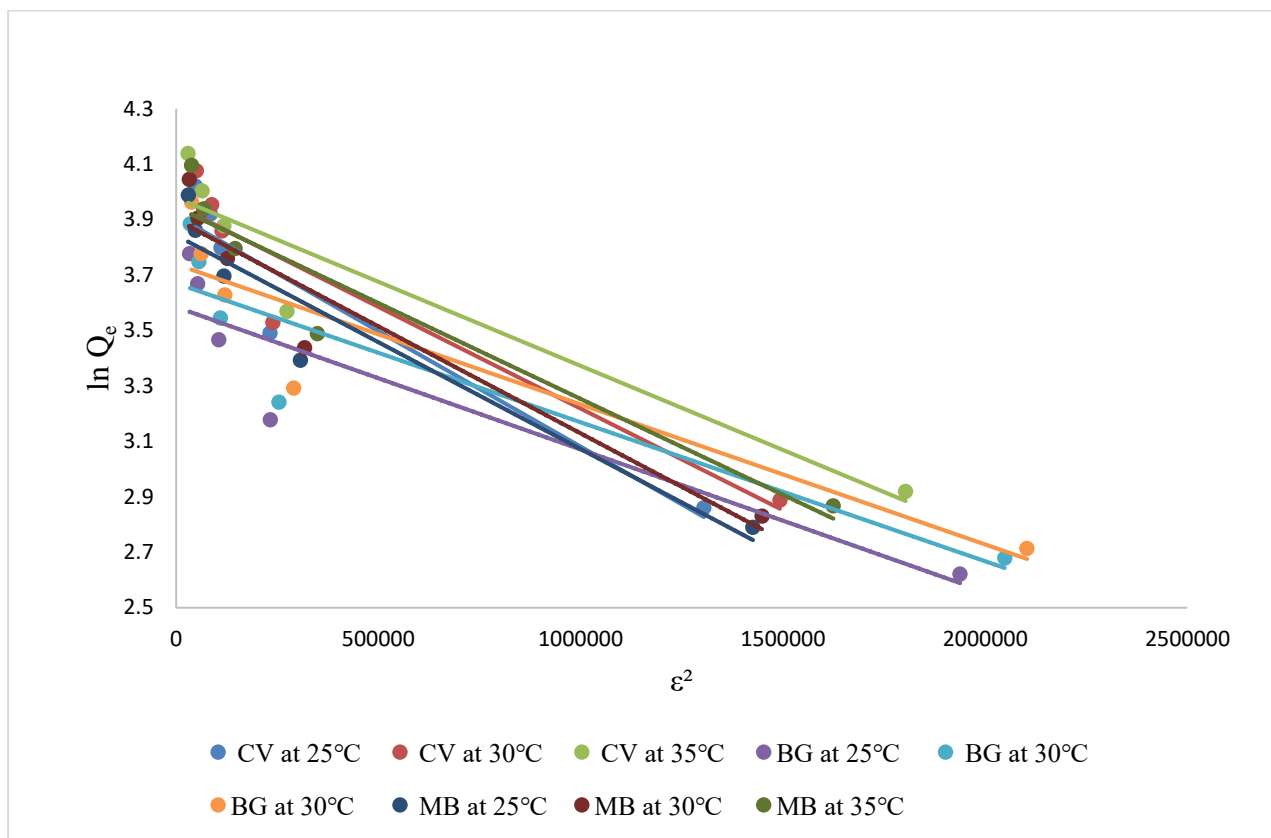
Figure 4.2.45- D-R isotherms for single dye system using ZFN-MS
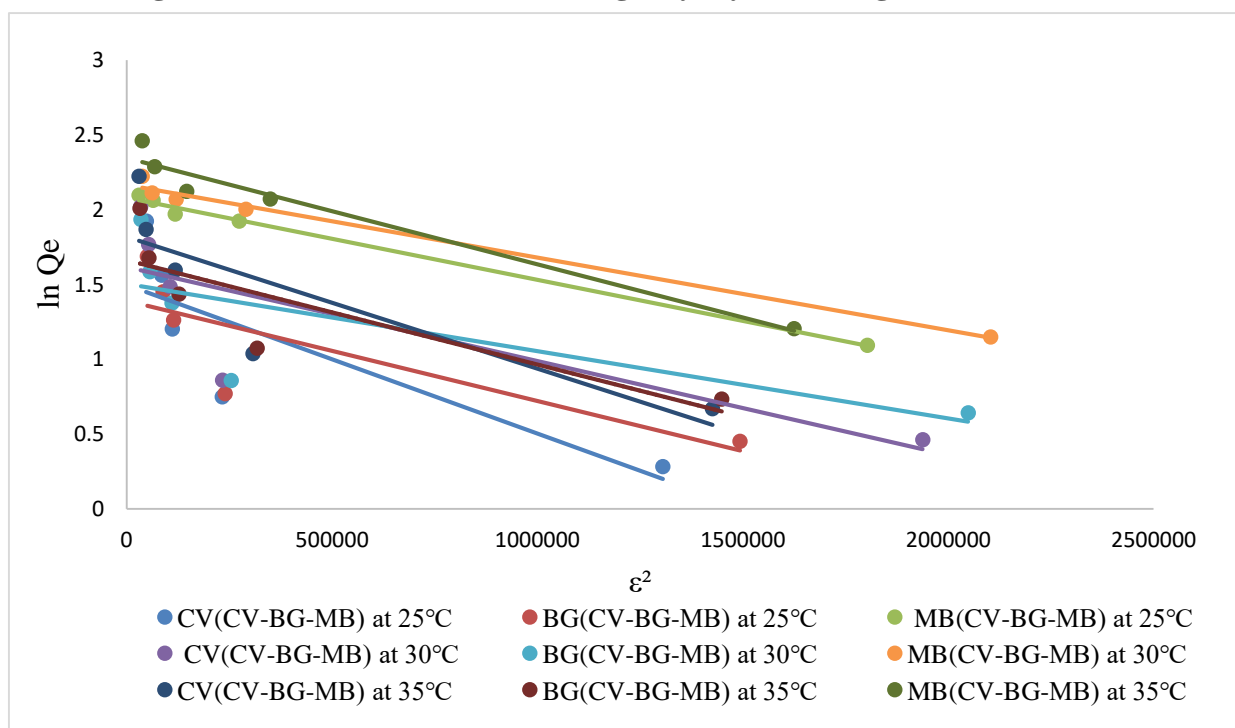
Figure 4.2.46- D-R isotherms for ternary dye system using ZFN-MS

Table 4.2.10- Isotherm constants for single dye system using ZFN-MS

SYSTEM		CV			BG			MB		
Isotherm Model	Const.	25°C	30°C	35°C	25°C	30°C	35°C	25°C	30°C	35°C
Langmuir	Q	134.5	138.6	142.9	95.6	97.9	101.2	97.2	101.4	105.8
	b	0.031	0.038	0.043	0.049	0.052	0.059	0.032	0.037	0.044
	R^2	0.962	0.954	0.949	0.990	0.983	0.969	0.971	0.982	0.963
	SD	0.031	0.068	0.022	0.008	0.004	0.007	0.049	0.093	0.074
	R_L	0.138	0.122	0.109	0.012	0.013	0.029	0.133	0.098	0.090
Freundlich	K_f	1.204	1.363	1.692	0.703	0.769	0.914	1.022	1.493	1.576
	1/n	0.509	0.523	0.496	0.721	0.732	0.706	0.524	0.521	0.516
	R^2	0.998	0.993	0.998	0.997	0.998	0.997	0.999	0.982	0.993
	SD	0.052	0.058	0.032	0.039	0.046	0.052	0.082	0.035	0.071

	Q_m	11.2	12.8	13.9	5.9	6.2	7.4	11.1	12.3	13.9
D-R	K_{DR}	2.9×10^{-5}	2.4×10^{-5}	1.8×10^{-5}	1.9×10^{-5}	2.9×10^{-5}	1.8×10^{-5}	3.8×10^{-5}	2.9×10^{-5}	2.3×10^{-5}
	R^2	0.826	0.855	0.923	0.798	0.838	0.873	0.856	0.879	0.892
	E	144.6	173.8	200.5	428.9	456.6	494.3	132.5	152.2	183.6
	SD	0.966	0.113	0.108	0.153	0.152	0.143	0.128	0.109	0.102
Temkin	b_T	702.3	648.1	632.5	984.6	945.1	939.3	692.4	618.2	605.4
	A	0.244	0.274	0.402	0.501	0.518	0.632	0.242	0.296	0.321
	R^2	0.992	0.991	0.989	0.912	0.923	0.946	0.989	0.972	0.981
	SD	0.132	0.292	0.182	0.754	0.722	0.602	0.124	0.278	0.243

Table 4.2.11- Isotherm constants for ternary dye system using ZFN-MS

SYSTEM		CV in CV-MB-BG			BG in CV-MB-BG			MB in CV-MB-BG		
Isotherm Model	Const.	298K	303K	308K	298K	303K	308K	298K	303K	308K
Langmuir	Q	65.4	66.1	66.8	48.4	52.6	53.8	45.4	48.9	54.5
	b	0.065	0.091	0.096	0.091	0.118	0.127	0.058	0.043	0.061
	R^2	0.936	0.909	0.961	0.998	0.997	0.991	0.992	0.991	0.996
	SD	0.042	0.044	0.039	0.009	0.006	0.009	0.014	0.008	0.007
	R_L	0.149	0.125	0.097	0.114	0.089	0.092	0.188	0.191	0.167
Freundlich	K_f	0.684	0.873	1.189	1.072	1.407	1.705	0.692	0.726	0.923
	1/n	0.729	0.814	0.807	0.677	0.641	0.618	0.729	0.721	0.698
	R^2	0.995	0.997	0.993	0.996	0.998	0.997	0.996	0.995	0.998
	SD	0.113	0.146	0.085	0.012	0.024	0.051	0.033	0.041	0.065
D-R	Q_m	6.102	5.998	6.571	6.091	6.401	6.831	5.873	5.898	6.104

		K_{DR}	2.5×10^{-6}	1.5×10^{-6}	1.8×10^{-7}	1.4×10^{-7}	8×10^{-7}	8×10^{-7}	2×10^{-7}	2.9×10^{-7}	2.5×10^{-7}
		R^2	0.653	0.652	0.698	0.804	0.896	0.891	0.814	0.836	0.829
		SD	0.219	0.222	0.192	0.153	0.143	0.124	0.154	0.152	0.140
		E	452.5	618.7	772.1	592.8	741.5	829.4	419.1	439.5	514.1
Temkin		b_T	924.1	798.9	814.1	956.7	944.8	963.5	984.3	936.8	937.5
		A	0.472	0.671	0.678	0.794	1.062	1.325	0.504	0.514	0.629
		R^2	0.851	0.773	0.723	0.959	0.987	0.992	0.918	0.927	0.954
		SD	1.613	2.104	2.010	0.714	0.468	0.243	0.754	0.719	0.611

4.2.29 Thermodynamics of adsorption

The thermodynamics of adsorption is significant because thermodynamic parameters like free energy change, entropy change and enthalpy change gave valuable information about the feasibility of adsorption process. Various thermodynamic constants were calculated from the slopes and intercepts of the graph between ln K_d and 1/T for CV, BG and MB dyes in single and ternary dye systems (Figures 4.2.47 and 4.2.48). The thermodynamic constants are depicted in table 4.2.12 which were calculated for removal of dyes in both systems using ZFN-MS magnetic green composite. $\Delta H°$ and $\Delta S°$ values were both positive, indicating an endothermic process with more randomness at the surface of adsorbent. Negative $\Delta G°$ values reveals the spontaneous nature of adsorption of dyes by ZFN-MS magnetic green composite from aqueous solution.
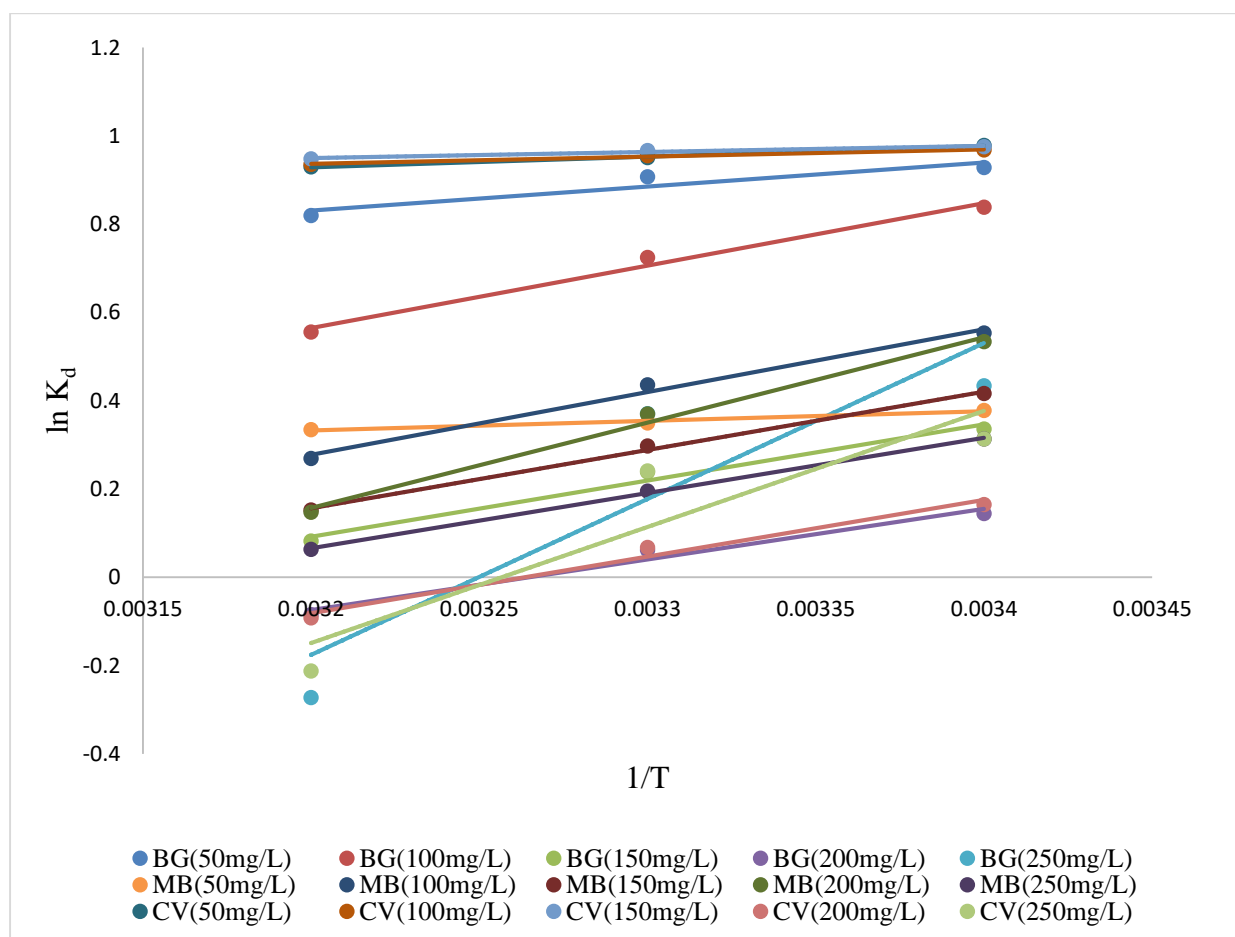
Figure 4.2.47- Graph between ln K_d and 1/T for single dye system using ZFN-MS
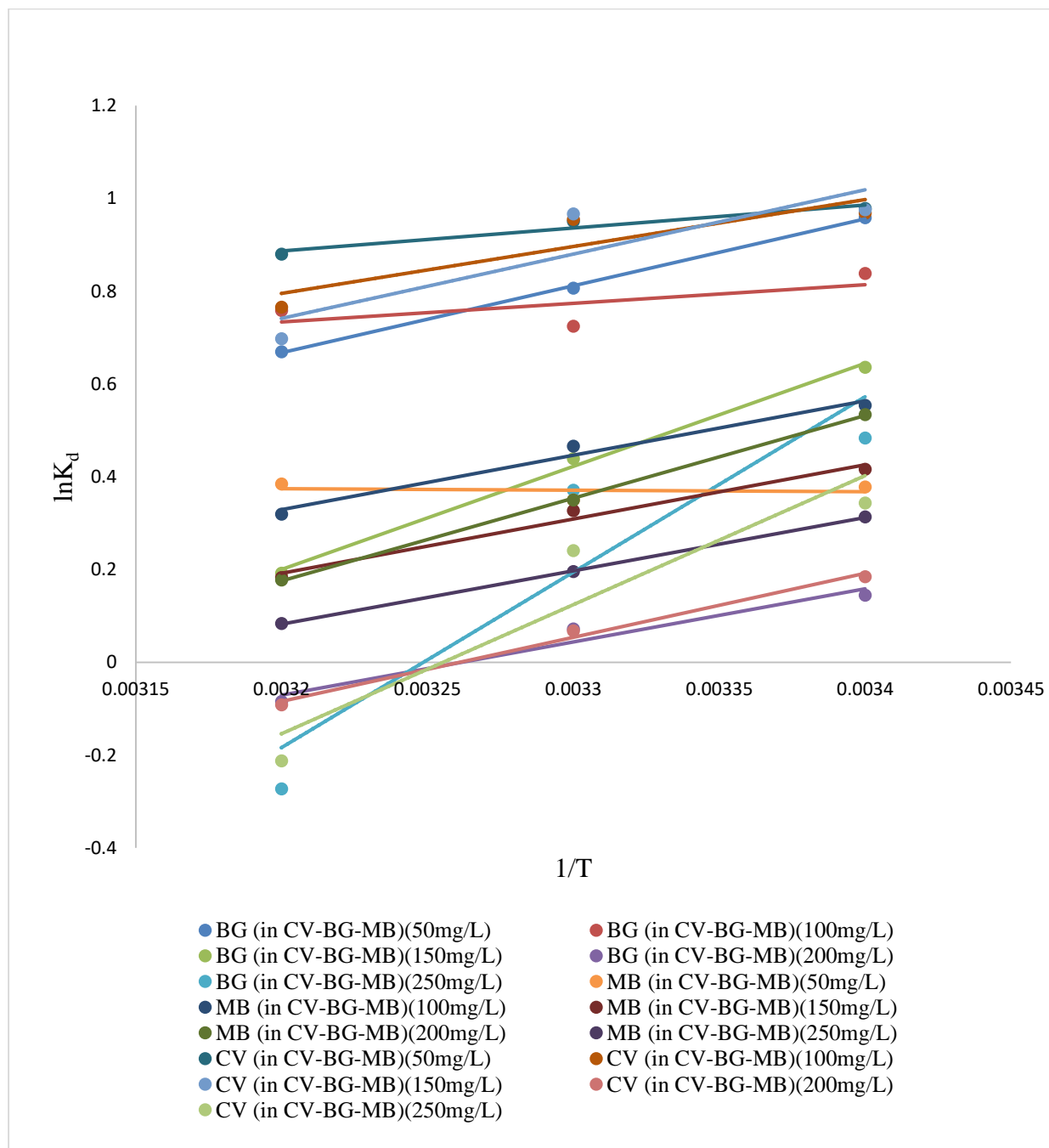
Figure 4.2.48- Graph between ln K_d and 1/T for ternary dye system using ZFN-MS

Table 4.2.12- Thermodynamic constants for single and ternary dye systems using ZFN-MS

Dye system	Conc. in mg L^{-1}	ΔH^o in kJ mol^{-1}	ΔS^o in Jmol^{-1}K^{-1}	ΔG^o at 25ºC in kJmol^{-1}	ΔG^o at 30ºC in kJmol^{-1}	ΔG^o at 35ºC in kJmol^{-1}
CV	50	38.225	0.112	-2.714	-2.472	-1.651
	100	45.761	0.133	-3.611	-2.955	-2.212
	150	32.543	0.084	-4.120	-3.794	-3.337
	200	41.201	0.114	-5.551	-4.676	-4.114
	250	29.502	0.072	6.104	5.378	5.102
BG	50	13.428	0.061	-3.805	-4.112	-4.559
	100	48.751	0.169	-2.950	-3.723	-4.442
	150	92.263	0.312	-1.602	-3.058	-4.478
	200	79.812	0.271	-0.002	-1.413	-2.973
	250	45.228	0.131	1.514	0.962	0.307
MB	50	35.813	0.097	3.114	2.655	2.115
	100	49.528	0.132	-3.773	-3.118	-2.553

	150	43.651	0.138	-4.513	-4.105	-3.275
	200	32.109	0.096	-5.104	-4.787	-4.324
	250	26.004	0.072	5.972	5.576	5.446
CV in CV-BG-MB	20	60.584	0.202	0.992	0.022	-0.964
	40	72.432	0.222	2.655	1.513	0.423
	60	60.204	0.191	-1.978	-0.978	-0.062
	80	88.394	0.293	-2.43	-0.859	-0.555
	100	75.268	0.264	-2.356	-1.219	-0.033
BG in CV-BG-MB	20	38.441	0.121	0.142	-0.456	-1.068
	40	55.111	0.174	0.738	-0.114	-0.946
	60	49.471	0.161	-1.491	-0.615	-0.158
	80	28.113	0.092	-1.814	-1.339	0.935
	100	29.352	0.084	-2.226	-1.797	-1.512
	20	22.551	0.075	1.745	1.495	1.132

MB in CV-BG-MB	40	27.814	0.091	2.343	1.984	1.628
	60	28.338	0.088	-2.491	-2.137	-1.773
	80	19.273	0.064	-3.102	-2.962	-2.694
	100	21.112	0.059	-3.334	-3.108	-2.786

4.2.30 Regeneration of ZFN-MS

After the adsorption, the performance of the adsorbent is assessed using regeneration. Regeneration is criteria to check whether the adsorbent is cost effective or not. After adsorption of different dyes with ZFN-MS magnetic green composite, the regeneration of adsorbent was done by using desorbing agent 0.1N HCl to regenerate ZFN-MS magnetic green composite. Table 4.2.13 shows theregenerability of ZFN-MS magnetic green composite for CV, BG, MB dyes in single and ternary dye systems. ZFN-MS composite was 90.1%, 88.1% and 90.4% efficient to remove CV, BG and MB dyes, respectively in single dye system. In ternary dye system, ZFN-MS was efficient to remove the aforementioned dyes upto 80.4%, 84.6% and 82.8%. These results indicated that ZFN-MS magnetic green adsorbent has good re-usability and is a cost-effective adsorbent.

Table 4.2.13- Regeneration efficiency of ZFN-MS for single and ternary dye systems

Regeneration Cycle	Regeneration efficiency for single system			Regeneration efficiency for ternary system		
	% CV	% BG	% MB	% CV	% BG	% MB
1	98.3	97.9	98.1	97.5	97.5	97.3
2	97.5	96.6	97.6	94.3	95.8	94.9
3	95.2	93.3	96.3	89.6	91.8	92.1
4	94.8	90.4	93.5	84.6	89.3	89.4
5	90.1	88.1	90.4	80.4	84.6	82.8

4.2.31 General mechanism of adsorption for dyes with magnetic green adsorbents

In this study, silica was extracted from rice husk having reactive functional groups like silanol, starch was extracted from mango seed kernel having hydroxyl and carboxylic functional groups and carboxy methyl starch had been synthesized using mango starch (extracted from mango seed kernel) having carboxy methyl functional group which may play significant role in the adsorption of dyes. When rice husk silica is combined with zinc ferrite,

it provides active sites on surface of zinc ferrite-rice husk silica (ZFN-RHS). Similarly, when mango starch and carboxy methyl starch is combined with Zinc ferrite, these provide active sites on the surfaces of Zinc ferrite-mango starch (ZFN-MS) and Zinc ferrite-carboxy methyl starch (ZFN-MS and ZFN-CMS). The cationic dyes Crystal violet (CV), Methylene blue (MB), Malachite green (MG) and Brilliant green (BG) shows strong affinity towards the functional groups attached to magnetic green adsorbents surface (ZFN-RHS/ZFN-MS/ZFN-CMS) due to the presence of opposite surface charge i.e., cationic dyes having positive charge and surface of the adsorbent having negative charge due to presence of functional groups. This may lead to electrostatic interactions between molecules of dye and adsorbent. Further, the study revealed that the nature of adsorption was chemical which again support this argument. On the basis of this discussion, a general mechanism for dye adsorption has been proposed and represented in Figure 4.2.49 for the removal of selected cationic dyes using magnetic green adsorbents (ZFN-RHS/ZFN- MS/ZFN-CMS). Further, as the surface charge of the adsorbent is negatively charged so this adsorbent can be used selectively for removal of cationic pollutants from wastewater.
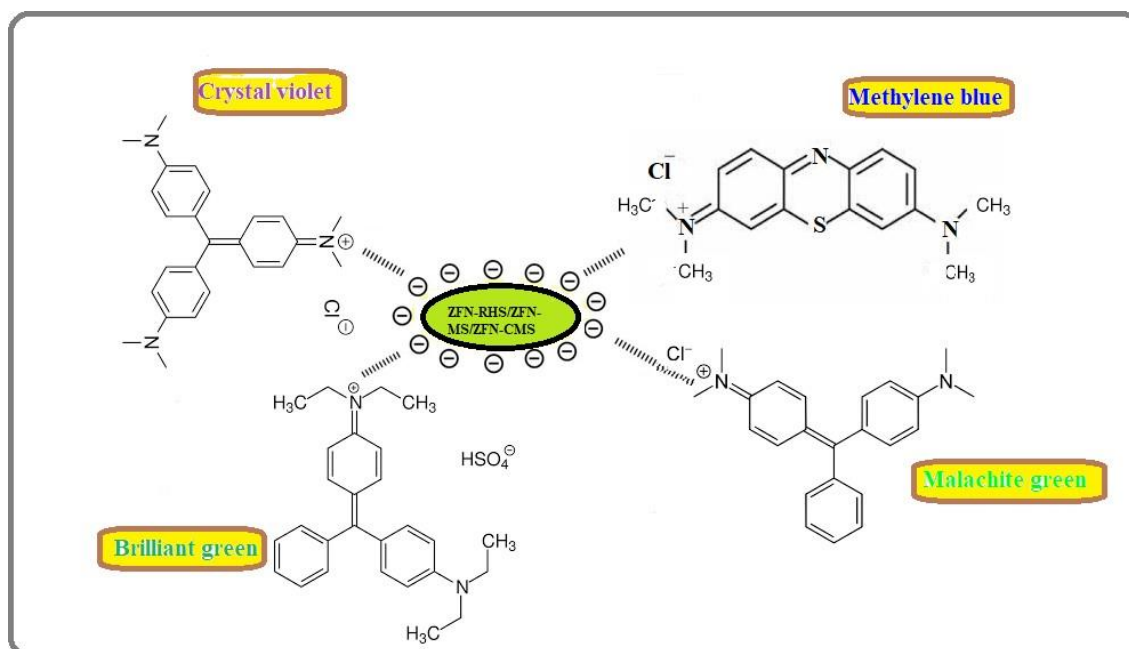
Figure 4.2.49- General mechanism of adsorption of cationic dyes by magnetic green adsorbents(ZFN-RHS/ ZFN-MS/ ZFN-CMS)

Part III

4.3 Batch adsorption studies with fluoride ions

4.3.1   Adsorption of fluoride ions using ZFN-RHS, ZFN-MS and ZFN-CMS magnetic green composites in single ion system

The batch mode of adsorption was utilised for examining adsorption behavior of fluoride ions in single ion system using ZFN-RHS, ZFN-MS and ZFN-CMS magnetic green composites. The flasks were shaken at 200 rpm for two hrs on a thermostatic shaker with 50 mL solution containing 5mg/L of fluoride ions and 0.1g of magnetic green composites. Fluoride ions were analysed spectrophotometrically using the SPADNS method[32]. The absorbance of solution containing fluoride ions was recorded at 570 nm utilising the SPADNS method and UV-VIS spectrophotometer and from this data residual concentration of fluoride ions was calculated. The effect of time, pH, adsorbate concentration, amount of adsorbent, and temperature were studied for removing fluoride ions using ZFN-RHS, ZFN-MS and ZFN-CMS magnetic green composites. Results on various parameters studied for fluoride ion removal have been discussed in the following section.

4.3.2   Effect of contact time

Fluoride ion solution at a fixed concentration (5 mg/L) were taken in various flasks (250 mL). On a thermostatic shaker set at 200 rpm, 0.1g of magnetic green composites (ZFN-RHS, ZFN-MS and ZFN-CMS) were added to each flask. The sample solutions were drawn after fixed interval of time about 10 min. and then residual concentration of F[-] ions was measured (utilising SPADNS method at 570 nm). Effect of time on removal of Fluoride ions using ZFN-RHS, ZFN-MS and ZFN-CMS magnetic green composites is shown in figure 4.3.1. Figure 4.3.1 shows that the percentage removal of fluoride ions was rapid initially, it eventually reached equilibrium after 120 min. Because initially there were abundant vacant sites present on the surface of magnetic green composites which got filled with the passage of time with fluoride ions. When all of these vacant sites were filled with fluoride ions, an equilibrium stage reached[33].
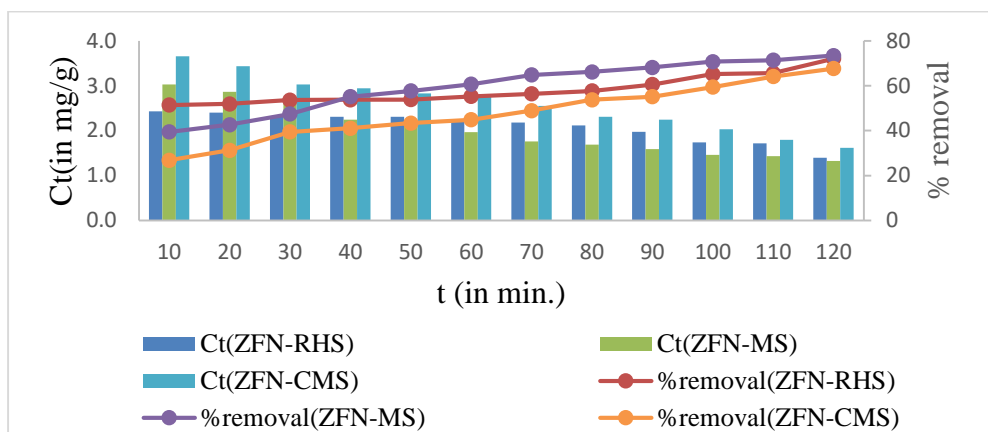
Figure 4.3.1- Effect of time on removal of fluoride ions using ZFN-RHS, ZFN-MS and ZFN-CMS

4.3.3 Kinetics of adsorption

The rate of fluoride ions adsorption on ZFN-RHS, ZFN-MS and ZFN-CMS magnetic green composites was investigated using adsorption kinetics. Utilising the available adsorption data,Lagergren pseudo-first order, Pseudo-second order and Elovich models were applied to calculate the relevant adsorption kinetic parameters. Figures 4.3.2, 4.3.3, 4.3.4 show Lagergren pseudo first order model, Pseudo second order model and Elovich models, respectively, for removing fluoride ions using magnetic green composites (ZFN-RHS, ZFN-MS and ZFN-CMS). Table 4.3.1 depicts the values of kinetic parameters calculated from the graphs of kinetic models for removal of fluoride ions utilising ZFN-RHS, ZFN-MS and ZFN-CMS magnetic green composites.
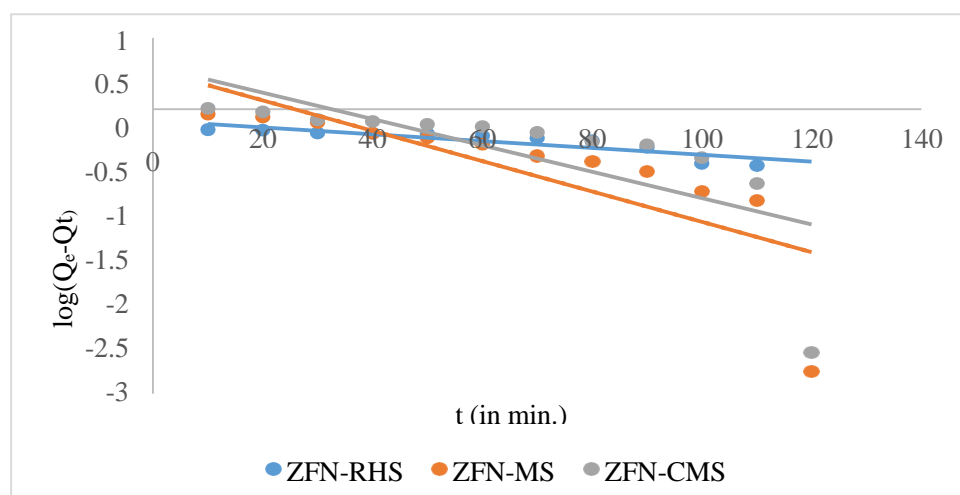
Figure 4.3.2- Lagergren pseudo first order kinetics for removal of fluoride ions using ZFN- RHS, ZFN-MS and ZFN-CMS

124
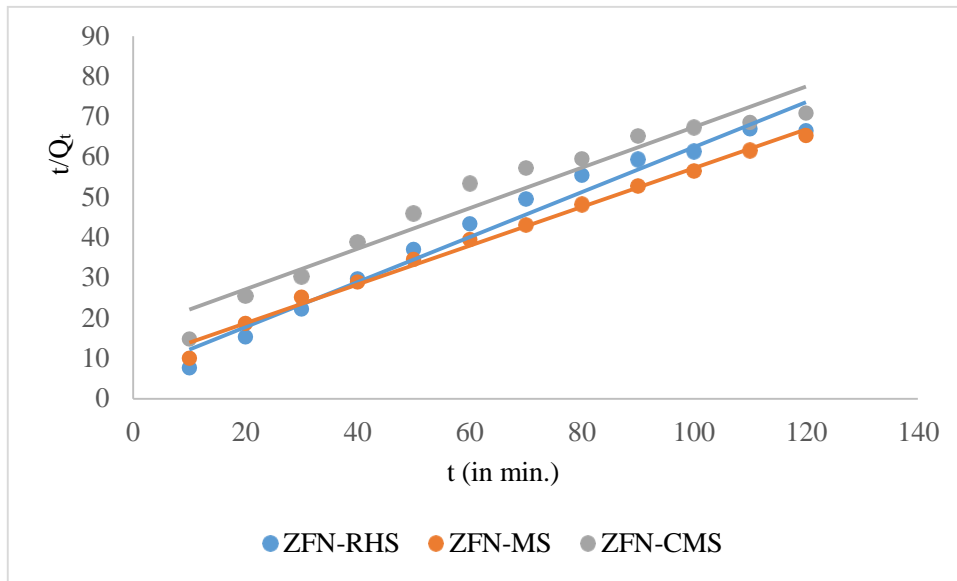
Figure 4.3.3- Pseudo second order kinetics for removal of fluoride ions using ZFN-RHS, ZFN-MS and ZFN-CMS
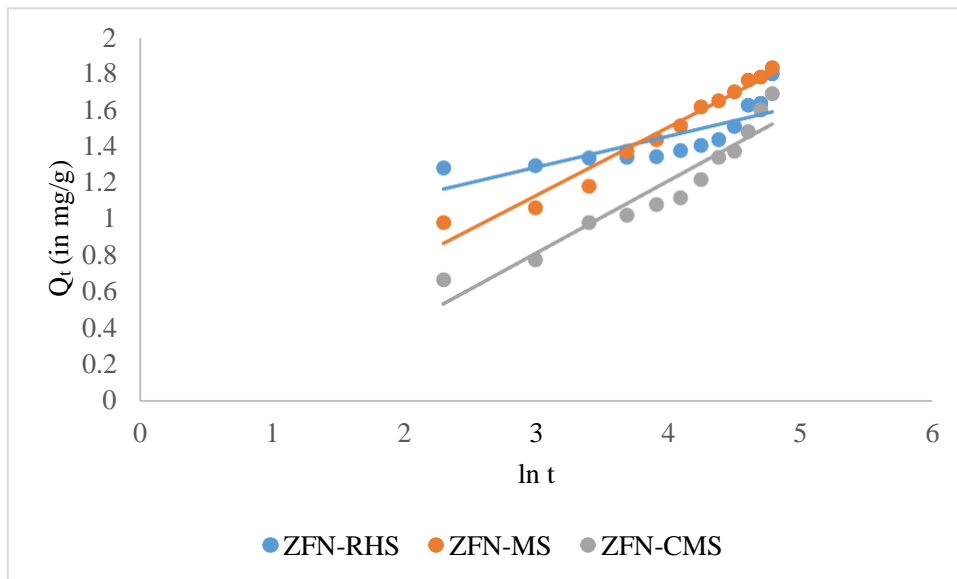
Figure 4.3.4- Elovich model for removal of fluoride ions using ZFN-RHS, ZFN-MS and ZFN-CMS

125

Table 4.3.1- Kinetic constants for removal of fluoride ions using ZFN-RHS, ZFN-MS and ZFN-CMS

Kinetics Model ↓	constants	For ZFN-RHS	For ZFN-MS	For ZFN-CMS
Lagergren Pseudo first order	Q_e	0.619	3.562	3.970
	K_1	0.011	0.049	0.042
	R^2	0.796	0.616	0.510
	S D	0.177	0.189	0.199
Pseudo Second order	Q_{2e}	1.793	2.079	1.989
	h	0.148	0.108	0.058
	K_2	0.046	0.025	0.014
	R^2	0.970	0.965	0.992
	S D	0.949	0.985	0.282
Elovich model	α	16.165	0.382	0.154
	β	5.865	2.666	2.519
	R^2	0.637	0.945	0.909
	S D	0.212	0.052	0.109

According to the data above presented in table 4.3.1, pseudo second order model had the highest regression coefficient value (R^2). Thus, to remove fluoride ions using ZFN-RHS, ZFN-MS and ZFN-CMS magnetic green composites in single ion system, pseudo second order model was best fitted. This means that nature of adsorption was chemisorption[34]. Figure 4.3.5 represents Weber Morris intra particle diffusion model for the removal of fluoride ions using ZFN-RHS, ZFN-MS and ZFN-CMS magnetic green composites. From figure 4.3.5, it is clear that as the graphs do not pass through origin so this is not rate limiting step. It revealed that besides intra particle diffusion, some other factors (like electrostatic interactions etc.) also affected the removal of fluoride ions[35].
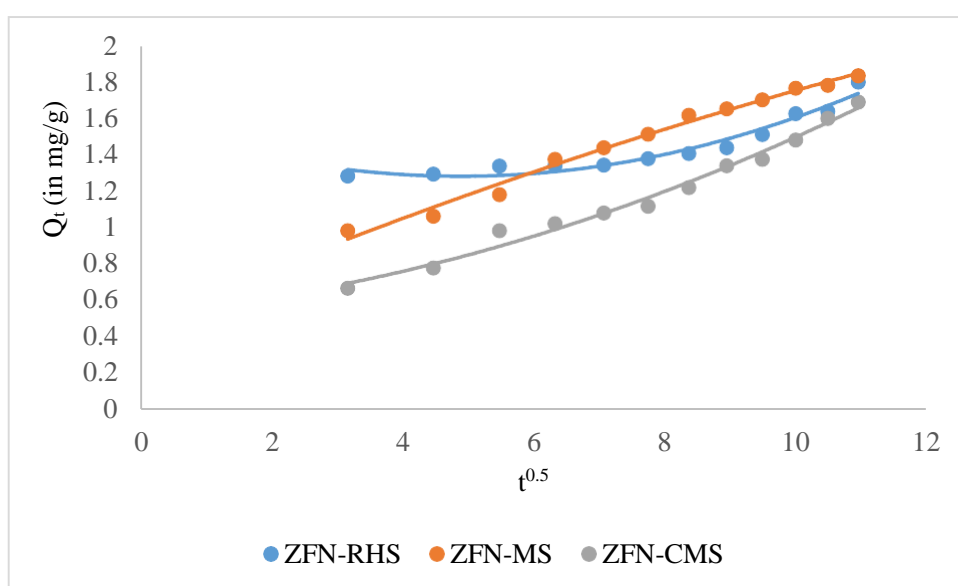
Figure 4.3.5- Weber Morris intra particle diffusion model for the removal of fluoride ions using ZFN-RHS, ZFN-MS and ZFN-CMS

4.3.3 Effect of adsorbent dose

Adsorbent dose was increased from 0.1-0.5g in 50 mL of fluoride ion solution of 5 mg/L concentration. The effect of adsorbent dose for removing fluoride ions using ZFN-RHS, ZFN-MS and ZFN-CMS magnetic green composites is shown in figure 4.3.6. According to Figure 4.3.6, when adsorbent dosage was increased, percentage removal of fluoride ions also increased. For ZFN-RHS removal efficiency of fluoride ions increased from 72.1 to 78.9 percent, for ZFN-MS from 73.5 to 79.8 percent, and for ZFN-CMS from 67.7 to 74.4 percent with increase in the adsorbent dose. This was observed because the number of active sites increased with increase in dose of ZFN-RHS, ZFN-MS and ZFN-CMS magnetic green composites[36].

The adsorption capacities (Q_e) decreased for the removal of fluoride ions using ZFN-RHS, ZFN-MS and ZFN- CMS magnetic green composites. This was observed because of the presence of more vacant active sites on surface of adsorbent for same number of fluoride ions[34].
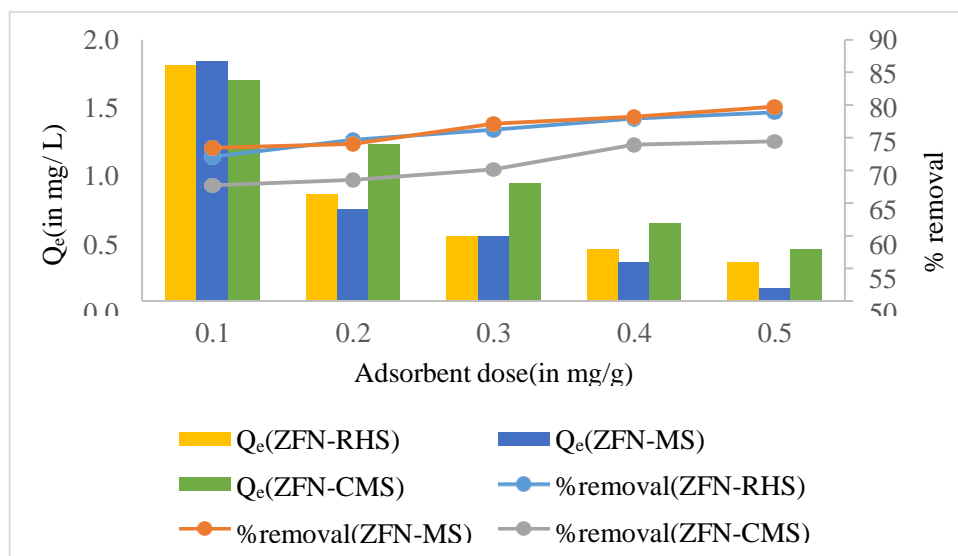
Figure 4.3.6- Effect of adsorbent dose on removal of fluoride ions using ZFN-RHS, ZFN-MS and ZFN-CMS

4.3.4 Effect of pH

The effect of pH for removing fluoride ions from aqueous solution was studied by using a fixed amount of adsorbent (0.1g) at 200 rpm and 25°C with fixed concentration of F⁻ ions (5 mg/L) in 50 mL solution. At various initial pH levels (3-10), the adsorption behavior of fluoride ions using ZFN-RHS, ZFN-MS and ZFN-CMS magnetic green composites was examined and is shown in figure 4.3.7.The percentage removal of fluoride ions was highest with ZFN-RHS at pH 5, ZFN-MS at pH 8, and ZFN-CMS at pH 7. The maximum efficiency for removing fluoride ions from aqueous solution using ZFN-RHS, ZFN-MS and ZFN-CMS magnetic green composites were found to be 72.5%, 73.8% and 68.7%, respectively. It was noted that fluoride ions removal percentage grew steadily as the pH of solution increased before declining at higher pH values.
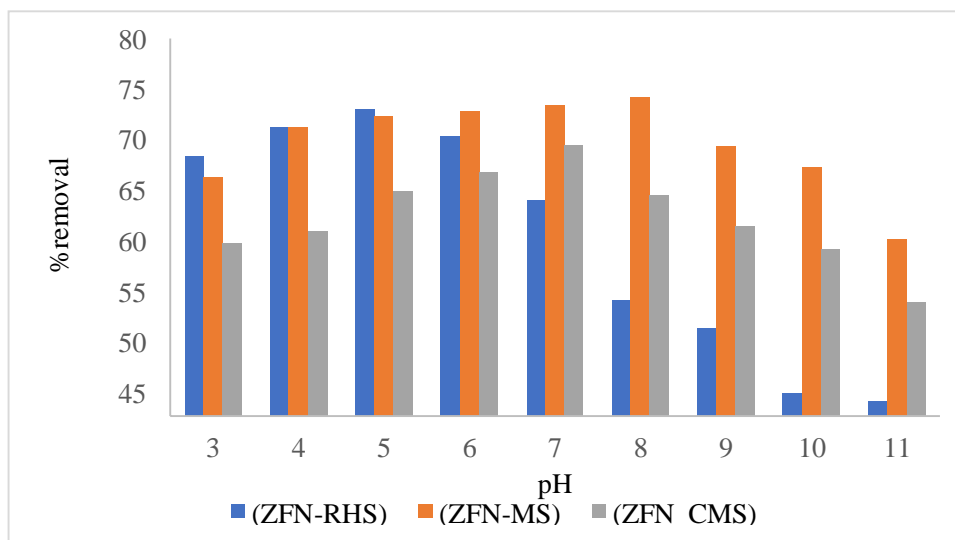
Figure 4.3.7- Effect of pH on removal of fluoride ions using ZFN-RHS, ZFN-MS and ZFN-CMS

4.3.6 Effect of concentration and temperature

Concentration of fluoride ions was altered from 5-25 mg/L to study the effect of concentration and temperature varied from 25°C to 35°C with ZFN-RHS, ZFN-MS and ZFN-CMS. Due to increase in the concentration of fluoride ions, interactions between fluoride ions and magnetic green composites (ZFN-RHS, ZFN-MS and ZFN-CMS) increased, therefore, Q_e (adsorption capacity) also increased. As the concentration increased, the percentage removal of fluoride ions decreased. It occurred because number of active sites decreased with respect to increase in concentration of fluoride ions[37]. Figure 4.3.8, shows the effect of concentration and temperature for removing fluoride ions using ZFN-RHS, ZFN-MS and ZFN-CMS magnetic green composites. Figure 4.3.8 shows that when temperature increased, adsorption of fluoride ions increased because higher interactions occurred between adsorbate and adsorbent molecules due to increase in kinetic energy of the system. It was observed because of their increased collisions by overcoming the activationenergy (provided by increased temperature). With increase in temperature, some of the poresof the adsorbent became large which resulted in increase of surface area available for adsorption of fluoride ions[38].
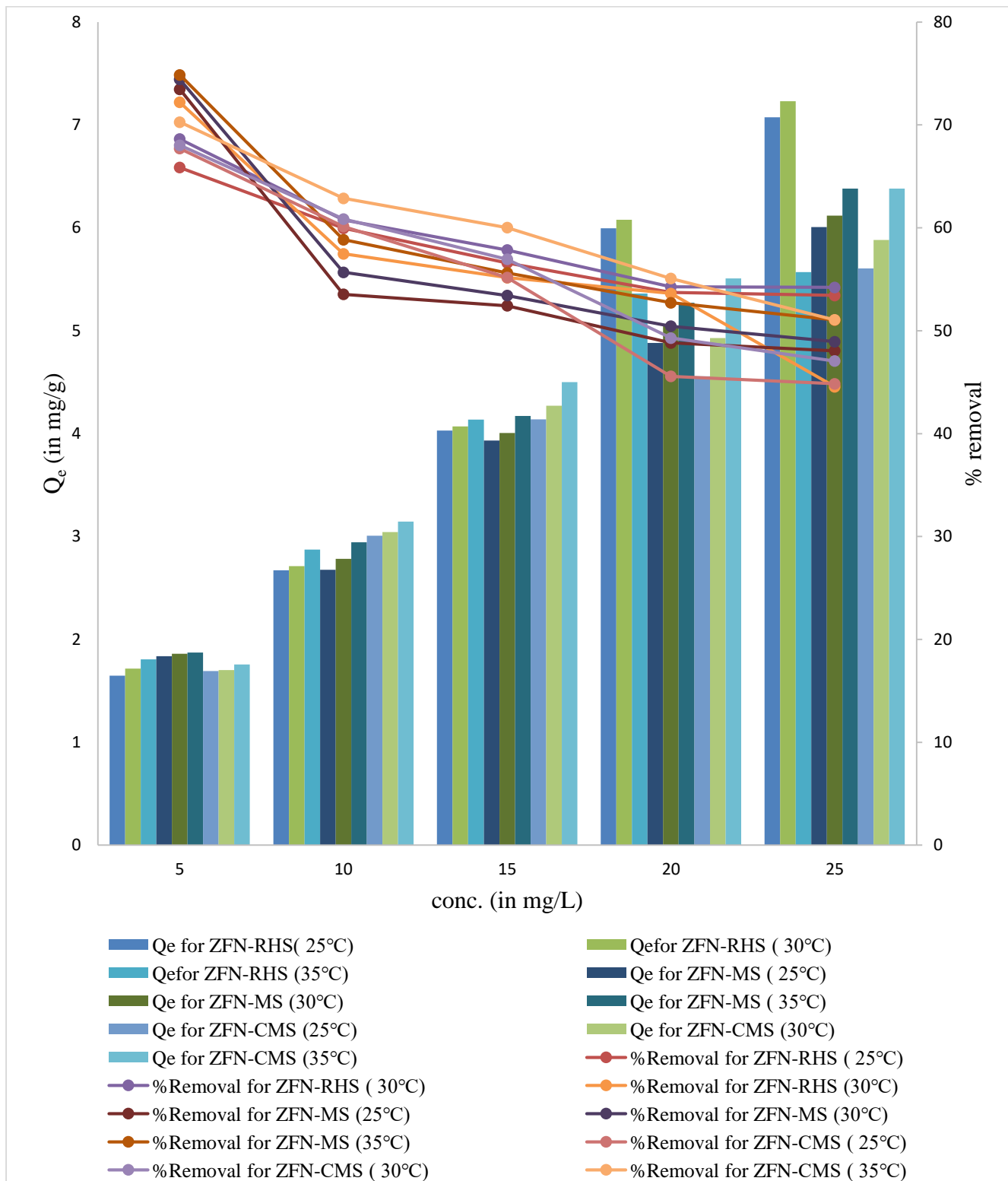
Figure 4.3.8- Effect of concentration and temperature on the removal of fluoride ion using ZFN-RHS, ZFN-MS and ZFN-CMS

4.3.7 Adsorption isotherms

Adsorption isotherms are used to study an adsorbent's adsorption behavior. The adsorption data obtained using magnetic green composites (ZFN-RHS, ZFN-MS, and ZFN-CMS), for removing fluoride ions was fitted to Langmuir, Freundlich, Temkin and Dubinin-Raduskevich (D-R) isotherm models and respective plots are shown in figures 4.3.9 to 4.3.12. From these graphs different isotherm constants for the removal of fluoride ion from aqueous using ZFN-RHS, ZFN-MS and ZFN-CMS magnetic green composites had been calculated and are represented in table 4.3.2.
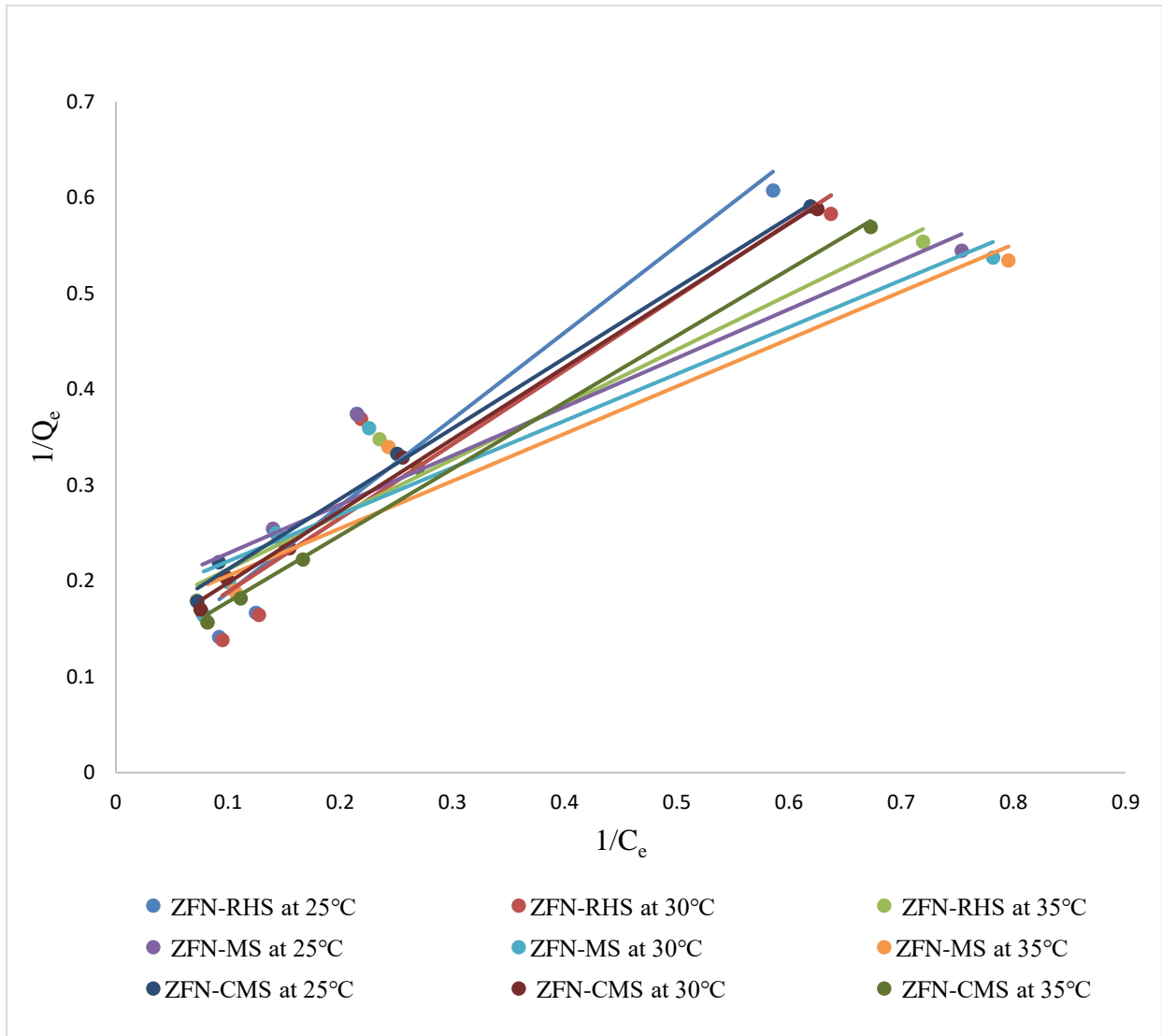
Figure 4.3.9- Langmuir isotherm for removal of fluoride ions using ZFN-RHS, ZFN-MS and ZFN-CMS
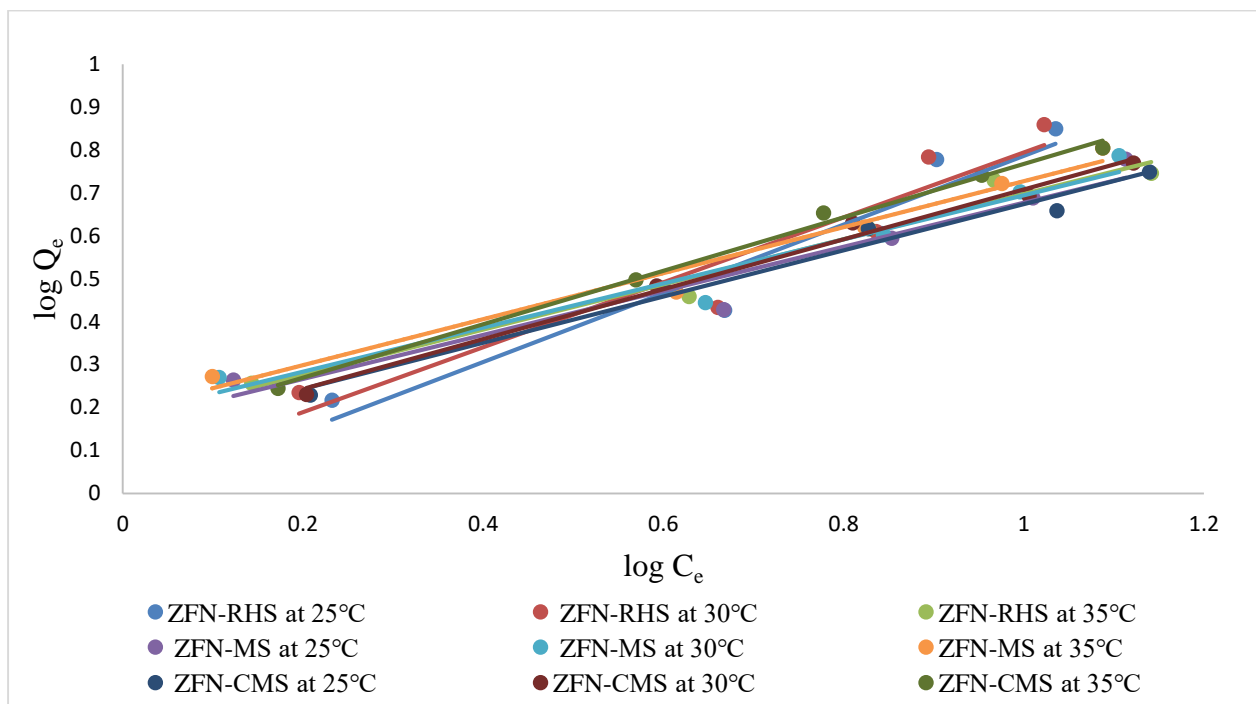
Figure 4.3.10- Freundlich isotherm for removal of fluoride ions using ZFN-RHS, ZFN-MS and ZFN-CMS
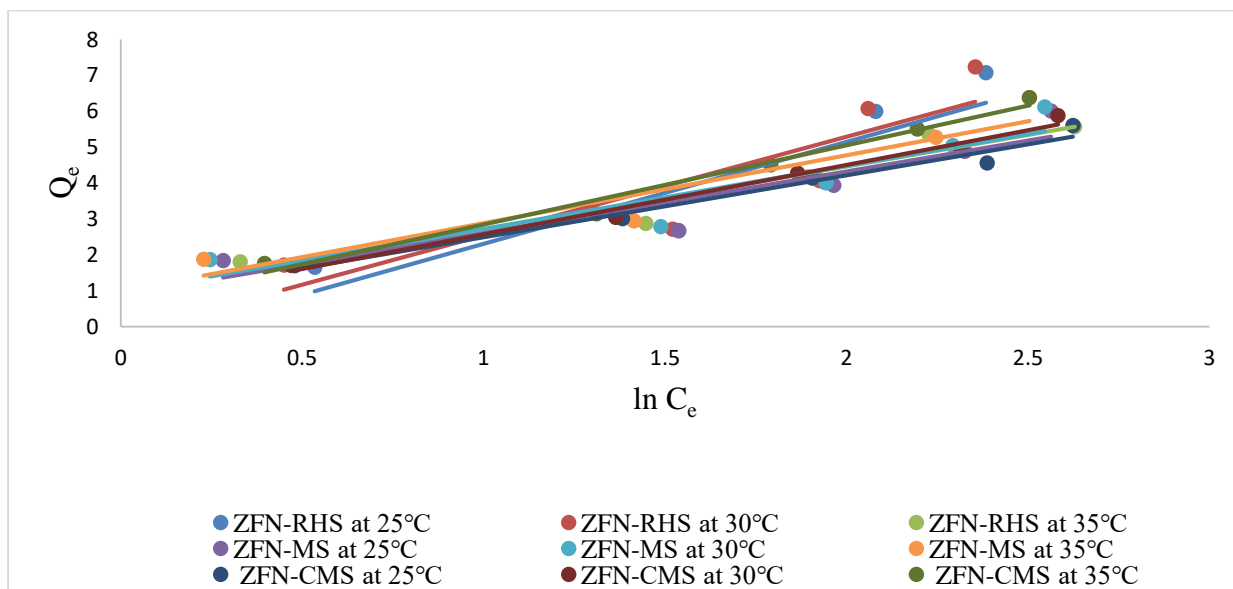
Figure 4.3.11- Temkin isotherm for removal of fluoride ions using ZFN-RHS, ZFN-MS and ZFN-CMS
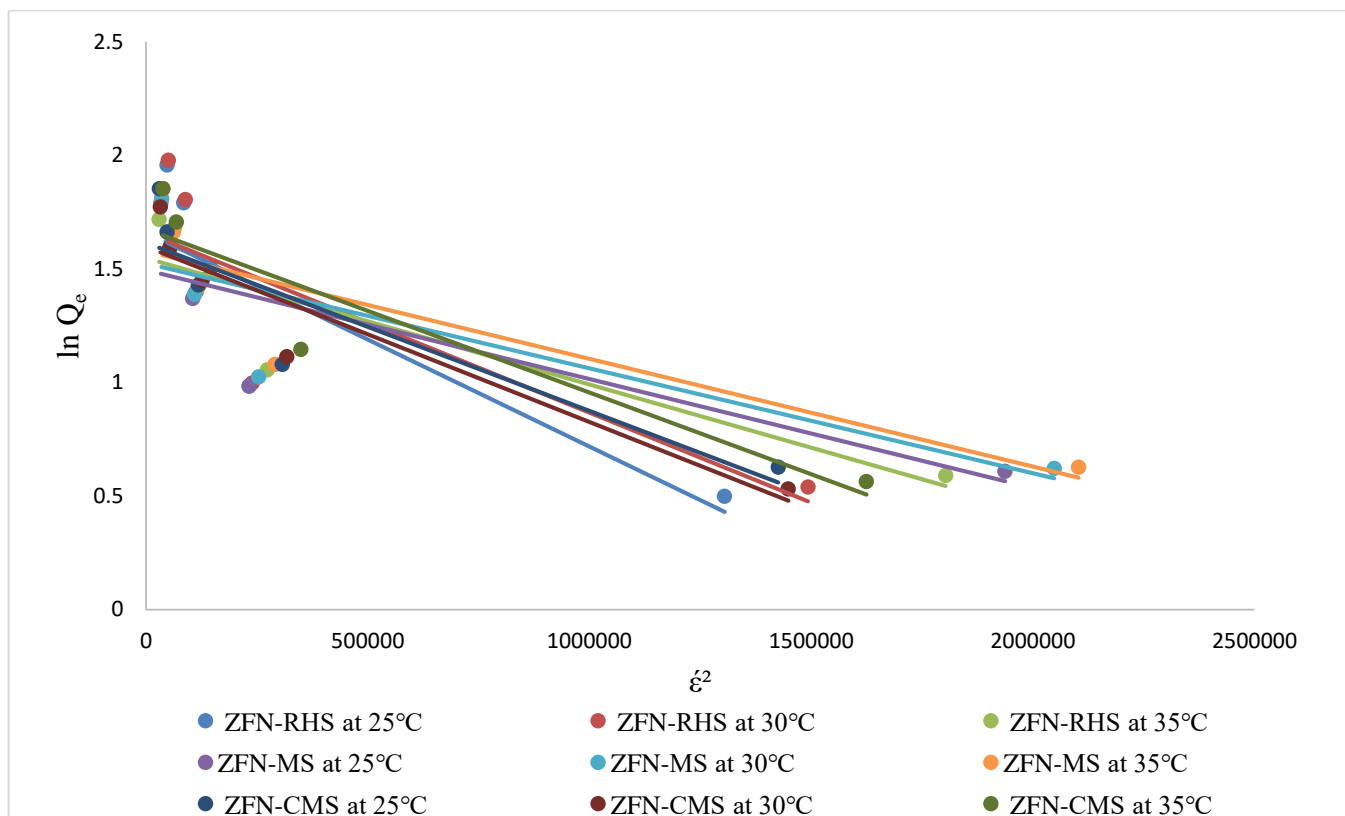
Figure 4.3.12- D-R isotherm for removal of fluoride ions using ZFN-RHS, ZFN-MS and ZFN-CMS

According to Table 4.3.2, Freundlich isotherm model is most suited for removing fluoride ions from aqueous solutions employing magnetic green composites (ZFN-RHS, ZFN-MS and ZFN-CMS), since it has the highest R^2 value. The adsorption capabilities (Q_e) for removing fluorideions from aqueous solution by employing ZFN-RHS, ZFN-MS, and ZFN-CMS, respectively, were 10.2, 6.4, and 9.2 mg/g. In this study, the values of the separation factors (R_L) is between 0 and 1 i.e. for ZFN-RHS, ZFN-MS, and ZFN-CMS the values of R_L were 0.649, 0.387, and 0.561, respectively. This indicated that removal of fluoride ions using magnetic green composites (ZFN-RHS, ZFN-MS and ZFN-CMS) was favourable. The calculated value of adsorption energy which is a parameter associated with D-R isotherm was more than 100 kJ/mol which confirmed that removal of fluoride ions using ZFN-RHS, ZFN-MS and ZFN- CMS followed chemical adsorption[34]. Maximum adsorption capacity for the removal of fluoride ions using ZFN-RHS, ZFN-MS and ZFN-CMS magnetic green composites were found to be 10.2, 6.4 and 9.1 mg/g, respectively.

133

Table 4.3.2- Isotherm constants for removal of fluoride ions using ZFN-RHS, ZFN-MS andZFN-CMS

SYSTEM		For ZFN-RHS			For ZFN-MS			For ZFN-CMS		
Isotherm Model	Const.	25ºC	30ºC	35ºC	25ºC	30ºC	35ºC	25ºC	30ºC	35ºC
Langmuir	Q	6.459	8.968	10.245	5.617	5.824	6.402	7.204	8.097	9.191
	b	0.270	0.144	0.108	0.349	0.351	0.316	0.189	0.164	0.156
	R^2	0.923	0.902	0.951	0.884	0.901	0.932	0.995	0.996	0.994
	S D	0.0106	0.0079	0.0032	0.0011	0.0029	0.0048	0.0075	0.0100	0.0088
	R_L	0.425	0.581	0.649	0.364	0.362	0.387	0.514	0.549	0.561
Freundlich	K_f	0.967	1.090	1.481	1.459	1.517	1.553	1.366	1.341	1.396
	1/n	0.801	0.756	0.526	0.512	0.513	0.536	0.538	0.580	0.622
	R^2	0.926	0.908	0.969	0.944	0.956	0.974	0.980	0.989	0.995
	S D	0.020	0.019	0.027	0.029	0.024	0.021	0.046	0.026	0.037
Dubinin-Raduskevich	Q_m	5.262	5.256	4.698	4.459	4.589	4.484	5.030	4.944	5.338
	K_{DR}	9×10^{-7}	8×10^{-7}	6×10^{-7}	5×10^{-7}	4.96×10^{-7}	4.94×10^{-7}	7×10^{-7}	8×10^{-7}	6.98×10^{-7}
	R^2	0.815	0.789	0.929	0.860	0.875	0.897	0.972	0.983	0.980
	E	745.3	790.5	912.8	1000	1008.2	1012.4	845.15	790.57	846.18

	SD	0.091	0.082	0.062	0.058	0.075	0.083	0.059	0.079	0.077
Temkin	b_T	871.8	917.3	1488.1	1439.7	1432.2	1351.7	1435.3	1303.9	1158.1
	A	0.004	1.542	6.181	7.043	6.183	6.821	9.431	20.236	33.018
	R^2	0.716	0.689	0.794	0.691	0.711	0.747	0.806	0.892	0.874
	SD	0.156	0.104	0.058	0.071	0.043	0.082	0.212	0.157	0.113

4.3.8 Thermodynamics of adsorption

It is necessary to interpret the behavior, and interactions of the various components that make up the adsorption process. Therefore, studying thermodynamics is important. Adsorption thermodynamic parameters such as enthalpy change (ΔH^o), free energy change (ΔG^o) and entropy change (ΔS^o) were determined by using different thermodynamic relationships (Gibbs Helmholtz equation and Van't Hoff equation) as mentioned in chapter 3 (section 3.7). From the slopes and intercepts of graph between ln K_d and 1/T (figure 4.3.13), various thermodynamic variables like enthalpy change, entropy change and Gibb's free energy changewere calculated and are depicted in table 4.3.3 at various concentrations. Positive ΔH^o values indicated that the removal of fluoride ions from aqueous solutions using magnetic green composites (ZFN-RHS, ZFN-MS and ZFN-CMS) was endothermic, and positive ΔS^o values indicated that there was a significant amount of randomization at the surface of ZFN-RHS, ZFN-MS and ZFN-CMS. Negative ΔG^o values indicated a spontaneous process for removing fluoride ions utilising magnetic green composites (ZFN-RHS, ZFN-MS and ZFN-CMS). ΔG^o values were negative at lower concentrations, but at higher concentrations it came out to be positive. It revealed that the process was spontaneous at lower concentrations whereas it became non-spontaneous at higher concentrations.
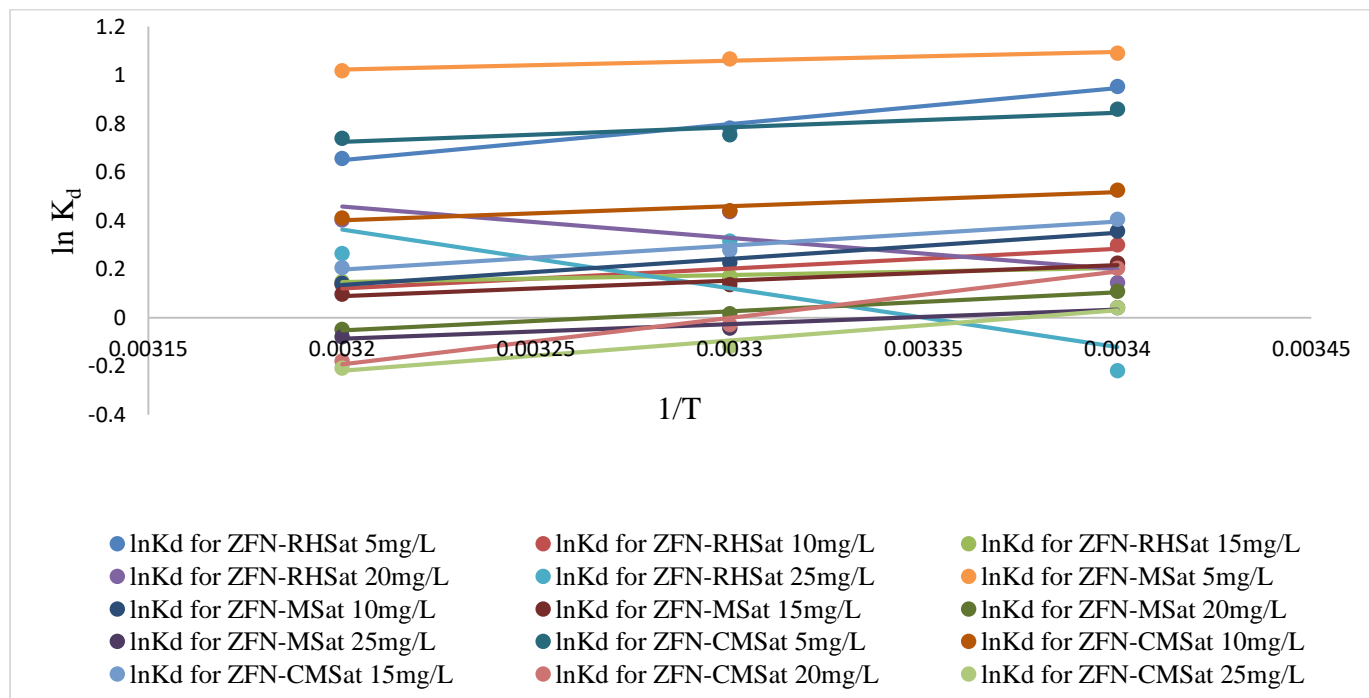
Figure 4.3.13- Graph between lnK$_d$ and 1/T for removal of fluoride ion using ZFN-RHS, ZFN-MS and ZFN-CMS

Table 4.3.3- Thermodynamic variables for removal of fluoride ion using ZFN-RHS, ZFN-MS and ZFN-CMS

Adsorbent used	Conc. (mg L^{-1})	ΔS^o (J mol^{-1}K^{-1})	ΔH^o (kJ mol^{-1})	ΔG^o at 25°C (kJ mol^{-1})	ΔG^o at 30°C (kJ mol^{-1})	ΔG^o at 35°C (kJ mol^{-1})
ZFN-RHS	5	0.064	12.367	-1.627	-1.939	-2.364
	10	0.114	16.818	-0.340	-0.418	-0.746
	15	0.074	11.389	-0.370	-0.324	-0.312
	20	0.068	10.757	1.112	1.085	1.059
	25	0.047	9.107	1.657	1.583	1.441
ZFN-MS	5	0.121	23.021	-2.566	-2.690	-2.749
	10	0.077	28.983	-1.357	-1.574	-1.901
	15	0.112	25.350	-0.244	-1.344	-1.568
	20	0.084	26.488	0.119	0.044	0.039
	25	0.071	24.982	0.196	0.106	0.105
ZFN-CMS	5	0.069	14.990	-1.895	-1.933	-0.202
	10	0.062	14.800	-1.053	-1.130	0..349
	15	0.064	18.257	-0.531	-0.715	1.040
	20	0.052	15.873	1.255	1.172	1.121
	25	0.054	19.358	2.529	2.302	2.108

4.3.9 Regeneration of ZFN-RHS, ZFN-MS and ZFN-CMS

Regeneration is required to evaluate the effectiveness of the adsorbent as its affordability depends on how easily it can be recycled and reused. The fixed amount of adsorbent saturated with fluoride ions was taken in a flask containing 50 mL solution of desorbing agent (0.5N HCl) and placed at 200 rpm for three hours to regenerate the magnetic green composites (ZFN-RHS, ZFN-MS, and ZFN-CMS). The regeneration process was studied up to five cycles, and depicted in table 4.3.4. According to table 4.3.4, the regeneration effectiveness of ZFN-RHS, ZFN-MS and ZFN-CMS were 73.6%, 84.6% and 84.1%, respectively after 5 cycles. This indicated the regenerated composites performed good even after 5 cycles. Thus, it can be concluded that these composites can serve as cost effective alternative.

Table 4.3.4- Regeneration efficiencies of ZFN-RHS, ZFN-MS and ZFN-CMS used for removal of fluoride ions

Regeneration cycle	For ZFN-RHS	For ZFN-MS	For ZFN-CMS
1	97.6	98.4	97.6
2	90.0	96.3	98.4
3	78.6	91.1	92.2
4	76.3	90.7	86.7
5	73.6	84.6	84.1

Part IV

4.4 Batch adsorption studies with Ni (II) ions

4.4.1 Adsorption of Ni (II) ions using ZFN-MS and ZFN-CMS magnetic green composites in single ion system

The adsorption potential of ZFN and its magnetic green composites viz. ZFN-MS and ZFN-CMS was investigated in preliminary studies for removing Ni (II) ions from aqueous solution.It was observed that Zinc ferrite composites (ZFN-MS and ZFN-CMS) had higher removal efficiencies for removing Ni (II) ions as compared to pure ZFN. So, zinc ferrite composites with Mango starch (MS) and carboxy methyl starch (CMS) were selected for removing Ni (II)ions from aqueous solutions. The effect of different parameters, viz. pH, adsorbent dose, contact time, concentration and temperature, for removal of Ni (II) ions was studied utilising the batch adsorption method.

4.4.2 Effect of contact time

A known concentration (100 mg/L) and volume (50 mL) of Ni (II) ions were kept in contact with 0.1 g of adsorbents, at a fixed temperature, for examining effect of contact time on the adsorption behavior of ZFN-MS and ZFN-CMS. The removal of Ni (II) ions using magnetic green composites ZFN-MS and ZFN-CMS is depicted in Figure 4.4.1 as a function of time. It was noted that as time passed, percentage removal of Ni (II) ions increased while residual concentration decreased. Adsorption of Ni (II) ions was rapid initywhich slowed down with the passage of time and ultimately achieved equilibrium after 110 min. This was due to the fact that initially, the surfaces of magnetic green composites (ZFN-MS and ZFN-CMS) had more unoccupied sites accessible, but with time, these sites were taken up by Ni (II) ions[39]. The percent removal of Ni (II) ions at equilibrium using ZFN-MS composite was found to be 59.3% whereas with ZFN-CMS it was found to be 52.4%.
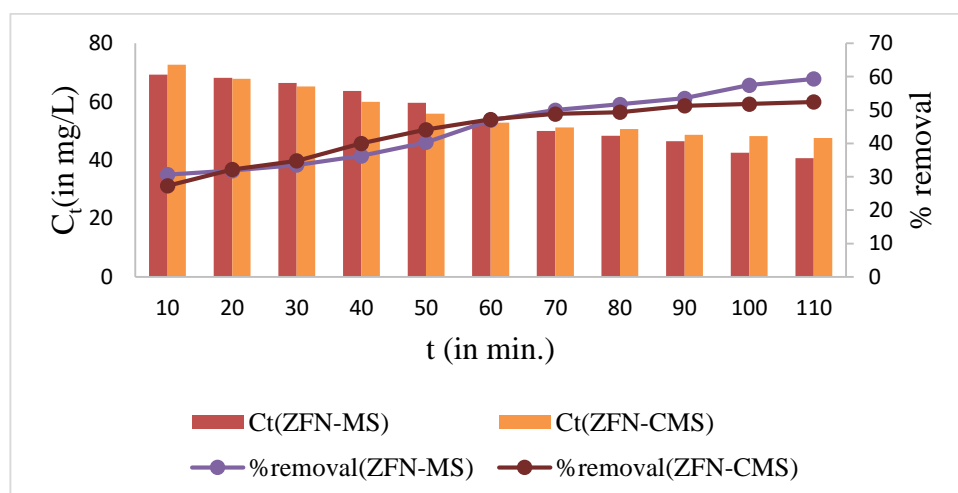
Figure 4.4.1- Effect of contact time on removal of Ni (II) ions using ZFN-MS and ZFN-CMS

4.4.3 Kinetics of adsorption

Adsorption data for removal of Ni (II) ions using magnetic green composites (ZFN-MS and ZFN-CMS) was fitted to kinetic models, viz. Lagergren pseudo first order, Pseudo second order, and Elovich model. The graphs for these models are shown in figures 4.4.2 to 4.4.4. Different kinetic constants derived from the plots of these graphs have been depicted in table 4.4.1.
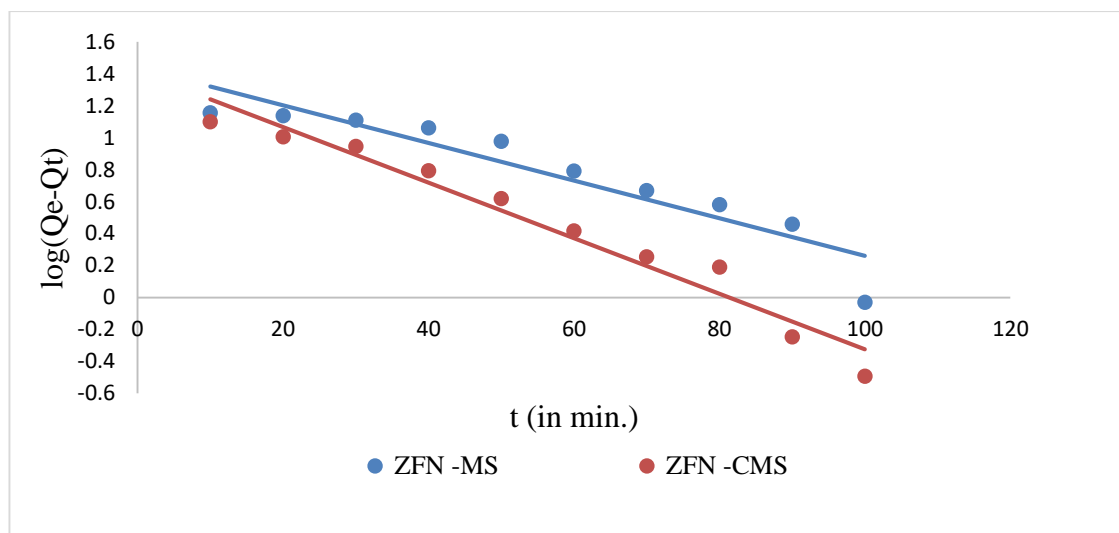
Figure 4.4.2- Lagergren pseudo first order kinetics for the removal of Ni (II) ions using ZFN-MSand ZFN-CMS
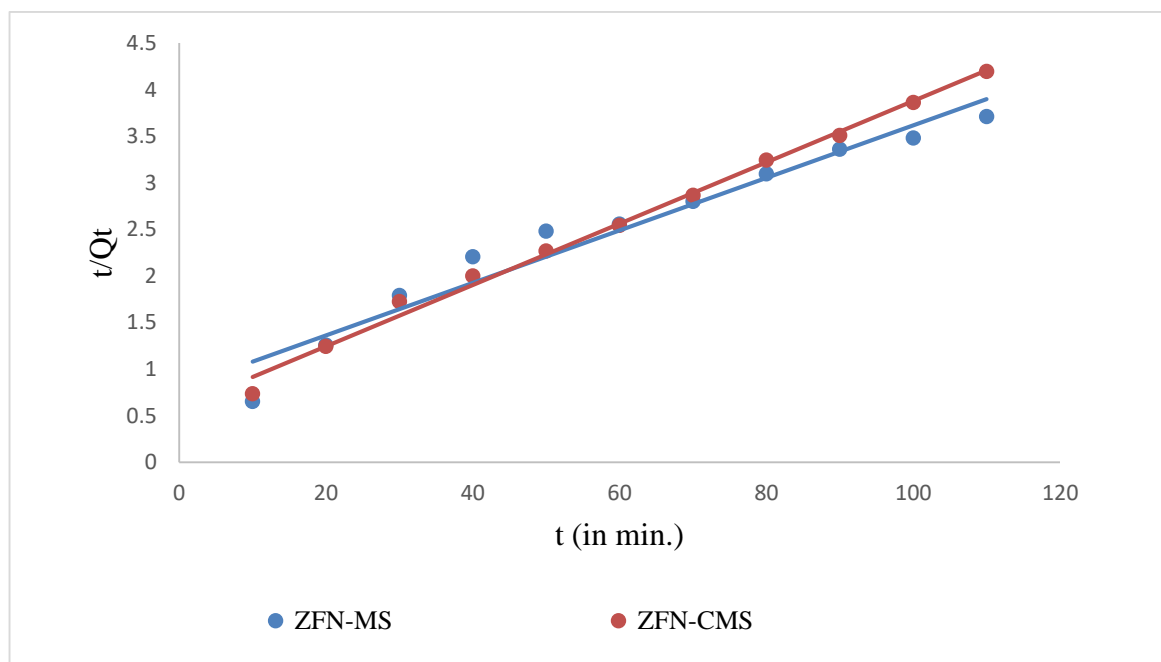
Figure 4.4.3- Lagergren pseudo second order kinetics for the removal of Ni (II) ions using ZFN-MSand ZFN-CMS

140
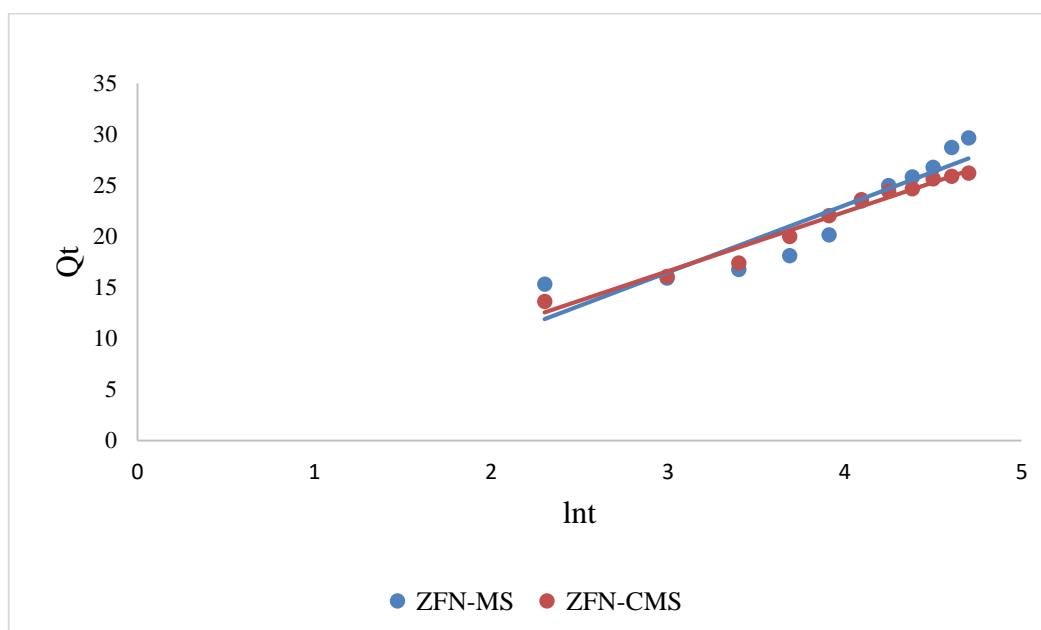
Figure 4.4.4- Elovich model for the removal of Ni (II) ions using ZFN-MS and ZFN-CMS

Table 4.4.1- Kinetic constant values for the removal of Ni (II) ions using ZFN-MS and ZFN-CMS

Kinetics Model ↓	constants	For ZFN-MS	For ZFN-CMS
Lagergren Pseudo first order	Q_{e1}	27.491	25.989
	K_1	0.0271	0.021
	R^2	0.8757	0.9586
	SD	0.381	0.537
Pseudo second order	Q_{e2}	35.46	30.39
	h	1.253	1.706
	K_2	0.001	0.002
	R^2	0.9531	0.9942

	SD	0.957	1.095
Elovich model	**α**	4.016	5.078
	β	0.152	0.172
	R^2	0.8617	0.9735
	SD	5.274	4.374

Regression coefficient (R^2) value was used to determine which kinetic model fitted data the best. It was evident from the study of the above table that pseudo-second order model had the highest R^2 value. This indicated that the removal of Ni (II) ions utilising magnetic green composites (ZFN-MS and ZFN-CMS) followed pseudo second order kinetics. This revealed that the nature of adsorption was chemisorption.

The plot for Weber Morris intra particle diffusion model for removing Ni (II) ions using magnetic green composites (ZFN- MS and ZFN-CMS) is shown in figure 4.4.5. From the figure it is clear that line is not passing through origin revealing that a number of other variables are also affecting removal of nickel ions using ZFN-MS and ZFN-CMS magnetic green composites along with the intra particle diffusion.
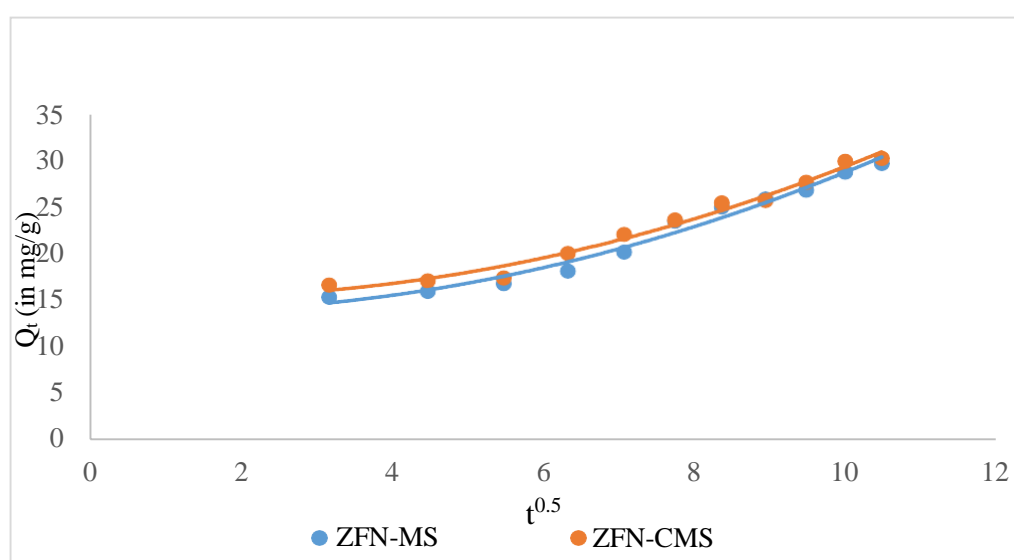
Figure 4.4.5- Weber Morris intra particle diffusion model for the removal of Ni (II) ions using ZFN-MS and ZFN-CMS

4.4.3 Effect of adsorbent dose

Adsorbent dose was increased from 0.1-0.5g in a 50 mL of known concentration metal ion solution (100mg/L) keeping other parameters constant. Effectof adsorbent dose for removing Ni (II) ions using ZFN-MS and ZFN-CMS magnetic green composites in single ion system is shown in figure 4.4.6. The graph demonstrates that percentage removal of Ni (II) ions increased along with increase in the amount of magnetic green composites (ZFN- MS and ZFN-CMS) because the active sites for the adsorption of Ni (II) ions increased as the dosage of the adsorbent was increased. For ZFN-MS removal efficiency of Ni (II) ions increased from 59.5% to 65.5%, for ZFN-CMS from 52.4% to 60.2% with increase in the adsorbent dose. Additionally, as the adsorbent dosage rose, the metal ion adsorption capacities (Q_e) decreased. The unsaturation of adsorption sites caused by the adsorption process was the cause of the drop in Q_e with increased adsorbent dosage[40].
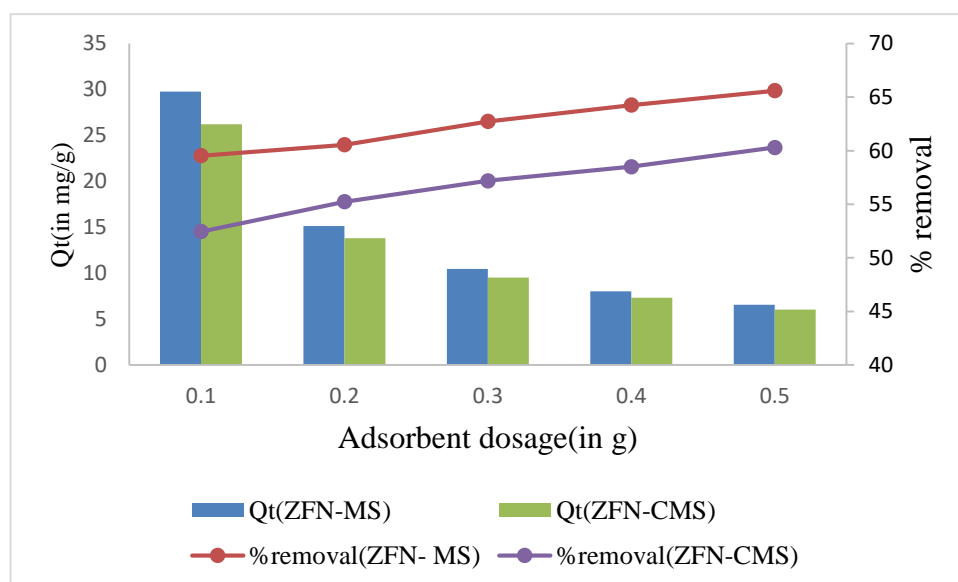
Figure 4.4.6- Effect of adsorbent dose for the removal of Ni (II) ions using ZFN-MS and ZFN- CMS

4.4.4 Effect of pH

The adsorption of Ni (II) ions utilising magnetic green composites (ZFN-MS and ZFN-CMS) was examined by altering the initial pH (from 3-11) of the metal ion solution. Figure 4.4.7 shows effect of pH on ZFN-MS and ZFN-CMS for removing Ni (II)from aqueous solution. Results showed that Ni (II) ions were removed to their maximum extent at pH 7 using ZFN-

CMS and at pH 8 using ZFN-MS. The maximum pH value correlates with the pH_{PZC} of ZFN-MS (pH_{PZC} =7.4) and ZFN- CMS (pH_{PZC} =7.2). Therefore, in these ideal pH ranges, all other adsorption parameters were examined. When the pH exceeded from pH_{PZC} value, the suface of magnetic green adsorbents (ZFN-MS and ZFN-CMS) became negatively charged and therefore, positively charged metal ions get attached with the surface of the adsorbent. The maximum efficiency for removing Ni (II) ions using ZFN-MS and ZFN-CMS for were found to be 60.3 and 52.2, respectively.
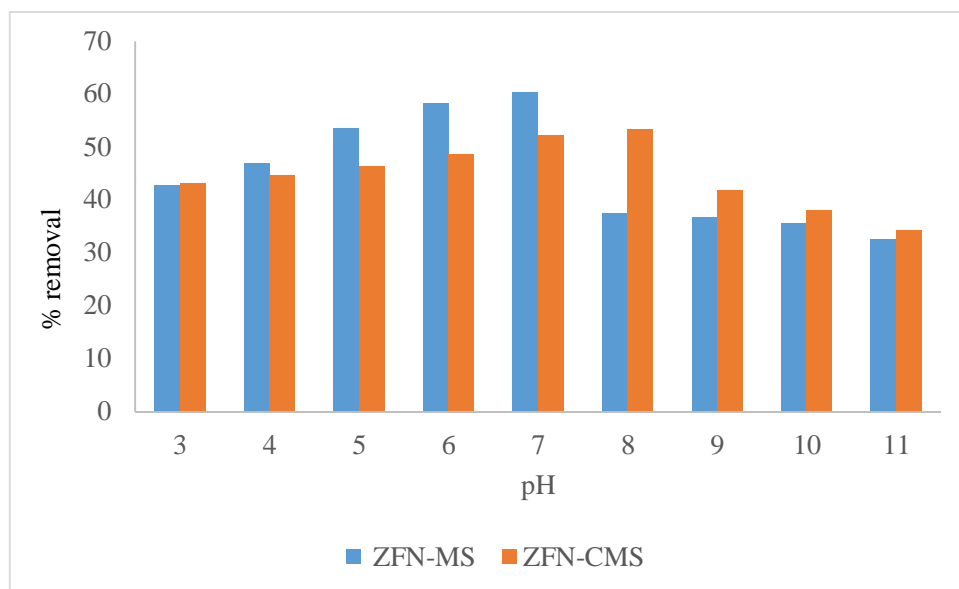
Figure 4.4.7- Effect of pH on removal of Ni (II) ions using ZFN-MS and ZFN-CMS

4.4.5 Effect of concentration and temperature

Concentration and temperature significantly affects the removal of metal ions from aqueous solution. Figure 4.4.8 illustrates the effect of concentration and temperature for removing Ni (II) ions using magnetic green composites (ZFN-MS and ZFN-CMS) in the concentration range of 100 to 500 mg/L in single ion system. The graph demonstrates that as concentration of metal ion increased, percentage of Ni (II) ions removed by ZFN-MS and ZFN-CMS dropped. The decrease of active sites on adsorbent's surface is what caused this trend to be seen. With an increase in metal ion concentration, adsorption capacity (Q_e) also increased. This was observed due to higher interactions between the adsorbate and the adsorbent. Three different temperatures-25ºC, 30ºC, and 35ºC were used for studying effect of temperature on removal of

nickel ions, and results demonstrated that percentage removal of Ni (II) ions increased with temperature or adsorption of Ni (II) ions increased with increase in temperature. This revealed endothermic nature of adsorption process. The increase in adsorption capacity with temperature was observed due to higher interactions between molecules of adsorbate and adsorbent due to increase in the kinetic energy at higher temperatures. With increase in temperature, the pore size of adsorbent became enlarged which resulted in the increase of surface area available for adsorption of Ni (II) ions[41].
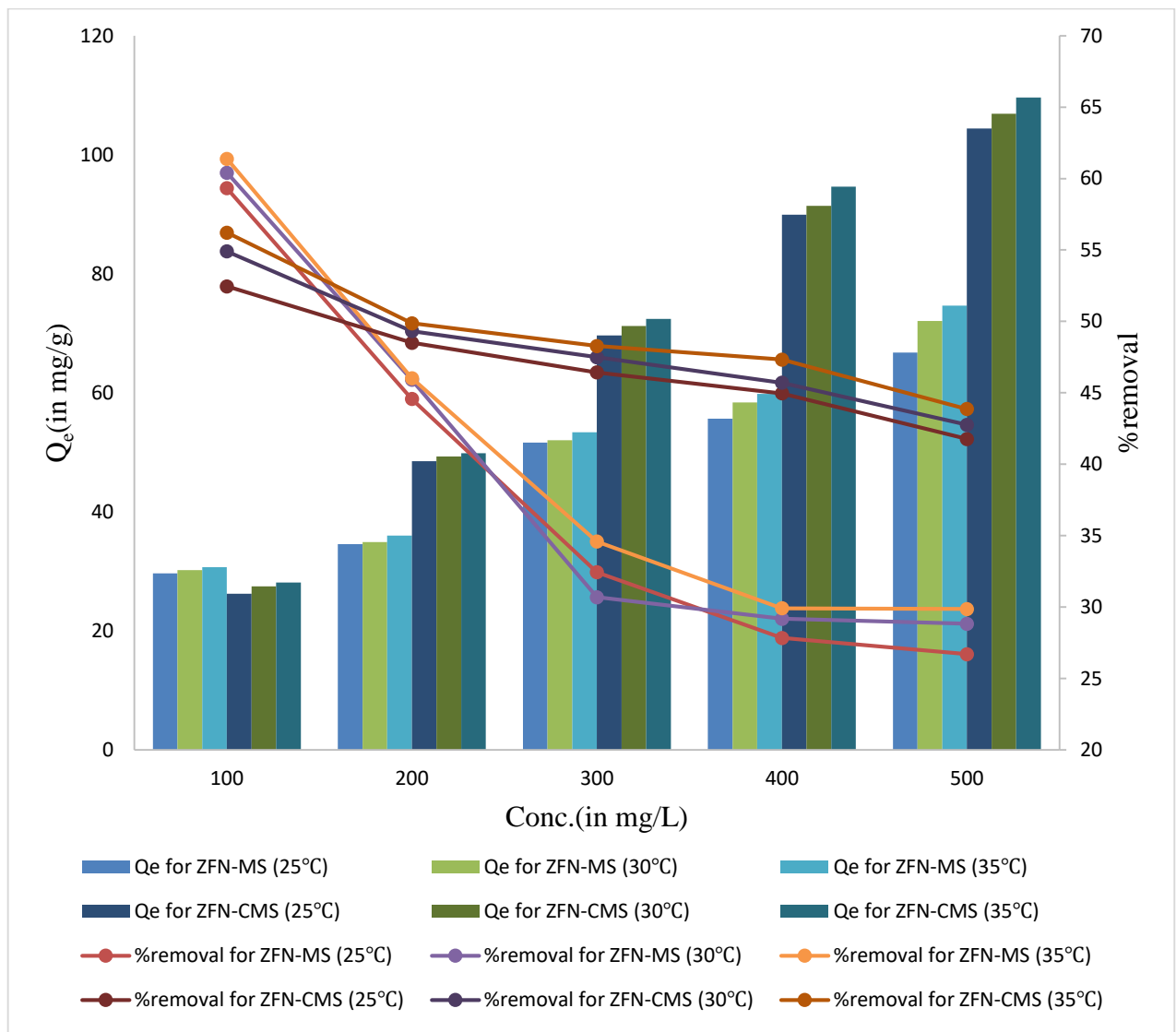
Figure 4.4.8- Effect of concentration and temperature on removal of Ni (II) ions using ZFN-MS and ZFN-CMS

4.4.6 Adsorption isotherms

Adsorption isotherm is the description of adsorbate in solution (C_e) and solid phase (Q_e) at equilibrium. Adsorption isotherms are crucial for the design of an adsorption system. A number of isotherms, viz. Langmuir, Freundlich, Temkin, and D-R were applied to describe the adsorption of Ni (II) ions from aqueous solutions using the adsorbents used in this study. The graphs for these isotherms are shown in figures 4.4.9 to 4.4.12. Using these graphs, different isotherm constants were calculated and are represented in table 4.4.2.

Table 4.4.2 results showed that the Freundlich isotherm fitted best for the removal of Ni (II) ions,since its R^2 value (regression coefficient) was highest for both ZFN-MS and ZFN-CMS (R^2=0.881 and R^2=0.998, respectively). As a result, according to Freundlich adsorption isotherm hypothesis, ZFN-MS and ZFN-CMS magnetic green composites have active sites which were non-uniformly distributed on their surface, and adsorption of Ni (II) ions resulted in the formation of multilayer on the surface of adsorbents.

From D-R isotherm, adsorption energy (E) can be calculated which indicated whether adsorption is chemical or physical in nature. If its value is more than 40 kJ/mol then it is referred to as chemical adsorption otherwise physical adsorption[8]. When Ni (II) ions were removed from aqueous solution utilising ZFN-MS and ZFN-CMS magnetic green composites, the amount of adsorption energy determined from the D-R model for ZFN-MS was found to be 70.71 KJ/mol and for ZFN- CMS, it was 55.38 kJ/mol. This revealed that adsorption process was chemical in nature.

From table 4.4.2, the separation factor (R_L) value associated with Langmuir isotherm was found to be between 0 and 1, corresponding to 0.322 for ZFN-MS and 0.833 for ZFN-CMS. According to values based on R_L , adsorption is categorized into four types: irreversible (R_L =0), linear (R_L =1), favourable ($0< R_L <1$), and unfavourable ($R_L >1$)[21]. This indicated that the process of removing Ni (II) ions using magnetic green composites (ZFN-MS and ZFN-CMS) was favourable.

Maximum adsorption capacity for the removal of Ni (II) ions using ZFN-MS and ZFN-CMS magnetic green composites were found to be 65.3 and 208.3 mg/g, respectively.
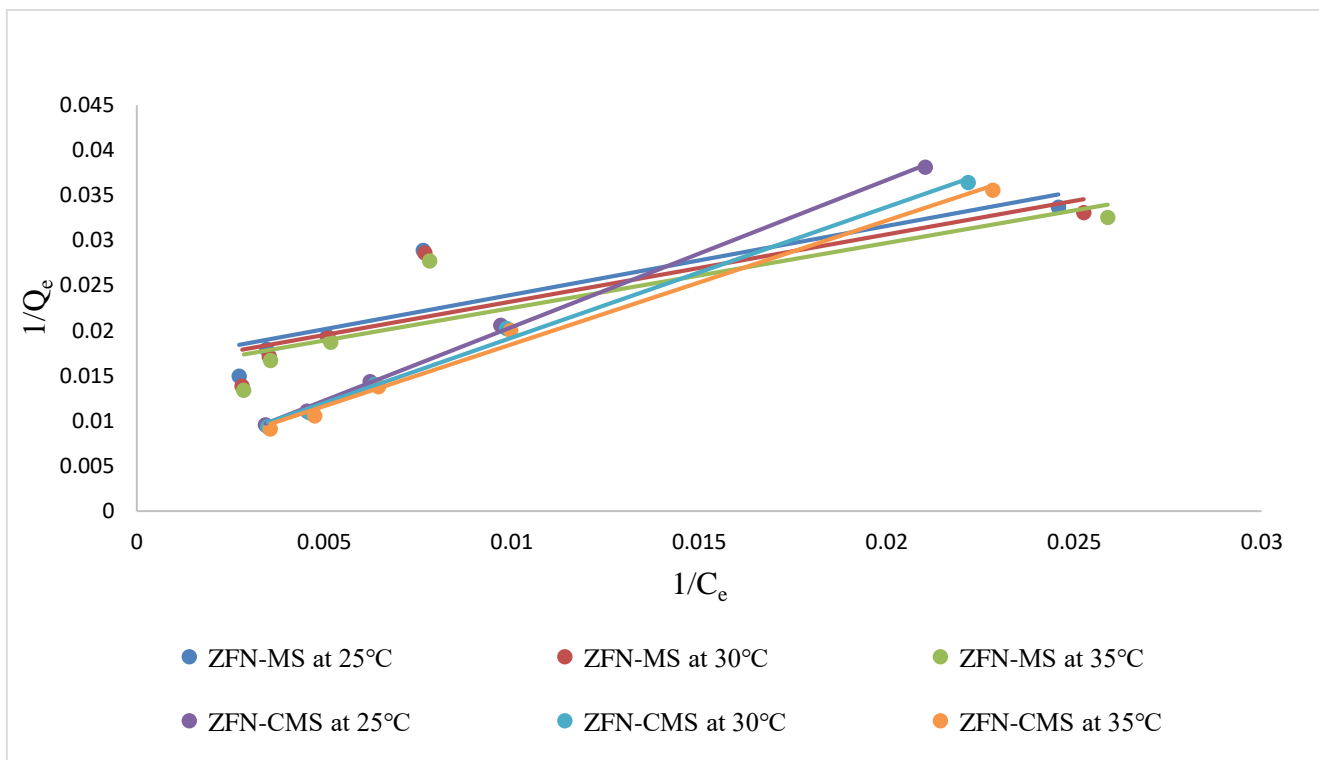
Figure 4.4.9- Langmuir isotherm for the removal of Ni (II) ions using ZFN-MS and ZFN-CMS
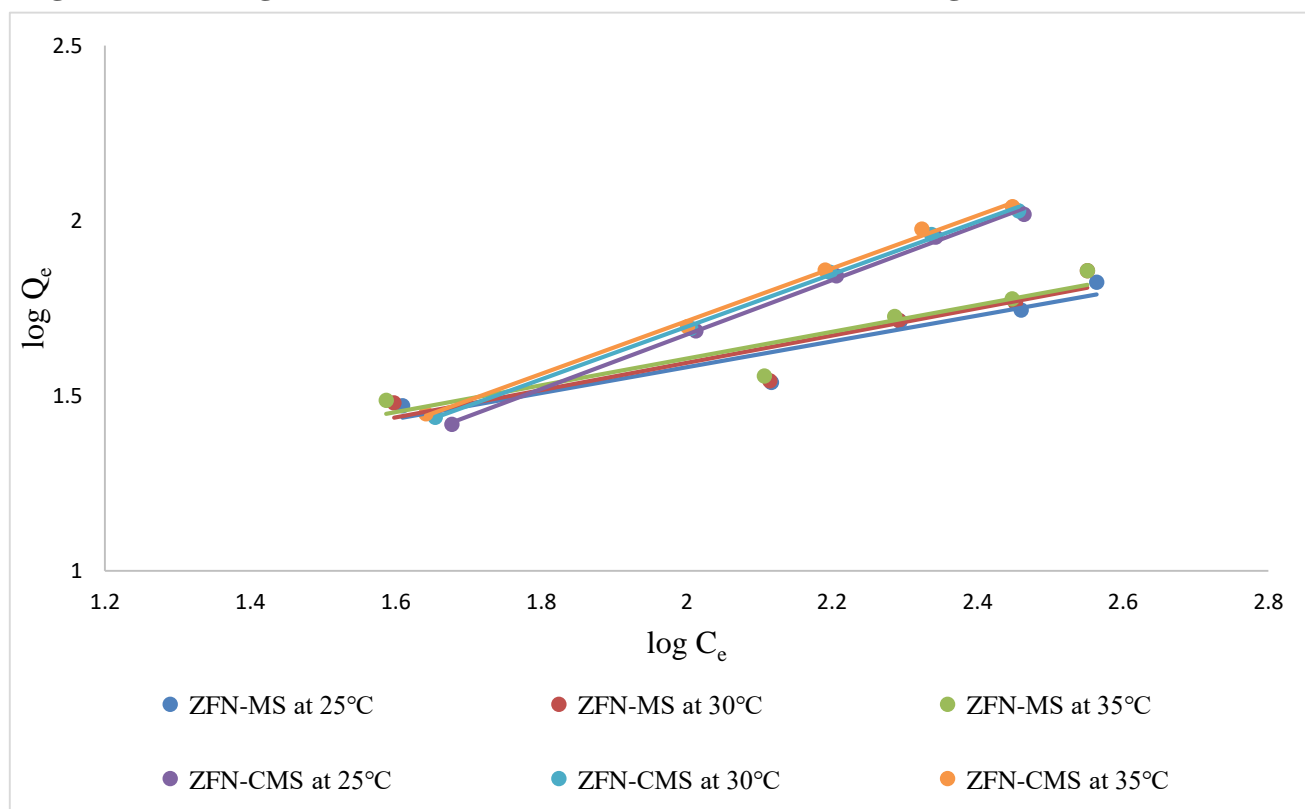
Figure 4.4.10- Freundlich isotherm for the removal of Ni (II) ions using ZFN-MS and ZFN-CMS
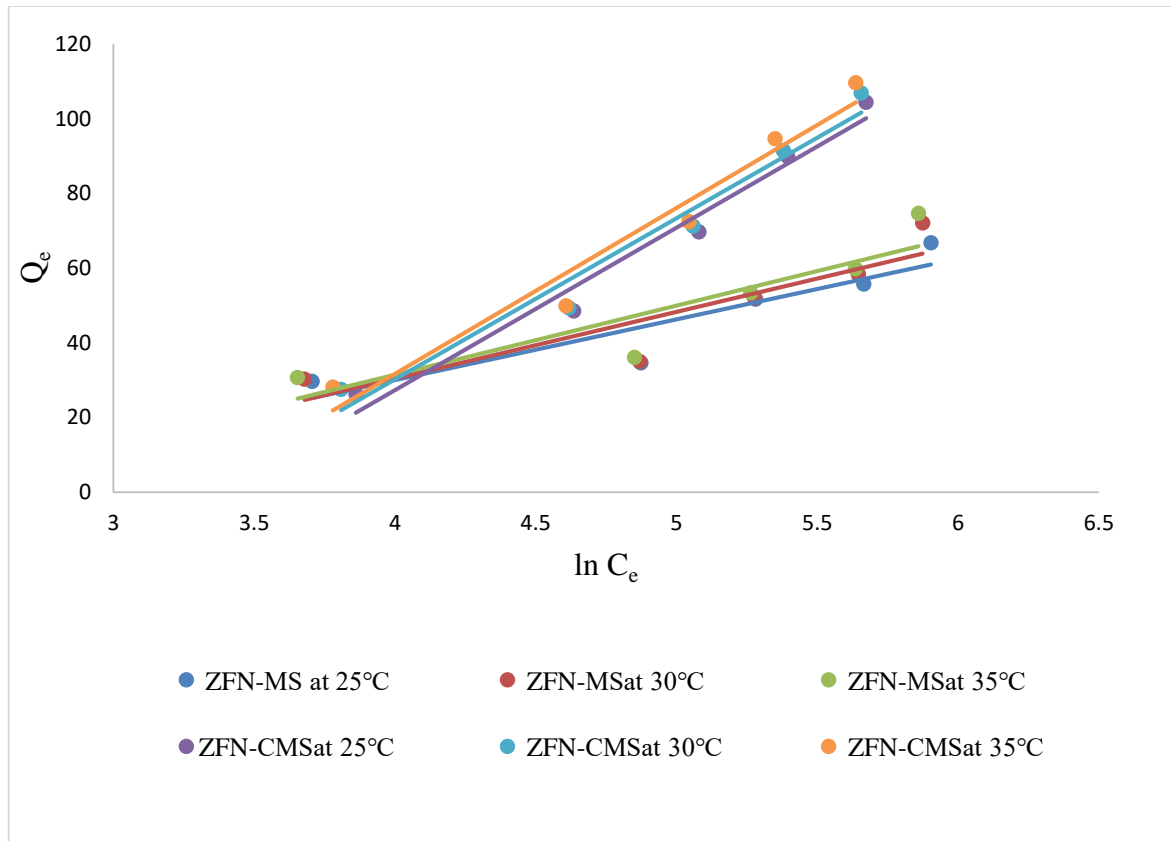
Figure 4.4.11- Temkin isotherm for the removal of Ni (II) ions using ZFN-MS and ZFN-CMS
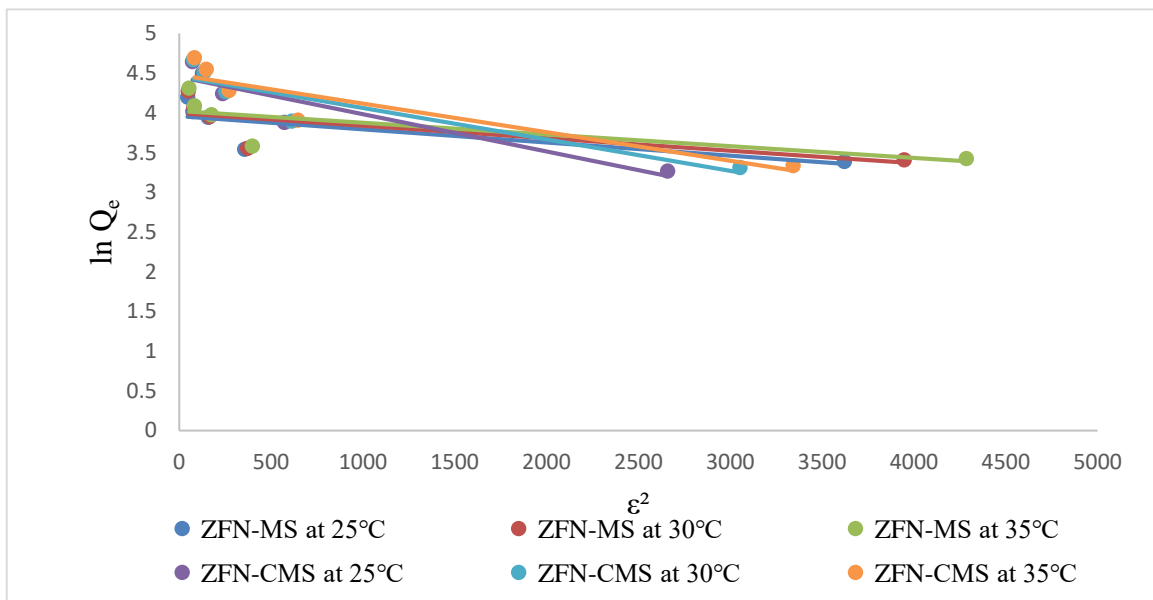
Figure 4.4.12- D-R isotherm for the removal of Ni (II) ions using ZFN-MS and ZFN-CMS

Table 4.4.2- Isotherm constant values for the removal of Ni (II) ion using ZFN-MS and ZFN-CMS

Isotherm Model	Constant	For ZFN-MS			For ZFN-CMS		
		25°C	30°C	35°C	25°C	30°C	35°C
Langmuir	Q	60.97	63.29	65.35	203.9	208.3	208.3
	b	0.021	0.022	0.023	0.002	0.003	0.004
	R^2	0.758	0.731	0.745	0.998	0.995	0.992
	SD	0.011	0.011	0.011	0.011	0.010	0.009
	R_L	0.322	0.312	0.303	0.833	0.769	0.714
Freundlich	K_f	6.983	6.57	6.956	1.32	1.575	1.615
	1/n	0.369	0.388	0.382	0.777	0.750	0.753
	R^2	0.881	0.864	0.880	0.998	0.998	0.997
	SD	0.396	0.389	0.385	0.321	0.316	0.312
D-R	Q_m	52.49	54.38	55.99	85.78	86.44	88.08
	K_{DR}	2×10^{-4}	2×10^{-4}	1×10^{-4}	5×10^{-4}	4×10^{-4}	4×10^{-4}
	R^2	0.575	0.541	0.550	0.862	0.843	0.829
	E	50.00	49.98	70.71	51.62	55.36	55.38
	SD	0.109	0.117	0.122	0.041	0.055	0.140
Temkin	b_T	152.4	138.7	133.9	56.92	57.36	55.78
	A	0.628	0.647	0.647	0.743	0.738	0.737
	R^2	0.841	0.811	0.812	0.972	0.966	0.957
	SD	0.889	0.992	0.893	0.964	0.992	0.814

4.4.3 Thermodynamics of adsorption

The study of thermodynamics is necessary for the prediction of nature of adsorption processes. Thermodynamic characteristics like Gibbs free energy change, enthalpy change, entropy change, etc. are crucial factors in thermodynamics. For the calculation of thermodynamic variables (ΔH^o, ΔS^o and ΔG^o) for removal of Ni (II) ions using ZFN-MS and ZFN-CMS, equations mentioned in section 3.7 were used (Van't Hoff equation and Gibb's Helmohltz equation). The graph between lnK_d and 1/T is depicted in figure 4.4.13 and values of ΔH^o, ΔS^o and ΔG^o are depicted in table 4.4.3.
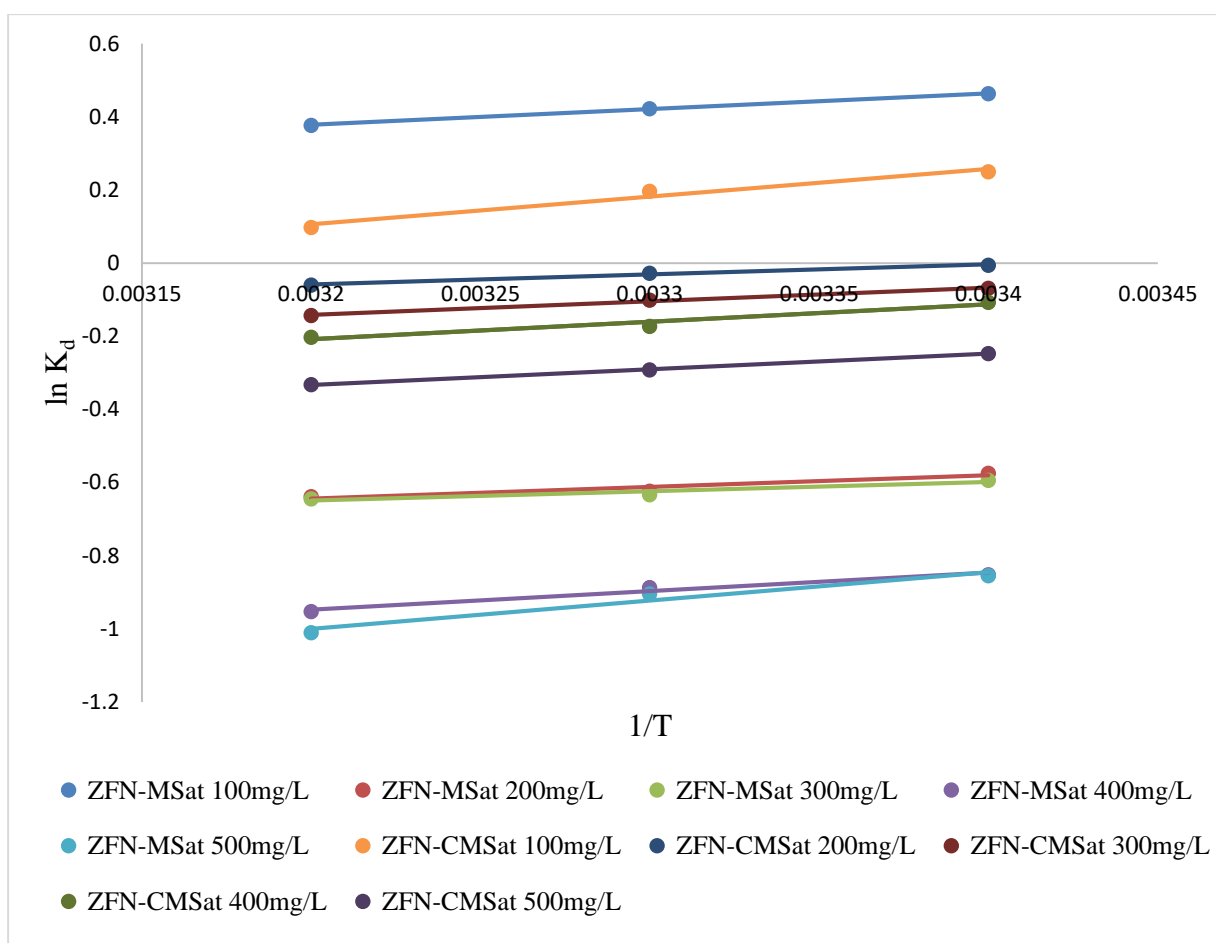
Figure 4.4.13- ln K_d versus 1/T graph for removal of Ni (II) ions using ZFN-MS and ZFN-CMS

Table 4.4.3- Thermodynamic constants for removal of Ni (II) ions using ZFN-MS and ZFN-CMS

Adsorbent	Conc. in mg L^{-1}	ΔS^o in J mol^{-1}K^{-1}	ΔH^o in kJ mol^{-1}	ΔG^o at 25°C in kJ mol^{-1}	ΔG^o at 30°C in kJ mol^{-1}	ΔG^o at 35°C in kJ mol^{-1}
ZFN-MS	100	0.008	3.579	-0.934	-1.063	-1.185
	200	0.013	2.645	1.580	1.569	1.469
	300	0.012	2.106	1.595	1.592	1.518
	400	0.021	4.204	2.358	2.143	2.179
	500	0.029	6.468	2.499	2.151	2.186
ZFN-CMS	100	0.019	6.299	-0.242	-0.493	-0.637
	200	0.007	2.266	0.146	0.068	0.012
	300	0.011	3.088	0.354	0.254	0.174
	400	0.014	3.958	0.500	0.433	0.273
	500	0.014	3.546	0.822	0.733	0.629

The positive values of ΔG^o from above table revealed the non-spontaneous nature and positive ΔH^o values corresponded to the endothermic nature for removal of Ni (II) ions using magnetic green composites (ZFN-MS and ZFN-CMS). Positive ΔS^o revealed that in adsorption system, the randomness between the interfaces of adsorbate and adsorbent molecules increased[42].

4.4.3 Regeneration of ZFN-MS and ZFN-CMS

0.1 N HCl solution was used for the regeneration of magnetic green composites (ZFN-MS and ZFN-CMS), utilized for removing Ni (II) ions from aqueous solution. Regeneration was

completed up to five cycles, and findings are given in table 4.4.4. According to the table 4.4.4, the regeneration effectiveness of ZFN-MS dropped to 71.6% after 5 cycles, while for ZFN-CMS dropped to 78.7%. These results demonstrated the affordability of the magnetic green composites used in this study as the efficacy of the adsorbent remained higher even after 5 cycles. Therefore, these adsorbents can be used multiple times.

Table 4.4.4- Regeneration efficiency of ZFN-MS and ZFN-CMS for removal of Ni (II) ions

Regeneration cycle	Regeneration efficiency ZFN-MS	Regeneration efficiency ZFN-CMS
1	96.8	93.6
2	89.3	83.3
3	82.5	84.5
4	81.0	81.6
5	71.6	78.7

4.4.10 General mechanism of adsorption of Ni (II) ions by magnetic green adsorbents (ZFN- MS/ZFN-CMS)

Mango Starch (MS)/carboxy methyl mango starch (CMS) are long chain natural polysaccharides having hydroxyl and carboxy methyl group present in their structure. These groups get attached to ZFN during composite formation and as a result, zinc ferrite composites (ZFN-MS and ZFN- CMS) contain different functional groups on their surface. Such functional groups provide negative charge on surface of Zinc ferrite composites which can attract positively charged metal ions towards it. Fig. 4.4.14 represents general mechanism of Ni (II) ions adsorption on surface of Zinc ferrite composites (ZFN- MS and ZFN- CMS).
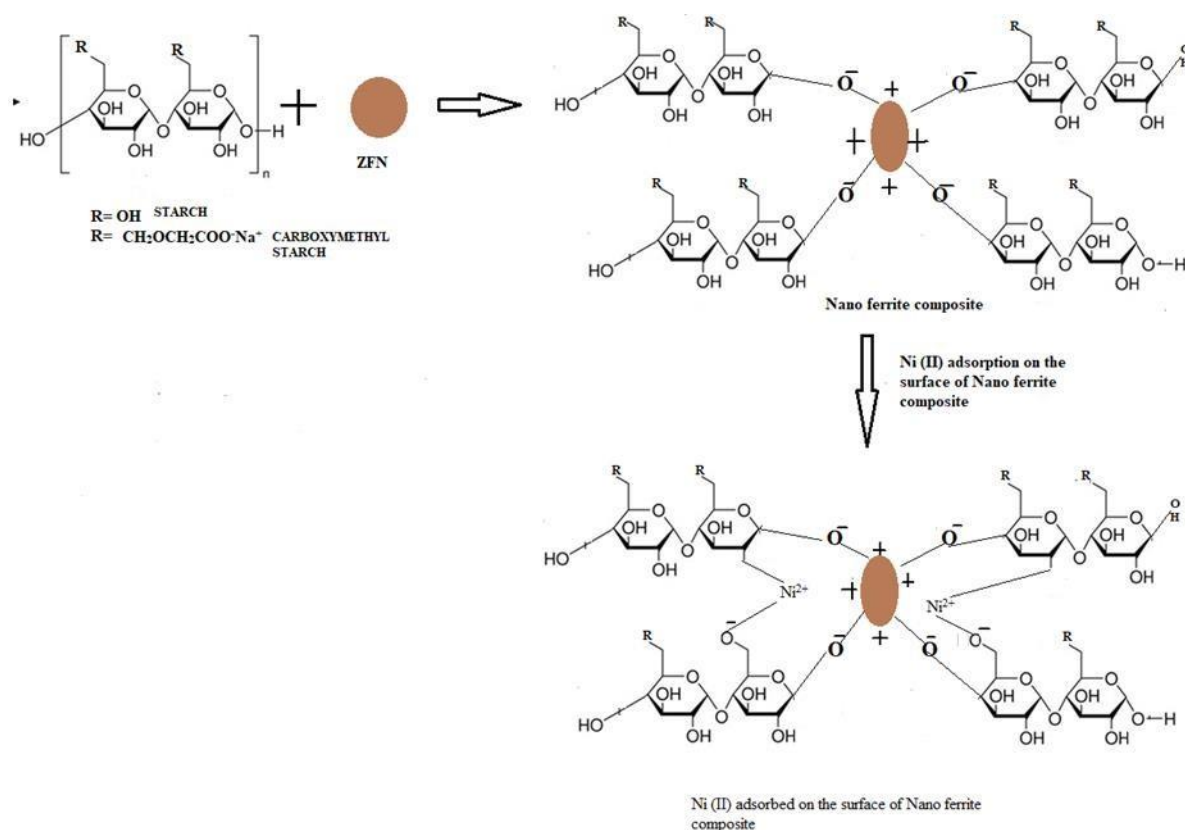
Figure 4.4.14- General mechanism of adsorption of Ni (II) ions on the surface of Zinc ferrite composites (ZFN-MS and ZFN-CMS)

4.4.11 Comparative analysis

Table 4.4.5 depicts comparative adsorption behavior of different cationic dyes/fluoride ions and Ni (II) ions using magnetic green adsorbents synthesized in this study. The comparative analysis demonstrated that the magnetic green adsorbents used in this study had a higher potential for removing pollutants (dyes/fluoride ions/Ni (II) ions) in single and multiple systems. The results demonstrated high removal efficiencies of ZFN-RHS/ZFN-MS and ZFN-CMS composites as compared to previous adsorbents used for the removal of pollutants (dyes/fluoride ions/Ni (II) ions). It revealed that ZFN-RHS, ZFN-MS and ZFN-CMS proved to be suitable eco-friendly adsorbents for the removal of pollutants from aqueous solution.

Table 4.4.5 Adsorption capabilities for removal of dyes (MB/MG/BG/CV), fluoride ions and NI (II) ions from aqueous solutions utilising magnetic green adsorbents (ZFN-RHS/ZFN-MS/ZFN-CMS)

Sr. no.	Adsorbent used	Pollutant removed	Adsorption capacity(in mg/g)	References
1	Palm kernel fibre	MB	95.4	[43]
		CV	78.9	
2	$CaFe_2O4$	CV	0.84	[44]
3	ZnFN- alg	CV	123.5	[26]
		BG	99.9	
4	ZFNCS	CV	14.3	[8]
		BG	20.0	
5	$CoFe_2O_4$	CV	105.04	[45]
6	$CoFe_2O_4$-SDS	CV	105	[18]
7	Activated carbon from Ficus carica bast	MB	47.6	[46]
8	$Fe_3O_4/SiO_2/Chitosan$	MB	43.0	[47]
9	$NiFe_2O_4$-Zeolite-Sodium Alginate	MB	54.0	[48]
10	ZFN-RHS	CV	138.8	Present study
		MB	84.8	
11	ZFNMS	CV	142.9	Present study
		BG	101.2	
		MB	105.8	
12	Marble waste powder	F^-	1.20	[49]
13	Chemically modified palm kernel shell	F^-	2.35	[50]
14	Ceramic	F^-	2.16	[51]

15	ZFN-CS	F$^-$	6.3	[34]
16	ZFN-RHS ZFN-MS ZFN-CMS	F$^-$	10.2 6.4 9.2	Present study
17	Modified coconut coir pith	Ni (II)	24.39	[23]
18	Scrap tire	Ni (II)	25	[52]
19	Chitosan/magnetic composite beads	Ni (II)	52.55	[53]
20	Bagasse fly ash	Ni (II)	1.70	[54]
21	Tea factory waste	Ni (II)	15.26	[55]
22	ZFN- MS ZFN-CMS	Ni (II)	65.3 208.3	Present study

References

(1)   Kumar, M.; Dosanjh, H. S.; Singh, H. Synthesis of Spinel ZnFe2O4 Modified with SDS via Low Temperature Combustion Method and Adsorption Behaviour of Crystal Violet Dye. *Asian J. Chem.* **2017**, *29* (9), 2057–2064. https://doi.org/10.14233/ajchem.2017.20827.

(2)   Azmi, M. A.; Ismail, N. A. A.; Rizamarhaiza, M.; Hasif, A. A. K. W. M.; Taib, H. Characterisation of Silica Derived from Rice Husk (Muar, Johor, Malaysia) Decomposition at Different Temperatures. *AIP Conf. Proc.* **2016**, *1756*. https://doi.org/10.1063/1.4958748.

(3)   Tesfaye Bahir, T.; Eitex, T. T. Valorisation of Mango Fruit By-Products: Physicochemical Characterisation and Future Prospect Crystalline Nanocellulose View Project Valorization of Corncobs View Project Valorisation of Mango Fruit By-Products: Physicochemical Characterisation and Future. **2017**, *50* (Figure 2), 22–34.

(4)   Hassan Musa, S.; Sagagi, B. S. Extraction and Some Characteristics of Mango Seed Kernel Starch for Industrial Applications. *Sci. Lett.* **2023**, *17* (2), 81–90.

(5)   Kaur, M.; Singh, N.; Sandhu, K. S.; Guraya, H. S. Physicochemical, Morphological, Thermal and Rheological Properties of Starches Separated from Kernels of Some Indian Mango Cultivars (Mangifera Indica L.). *Food Chem.* **2004**, *85* (1), 131–140. https://doi.org/10.1016/j.foodchem.2003.06.013.

(6)   Agwamba, E. C.; Hassan, L. G.; Achor, M.; Tsafe, A. I.; Sokoto, A. M. Physicochemical Analysis of Carboxymethyl Mango (Mangifera Indica) Starch. **2016**, *9* (12), 69–74. https://doi.org/10.9790/5736-0912016974.

(7)   Patade, S. R.; Andhare, D. D.; Somvanshi, S. B.; Kharat, P. B.; More, S. D.; Jadhav, K. M. Preparation and Characterisations of Magnetic Nanofluid of Zinc Ferrite for Hyperthermia. *Nanomater. Energy* **2020**, *9* (1), 8–13. https://doi.org/10.1680/jnaen.19.00006.

(8)   Kumar, M.; Dosanjh, H. S.; Singh, H. Magnetic Zinc Ferrite–Chitosan Bio-Composite: Synthesis, Characterization and Adsorption Behavior Studies for Cationic Dyes in Single and Binary Systems. *J. Inorg. Organomet. Polym. Mater.* **2018**, *28* (3), 880–898. https://doi.org/10.1007/s10904-017-0752-0.

(9)   Deraz, N. M.; Alarifi, A. Microstructure and Magnetic Studies of Zinc Ferrite Nano-Particles. *Int. J. Electrochem. Sci.* **2012**, *7* (7), 6501–6511.

(10)   Liou, T. H. Preparation and Characterization of Nano-Structured Silica from Rice Husk. *Mater. Sci. Eng. A* **2004**, *364* (1–2), 313–323. https://doi.org/10.1016/j.msea.2003.08.045.

(11)   Gündüz, F.; Bayrak, B. Synthesis and Performance of Pomegranate Peel-Supported Zero-Valent Iron Nanoparticles for Adsorption of Malachite Green. *Desalin. Water Treat.* **2018**, *110*, 180–192. https://doi.org/10.5004/dwt.2018.22185.

(12) Benhalima, T.; Ferfera-Harrar, H. Eco-Friendly Porous Carboxymethyl Cellulose/Dextran Sulfate Composite Beads as Reusable and Efficient Adsorbents of Cationic Dye Methylene Blue. *Int. J. Biol. Macromol.* **2019**, *132*, 126–141. https://doi.org/10.1016/j.ijbiomac.2019.03.164.

(13) Almethen, A. A.; Alotaibi, K. M.; Alhumud, H. S.; Alswieleh, A. M. Highly Efficient and Rapid Removal of Methylene Blue from Aqueous Solution Using Folic Acid-Conjugated Dendritic Mesoporous Silica Nanoparticles. *Processes* **2022**, *10* (4). https://doi.org/10.3390/pr10040705.

(14) Lagoa, R.; Rodrigues, J. R. Evaluation of Dry Protonated Calcium Alginate Beads for Biosorption Applications and Studies of Lead Uptake. *Appl. Biochem. Biotechnol.* **2007**, *143* (2), 115–128. https://doi.org/10.1007/s12010-007-0041-4.

(15) Abbasi, S. Adsorption of Dye Organic Pollutant Using Magnetic ZnO Embedded on the Surface of Graphene Oxide. *J. Inorg. Organomet. Polym. Mater.* **2020**, *30* (6), 1924–1934. https://doi.org/10.1007/s10904-019-01336-4.

(16) El-Azazy, M.; Kalla, R. N.; Issa, A. A.; Al-Sulaiti, M.; El-Shafie, A. S.; Shomar, B.; Al-Saad, K. Pomegranate Peels as Versatile Adsorbents for Water Purification: Application of Box–Behnken Design as a Methodological Optimization Approach. *Environ. Prog. Sustain. Energy* **2019**, *38* (6), 1–12. https://doi.org/10.1002/ep.13223.

(17) Bouaziz, F.; Koubaa, M.; Kallel, F.; Ghorbel, R. E.; Chaabouni, S. E. Adsorptive Removal of Malachite Green from Aqueous Solutions by Almond Gum: Kinetic Study and Equilibrium Isotherms. *Int. J. Biol. Macromol.* **2017**, *105*, 56–65. https://doi.org/10.1016/j.ijbiomac.2017.06.106.

(18) Singh, M.; Dosanjh, H. S.; Singh, H. Surface Modified Spinel Cobalt Ferrite Nanoparticles for Cationic Dye Removal: Kinetics and Thermodynamics Studies. *J. Water Process Eng.* **2016**, *11*, 152–161. https://doi.org/10.1016/j.jwpe.2016.05.006.

(19) Kandisa, R. V.; Saibaba KV, N. Dye Removal by Adsorption: A Review. *J. Bioremediation Biodegrad.* **2016**, *07* (06). https://doi.org/10.4172/2155-6199.1000371.

(20) Reddy, D. H. K.; Yun, Y. S. Spinel Ferrite Magnetic Adsorbents: Alternative Future Materials for Water Purification? *Coord. Chem. Rev.* **2016**, *315*, 90–111. https://doi.org/10.1016/j.ccr.2016.01.012.

(21) Chandrasekhar, S.; Pramada, P. N. Rice Husk Ash as an Adsorbent for Methylene Blue-Effect of Ashing Temperature. *Adsorption* **2006**, *12* (1), 27–43. https://doi.org/10.1007/s10450-006-0136-1.

(22) Tu, Y. J.; You, C. F.; Chang, C. K. Kinetics and Thermodynamics of Adsorption for Cd on

Green Manufactured Nano-Particles. *J. Hazard. Mater.* **2012**, *235–236*, 116–122. https://doi.org/10.1016/j.jhazmat.2012.07.030.

(23)   Ratan, S.; Singh, I.; Sarkar, J.; RM, N. The Removal of Nickel from Waste Water by Modified Coconut Coir Pith. *Chem. Sci. J.* **2016**, *7* (3). https://doi.org/10.4172/2150-3494.1000136.

(24)   Etemadinia, T.; Barikbin, B.; Allahresani, A. Removal of Congo Red Dye from Aqueous Solutions Using Znfe2o4/Sio2/Tragacanth Gum Magnetic Nanocomposite as a Novel Adsorbent. *Surfaces and Interfaces* **2019**, *14*, 117–126. https://doi.org/10.1016/j.surfin.2018.10.010.

(25)   Patil, M. R.; Shrivastava, V. S. Adsorption of Malachite Green by Polyaniline–Nickel Ferrite Magnetic Nanocomposite: An Isotherm and Kinetic Study. *Appl. Nanosci.* **2015**, *5* (7), 809–816. https://doi.org/10.1007/s13204-014-0383-5.

(26)   Kumar, M.; Dosanjh, H. S.; Singh, H. Magnetic Zinc Ferrite–Alginic Biopolymer Composite: As an Alternative Adsorbent for the Removal of Dyes in Single and Ternary Dye System. *J. Inorg. Organomet. Polym. Mater.* **2018**, *28* (5), 1688–1705. https://doi.org/10.1007/s10904-018-0839-2.

(27)   Mahmoodi, N. M.; Abdi, J.; Bastani, D. Direct Dyes Removal Using Modified Magnetic Ferrite Nanoparticle. *J. Environ. Heal. Sci. Eng.* **2014**, *12* (1), 1–10. https://doi.org/10.1186/2052-336X-12-96.

(28)   Keyhanian, F.; Shariati, S.; Faraji, M.; Hesabi, M. Magnetite Nanoparticles with Surface Modification for Removal of Methyl Violet from Aqueous Solutions. *Arab. J. Chem.* **2016**, *9*, S348–S354. https://doi.org/10.1016/j.arabjc.2011.04.012.

(29)   Kumar, K. V.; Kumaran, A. Removal of Methylene Blue by Mango Seed Kernel Powder. *Biochem. Eng. J.* **2005**, *27* (1), 83–93. https://doi.org/10.1016/j.bej.2005.08.004.

(30)   Achour, Y.; El Kassimi, A.; Khouili, M.; Hafid, A.; Laamari, M. R.; El Haddad, M.; Melliani, S. Competitive Removal of Ternary Dyes Mixture from Aqueous Media: Equilibrium, Kinetic, Isotherm, Thermodynamic and DFT Studies. *J. Iran. Chem. Soc.* **2022**. https://doi.org/10.1007/s13738-022-02555-2.

(31)   Jasrotia, R.; Singh, J.; Mittal, S.; Singh, H. Synthesis of CTAB Modified Ferrite Composite for the Efficient Removal of Brilliant Green Dye. *Int. J. Environ. Anal. Chem.* **2022**, *0* (0), 1–17. https://doi.org/10.1080/03067319.2022.2098485.

(32)   Shanker, A. S.; Srinivasulu, D.; Pindi, P. K. A Study on Bioremediation of Fluoride-Contaminated Water via a Novel Bacterium Acinetobacter Sp. (GU566361) Isolated from Potable Water. *Results Chem.* **2020**, *2*, 100070.

https://doi.org/10.1016/J.RECHEM.2020.100070.

(33)   Tan, T. L.; Krusnamurthy, P. A.; Nakajima, H.; Rashid, S. A. Adsorptive, Kinetics and Regeneration Studies of Fluoride Removal from Water Using Zirconium-Based Metal Organic Frameworks. *RSC Adv.* **2020**, *10* (32), 18740–18752. https://doi.org/10.1039/d0ra01268h.

(34)   Kumar, M.; Dosanjh, H. S.; Singh, H. Biopolymer Modified Transition Metal Spinel Ferrites for Removal of Fluoride Ions from Water. *Environ. Nanotechnology, Monit. Manag.* **2019**, *12* (May 2018), 100237. https://doi.org/10.1016/j.enmm.2019.100237.

(35)   Tanhaei, B.; Ayati, A.; Lahtinen, M.; Sillanpää, M. Preparation and Characterization of a Novel Chitosan/Al2O3/Magnetite Nanoparticles Composite Adsorbent for Kinetic, Thermodynamic and Isotherm Studies of Methyl Orange Adsorption. *Chem. Eng. J.* **2015**, *259*, 1–10. https://doi.org/10.1016/j.cej.2014.07.109.

(36)   Sengupta, P.; Saha, S.; Banerjee, S.; Dey, A.; Sarkar, P. Removal of Fluoride Ion from Drinking Water by a New Fe(OH)3/ Nano CaO Impregnated Chitosan Composite Adsorbent. *Polym. Technol. Mater.* **2020**, *59* (11), 1191–1203. https://doi.org/10.1080/25740881.2020.1725567.

(37)   Borgohain, X.; Boruah, A.; Sarma, G. K.; Rashid, M. H. Rapid and Extremely High Adsorption Performance of Porous MgO Nanostructures for Fluoride Removal from Water. *J. Mol. Liq.* **2020**, *305*, 112799. https://doi.org/10.1016/J.MOLLIQ.2020.112799.

(38)   Alkurdi, S. S. A.; Al-Juboori, R. A.; Bundschuh, J.; Bowtell, L.; McKnight, S. Effect of Pyrolysis Conditions on Bone Char Characterization and Its Ability for Arsenic and Fluoride Removal. *Environ. Pollut.* **2020**, *262* (September 2018), 114221. https://doi.org/10.1016/j.envpol.2020.114221.

(39)   Lin, S.; Zou, C.; Liang, H.; Peng, H.; Liao, Y. The Effective Removal of Nickel Ions from Aqueous Solution onto Magnetic Multi-Walled Carbon Nanotubes Modified by β-Cyclodextrin. *Colloids Surfaces A Physicochem. Eng. Asp.* **2021**, *619* (8), 126544. https://doi.org/10.1016/j.colsurfa.2021.126544.

(40)   Kucukcongar, S.; Akbari, A.; Turkyilmaz, M. Removal of Nickel from Aqueous Solutions Using Magnetic Nanocomposite Synthesised with Agricultural Waste. *Int. J. Environ. Anal. Chem.* **2020**, *102*, 1–19. https://doi.org/10.1080/03067319.2020.1790549.

(41)   Aji, M. P.; Wiguna, P. A.; Karunawan, J.; Wati, A. L.; Sulhadi, S. Removal of Heavy Metal Nickel-Ions from Wastewaters Using Carbon Nanodots from Frying Oil. *Procedia Eng.* **2017**, *170*, 36–40. https://doi.org/10.1016/j.proeng.2017.03.007.

(42)   Gautam, R. K.; Gautam, P. K.; Banerjee, S.; Soni, S.; Singh, S. K.; Chattopadhyaya, M. C.

Removal of Ni(II) by Magnetic Nanoparticles. *J. Mol. Liq.* **2015**, *204*, 60–69. https://doi.org/10.1016/j.molliq.2015.01.038.

(43) El-Sayed, G. O. Removal of Methylene Blue and Crystal Violet from Aqueous Solutions by Palm Kernel Fiber. *Desalination* **2011**, *272* (1–3), 225–232. https://doi.org/10.1016/j.desal.2011.01.025.

(44) An, S.; Liu, X.; Yang, L.; Zhang, L. Enhancement Removal of Crystal Violet Dye Using Magnetic Calcium Ferrite Nanoparticle: Study in Single- and Binary-Solute Systems. *Chem. Eng. Res. Des.* **2015**, *94*, 726–735. https://doi.org/10.1016/j.cherd.2014.10.013.

(45) Li, X. H.; Xu, C. L.; Han, X. H.; Qiao, L.; Wang, T.; Li, F. S. Synthesis and Magnetic Properties of Nearly Monodisperse CoFe2O4nanoparticles through a Simple Hydrothermal Condition. *Nanoscale Res. Lett.* **2010**, *5* (6), 1039–1044. https://doi.org/10.1007/s11671-010-9599-9.

(46) Pathania, D.; Sharma, S.; Singh, P. Removal of Methylene Blue by Adsorption onto Activated Carbon Developed from Ficus Carica Bast. *Arab. J. Chem.* **2017**, *10*, S1445–S1451. https://doi.org/10.1016/J.ARABJC.2013.04.021.

(47) Zheng, X.; Zheng, H.; Zhao, R.; Xiong, Z.; Wang, Y.; Sun, Y.; Ding, W. Sulfonic Acid-Modified Polyacrylamide Magnetic Composite with Wide PH Applicability for Efficient Removal of Cationic Dyes. *J. Mol. Liq.* **2020**, *319*, 114161. https://doi.org/10.1016/j.molliq.2020.114161.

(48) Bayat, M.; Javanbakht, V.; Esmaili, J. Synthesis of Zeolite/Nickel Ferrite/Sodium Alginate Bionanocomposite via a Co-Precipitation Technique for Efficient Removal of Water-Soluble Methylene Blue Dye. *Int. J. Biol. Macromol.* **2018**, *116* (2017), 607–619. https://doi.org/10.1016/j.ijbiomac.2018.05.012.

(49) Mehta, D.; Mondal, P.; George, S. Utilization of Marble Waste Powder as a Novel Adsorbent for Removal of Fluoride Ions from Aqueous Solution. *J. Environ. Chem. Eng.* **2016**, *4* (1), 932–942. https://doi.org/10.1016/j.jece.2015.12.040.

(50) Bashir, M. T. Fluoride Removal by Chemical Modification of Palm Kernel Shell-Based Adsorbent : A Novel Agricultural Waste Utilization Approach FLUORIDE REMOVAL BY CHEMICAL MODIFICATION OF PALM KERNEL SHELL-BASED ADSORBENT : A NOVEL AGRICULTURAL WASTE UTILIZATION APPROA. **2015**, No. November. https://doi.org/10.13140/RG.2.1.5039.3043.

(51) Chen, N.; Zhang, Z.; Feng, C.; Li, M.; Zhu, D.; Chen, R.; Sugiura, N. An Excellent Fluoride Sorption Behavior of Ceramic Adsorbent. *J. Hazard. Mater.* **2010**, *183* (1–3), 460–465. https://doi.org/10.1016/j.jhazmat.2010.07.046.

(52) Gupta, V. K.; Suhas; Nayak, A.; Agarwal, S.; Chaudhary, M.; Tyagi, I. Removal of Ni (II) Ions from Water Using Scrap Tire. *J. Mol. Liq.* **2014**, *190*, 215–222. https://doi.org/10.1016/j.molliq.2013.11.008.

(53) Tran, H. V.; Tran, L. D.; Nguyen, T. N. Preparation of Chitosan/Magnetite Composite Beads and Their Application for Removal of Pb(II) and Ni(II) from Aqueous Solution. *Mater. Sci. Eng. C* **2010**, *30* (2), 304–310. https://doi.org/10.1016/j.msec.2009.11.008.

(54) Singh, H.; Rattan, V. K. Adsorption of Nickel from Aqueous Solutions Using Low Cost Biowaste Adsorbents. **2011**, 239–249. https://doi.org/10.2166/wqrjc.2011.024.

(55) Tripathi, A.; Rawat Ranjan, M. Heavy Metal Removal from Wastewater Using Low Cost Adsorbents. *J. Bioremediation Biodegrad.* **2015**, *06* (06). https://doi.org/10.4172/2155-6199.1000315.
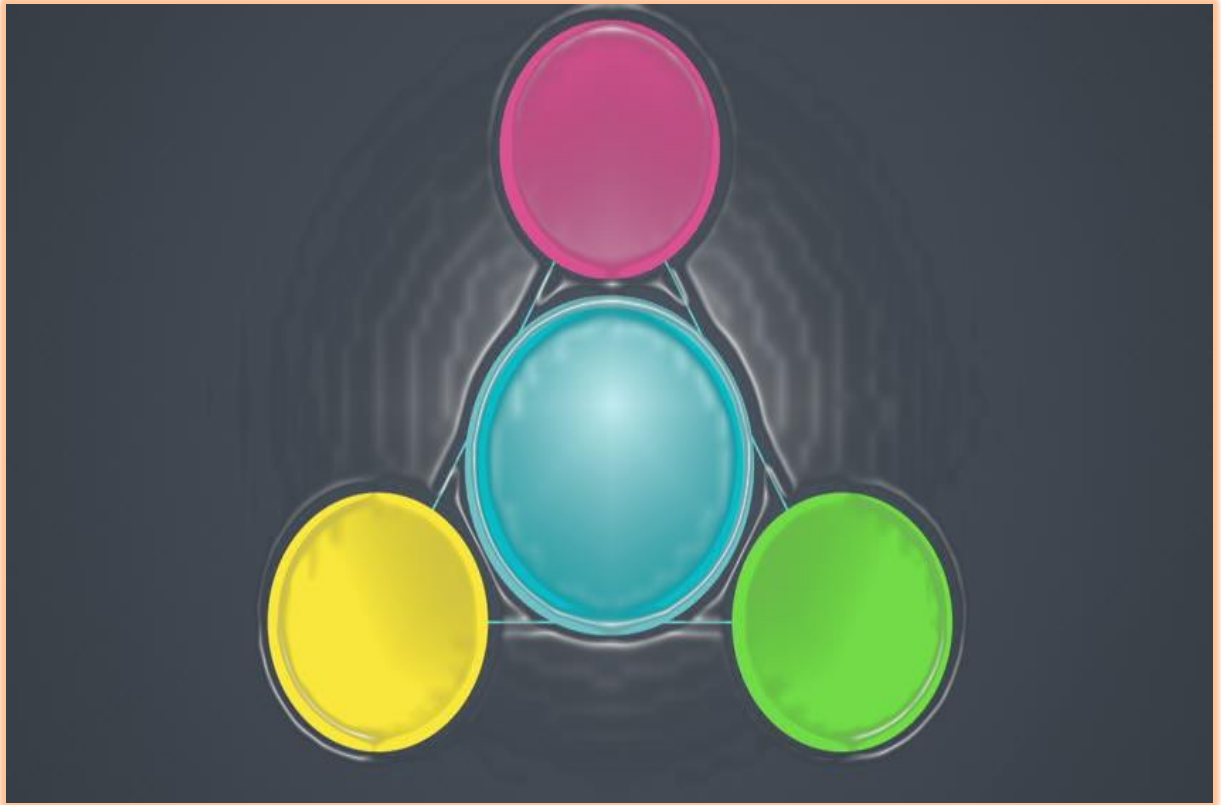
Chapter 5

Summary and Conclusions

5.0 Summary and Conclusions

In the present work, spinel metal ferrites (Zinc ferrite, Nickel ferrite and Copper ferrite) and their magnetic green composites with rice husk silica, mango starch and carboxy methyl starch were synthesized. The potential of these magnetic green composites was analysed for removing cationic dyes (MG/CV/BG/MB) in single and multiple dye systems; Ni (II) ions and F⁻ ions in single system. From preliminary studies, Zinc metal ferrite magnetic green composites viz. Zinc ferrite-rice husk silica, Zinc ferrite-mango starch and Zinc ferrite-carboxy methyl starch (ZFN-RHS, ZFN-MS and ZFN-CMS) were observed to perform better for the removal of pollutants from aqueous solution. So, these were selected for further study. Various characterization techniques like Fourier Transform Infra-Red Spectroscopy (FTIR), X-Ray Diffraction (XRD), Fe- Scanning Electron Microscope (FESEM), Energy Dispersive Spectra (EDS), Brunnauer-Emmett-Teller (BET), Thermo gravimetric Analysis (TGA) and pH of point zero charge (pH$_{PZC}$) were utilised for structural and morphological analysis of selected magnetic green composites. The important conclusions drawn from this study are given below:

A. Characterization of magnetic green composites

(1) Fourier transform infrared spectroscopy (FTIR) :

- In FTIR spectra of ZFN, two peaks below 600 cm^{-1} confirmed the formation of spinel Zinc metal ferrite.

- In FTIR spectra of ZFN-RHS, peaks at 1064 and 795 cm^{-1} corresponded to asymmetric stretching and bending respectively which depicted silicon-oxygen-silicon bonds and peak at 3375 cm^{-1} confirmed the presence of hydroxyl group. Similar, peaks were also present in the FTIR spectra of pure rice husk silica. Two peaks at 554 cm^{-1} and 423 cm^{-1}
  were present in FTIR spectra of ZFN-RHS which was similar to ZFN spectra indicating the retention of spinel character.

- In FTIR spectra of ZFN-MS, peak seen at 2930 cm^{-1} was also present in the spectra of pure mango starch which depicted C-H stretching. Peak at 3200 cm^{-1} represents the presence of hydroxyl group in ZFN-MS. Similarly, two peaks observed below 600 cm^{-1} corresponded to retention of spinel character in ZFN-MS.

- In FTIR spectra of ZFN-CMS, absorption band at 1557.57 cm^{-1} confirmed the presence of –COO$^-$ group. The bands at 3375 cm^{-1} and 2900 cm^{-1} which were found in spectra of both CMS and ZFN-CMS indicated the presence of hydroxyl and alkyl groups in them. Two peaks at 554 cm^{-1} and 423 cm^{-1} found in the FTIR spectra of ZFN-CMS demonstrated that ZFN-CMS had spinel character.

(2) X-Ray Diffraction analysis (XRD):

- X-Ray Diffraction analysis (XRD) confirmed the spinel character of Zinc metal ferrite(ZFN) and its magnetic green composites viz. ZFN-RHS, ZFN-MS and ZFN-CMS.

- Using Scherrer formula, the average crystallite size of ZFN, ZFN-RHS, ZFN-MS andZFN-CMS were found to be 28nm, 31nm, 43nm and 38nm, respectively.

- The crystallite size indicated that all synthesized materials were in nano size range.

(3) Fe-Scanning electron microscopy (FESEM):

- From FESEM, the detailed information about the shape and structure of Zinc ferriteand its composites was observed.

- Small granules appeared on the surface of ZFN-RHS composite upon modification ofzinc ferrite with rice husk silica.

- The surface of ZFN-MS becomes flaky when mango starch was attached with ZFN.

- The structure of zinc ferrite-carboxy methyl starch (ZFN-CMS) was found to beirregular.

(4) Brunauer-Emmett-Teller analysis (BET)

- From BET analysis, the specific surface area of ZFN, ZFN-RHS, ZFN-MS and ZFN-CMS were found to be 3.7020, 3.0233, 2.7790, 0.4268 m^2g^{-1}, respectively.

- Average pore diameter of ZFN, ZFN-RHS, ZFN-MS and ZFN-CMS were 410.79, 454.25, 416.87 and 423.82 A^o, respectively.

- Pore volume of ZFN, ZFN-RHS, and ZFN-CMS were 0.6519, 3.6785, 1.0954 and 1.30201 cm^3g^{-1}, respectively.

- The decreased surface area and increased particle size as well as pore size of magneticgreen composites confirmed the attachment of RHS, MS and CMS on the surface of ZFN.

(5) Thermo gravimetric analysis (TGA)

- According to the TGA data of ZFN-MS it was found that 0.40g of starch was attachedin 1g of ZFN-MS magnetic green composite.

- Based on the TGA data of ZFN-CMS it was estimated that 0.45g of carboxy methylstarch was attached with 1g of ZFN-CMS.

- Based on the data of ZFN-RHS it was found that 0.50g of silica was attached with 1g of ZFN-RHS.

(6) Point zero charge pH (pH$_{pzc}$)

- The pH$_{pzc}$ of ZFN, ZFN-RHS, ZFN-MS and ZFN-CMS was 8.4, 4.3, 7.4 and 7.2 respectively.

- The pH of point zero charge revealed that above pH$_{pzc}$, there will be a net negative charge and

below pH_{pzc}, there will be a net positive charge on the surface of magnetic green composites.

B. Adsorption of cationic dyes (CV, BG, MB, MG), Ni (II) ions and F⁻ ions with magnetic green composites (ZFN-RHS, ZFN-MS and ZFN-CMS)

1) The adsorption study revealed the use of magnetic green composites (ZFN-RHS, ZFN-MS and ZFN-CMS) towards various dyes, metal ion and fluoride ions.

- ZFN-CMS was used in the removal of CV, BG, MB and MG for single dyes.

- ZFN-RHS was used for removing MB and CV in single and binary system of dyes.

- ZFN-MS was used in removal of MB, BG and CV dyes in single and ternary system of dyes.

- ZFN-MS and ZFN-CMS were used in the removal of Ni (II) ions from aqueous solution in a single system.

- ZFN-RHS, ZFN-MS and ZFN-CMS were utilised for removing F⁻ ions from aqueous solution.

- Effect of contact time, adsorbent dose, pH, concentration and temperature was studied.

2) Adsorption behavior of magnetic green composites showed that in binary and ternary system of dyes, the removal efficiency was less as compared to single system of dyes. This was observed due to antagonistic effect of dyes (electrostatic forces and π-π interactions). These strong interactions lessened the removal efficiency of dyes in multiple dye system.

3) From the study of effect of contact time on the removal of pollutants (dyes/fluoride ions/Ni (II) ions) using ZFN-RHS, ZFN-MS and ZFN-CMS, it was found that the residual concentration decreased and percent removal of pollutants increased with time and eventually reached at equilibrium stage. This happened because initially there were vacant sites present on the surface of magnetic green composites which got filled with dyes/fluoride ions/Ni (II) ions with time and equilibrium was attained.

4) From the kinetic studies, it was found that pseudo second order model best fitted the data obtained for dyes (in single, binary, ternary system); Ni (II) ions and F⁻ ions in single system. It was concluded that process of removal of dyes in single or multiple dye system; Ni (II) ions and F⁻ ions in single system, followed the chemisorption process. The lines in the plots of Weber Morris intra particle diffusion model did not pass through the origin which revealed that a lot of other factors also affected the adsorption process in the present study besides intra particle diffusion.

5) pH studies revealed that maximum percentage removal of dyes/F⁻ ions using ZFN-RHS was achieved at pH 5 and using ZFN-MS, ZFN-CMS for removal of dyes; Ni (II) ions and F⁻ ions at pH 8. These pH values are quite close to their respective pH_{PZC} values.

6) By increasing the adsorbent dose, the percentage removal of dyes/Ni (II) ions/F⁻ ions also increased. Because the number of active sites used for adsorption of dyes/Ni (II) ions/F⁻ ions, increased. For ZFN-CMS, removal efficiency of MG, BG, MB and CV dyes increased from 69.1% to 79.9%, 47.3% to 59.1%, 69.4% to 77.5% and 57.5% to 74.4%, respectively. Using ZFN-RHS, removal efficiency of MB and CV dyes increased from 69.4% to 77.6% and 57.6% to 74.4% respectively in single dye system. In binary dye system, it increased from 57.1% to 66% and 56% to 67.7% for MB and CV dyes respectively. Using ZFN-MS, removal efficiency of MB, CV and BG dyes increased from 69.4% to 77.5%, 59.2% to 79.5% and 53.5% to 75.5% respectively in single dye system. In ternary dye system with ZFN-MS, removal efficiencies of dyes MB, CV and BG increased from 52.4% to 75.2%, 55.5% to 74.4% and 53.1% to 72%, respectively. Using ZFN-RHS, removal efficiencies of fluoride ions increased from 72.1% to 78.9%, for ZFN-MS from 73.5% to 79.8% and for ZFN-CMS from 67.7% to 74.4% with increase in the adsorbent dose. For ZFN-MS, removal efficiencies of Ni (II) ions increased from 59.5% to 65.5%, for ZGN-CMS from 52.4% to 60.2% with increase in the adsorbent dose.

7) With increase in concentration, removal efficiency of dyes (in single and multiple systems)/ Ni (II) ions/F⁻ ions, decreased. Adsorption capacity (Q_e) values increased with increase in concentration due to increase in interactions between adsorbate and adsorbent molecules. The adsorption of magnetic green composites were analysed at three temperatures viz. 25°C, 30°C and 35°C. It was found that with rise in temperature, adsorption of dyes/Ni (II) ions/F⁻ ions, increased. This was observed because with the increase in temperature, higher interactions occurred between adsorbate and adsorbent molecules due to increase in kinetic energy of the system. Also size of pores of adsorbent became large with increase in temperature which provided large surface area for the adsorption of pollutants on the surface of adsorbent.

8) The adsorption data obtained from dyes/Ni (II) ions/ F⁻ ions were fitted to Langmuir, Freundlich, Temkin and D-R isotherms.

- It was found that using ZFN-CMS in single dye system, Langmuir and Temkinisotherms fitted best.

- In single and binary dye system using ZFN-RHS, Freundlich isotherm fitted best.

- In single and ternary system of dyes using ZFN-MS as adsorbent, Freundlich adsorptionisotherm was best fitted.

- Similarly, for adsorption of Ni (II) ion and F⁻ ions, Freundlich adsorption isotherm wasfitted best.

- The value of adsorption energy which was one of the parameter associated with D-R isotherm calculated for removing MG, BG, MB and CV in single system were 119,132.109 and 133 kJ mol^{-1}, respectively. Using ZFN-RHS in single system for dyes CV and MB, adsorption energy was 129 and 223 kJ mol^{-1}, respectively whereas in binary dye system adsorption energy was 914 and 408 kJ mol^{-1} for removal of CV and MB dyes. For removal of F$^-$ ions using ZFN- RHS, ZFN-MS and ZFN-CMS adsorption energy values were 912, 1008.2 and 846.18 kJ mol^{-1}, respectively. For removal of Ni (II) ions, adsorption energies were calculated to be 70.7 and 55.4 kJ mol^{-1} for ZFN-MS and ZFN-CMS, respectively. These high values of adsorption energies revealed the endothermic and chemisorption nature of the adsorption process by these magnetic green composites.

- The values maximum of adsorption capacities for single dye system using ZFN-CMS were found to be 101.3, 132.1, 98.3 and 114.9mg/g for removal of MG, BG, MB and CV dyes respectively. For ZFN-RHS in single dye system, the maximum adsorption capacities for removal of CV and MB dyes were found to be 138.8 and 84.7 mg/g respectively whereas in binary system it was found to be 15.4 and 22.2 mg/g for CV and MB dyes respectively. Using ZFN-MS, maximum adsorption capacities for CV, BG and MB dyes were found to be 142.9, 101.2 and 105.8 mg/g respectively. In ternary dye system, for ZFN-MS, the values of maximum adsorption capacities were found to be 66.8 and 53.8 mg/g respectively. For removal of fluoride ions using ZFN-RHS, ZFN-MS and ZFN-CMS magnetic green composites, the maximum adsorption capacities were found to be 10.2, 6.4 and 9.1 mg/g respectively. Using ZFN-MS for the removal of Ni (II) ions, maximum adsorption capacity was found to be 65.3 mg/g whereas for ZFN-CMS it was found to be 208.3 mg/g.

- The value of separation constant (R$_L$) associated with Langmuir isotherm was found to be in between 0 and 1 for all the magnetic green composites used in this study for the removal of dyes/fluoride ion/Ni (II) ions which depicted the favorable nature of adsorption process by these adsorbents.

9) The different adsorption parameters (ΔH^o, ΔS^o and ΔG^o) were calculated with magnetic green composites (ZFN-RHS, ZFN-MS and ZFN-CMS).

- The results revealed that for removal of dyes using magnetic green composites (ZFN- RHS, ZFN-MS and ZFN-CMS), values of ΔH^o and ΔS^o were positive. This suggested that adsorption process was endothermic in nature and there was more randomness at the surface of magnetic green composites, ΔG^o values were negative which showed the spontaneous nature of adsorption by magnetic green composites.

- For the removal of F$^-$ ions, adsorption parameters ΔH^o and ΔS^o were positive and ΔG^o was

negative. It was concluded that process of removal of fluoride ions was endothermic and spontaneous in nature and more randomness was at the surface of magnetic green composites.

- For the removal of Ni (II) ions using ZFN-MS and ZFN-CMS, ΔG^o was positive, which revealed the non-spontaneous nature of the adsorption process by magnetic green composites.

- The values of ΔG^o were found to be negative at lower concentrations and positive at higher concentrations. This indicated that the process of removal of dyes/fluoride ions/ Ni (II) ions using magnetic green composites (ZFN-RHS, ZFN-MS and ZFN-CMS) was spontaneous at lower concentrations whereas it became non-spontaneous at higher concentrations.

10) Magnetic green composites were recycled for 5 times. Results showed that ZFN-CMS retained 93% efficiency in single system; ZFN-RHS retained 80% efficiency in single system and 71% in binary system of dyes. ZFN-MS retained 90% efficiency in single and 82% in binary system of dyes. ZFN-MS and ZFN-CMS retained 72% and 79% efficiency in removal of Ni (II) ions from aqueous solution. ZFN-RHS, ZFN-MS and ZFN-CMS retained 74%, 85% and 84% efficiency, respectively in removal of fluoride ions from aqueous solution. These results demonstrated the affordable nature of magnetic green adsorbents used in this study as the efficacy of these adsorbents remained higher even after 5 cycles. So, ZFN-RHS, ZFN-MS and ZFN-CMS magnetic green adsorbents can be used multiple times.

CONCLUSIONS

The present study concluded that

- Magnetic green composites used in this study (ZFN-RHS, ZFN-MS and ZFN-CMS) showed high efficiency for removing selected cationic dyes (MB/MG/BG/CV). These adsorbents can be economically and beneficially utilised for removing other cationic species/heavy metal ions as these have suitable functional groups attached to their moiety.
- The synthesized magnetic green adsorbents in the present work can also be tested further for the removal of industrial waste water impurities.
- ZFN-RHS, ZFN-MS and ZFN-CMS magnetic green composites were recycled for 5 times and still gave good results for removal of pollutants from water, so these are affordable.

List of publications:

Papers published

1. **D. Sharma,** R. Jasrotia, J. Singh, S. Mittal, and H. Singh, "Novel Zinc ferrite composite with starch and carboxy methyl starch from biowaste precursor for the removal of Ni(II) ion from aqueous solutions," *J. Dispers. Sci. Technol.*, vol. 0, no. 0, pp. 1–11, 2023, doi: 10.1080/01932691.2023.2222809.

2. **D. Sharma,** R. Jasrotia, J. Singh, and H. Singh, "Removal of cationic dyes in single as well as binary dye systems from aqueous solution using Zinc ferrite-rice husk silica composite," *Int. J. Environ. Anal. Chem.*, vol. 0, no. 0, pp. 1–22, 2022, doi: 10.1080/03067319.2022.2140416.

3. R.Singh, R.Jasrotia**., D.Sharma**, J. Singh, S.Mittal, and H. Singh, " Recyclable magnetic nickel ferrite–carboxymethyl cellulose–sodium alginate bio-composite for efficient removal of nickel ion from water," *J. Dispers. Sci. Technol.*, vol. 0, no. 0, pp. 1–12, 2024,doi.org/10.1080/01932691.2024.2320302.

4. R. Jasrotia, R. Singh, **D. Sharma**, J. Singh, S. Mittal, and H. Singh, "A Sustainable Approach for Enhancing Cationic Dyes Adsorption in Single and Multiple Systems using Novel Nano Ferrites Modified with Walnut Shell," *ChemistrySelect*, vol. 9, no. 18, p. e202304810, 2024, doi: https://doi.org/10.1002/slct.202304810.

Book chapter published

1. **Dimple sharma,** Sonika singh, Jandeep singh, and Harminder singh," Magnetic nanomaterials for waste water remediation." D.o.i 10.1201?9781003129042-5. **www.taylorfrancis.com/chapters.**

Papers communicated

1. **Sharma Dimple** and Jasrotia, Rimzim and Singh, Jandeep and Mittal, Sunil and Singh, Harminder, "Recyclable Magnetic Green Adsorbents for the Effective Removal of Fluoride Ions from Water."

2. **D. Sharma,** R. Jasrotia, J. Singh, and H. Singh," Novel magnetic metal ferrite-mango starch composite for the removal of dyes in single and ternary dyes mixture from aqueous solutions: Kinetics and thermodynamic studies."

3. R jasrotia, **D. Sharma,** R. Singh, J. Singh, S. Mittal, and H Singh, "Bio-waste based novel nano magnetic composite for removing Cu(II) ions from water: Kinetic and Thermodynamic studies."

Conferences

1. Paper presentation, on green adsorbents in treatment of waste water containing dyes and heavy metals as pollutants in the International Conference on Materials for Emerging Technologies (ICMET-21) held on February 18-19, 2022, organized by Department of Research Impact and Outcome, Division of Research and Development, Lovely Professional University, Punjab.

2. Poster presentation on Review on treatment of waste water containing dyes and heavy metals as pollutants in the International Conference on Recent advances in fundamental and applied sciences (RAFAS 2021)held on June 25-26, 2021, organized by Department of Research Impact and Outcome, Division of Research and Development, Lovely Professional University, Punjab

Submit an article | Journal homepage

Research Article

Removal of cationic dyes in single as well as binary dye systems from aqueous solution using Zinc ferrite-rice husk silica composite

Dimple Sharma, Rimzim Jasrotia, Jandeep Singh & Harminder Singh ✉ ⓘ

66 Download citation | https://doi.org/10.1080/03067319.2022.2140416 | Check for updates

Full Article | Figures & data | References | Citations | Metrics | Reprints & Permissions | Get access

ABSTRACT

49

Taylor & Francis Online

Home ▶ All Journals ▶ Engineering & Technology ▶ Journal of Dispersion Science and Technology ▶ List of Issues ▶ Latest Articles ▶ Novel Zinc ferrite composite with starch ...

Submit an article   Journal homepage

Research Article

Novel Zinc ferrite composite with starch and carboxy methyl starch from biowaste precursor for the removal of Ni (II) ion from aqueous solutions

Dimple Sharma, Rimzim Jasrotia, Jandeep Singh, Sunil Mittal & **Harminder Singh** ✉

66 Download citation   🔗 https://doi.org/10.1080/01932691.2023.2222809   ⟳ Check for updates

🖹 Full Article   🖼 Figures & data   📖 References   🖽 Supplemental   66 Citations   📊 Metrics   🔒 Reprints & Permissions   Read this article

Abstract

In the present work, Zinc ferrite composites with Mango starch (MS) and

Related research 🔵

People also read   Recommended articles   Cited by

Recyclable magnetic nickel ferrite–carboxymethyl cellulose–sodium alginate bio-composite for efficient removal of nickel ion from water

Rajinder Singh[a], Rimzim Jasrotia[a], Dimple Sharma[a], Jandeep Singh[a], Sunil Mittal[b], and Harminder Singh[a]

[a]School of Chemical Engineering and Physical Sciences, Lovely Professional University, Phagwara, India; [b]Department of Environmental Science and Technology, Central University of Punjab, Bathinda, India

ABSTRACT

In waste water treatment, magnetic bio-composites are frequently investigated as an adsorbent recently due to their great capacity for adsorption and affordability. In this current work, an attempt has been made to develop spinel nickel ferrite-carboxymethyl cellulose (NiFCMC) composite and modified its surface by alginate polymer to form NiFCMC–Alg composite. Several techniques were utilized to characterize these adsorbents including Fourier transform infrared spectroscopy, x-ray diffraction, field emission scanning electron microscopy, energy-dispersive spectra, thermogravimetric analysis, vibration sample magnetometry and pH of point zero charge. These adsorbents were explored to check their potentiality to remove Ni (II) ions in aqueous medium on various parameters such as contact time, initial metal ion concentration, pH, adsorbent dose and temperature. The optimum time for establishment of equilibrium was 180 minutes at pH 8 with adsorbent dose of 0.1 g. Results of kinetic studies revealed that the best fit for the metal ion adsorption data was the Lagergren pseudo-second-order mode indicating the chemisorption nature. Likewise, the Langmuir isotherm model also showed good agreement with adsorption equilibrium data with maximum adsorption capacities 47.84 ± 2.39 and 60.24 ± 3.01 mg/g for NiFCMC and NiFCMC–Alg respectively. The calculated adsorption thermodynamic parameters confirmed the spontaneous nature of adsorption process. The regeneration efficiency of both adsorbents was studied for five cycles and showed significant results. This study has shown that NiFCMC and NiFCMC–Alg can be a good substitute for removing Ni (II) ions in aqueous medium.

GRAPHICAL ABSTRACT

A Sustainable Approach for Enhancing Cationic Dyes Adsorption in Single and Multiple Systems using Novel Nano Ferrites Modified with Walnut Shell

Rimzim Jasrotia,[a] Rajinder Singh,[a] Dimple Sharma,[a] Jandeep Singh,[a] Sunil Mittal,[b] and Harminder Singh*[a]

Walnut shell has been used in various experimental studies for different dyes removal, but it is exciting to study the adsorption behaviour of bio-waste (walnut shell) in combination with spinel zinc ferrite which resulted in the formation of a novel material having magnetic properties and help in easy separation after the wastewater treatment. Novel magnetic walnut shell zinc ferrite (WSZF) composite has been synthesized and used to remove Malachite Green and Methylene Blue from aqueous solution in single and binary dye systems. Different techniques have been used to characterize the composite such as Fourier Transform Infrared Spectroscopy, X-Ray Diffraction, Field Emission Scanning Electron Microscopy, Energy Dispersive Spectroscopy, Thermogravimetric Analysis and pHzpc. Adsorption of dyes were studied to see the effect of time, pH, adsorbent dose, dye concentration and temperature. The Lagergren pseudo second order model fitted well among various kinetic models employed. Langmuir adsorption isotherm best fitted with maximum adsorption capacities of 86.20 and 169.5 mg/g in single dye and 23.92 and 18 mg/g respectively in binary dye system for Malachite Green and Methylene Blue. Process was spontaneous and ΔH° were found positive, confirmed endothermic process of adsorption. The composite's regeneration capacity was studied for five cycles and at the end of five cycle the efficiency of the material was found to be around 80% for both single as well as binary dye systems. It is concluded that the chosen WSZF will be the optimum solution for cationic dyes removal.

1. Introduction

Rapid increase in population growth, various industrial activities, climatic variations etc. leads to the deterioration of available fresh water resources in the whole world.[1] Industries such as paint, plastic, leather, food processing, textile, pharmaceutical industries etc. are using dyes as colorants in their production process.[2a] Dyes are used by industries in large quantities and discharged directly into water bodies without their treatment.[3] The discharge of harmful pollutants into water bodies can cause mutagenicity, embryo toxicity and carcinogenicity.[4] The dyes are of basically synthetic origin which possess complex molecular structure, thus shows more stability and difficulty in biodegradation.[5] The dyes can be categorized as cationic, anionic and non-ionic dyes.[5] Approximately ten thousand types and about 7×10^5 tons of different dyes are produced by these industries annually.[6] Even at very low concentration, dyes are easily visible to naked eye. Dyes contain harmful components which are toxic in nature that can damage aquatic life, human life and may also results in the

disruption of ecological balance. Therefore, presence of dyes in the water body beyond maximum permissible limits affects the quality of water and also results in the inhibition of sunlight penetration which ultimately affects the photosynthetic activity.

Different treatment methods available for the degradation of dyes from wastewater depending upon wastewater source are as- Advanced Oxidation process, Coagulation/flocculation, Adsorption, Membrane filtration, Photocatalytic degradation etc.[7]

Adsorption techniques are effective practices that are extensively used in the industrial sector to remediate organic as well as inorganic pollutants due to their low cost, ease of operation, minimum sludge creation, regeneration ability and other benefits.[8–10]

Nanotechnology has emerged as an excellent alternative to wastewater treatment. Because the nanoparticles show numerous advantages such as high active surface sites, increased strength, short density and so on.[11] The size of nanoparticles ranges from diameter 1–100 nm. There are different materials which can be used as nanoparticles. In this experimental study, ferrites were chosen as efficient nano materials. Ferrites represent a type of magnetic nanoparticles that are derived from various metal oxides as well as hematite and magnetite.[12] Ferrites have exceptional electrical and magnetic characteristics.[13] According to literature studies, spinel ferrites are widely used for wastewater treatment. However, in some cases magnetic nanoparticles show certain disadvantages such as limited efficiency, short shelf life.[14–15] To overcome these limitation, different materials are used to coat nano particles for

[a] R. Jasrotia, R. Singh, D. Sharma, J. Singh, H. Singh
School of Chemical Engineering and Physical Sciences, Lovely Professional University, Phagwara, Punjab, 144411, India
E-mail: harminder_env@yahoo.com

[b] S. Mittal
Department of Environmental Science and Technology, Central University of Punjab, Bathinda, Punjab, India

☐ Supporting information for this article is available on the WWW under https://doi.org/10.1002/slct.202304810

About Us   Subjects ∨   Browse ∨   Products ∨   Request a trial   Librarian Resources   What's New!!

Chapter

Magnetic Nanomaterials for Wastewater Remediation

By *Dimple Sharma, Sonika Singh, Jandeep Singh, Harminder Singh*

Book   Nanomaterials for Environmental Applications

Edition   1st Edition

First Published   2022

You do not have access to this content currently. Please click 'Get Access' button to see if you or your institution have access to this content.

GET ACCESS

To purchase a print version of this book for personal use or request an inspection copy »

53

DIVISION OF RESEARCH AND DEVELOPMENT

[Under the Aegis of Lovely Professional University, Jalandhar-Delhi G.T. Road, Phagwara (Punjab)]

Certificate No.240190

Certificate of Participation

This is to certify that **Ms. Dimple Sharma** of **Lovely Professional University, Phagwara, Punjab, India** has presented paper on **Review on green adsorbents in treatment of waste water containing dyes and heavy metals as pollutants** in the **International Conference on Materials for Emerging Technologies (ICMET-21)** held on February 18-19, 2022, organized by Department of Research Impact and Outcome, Division of Research and Development, Lovely Professional University, Punjab.

Date of Issue: 16-03-2022
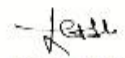Place: Phagwara (Punjab), India

Prepared by
(Administrative Officer-Records)

Dr. Vipul Srivastava
Convener
(ICMET-21)

Dr. Manish Vyas
Organizing Secretary
(ICMET-21)

Dr. Chander Prakash
Co-Chairperson
(ICMET-21)

Certificate of Participation

This is to certify that Prof./Dr./Mr./Ms. **Ms. Dimple Sharma**

of **Lovely Professional University**

has given poster presentation on **Review on treatment of waste water containing dyes and heavy metals as pollutants**

in the International Conference on 'Recent Advances in Fundamental and Applied Sciences" (RAFAS 2021) held on June 25-26, 2021, organized by School of Chemical Engineering and Physical Sciences, Lovely Faculty of Technology and Sciences, Lovely Professional University, Punjab.

Date of Issue : 15-07-2021
Place of Issue: Phagwara (India)

Prepared by
(Administrative Officer-Records)

Organizing Secretary
(RAFAS 2021)

Convener
(RAFAS 2021